ENGINEERING TOOLS TO SUPPORT THE DESIGN AND OPERATION OF INITIAL CAPTURE CHROMATOGRAPHY

A thesis submitted to the University of London
for the degree of Doctor of Engineering
in Biochemical Engineering

by

John Joseph

September 2007

The Advanced Centre for Biochemical Engineering
Department of Biochemical Engineering
University College London
Torrington Place
London WC1E 7JE

ProQuest LLC
789 East Eisenhower Parkway
P.O. Box 1346
Ann Arbor, MI 48106-1346

ABSTRACT

Monoclonal antibodies are the largest and most rapidly expanding category of biopharmaceuticals today with applications across a wide range of diseases. While Protein A affinity chromatography has been almost universally applied as the primary purification step for process-scale production of these molecules, it suffers from disadvantages of high cost, limited throughput and the need for extensive methods development. These issues are magnified by dramatic increases in cell culture titres, which have shifted the burden to downstream processing in the race for increased manufacturing productivity and decreased cost of goods (COG/g). The aim of this thesis is the development of a decisional framework with which to address these concerns; allowing for the rapid visual representation and comparison of process performance and key process trade-offs that result from the adoption of various column-based processing strategies.

An empirical framework has been developed which significantly reduces the number of small scale studies required to predict flow conditions at increasing scale. Predictions were found to be within 10% of published data for columns at production-scale. Column hydrodynamics are closely related to the rigidity of the chromatographic resin used. Given the inherent physicochemical nature of chromatographic separations, techniques are developed with which to investigate the effect that pH changes have on resin rigidity during multi-cycle operation. Results demonstrate the importance of considering the impact on resin stability when operating over long campaigns. Trials with a range of existing and prototype resins are used to both verify the approach and to illustrate the nature of the process insights which may be gained. For example, it was found that increasing back-bone resin rigidity by 7 fold resulted in a 6 fold increase in compressive strength under high pH mobile phase conditions.

Knowledge of column behaviour at large scales provides a more realistic basis for the prediction of the throughput limits of chromatographic operation. This is

accomplished through an integrated graphical framework, based on a verified mathematical model for the design and analysis of a Protein A affinity chromatography step. A case study is used to illustrate the methodology and investigates the effect of different column sizes and linear flow rates on operational costs and scheduling, so as to identify the optimum column size and operation for a given process duty. The study also considers resin choice and the use of ultrafiltration pre-concentration prior to the chromatographic step. Results show that conditions of maximal column productivity are not equivalent to conditions of minimum COG/g. Cost minimisation was found to occur when the number of cycles of production were minimised by maximising resin binding capacity. The framework was further extended to investigate optimal operation of the chromatographic cycle with particular reference to the post-load washing stage. Studies show the interaction between the washing and loading strategy and demonstrate that wash and adsorption stages should be considered as a single integrated stage within the chromatographic cycle. Alternative washing strategies for various resin materials are compared and evaluated.

The strategies developed in this thesis enable rapid development of optimal process-scale chromatographic design and also bear significant implications for the economics of antibody production. Moreover, the approaches and techniques developed are generic and should be broadly applicable to most packed bed chromatographic separations.

ACKNOWLEDGEMENTS

I wish to acknowledge the help of many individuals who have contributed to bringing this work to fruition. I would first like to express my sincere thanks and gratitude to my supervisors Professor Nigel Titchener-Hooker and Dr Yuhong Zhou for the numerous opportunities and experiences that have come my way throughout my tenure at the department of Biochemical Engineering. Their advice, energy, enthusiasm and most importantly their 'open door' policy were invaluable in my progress.

I am also indebted to Dr Karol Lacki (GE Healthcare, Uppsala, Sweden) for his patience, expert advice and support. Certainly his 'what's the problem?' adage proved to be a source of encouragement (and frustration!). I would also like to thank Dr Henry Charlton (Prometic Biosciences, Cambridge, UK) for adding an interesting dimension to this study.

I would also like to express my appreciation to many colleagues at UCL for their input and encouragement in this work. Particular thanks go to Richard Tran for his help with the experimental portion of this study as well as for many fruitful discussions. Without his assistance, this doctoral study may have taken an extra year to complete. Special thanks must also be given to Dr Daniel Bracewell and Dr Suzanne Farid for their expert advice as well as to Dr Janice Lim, Dr Samir Ujam and Janahan Paramesvaran for their friendship and support.

TABLE OF CONTENTS

LIST OF FIGURES

LIST OF TABLES

1 SCOPE AND BACKGROUND

1.1 Introduction

The biopharmaceutical industry faces enormous pressures to achieve timely delivery of drugs to market whilst reducing costs. The manufacture of antibody therapeutics faces several critical challenges including improving process economics and efficiency, meeting demanding regulations and reducing costs (Roque *et al.*, 2004). Greater than 50% of the total manufacturing cost of a therapeutic antibody is incurred during the downstream processing with the majority of this cost attributable to chromatographic unit operations (Roque *et al.*, 2004; Aldridge, 2006). Due to its high selectivity and stability chromatography has become the pre-eminent technique for the large-scale purification of proteins for therapy. Therefore improving the economy and efficiency of chromatographic systems is critical to the streamlining of timelines and reducing the cost of goods of a manufacturing process. This can be achieved through seamless process development.

Early planning of process development activities, recognition of lead times and efficient resource utilisation can help to achieve these objectives. This is particularly the case as production technologies for new drugs are becoming progressively more complex (Bryom, 2000). As a consequence the application of computer-aided design tools to facilitate process design and development of large-scale chromatography systems is of interest. This thesis explores the creation of an integrated modelling framework which aims to provide a rigorous approach to designing large-scale chromatography systems.

The aim of this introductory chapter is to provide an overview of the biopharmaceutical industry with its key manufacturing concerns, highlighting the role of downstream processing and in particular chromatography. Section 1.2 gives a brief overview of the biopharmaceutical market describing the economic potential of manufacturing therapeutic drugs and in particular, monoclonal antibodies (MAbs). The process for the production of MAbs is tackled in Section 1.3. Section 1.4 highlights the current platform purification process that is currently being

implemented in industry. The main concerns experienced by firms within this process are also addressed in Section 1.5, which provides the basis and focus of this work. The challenges and benefits of using bioprocess simulation to tackle these issues are examined in Section 1.6. Finally, the objectives and organisation of this thesis are highlighted in Section 1.7.

1.2 The commercial potential of monoclonal antibodies

In the drug industry as a whole 101 drugs each brought in more than $1 billion in worldwide sales in 2006 (Lawrence, 2007). Of these, 18 were biotech drugs. As an industry, biotech will account for 24% of the 2007 pharmaceutical market sales growth of $35billion[a]. Even as the total number of $1 billion-plus drugs has grown, biotech has more than doubled its share of blockbusters over the past six years. In addition, last year three biotech drugs that were approved in 2004 brought in more than $1billion each, two of which were monoclonal antibodies (MAbs) used in cancer treatment.

Since the development of hybridoma technology in the mid 1970s, MAbs have played a role in several of the important advances in pharmacotherapy; agents such as, Synagis™, Herceptin™, Avastin™ and Remicade™ have contributed to the treatment of infectious diseases, cancer and autoimmune diseases, respectively (Torphy, 2002). MAbs came of age as therapeutic products in the early 1990s (Walsh, 2000). In the past decade, the manufacturing requirements for purified MAbs have advanced exponentially in order to meet the ever-growing clinical and commercial demand (Kelly, 2001). However, they are amongst the most expensive of all drugs - the annual cost per patient can reach $55,000 for antibodies treating cancer conditions (Farid, 2006). These high prices are a reflection of the fact that antibodies are now marketed for chronic conditions and of their relatively low potency which results in the need for high cumulative doses (grams rather than milligrams). Consequently expensive large-scale production capacity is required to fulfil market demand and produce 10–100s kg/year (Birch, 2005; Farid 2006). The importance of access to large scale manufacturing capacity was clearly demonstrated

[a] IMS health, www.imshealth.com, 2006

when demand in 2000 for the antibody fusion protein, Enbrel™, exceeded available capacity. These trends, as well as industry pressures, have triggered renewed interest in assessing the financial burden associated with manufacturing and hence its contribution to overall corporate economic success.

Monoclonal antibodies are typically large glycosylated molecules and are most often produced commercially by deep tank mammalian cell culture of up to 20,000L (Chadd *et al.*, 2001). To date, successful large-scale cell culture techniques have been engineered to yield multi-kilogram MAb per batch (Wurm, 2004; Sommerfeld *et al.*, 2005). The challenge is to develop and scale purification processes that are capable of yielding kilogram quantities of purified MAb at the lowest possible cost. The aim of this study is to outline an approach which provides a design tool that can be used in the search for a resolution to this issue.

1.3 MAb Production

The production of monoclonal antibodies can occur through growth via fermentation of different mammalian cell lines. Originally, MAbs were produced in hybridoma cells (Koheller *et al.*, 1985). For modern in vitro production processes, the following cell lines are used:

- Chinese Hamster Ovary (CHO)
- Mouse Myeloma (NSO, Sp2/0)
- Monkey Kidney (COS)
- Baby Hamster Kidney (BHK).

The selection of cell is dependent on a set of criteria. Firstly, the cell line must provide a close match to human glycosylation pattern. The cell line must have a stable expression system so as to produce the desired protein. This is necessary because the product is only produced when the cells accept foreign DNA in which the antibody information is stored. And lastly, the specific production rate of the cells should be as high as possible. To achieve this, different amplification systems are used. One of the most common systems is the glutamine synthetase (GS) system

which is used for some monoclonal antibodies and which is licensed to Lonza Biologics (Brown *et al.*, 1992).

The previously described cell line selection criteria are best met by the CHO and mouse myeloma cells since they each provide a near human glycosylation pattern as well as the chance to establish a stable expression system. Furthermore, these cell lines are known very well so that there is extensive experience in culturing and modifying them (Peakman *et al.*, 1994). During the fermentation process, cells secrete product into the fermentation broth so that the product has to be separated from a complex mixture of different substances. The cell culture medium comprises of amino acids, inorganic salts, vitamins, glucose and other organic substances. Moreover, certain proteins are added as a supplement, exacerbating the purification of the product protein. Other problems arise from the cells since DNA, viruses and lipids can get into the fermentation broth when the cells are destroyed or when cell lysis occurs during fermentation. Moreover, certain host cell proteins (HCP) are secreted and have to be separated from the product protein.

1.4 MAb purification

The purification of MAbs involves the use of different chromatographic techniques. Chromatographic separations have been the workhorse in the downstream processing of MAb therapeutics since the beginning of the industry, by virtue of its high resolving power (Thommes *et al.*, 2007). Various combinations of chromatographic steps have been employed for the purification of monoclonal antibodies (Naveh *et al.*, 1991; Shadle, 1995; Ostlund, 1996). Typically a Protein A affinity capture column is used for the direct capture of MAbs from cell culture fluid. Protein A affinity chromatography can remove greater than 99.5% of product impurities in a single step with high yields and often minimal methods development (Follman *et al.*, 2004 ; Lacki *et al.*, 2003). The high degree of purification from this process step alone helps make the entire downstream process very robust since in general only trace contaminants need to be removed after this unit operation (high molecular aggregates, residual host cell proteins and leached Protein A). Usually only one or two chromatographic steps are required following the Protein A capture step (Fahrner *et al.*, 2001). Ion exchange chromatography is normally used in

conjunction with various filtration and virus clearance steps (Thommes *et al.*, 2007). This has helped firms move towards platform processes as shown in Figure 1.1 for antibody production (Blank, 2005; Hubbard 2005; Ghose, 2005).

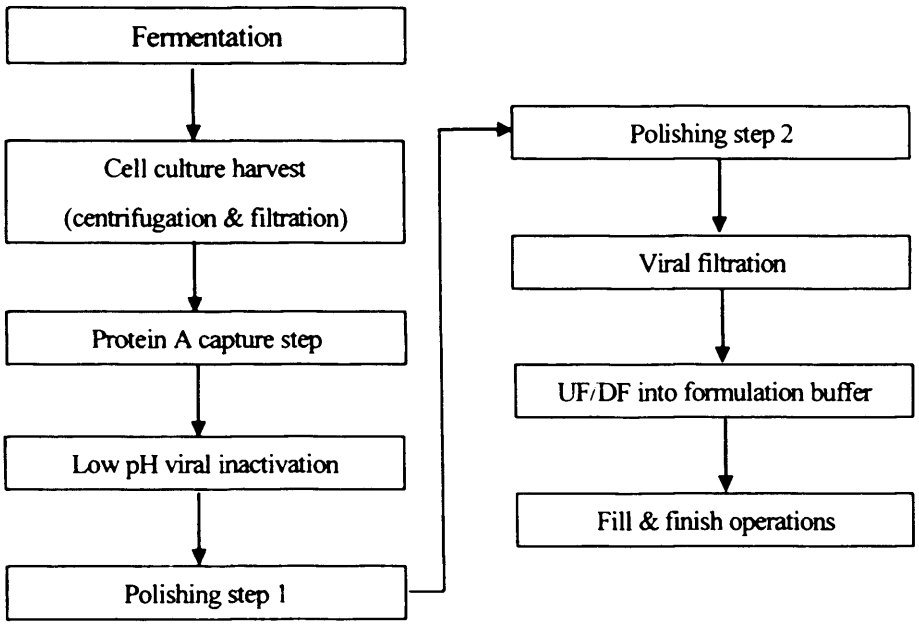

Figure 1.1 Generic manufacturing process for a recombinant monoclonal antibody

1.5 Concerns in large scale MAb Production

A major issue in the development of antibody-based therapies is the cost of production which can be as high as $1,000 per gram (Gura, 2002; Sommerfield *et al.*, 2005; Farid, 2006). In order for the industry to maintain an acceptable margin on future production, there are significant pressures to reduce manufacturing costs at commercial scale (Chadd *et al.*, 2001). Millipore Corp recently carried out an industry-wide survey of managers in the field of antibody process development and manufacturing to assess their performance indicators and how these could be improved (Morrow, 2006). In terms of operational improvements, innovations in cell culture and fermentation were the most frequently cited. This supports the belief that even though yields per cell have exploded in recent years, there is still much room for further increases. The next most cited priority was process chromatography. The recent advances in the upstream production of antibodies have increased both the

time-to-market and cost-efficiency pressures on these downstream processes (Morrow, 2006).

Efficient recovery and purification of antibodies from cell culture media plays a crucial part in minimising manufacturing costs (Keller *et al.*, 2001). As shown in Figure 1.2 a significant percentage (~30-40 %) of the total manufacturing cost of therapeutic antibodies is incurred during purification (Myers, 2000). In fact, with significant improvements in cell culture titres (> 5g/L), downstream purification has the potential to become the bottleneck in antibody drug production. Thus the commercial success of these biomolecules may be said to hinge on the rapid and successful development of economic, robust and efficient downstream process operations. It is this assertion which provides the context for the research presented in this thesis.

The costs breakdown for a typical monoclonal antibody purification process (Figure 1.3) points out one of the clear disadvantages of chromatography – high cost. Protein A resins can cost up to 10 times as much as other non-affinity chromatographic resins and therefore could account for up to 50% of the total chromatographic cost for a purification process (Van Reis, 2006). Through this reasoning, a Protein A capture step can contribute up to 8 % to the overall cost of production (Rouf *et al.*, 2001). As such, the economics of this chromatographic step alone should reflect how process-wide COG/g might fluctuate as a result of process and operational strategies and options.

To reduce the costs associated with the Protein A unit operation firms have recoursed to extensive cycling of Protein A columns (Ghose *et al.*, 2004). While this reduces the financial investment, more cycles are required despite the fact that there are only a finite number of useful cycles for Protein A affinity resins (see Chapter 2). Furthermore, because chromatographic separations involve equilibration, wash, elution, regeneration and sanitisation steps, substantial buffer volumes are required. These volumes also have to be prepared, stored and disposed of properly (Van Reis, 2006).

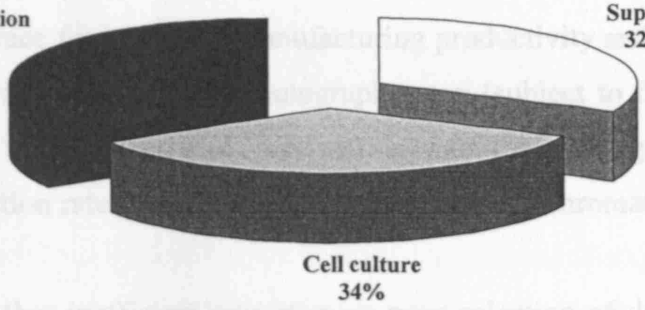

Figure 1.2 Representative distributions of costs in an antibody production process (Myers, 2000).

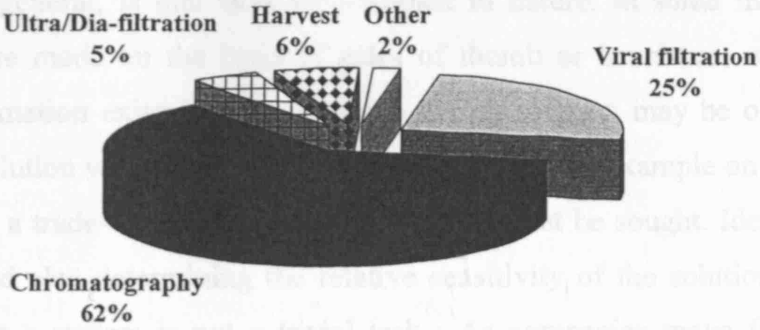

Figure 1.3 Cost distribution of a typical monoclonal antibody purification process (adapted from Myers, 2000).

Another significant driver in bioprocessing is production rate or throughput (Fahrner *et al.*, 1999; Iyer *et al.*, 2002). Advances in cell culture technology and the expansion of the monoclonal antibody market have shifted the burden to downstream processing in the race for increased manufacturing productivity and decreased cost of goods (COGs). Often, the first chromatography step (subject to the largest volume load and lowest concentration of product) is rate limiting (Iyer *et al.*, 2002). Therefore, production rate remains a concern for Protein A chromatography.

It is clear that inefficient operation or poor selection of design for this step can lead to large impacts on the cost and productivity of the production process as a whole. As production technologies for new drugs become progressively more complex, rapid process design and development will be needed to enhance manufacturing operations by shortening time lines with a view to reducing the cost of goods. Recently, computer simulations have been used as a powerful tool in accelerating bioprocess design (Petrides *et al.*, 2002).

1.6 A computer-aided approach to design

The problem of process design for purification systems, as with bioprocess unit operations in general, is that they are complex in nature. In some instances, design decisions are made on the basis of rules of thumb or heuristics, whilst in others design information exists so that a unique design solution may be obtained. Often the design solution will represent a compromise, based for example on a target selling price where a trade-off between yield and purity must be sought. Identifying the best design, and also determining the relative sensitivity of the solution to the variables governing a system is not a trivial task. As companies move from the discovery phase, through clinical trials toward efficacy data and to commercialisation so the issues of production and of process design and operation are becoming more important. In the past it may have been acceptable for a company to run production-scale processes with severely suboptimal levels of performance, just in order to gain fast access to the market in the anticipation of recouping the vast initial outlay incurred in drug development (Zhou *et al.*, 1999). However, the cost pressures are now irresistible (Pisano, 1997), and companies need to develop efficient and robust processes for the manufacture of increasingly sophisticated biological entities.

Further to this, since the 'product is determined by the process' in biotechnology (Petrides *et al.*, 2002), further optimisation is costly and time-consuming after the first clinical lot has been produced meaning that large-scale optimisation needs to be conducted early in the development process.

These issues hold true particularly in the design of chromatographic systems, whose complex mix of interacting design variables can lead to time consuming process development and which relies heavily on the use of expensive pilot-plant facilities in which to test out proposed new strategies. Moreover, the feasibility and reliability of large –scale chromatographic processes is subject to a much higher level of uncertainty due to lack of fundamental approaches to design. As will be demonstrated in this work, computer-aided processes can facilitate this.

Traditionally, chromatographic purification processes are optimised empirically. Separation media, running conditions and sequence of purification steps are all selected according to the expertise of the responsible scientists or engineers (Jungbauer *et al.*, 1996). Given the highly complex nature of chromatographic separation computer-aided methods cannot completely replace this approach but a computer-assisted strategy can reduce the quantity of experiments that need to be performed. The integration of experimental results and computer modelling allows the investigation to accelerate the development of chromatographic separation processes, as demonstrated previously for analytical chromatography (Snyder *et al.*, 1990). Process design can follow a methodology which uses the results from a limited number of strictly controlled experiments and from which parameters required for simulation can be extrapolated (Whitely *et al.*, 1989a, 1991). The simulated peak profiles are used to identify the optimum conditions by applying the conventional rules for assessing separation conditions.

The advantages of using such approaches towards chromatographic optimisation are clear in the context of separation performance. Studies had been carried out to investigate the optimised conditions for a single chromatographic separation (Golshan-Shirazi *et al.*, 1992; Jacobson *et al.*, 1992; Mao *et al.*, 1996a; Felinger *et al.*, 1996, 1998; Dünnebier *et al.*, 2000, Teoh *et al.*, 2001, Ngiam *et al.*,

2002, Salisbury *et al.*, 2006). However, when considering chromatographic operations at manufacturing scale, additional factors need to be considered.

While current techniques enable initial design decisions to be made, the interaction of the chromatography unit with the prior and/or subsequent unit operations in the process will require a more detailed examination of the effects on the selected design. Further to this, operation determined by system (biological, physical and chemical) and process (engineering) constraints and correlations, place limitations on large-scale performance. For example, the flow velocities used in small scale optimisation studies may not be viable at production scale (see Chapter 3). Also, when considering the design of a Protein A capture step in particular, the processing and economic constraints associated with this step (see Chapter 2), indicate that these criteria should be included in any design practises. All in all, it is apparent that a fully integrated approach to chromatographic process design is necessary for optimal performance in manufacturing. At present, however, there seems to be a dearth of models that can fully predict performance of large-scale columns within a manufacturing environment. Work reported in the literature has focused more on individual aspects of chromatography design, whether it be in terms of operational limits, process performance or economics.

1.7 Aims of the thesis

The preceding sections have provided a description of the pertinent features of the biopharmaceutical manufacturing process for the production of MAbs, highlighting the role of Protein A chromatography as the primary capture step in these processes. Chromatographic modelling in process development is becoming more common in industry given its propensity to reduce development times and costly development processes. However, as yet, there seem to be a lack of integrated process techniques in the development of large-scale chromatography systems.

The particular need that is addressed in this thesis is that of process design where biotech companies currently have only limited tools available for the predictive design of large-scale chromatographic operations. The aim was to investigate the possibility of capturing both the technical and business perspectives

of chromatographic manufacturing processes. In order to achieve this aim, a variety of different tools and techniques are described throughout this study, each addressing a particular design consideration in large-scale chromatography. The combination of these techniques into a single consistent framework provides for a structured, fully integrated approach to designing large-scale high resolution systems. This can facilitate more informed decision making when evaluating manufacturing alternatives. The design, implementation and application of the framework was applied to a Protein A affinity capture step in the production of monoclonal antibodies based on cell culture. Protein A chromatography was specifically selected for investigation given its sizeable impact on production as whole, making its design and development key for successful processing. However, the techniques and methodologies presented herein can be applied to any packed-bed adsorption chromatography. The aspects considered in the design and development of a Protein A chromatography step form the individual objectives of the proceeding chapters outlined below.

Chapter 2 provides a background to the Protein A chromatography step highlighting the areas of concern associated with this step during manufacturing. Also described are the newer technologies developed which aim to replace the Protein A process in the future.

In Chapter 3 an empirical framework is outlined for the evaluation of the limits placed on the maximum operable velocities that can be attained through large-scale chromatographic packed-bed systems. Such a methodology might be used to reduce development times when evaluating such limits.

The methodologies developed in Chapter 3 are then further applied in Chapter 4 to investigate the limits on flow velocity and bed stability that can arise through the physicochemical interactions that are inherent during a chromatographic separation. The effects are considered during multi-cycle operation, providing for an indication of the structural integrity of the chromatographic bed over time.

In Chapter 5, a conceptual framework is presented to facilitate the evaluation of chromatography manufacturing design alternatives. The main characterises of the manufacturing problem domain are identified early in the chapter, as well as the scope of the modelling effort. A hierarchical approach to represent the key activities and considerations when designing a Protein A capture step are identified. Features and parameters that satisfy both process and business applications are discussed and the design equations used to determine the product mass and costs are described.

The implementation of the conceptual framework into a simulation based decision-support tool for modelling design and operation of a Protein A capture step is described in Chapter 6. A hypothetical case is set up to assess the process economics and productivity of varying column sizes and operational strategies. The Windows of Operation technique is used to highlight the feasible column strategies under given product and process specific conditions. The functionality of the tool is then further demonstrated through its use when investigating the process options available when trying to meet more intensive performance requirements: including changes in the process flowsheet and selection of resin.

Once column size and the limits of operation have been established, the analysis may be taken a step further in Chapter 7, where the framework is used to investigate the most favourable operating conditions for the chromatographic cycle. The case-study emphasises the interactive nature of load volume, post-load washing and clean-in-place strategy and discusses the implications when operating with different types of chromatographic resin.

The modelling framework is utilised in a commercial setting in Chapter 8. Here the model is used in business decision making when selecting between two commercially available chromatographic resins based on the in-house company constraints.

Chapter 9 then moves on to discuss the related validation and regulatory issues concerning initial capture design and operation.

Finally Chapter 10 provides a summary of the main contributions of this work and Chapter 11 presents suggestions for future work.

The attached Appendices provide more detailed theory and results. Appendix A provides the theory of chromatographic performance as used in Chapter 4. Appendix B provides the raw experimental data and model fits performed in determining the chromatographic model parameters used in Chapters 6, 7 and 8.

2 PROTEIN A AFFINITY CHROMATOGRAPHY

2.1 Introduction

Staphylococcal Protein A, or SpA, is a type I membrane protein from the bacterium *Staphylococcus aureus*. Protein A has a high specificity for the Fc region of antibodies which has lead to its widespread use as a powerful affinity ligand for several immunological and purification applications. Protein A itself is a 42kDa protein consisting of a single polypeptide chain. The chain is made up of five homologous IgG binding domains of approximately 58 residues each, followed by a C-terminal region necessary for cell wall attachment (Gagnon, 1996). The IgG binding domains are designated as E, D, A, B, C (named in order of their discovery) and share 65-90% of the amino acid sequence identity (Hjelm *et al.*, 1975; Moks *et al.*, 1986). High selectivity and good physiochemical stability has made Protein A the preferred generic ligand for affinity purification of antibodies and molecules tagged with an antibody Fc-region.

The affinity of Protein A for immunoglobulins varies with species and subclass (Burton, 1985; Huse *et al.*, 2002). Human IgGs are bound with very strong affinities, except for IgG 3 which is very weakly bound (Langone, 1982). Some classes of murine antibodies have much lower affinities; however their binding can be enhanced by using high concentrations of kosmotropic salts, glycine and /or lower temperatures (Tu *et al.*, 1988; Schuler *et al*, 1991;Gagnon, 1996). The highly specific binding between the Fc-region of an antibody and Protein A leads to the widespread use of this chromatography as the capture step in the process. Further to this, it gives a large purification factor starting directly from complex solutions such as clarified cell culture harvest media. Since its discovery in 1972 (Hjlem *et al.*, 1972), Protein A chromatography has become the workhorse of antibody purification and has received growing attention as the importance of therapeutic antibodies in the biotech industry has continued to increase.

This chapter aims to provide a background to the Protein A affinity chromatography process highlighting the current issues and design considerations

associated with such a step in manufacture. Section 2.2 describes some of the characteristics of currently commercially available Protein A resins. Section 2.3 outlines the main issues which face the designer when faced with using Protein A chromatography step. Section 2.4 gives a brief summary of some of the newer and re-visited technologies which are being considered as alternative solutions to Protein A chromatography as an initial capture operation.

2.2 Commercialisation of Protein A

There are a number of commercially available Protein A resins that vary with respect to the origins of the Protein A ligand ('natural' wild type or 'recombinant') or bead characteristics (e.g. backbone resin, particle size, of the bead and pore size distribution). Several works (Hahn *et al.*, 2003, 2005; Swinnen *et al.*, 2006) have recently compared a large number of Protein A adsorbents with respect to their transport properties and equilibrium binding capacities using polyclonal human IgG as the feed material. Some of the most common commercially available Protein A resins are listed in Table 2.1.

The two leading manufacturers of Protein A chromatographic resins are GE Healthcare Biosciences and Millipore Corp. While Millipore has adopted the controlled pore glass (CPG) matrix for their resins, GE Healthcare employs agarose with varying degrees of cross-linking as their backbone of choice. This is important because non-specific interactions can occur with the backbone leading to variation in the Protein A eluate purities with respect to host cell protein levels. CPG is quite hydrophobic as compared to agarose and thus exhibits significantly higher levels of non-specific interactions. Several wash steps have been developed for Prosep A resins to address specifically this issue (Breece *et al.*, 2005), the effects of which will be investigated later in this work.

Despite increased non-specific binding of contaminants to the backbone, the Prosep™ A resins have the advantage of better pressure-flow characteristics due to the rigid CPG backbone. Agarose based resins however, are compressible leading to lower operable flowrates. MabSelect™ was introduced by GE Healthcare in 2000/01 to address this shortcoming in their Sepharose FF™ products. A higher degree of

Table 2.1 Commercially available Protein A resins for preparative chromatography.

Resin	Vendor	Source of Protein A	Backbone	Particle diameter (μm)
nProtein A Sepharose 4FF	GE Healthcare	Natural (coupled by cyanogens bromide activation)	4% cross-linked agarose	45-165
rmp Protein A Sepharose FF	GE Healthcare	Recombinant (multi-point attachment by reductive amidation	6% cross-linked agarose	45-165
MAbselect	GE Healthcare	Recombinant (Epoxy activation)	Highly cross-linked agarose	40-130
MAbselect Xtra	GE Healthcare	Recombinant	Highly cross-linked agarose	Avg. ~ 75
ProSep vA High capacity	Millipore	Natural	Controlled pore glass (1000A pore size)	75-125
ProSep rA High Capacity	Millipore	Recombinant	Controlled pore glass (1000A pore size)	75-125
ProSep-vA Ultra	Millipore	Natural	Controlled pores glass (700A pore size)	75-125
IPA-500	Repligen Corp	Natural	Cross-linked agarose	90
Protein A Ceramic HyperD	Pall	Recombinant	Polyacrylamide gel in ceramic macrobead	50
MAbsorbent A2P	Prometic Biosciences	Synthetic	6% cross-linked agarose	100 +/-25

cross-linking was employed in this bead making it more rigid. This resin is increasingly being adopted for newer products. The Prosep™ A resin comes in two pores-sizes – 700A and 1000A. The smaller pore size was recently introduced to give a larger surface area and thus increase binding capacity. The decreased pore size may however lead to increased mass transfer limitations for larger molecules (McCue *et al.*, 2003). Typically in the industry the choice of Protein A resin is application specific and depends on the best compromise between capacity, product purity and flow characteristics (which contribute to productivity).

2.3 Current issues for industrial Protein A Chromatography

The basic protocol of Protein A chromatography is relatively straightforward: bind at neutral pH and elute at acidic pH (Farhner *et al.*, 2001). Even an un-optimised Protein A step can yield a highly purified antibody. The ease and simplicity of methods development on this mode of chromatography has been a key reason for its widespread adoption for monoclonal antibody purification from the laboratory to large-scale production processes. The practically universally applicability of Protein A chromatography and the similarity of operating conditions has made the concept of generic purification processes possible for these classes of molecules. Despite these significant advantages, the use of Protein A chromatography for process scale purification does involve several critical challenges that are described below.

The primary disadvantage of Protein A affinity chromatography is the high cost of the resin. Figure 2.1 shows a comparison of the costs for some widely used resins on a per litre basis. As can be seen from the figure, Protein A media are almost an order of magnitude more expensive as compared to other traditional chromatographic media. The high cost coupled with the large production quantities for antibodies have caused binding capacity on Protein A to become a key parameter that has a significant influence on process economics in the industrial purification processes. Given this fact, resin manufacturers are continuously introducing new versions of Protein A media aimed at providing better binding capacity. Recent examples include the introduction of MabSelect Xtra™ from GE Healthcare and the introduction of Prosep™ A media from Millipore in a smaller pore size. These

changes in resin morphology also have their limits. For example, decreasing pore size will increase surface area binding but will ultimately lead to increased mass transfer resistance (McCue *et al.*, 2003). At present, there is no clear path that resin manufacturers can follow in order to further increase resin capacity.

As has been previously discussed in Chapter 1, to reduce the costs associated with this unit operation, firms have taken recourse to extensive cycling of Protein A columns. However, this strategy makes throughout or productivity a concern (Jandera *et al.*, 1997; Fahrner *et al.*, 1999a; Iyer *et al.*, 2002; Ghose *et al.*, 2004). Since media is very expensive, rather than using a large column to process a batch of antibody in a single cycle, typical bioprocess application run a smaller column for several cycles to purify a single batch. This reduces the risk of capital loss if the column is compromised during operation and also brings the column diameter into a practical range.

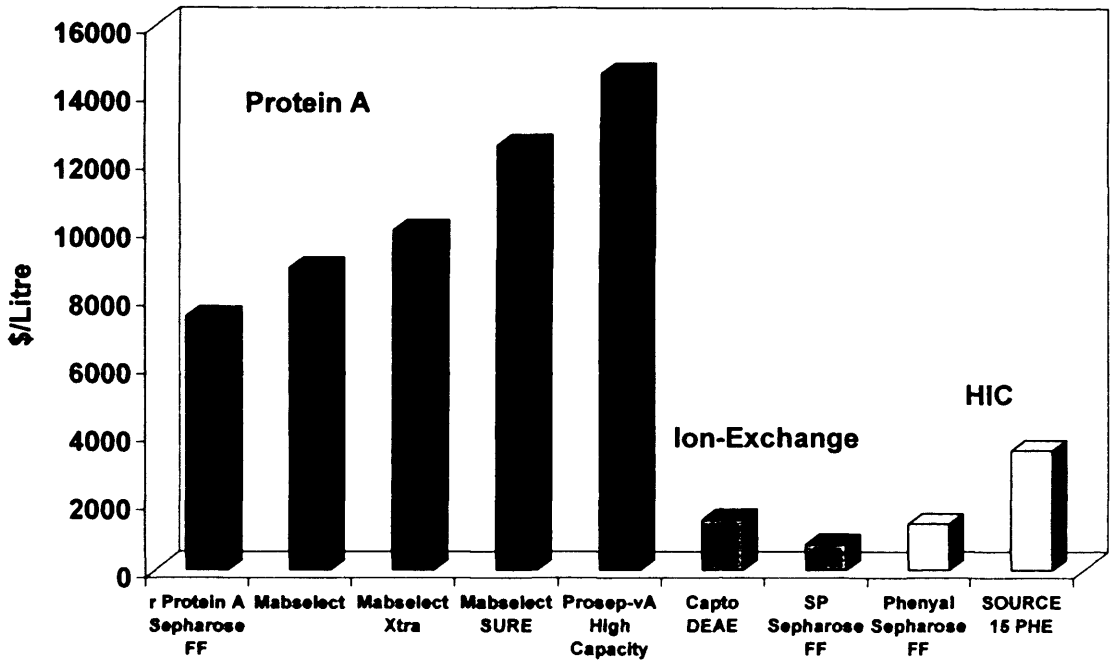

Figure 2.1 Typical costs of chromatographic resins.

Cycling increases the total purification time and thereby decreases productivity. Thus, processing time can be an important factor in Protein A step development. Fahrner *et al* (1999b) discuss the importance of considering the optimal flow velocity on Protein A and suggest that high velocities will reduce process time without significantly affecting process capacity. Unfortunately, the maximum flow velocity through the column is limited by the collapse of the resin due to stresses imposed by the fluid flowing through it. While frictional forces at the walls of the column can allow higher velocities by virtue of the so-called "wall-support" affect, these wall shear stresses decrease with increasing column diameter, and, as a result, the maximum operating linear velocity for large diameter columns can be limited. This places a constraint on the minimum processing times of column options. Processing time has been mentioned to be critical to process development for three reasons (Iyer *et al.*, 2002). Firstly, if purification is the limiting factor in a production facility, then a direct improvement in process time will increase throughput. Typically, Protein A is the first capture step and is often the rate limiting step due to the large volume loads and relatively low protein concentrations associated with the process. Secondly, the product stability in the harvested cell culture fluid can limit the allowable hold and processing times. Thirdly, cell culture fluid is a rich medium that can promote an increase in bio burden. Minimising processing time can help decrease the potential bio burden contamination. The authors even suggest using a resin with a slightly lower binding capacity but better flow characteristics to enable a decrease in the overall processing time. Fahrner *et al* (1999a) have compared the performance of several Protein A resins using both volumetric (amount of protein purified per unit time per unit volume) and production rates under different velocities for these resins.

Other works (Hinckley *et al.*, 2002, Swinnen *et al.*, 2006) have further extended this comparison by including a consideration of pressure-drop that will limit the maximum attainable velocity at a given bed diameter and column height. However, very often, productivity is not the sole consideration while selecting Protein A resins for a downstream process. Resin choice is frequently made earlier in clinical development and is dominated by product purity considerations. In addition, due to the high cost of the resin, binding capacity is one of the key parameters

affecting process economics. Hence, it is important to establish ways of maximizing productivity on a given resin while utilising efficiently binding capacity.

Protein A leaching is yet another associated problem with the use of this mode of chromatography. This is a serious concern for the drug industry because Protein A is known to cause immunogenic responses in humans and has been proven toxic in a number of clinical trials (Terman *et al.*, 1985). The downstream purification process of a typical antibody typically consist of two chromatographic polishing steps after the Protein A capture step. These are aimed at removing host cell protein contaminants and high molecular weight aggregate levels to acceptable values and also reduce leached Protein A to safe levels. In the commercial purification process for the marketed drug Enbrel™, a polishing step was specifically designed to remove leached Protein A to acceptable levels (Hubbard, 2003; Madani *et al*, 2003).

Efficient cleaning of the Protein A resin is crucial because the high cost of this resin makes extensive cycling of Protein A columns imperative. Sodium hydroxide solutions are commonly used for the cleaning and sanitisation of chromatographic systems in a cGMP manufacturing environment (Sofer *et al.*, 1989). This is due to such solutions being both an effective cleaning agent as well as being low cost. However, despite Protein A being physicochemically stable under strong acidic conditions, it cannot withstand strong alkaline conditions. It has been shown that this type of treatment causes a capacity loss of the adsorbent (Boschetti, 1994). Several works for predicting the performance of affinity resins take into account diverse operational and system parameters (Chase, 1994; Arnold *et al.*, 1985; Kang *et al.*, 1991), but little consideration is usually given to the extent to which chemical treatments have on either adsorption equilibrium or kinetics. It is clear that data such as these will be necessary for reliable modelling and scale up of these adsorption processes. To circumvent the problem of capacity loss, GE Healthcare has recently introduced a new version of Protein A resin (Mabselect SuRe™) that is expected to be resistant to alkaline conditions. To achieve this, they have employed protein engineering techniques to replace a number of asparagines (the most alkali sensitive

amino acid) residues in the B-domain of Protein A with other amino acids (Malmquist *et al.*, 2003; Johansson *et al.*, 2004).

2.4 Alternatives to Protein A

Even though Protein A chromatography is ubiquitous in monoclonal antibody purification, some of the issues described in the previous section have stimulated the search for alternative stationary phases or techniques that could give similar performance.

To increase throughput compared to traditional packed bed mode of operation, technologies such as simulated moving-bed chromatography (which increase throughput by moving into a continuous operation from a batch operation) has been evaluated for the Protein A affinity step (Gottschlich *et al.*, 1997; Thommes *et al.*, 2003). Additionally, expanded bed chromatography (which enables elimination of the cell harvest step and may also allow high flowrates during column loading) has been investigated with Protein A media (Farhner *et al.*, 1999c; Blank et *al.*, 2001). However, both these technologies have met limited success and are not currently employed at large-scale.

Numerous attempts have also been made to purify antibodies in three chromatographic steps or less without use of a Protein A step (Follman *et al.*, 2004; Ferreira, 2007) but such non-affinity purification schemes require significantly higher methods development time and resources, and are potentially less robust (Van Alstine *et al.*, 2006). More recently, efforts have focused on mimicking the binding phenomena involved in the antibody-Protein A interaction and some of these techniques are discussed below.

2.4.1 Aqueous two phase systems (ATPS)

The unit operation of ATPS has been studied extensively, especially in the recovery of industrial enzymes (Sinha *et al.*, 2000). However, despite early interest it has not had a successful adoption in bioprocesses (Rito-Palomares, 2004). Interest in its use for Mab recovery has been no exception, and been limited to few research

studies (Andrews *et al.*, 1996). However, this unit operation has certain advantages of scalability, the ability for continuous operation, and high capacity, some of which align quite well with the process needs of low cost and high throughput for antibodies. There have been efforts integrating ATPS with other unit operations, primarily affinity-separation, and utilizing temperature or solute-sensitive polymers. For example, Kamihira *et al.* (2000) have added the polymer carrier Eudragit, whose pH sensitivity to phase stability can be utilized to facilitate recovery of the extracted protein. Nevertheless, difficulties remain regarding use of this as a platform step due to issues related to complex interactions of the multiple components involved (as the poor understanding thereof) as well as potential sensitivities to feed stream variability.

2.4.2 Crystallisation

Another approach used in low cost industrial enzymes is crystallization, although its use as a unit operation for therapeutic protein purification has been limited (Lee *et al.*, 2000; Schmidt *et al.*, 2005), primarily due to the difficulty of crystallization from impure process streams and scalability. Crystallization in protein formulation can be more readily envisioned (Merkle, 2002), and though still limited in its application, has provided the impetus for development of large-scale crystallization processes. For monoclonal antibodies, crystallization poses a greater challenge even at small scales, due to their large size, glycosylation, and a high degree of segmental flexibility. Nevertheless, this technology has had a new revival at the process scale (Klyushnichenko, 2003) with the consideration of antibody crystals as a novel delivery vehicle (Yang *et al.*, 2003; Pechenov *et al.*, 2004).

2.4.3 Hydrophobic Charge Induction Chromatography

Another mode of chromatography that has been developed for immunoglobulin binding is hydrophobic charge induction chromatography (HCIC) (Burton *et al.*, 1998). This technique is based on the pH dependent behaviour of heterocyclic ligands that ionize at low pHs. While adsorption on this mode of chromatography occurs via hydrophobic interactions, desorption is facilitated by lowering the pH to produce charge repulsion between the ionisable ligand and the

bound protein (Blew *et al.*, 1987; Ngo, 1992). The origin of this mode of chromatography can be traced to the earlier development of thiophilic ligands (T-gels) (Boschetti *et al.*, 2000) and thiodipyridyl Avid AL gels (Boschetti, 2002). Lately, a number of papers that have described the use of HCIC resins for the capture and purification of immunoglobulins have reported purities ranging from 70% to >99% by SDS–PAGE analysis (Guerriar *et al.*, 2000; Schwartz *et al.*, 2001). The success of such technology has culminated in the commercialisation of such ligands most notably in the form of MEP Hypercel® from Pall. The ability of this mode of chromatography to bind both non-IgG model proteins and monoclonal antibodies has been shown recently (Ghose *et al.*, 2006). While the authors have shown that HCIC is not as selective as Protein A chromatography, they note that the unique combination of hydrophobic binding and charge induced repulsion confers this resin with properties that make it useful for protein purification in general.

2.4.4 Bio-mimetic synthetic ligands

In the last five years, several cheaper small molecule ligands that are reported to mimic the selectivity of Protein A chromatography have been introduced (Roque *et al.*, 2004; Vandeyvyver *et al.*, 2004, Newcombe *et al.*, 2005). Using techniques such as molecular modelling, protein engineering and phage display, several small protein domains have been constructed based on the IgG binding domain of Protein A (Sengupta *et al.*, 1999; Sinha *et al.*, 1999; Eklund *et al.*, 2002). Fassina *et al.* (1996, 1998, 2001) have identified a Protein A mimetic peptide (PAM) through synthesis and screening of synthetic multimeric peptide libraries composed of randomised synthetic molecules with a tetradendate lysine core.

Another approach has employed a combination of molecular modelling and synthetic chemistry to design small molecule ligands that can mimic the Fc-Protein A interaction. This effort has its origins in the use of dyes as bio mimetic ligands for protein binding (Lowe *et al.*, 1992; Curling, 2004). By X-ray crystallography, the dipeptide motif Phe-132: Tyr-133 has been shown to play an important role in the interaction of Protein A with the Fc portion of IgGs (Diesenhofer, 1981). Using 1,3,5-trichloro-triazine as the scaffold, Li *et al.* (1998) have designed and synthesized several molecules to mimic the Phe-132: Tyr-133 dipeptide. Anilino and tryramino

substitutions were found to mimic the side chains of Phe-132 and Tyr-133. In addition, further side chain substitutions were found to be useful. A2-aminoethylamino group was substituted at the third position of the triazine framework to act both as a spacer and to enable subsequent immobilization. The lead compound (named Artificial-protein-A or *ApA*) was shown to have an affinity constant of 105–106M−1. Based on this lead compound, a subsequent library of 88 adsorbents was generated on an agarose solid phase using combinatorial synthesis (Teng *et al.*, 1999). The lead immobilized ligand was further characterized and shown to bind IgG from human plasma and give a yield of 60–70% and approximately 90–99% purity by SDS–PAGE analysis (Teng *et al.*, 2000).

This work has led to the commercialization of two synthetic, non-peptidyl Protein A mimetic ligands—MAbsorbent™ A1P and A2P from ProMetic BioSciences (Cambridge, UK). These ligands are immobilized on a new, rigid, 6% cross-linked agarose matrix which has a narrow particle size distribution (80–130 μm) and can tolerate high flow velocities up to 700 cm/h (Baines *et al.*, 2001). Therefore, they are suitable for preparative chromatography and can potentially offer a promising cheap, easily sanitisable alternative for capture of monoclonal antibodies. In addition, unlike Protein A these ligands do not distinguish between polyclonal IgG subclasses and have been proposed as a new method for total IgG isolation from normal source and hyper-immune plasmas (Curling, 2001). Several conference presentations from the vendor company have discussed the application of these mimetic adsorbents to the purification of real immunoglobulin feed streams (Russell *et al.*, 1999; Duell *et al.*, 2002). They obtained comparable purity to Protein purification by sodium dodecylsulfate-polyelectrolye agarose gel electrophoresis (SDS–PAGE) analysis (90% purity). Recently, Newcombe *et al.* (2005) have reported optimized affinity purification of polyclonal antibodies from hyper immunized ovine serum using MAbsorbentA2P™. The purity of the eluted IgG was approximately 85% by SDS–PAGE and densitometric analysis. However, no comprehensive understanding of the selectivity of these bio mimetic resins exists so far. Rigorous comparisons of their selectivity with Protein A chromatography have not been carried out. As a result, it is unknown if the generic operating conditions that allow the widespread and rapid application of Protein A chromatography extend

to these resins or not. In addition, the choice between the two bio mimetic resins has been purely empirical and no real understanding exists about the selectivity difference that might exist due to the structural differences of these two ligands. A better understanding of binding on these resins will permit one to exploit them better for process-scale purification of antibodies.

Future challenges to the current paradigm in MAb purification will be provided by the scale of production for many of this class of product. Successful increases in cell culture titre are anticipated to continue for the next several years, making the downstream process rate limiting. A large part of the limitations stem from the perceived limitations of the Protein A affinity step; given its position in the DSP train (Shukla *et al.*, 2007). Generally, chromatographic separations suffer from the inability to increase large scale column diameters to beyond 2 metres in diameter without encountering issues of flow distribution and packing. Chromatographic operations thus become limited in terms of the throughout they can provide without necessitating extensive cycling to process a single cell culture batch. Further in the future, non-chromatographic purification techniques such as selective precipitation or liquid-liquid separations employing highly selective ligands are likely to emerge (Shukla *et al.*, 2007).

As has been described there are already a number of commercially available resins that are being promoted as alternatives to Protein A chromatography, however no clear understanding of their efficacy exists (Ghose *et al.*, 2006). Most of the work so far on these stationary phases has been from the resin manufacturers who have predominantly focused on the ability of these stationary phases to bind antibodies, without thoroughly investigating their specificity. All these alternative resins are significantly lower in costs, have fewer concerns with ligand leaching and can be easily sanitised with sodium hydroxide. Accordingly, they have generated significant interest in the downstream processing field. A clear understanding of how these resins work and what governs their selectivity is essential before wholesale use in production processes. Lack of clear understanding of binding and selectivity on these resins will limit their future use in the industry as they typically require high process development time with no assured results.

2.5 Summary

These alternatives to Protein A are likely to improve in terms of selectivity as their mechanisms will be better understood over time. For now until these concerns are met and despite the relative abundance of alternatives, Protein A chromatography remains the gold standard for antibody purification (Low *et al.*, 2007). As such, suitable platforms must continue to be made available to improve and enhance the efficiency of this initial capture process. The construction of a structured decision tool which aims to provide such a platform for more efficient process development is the focus of this thesis. The following chapter will begin the development of this tool by describing a framework for the evaluation of the maximum mobile phase velocity that can be passed through a given chromatographic step at manufacturing scale. Assessment of the limits of operation will aid the designer when considering the required productivity or throughput of the chromatographic step.

3 A FRAMEWORK FOR THE CHARACTERISATION AND EVALUATION OF FLOW HYDRODYNAMICS IN LARGE SCALE PACKED BED CHROMATOGRAPHY

3.1 Introduction

As indicated in previous chapters, processing time is critical when considering initial capture chromatography within a biopharmaceutical manufacturing process. Chromatographic process time, however, is restricted for a given process as the maximum operating linear velocity for chromatography columns is limited at production scale. The primary objective of this chapter was to generate an empirical model to predict this maximum operating velocity, the critical velocity, of compressible packed beds at varying scales and operating conditions. The aim was also to limit the range of scouting experiments necessary for application of the model, through the utilisation of system-specific variables expressing mobile phase viscosity and resin rigidity.

The remainder of this chapter is divided as follows: Section 3.2 provides a description of current scale-up techniques and of the necessity to account for flow hydrodynamics in production scale columns. Section 3.3 details the impact of various design parameters on the maximum flow velocity at which columns can be operated. This is followed by a description of the materials and methods used in this study in Section 3.4. Section 3.5 describes the findings of the experimental procedures. Section 3.6 provides a description of how the experimental data-set can be correlated into an empirically based model through the description of a modelling framework. The final section summarises the salient properties of the framework developed.

3.2 Considerations in the Scale-Up of chromatography processes

Chromatography processes are usually developed at bench scale with columns of diameters (D) less than 0.03m. Current chromatographic scale-up techniques typically involve increasing column diameter to accommodate the increase in process volume, whilst maintaining the bed height and superficial fluid velocity (Stickel *et al.*, 2001). A key-issue in the scale-up for columns packed with compressible

materials is that the maximum flow rate through the column is limited by the collapse of the resin due to compressive stresses imposed by the fluid flowing through it. This does not occur with beds packed with incompressible, rigid resins for which the bed volume and permeability remain constant giving rise to linear pressure-flow profiles in which increasing pressure drop is a result of increasing fluid velocity only. However, many of the chromatography resins available today exhibit compression to varying degrees, particularly the ubiquitous agarose-based resins. Beds packed with such materials exhibit exponential pressure-flow curves as opposed to the linear-profiles of their incompressible counterparts. The superficial fluid velocity at which the pressure-flow curves start to rise without limit is defined as the critical velocity (u_{crit}) (Stickel *et al.*, 2001) and places a practical boundary upon the operating flow rates which can be used for any chromatographic system utilising compressible media.

While frictional forces at the walls of the column provide a degree of bed support and can allow higher flow rates, the impact of shear wall stresses decreases with increasing column diameter (Keener *et al.*, 2002). A direct consequence of this "wall support" effect is that the superficial mobile phase velocities developed and used during bench-scale optimization may not necessarily be suitable for large scale operation. Further to this, temperature, viscosity, pH and ionic strength of the mobile phase can also have a dramatic effect on the structural support of compressible resins (Stickel *et al.*, 2001), as well as the packing techniques used (e.g. sedimentation time etc.).

Scale-up techniques therefore need to account not only for the effect of increasing column diameter but also other variables which will affect the critical velocity, such as bed height, the hydrodynamic properties of the mobile phase and the type of chromatographic resins used. Several studies have attempted to model pressure drop in compressible packed beds by accounting for the varying contribution of friction in conjunction with force balances for both mechanical and flow-induced compression (Keener *et al.*, 2004a; Keener *et al.*, 2004b; Keener *et al.*, 2002; Yuan *et al.*, 1999; Ostergren *et al.*, 1998; Soriano *et al.*, 1997; Colby *et al.*, 1996). However the complexity of these models limits their use in practical

applications. Other models (Mohammed *et al.*, 1992; Joustra *et al.*, 1967) provide quantitative laboratory-scale predictions of the pressure drop behaviour of compressible resins with scale but do not account for the decrease in bed height that is associated with flow induced compression and have not been verified at large scale. Stickel *et al.* (2001) propose a model which was evaluated for all scales and provides a quantitative prediction of the critical velocity (u_{crit}). However, due to the lack of variable terms expressing quantities such as mobile phase viscosity and resin rigidity, these correlations (Stickel *et al.*, 2001) use highly system-specific empirical constants and hence require significant experimental effort to be expended before they can be applied.

3.3 Effects of chromatographic system variables on critical velocity

Previous studies have shown there to be an inverse relationship between the critical velocity of a chromatographic system and the diameter of the packed bed (Stickel *et al.*, 2001; Mohammed *et al.*, 1992). The critical velocity of a system will decrease with increasing column diameter with the effect diminishing at column diameters greater than 0.1m. Similarly, the critical velocity of a chromatographic system is inversely proportional to the height of the packed bed, with lower superficial velocities possible with increasing bed height (Mohammed *et al.*, 1992). This is because longer bed lengths put more weight on resin particles at the bottom of the column. Coupled with the compression force arising from the fluid flow, the particles at the bottom of the column deform to a greater extent and thus the pressure drop increases. Therefore at any particular fluid flow rate, there is a greater compressive effect and higher column pressure drop, resulting in lower critical velocities. As with the wall support phenomenon, this effect diminishes with increasing bed heights.

Previous work, however, does not provide significant insight into the effect that mobile phase viscosity will have upon the critical velocity of a packed bed. Flow- induced compression of packed beds is primarily caused by the fluid drag forces exerted upon the beads of the resin by movement of the mobile phase. An increase in fluid viscosity will cause an increase in the drag forces, f_d, experienced by the chromatographic resins as given by Stokes Law (Bird *et al.*, 1960) where,

$$f_d = 6\,\pi\, r\, \mu\, u \qquad \textbf{(3.1)}$$

where, r, is the particle radius, μ, is the mobile phase viscosity, u, is the mobile phase/ particle velocity. The drag force exerted on the resin particles at the critical velocity can therefore be described by,

$$f_{d\,crit} = 6\,\pi\, r_{crit}\, u_{crit}\, \mu \qquad \textbf{(3.2).}$$

It can be assumed that the magnitude of the drag force exerted on the resin in order to cause critical compression, and the dimension of the resin particles when this point is reached, are both constant if bed height, column diameter and resin type are maintained. Under these conditions, a relationship between the critical velocity (u_{crit}) and the mobile phase viscosity can be derived from a rearrangement of Stokes Law.

The result of this rearrangement is shown in Equation (3.3):

$$u_{crit} = \frac{k}{\mu} \qquad \textbf{(3.3)}$$

where $k = \dfrac{f_{d\,crit}}{6\pi\, r_{crit}}$

In Equation (3.3), k is a lumped constant containing values expressing particle radius and the drag force required to deform the bed to such an extent equivalent to that realised at the critical velocity. From this it can be predicted that an inverse relationship will exist between the critical velocity of a chromatographic system and the viscosity of the mobile phase.

As is the case with mobile phase viscosity, a limited amount of work has been carried out in order to determine the effect of resin rigidity upon the critical velocity of a chromatographic system (Keener *et al.*, 2004 a; Keener *et al.*, 2004 b; Keener *et al.*, 2002; Stickel *et al.*, 2001; Ostergren *et al.*, 1998). Higher resin rigidity will lead to higher critical velocities, however, quantitative relationships between u_{crit} and resin rigidity have yet to be determined. The main cause of this is the difficulty in generating a suitable measure of resin rigidity.

In this study, experiments were carried out in order to determine the compression behaviour and critical velocity (u_{crit}) of a variety of different chromatographic systems. All were agarose-based resins (Sepharose 4FF, Sepharose 6FF, Sepharose CL-6B and 10% ABT Agarose-CL); with mobile phases exhibiting a range of viscosities typical of those encountered in industrial preparative chromatography and a range of different bed heights and column diameters. The resins, Sepharose 4FF and 6FF, were chosen to reflect for this study primarily because these two media bracket the range of rigidities exhibited by the majority of agarose based media commonly used.

The experiments performed sought to enable a correlation to be developed linking the critical velocity of a chromatographic system to the gravity settled bed height (L_0), column diameter (D), mobile phase viscosity (μ) and the compressibility of the resin used.

3.4 Materials and Methods

3.4.1 Experimental Equipment

The system for the experiments is shown in Figure 3.1. Three bench-scale columns with adjustable column lengths and inner diameters of 0.016, 0.026 and 0.05m (models XK16, XK26, XK50, GE Healthcare, Uppsala, Sweden) were used, in addition to one pilot scale column (BPG-100/500,GE Healthcare, Uppsala, Sweden) with an internal column diameter of 0.1m and adjustable length.

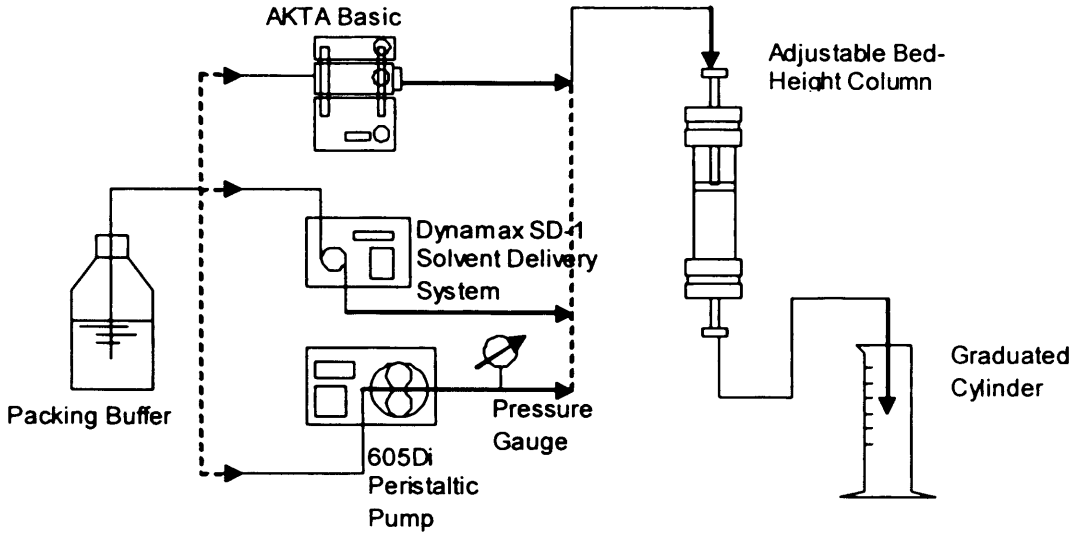

Figure 3.1 Experimental set-up used.

Due to the differences in the volumetric flow rates required in order to reach critical velocity for the different combinations of columns and resins tested, three different feed delivery and pressure measurement systems were used. The AKTA Basic P-900 (GE Healthcare, Uppsala, Sweden) was used in experiments involving the XK16 and the XK26 columns whilst for the XK50, a Dynamax Model SD-1 Solvent Delivery System (Rainin Instrument Co. Inc., Oakland, CA, US) was utilised. For the BPG-100 pilot scale column, a 605Di Peristaltic Pump (Watson Marlow, Wilmington, MA, US) was used for feed delivery.

Column pressure drops (ΔP) were measured using either internal pressure measurement devices present in the feed delivery systems (in the case of the AKTA basic and Dynamax Model SD-1) or needle pressure gauges inserted into the column inlet line (in the case of the pilot-scale system). The volumetric flow rate through the columns during all of the experiments was measured manually by collecting the column output in a graduated cylinder for a timed period.

In all cases, in order to reduce the extra-column pressure drop, column inlets were connected directly to injection valves whilst column outlet lines were fed directly into a waste collecting container, as opposed to a fraction collector.

3.4.2 Chromatography Media

Sepharose 4 Fast Flow (4FF), Sepharose 6 Fast Flow (6FF), Sepharose CL-6B-B (GE Healthcare, Uppsala, Sweden) and 10% ABT Agarose-CL (Agarose Bead Technologies, XC Corporation, Tampa, FL, US) were used in this study. All of the chromatographic media used are agarose based with an average particle size of 90μm, with actual bead diameters ranging from 46-106μm. The difference between the four resins is in the agarose content of the particles of each resin and also the degree of structural cross-linking present.

Sepharose 4FF and Sepharose 6FF are both made of spherical, highly crossed-linked agarose whilst Sepharose CL-6B and 10% ABT Agarose-CL are made up of simply cross-linked agarose beads. The Sepharose CL-6B also contains a functional ligand attached to the agarose base. The higher level of cross-linking present in the Fast Flow (FF) resins makes them more rigid than the simply cross-linked (CL) resins. Along with the degree of cross-linking, the rigidity of the different resins used in this study is also determined by the percentage of agarose present in the resin particles. 6FF and CL-6B particles are both made up of 6% agarose whilst 4FF particles contain 4% agarose and 10% ABT Agarose-CL particles contain 10% agarose. Higher agarose content leads to increased levels of rigidity and decreased resin compressibility. Thus of the four resins used in this study the least compressible is Sepharose 6FF, followed by Sepharose 4FF, then 10% ABT Agarose-CL with the most compressible resin being Sepharose CL-6B.

3.4.3 Experimental Procedure

To simulate the varying physical properties of feed streams found in industry, a range of different packing buffers were used. Feed streams of different viscosities were replicated by supplementing phosphate buffer (PBS, 20mM sodium phosphate + 100mM sodium chloride) with appropriate amounts (60%, 50%, 20%, 10%, 5%, 2.5%, 1.25%, 0% v/v) of glycerol. A 60% v/v glycerol solution was chosen as the top end of the viscosity range, as PBS blended with 60% glycerol provides a solution with a viscosity that is equivalent to approximately 0.11kg/ms. This corresponds to an IgG protein concentration of approximately 65g/L (Shire *et al.*, 2004; Hand, 1934). Viscous fingering is known to occur at protein concentrations upward of

70g/L (Hagel *et al.*, 1997) and so the viscosity range tested was deemed to be sufficient to cover possible operating extremes.

Absolute viscosity measurements were carried out with the use of a DV +II programmable viscometer (Brookfield, MA, US) with a CP-40 conical cone spindle. Samples of packing buffer (0.5mL) were taken for measurement of shear stress at a series of shear rates (1125, 900, 750 and $563s^{-1}$). Viscosity values were then calculated from the resulting plots of shear stress against shear rate.

To begin packing, a measured volume of slurry was poured into the column and allowed to gravity settle overnight. The top plate of the column was lowered into the supernatant and flow was started. For experiments involving XK columns, the packing buffers were initially pumped through the columns at 0.5mL/min for 30mins in order to flow pack the resin. The feed flow rate was then increased to 1mL/min for 15mins in order to equilibrate the packing. With the BPG-100 column, the feed solution was initially pumped through the column at 340mL/min for 30mins. Following this, the top adaptor of the column was lowered to the top of the bed, and measurements of the initial pressure drop and bed height were taken.

The flow rate of packing buffer through the column was gradually increased until a 35kPa increase in the pressure drop (ΔP) was seen, at which point measurements of bed height and fluid flow rate were taken. This procedure was repeated until the pressure measured did not settle on a particular value, but instead continued to increase without any further increase in delivered flow rate. It was deemed at this point that the critical velocity for the column had been reached. To ensure an accurate measurement of the critical velocity; when the critical point was approached, the volumetric flowrate out of the column was measured. The critical velocity was deemed to be the point at which any further increase in pump speed yielded a negligible change in the flowrate measured from the outlet of the column. Therefore the critical point was taken to be the point at which the pressure drop through the column started to increase to infinity.

The experiments described previously, were repeated using feeds of varying viscosities for all resins, in columns with different combinations of bed height and diameter. A single packed column was tested for the entire viscosity series. Columns were washed out with a 20% (v/v) ethanol solution prior to being allowed to decompress between changes in the mobile phase. In all cases the bed height returned to its gravity settled bed height (L_0) after being allowed to decompress for several hours, which demonstrated that damage to resin beads and loss of mechanical integrity had been avoided.

As a further test, to ensure that no long term effects of continual compression studies had resulted, the u_{crit} of the column run with a mobile phase of PBS (0% v/v Glycerol) was compared at the start and end of each series of experiments. In all cases the u_{crit} values for the reference case buffer were comparable (±5%).

3.5 Results and Discussion

3.5.1 Effect of Column Diameter and Bed Height

Figure 3.2 (a) shows the expected shift in pressure –flow curves to lower flow rates for increasing column diameters. This increase in cross column pressure drop at corresponding fluid flow rates, and general decrease in critical velocity is due to the effect of diminishing wall support at larger column diameters. This figure illustrates the significant and well-documented effect that wall support has on resistance to bed compression (Keener *et al.*, 2002; Stickel *et al.*, 2001; Soriano *et al.*, 1997; Hagel *et al.*, 1997). The effect bed height has on column pressure drop and critical velocity (Mohammed *et al.*, 1992) was also observed, as shown in Figure 3.2 (b). Increases in bed height resulted in higher column pressure drops at corresponding fluid velocities and also a general decrease in the critical velocity of the chromatography systems tested. This effect was seen across all of the resins tested.

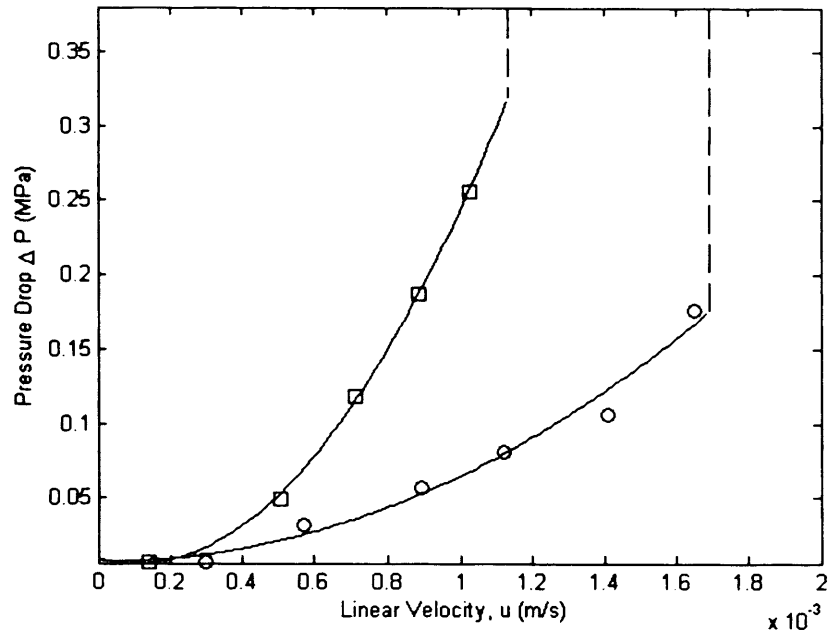

(a)

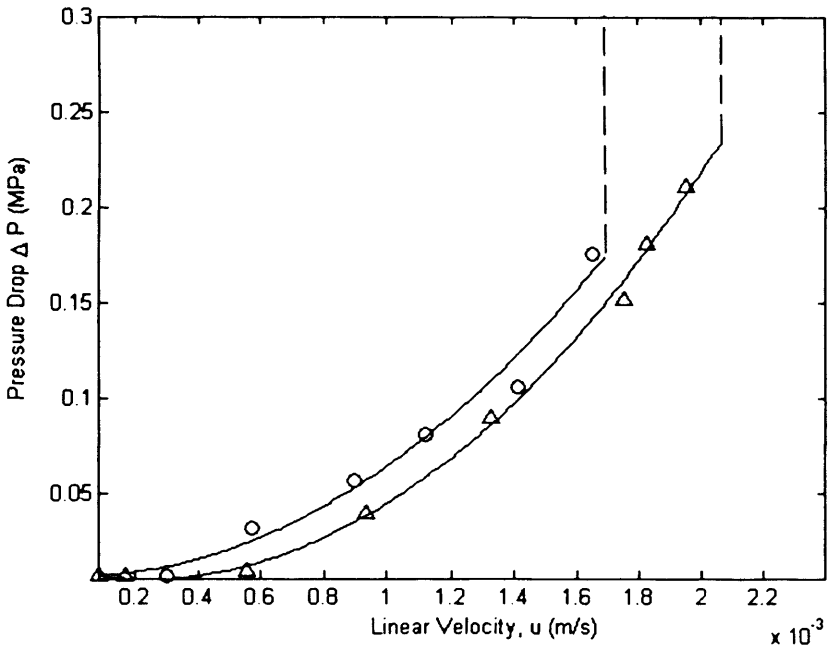

(b)

Figure 3.2 Pressure-flow profiles of bed packed at different bed heights and column diameters. Packing buffer is PBS at 22°C. **(a)** Sepharose 4FF packed to a gravity settled bed height of 0.13m in an (○) XK16; (□) XK50. **(b)** Sepharose 4FF packed into an XK16 at a gravity settled bed height of (○) 0.13m; (Δ) 0.09m.

3.5.2 Effect of Resin Rigidity

Figure 3.3 shows pressure-flow profiles for beds of the same geometry packed with the four different resins used in this study. For ease of comparison the plots are normalised for different bed lengths by multiplying the flow velocity by the gravity settled bed height. The non-linear profiles shown are characteristic of compressible resins (Hagel *et al.*, 1997). As expected by virtue of the higher level of cross-linking the Fast-Flow resins (4FF & 6FF) are much less compressible than the two cross-linked resins (CL-6B & 10% ABT Agarose-CL). This is shown by the relative critical velocities of the four resins, with lower critical velocities implying higher compressibility (less rigidity). The impact of cross-linking upon the rigidity of a resin can be observed by comparing the critical velocity of Sepharose 6FF to that of Sepharose CL-6B, since these have the same agarose content but different extent of cross-linking. This comparison shows over a ten-fold decrease in critical velocity, with a reduction in cross-linking. The percentage of agarose present in the resin particles plays a key role in determining the rigidity of each resin.

3.5.3 Quantification of Resin Rigidity

The rigidity of the resins was quantified in order to allow more effective interpretation of the data generated from this study. The rigidity of a resin will depend on a number of factors including the material from which the resin is made, the size and microscopic structure of the resin particles and hence the porosity of the beads. These factors all contribute to determining the drag forces required to compress a packed bed and also its critical velocity. In order to quantify the resin rigidity and to simplify the study, a measurement was developed to reflect the rigidity of a resin, which incorporated all of these different factors into a single quantity. This quantity was termed $u_{10\%}$, and was defined as the linear fluid velocity required to compress a packed bed, with initial dimensions of L_0=0.13m and D=1.6 x 10^{-2}m, by 10% using a mobile phase of phosphate buffer (PBS, 20mM sodium phosphate + 100mM sodium chloride).The rationale being that the $u_{10\%}$ will increase with increasing resin rigidity. The data generated from the experiments performed was used to plot superficial fluid velocity against reduction in bed height for all of the resins used in this study. Linear relationships, shown in Figure 3.4, were obtained

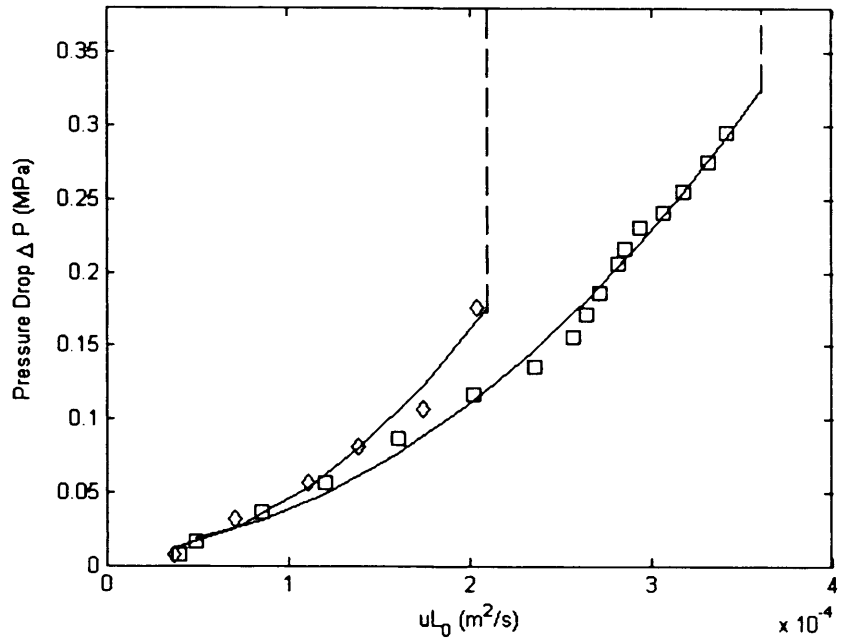

(a)

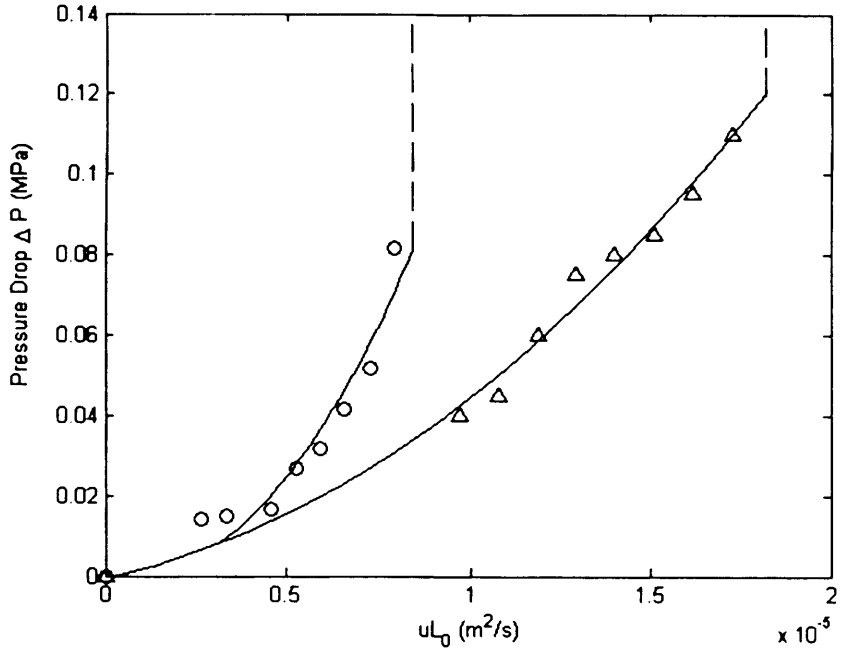

(b)

Figure 3.3 Pressure-flow profiles of beds packed with different compressible media at a gravity settled bed height of approximately 0.13m in an XK16. Packing buffer is PBS at 22°C. Superficial fluid velocities have been normalised for differences in bed height. **(a)** Fast flow resins: (◊) 4FF; (□) 6FF. **(b)** Cross-linked resins: (Δ) 6CL; (○) 10CL.

for all resins. If flowrate is assumed to reflect the stress placed upon the bed, and change in bed height is assumed to reflect the strain exhibited by the bed in response then the linear relationships obtained imply that the packed beds showed elastic behaviour during compression. These plots were then used to determine the $u_{10\%}$ values of Sepharose 4FF, 6FF, 6CL and 10CL. Table 1 summarises the $u_{10\%}$ values obtained for the resins used in this study.

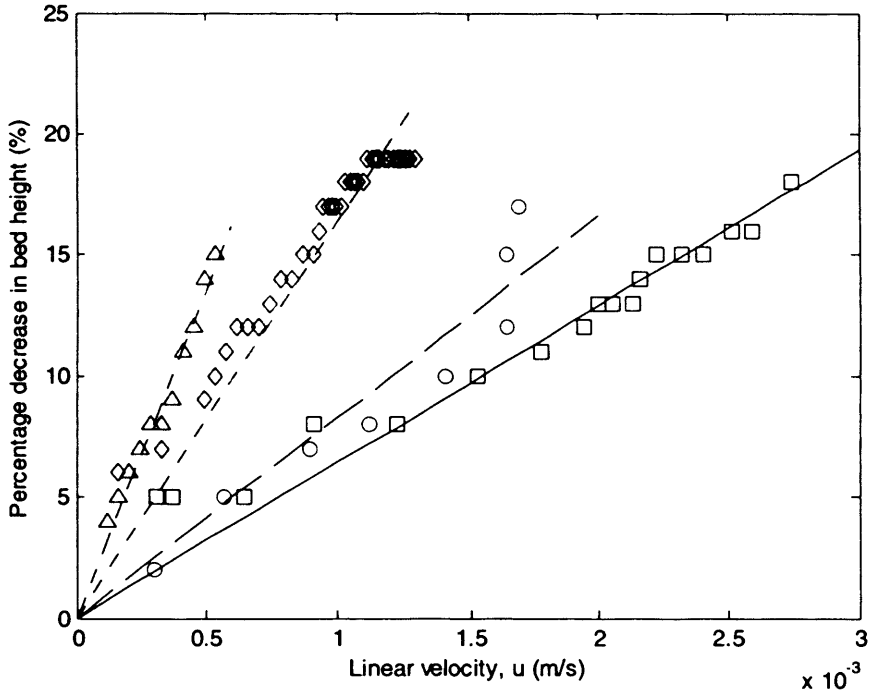

Figure 3.4 Experimental and predicted trends showing reduction in bed height with increasing linear velocity when packing with PBS at 22^{0}C for resins packed in an column of D = 1.6cm and L_0 = 13cm (approx). Resins tested: Sepharose 6FF (Δ); Sepharose 4FF (◊); Sepharose CL-6B (○); and Sepharose 10CL (□).

Table 3.1 Rigidity of resins used in the study, expressed in terms of $u_{10\%}$, determined by linear regression of data obtained from bed compression experiments.

Resin	Supplier	Resin Rigidity, $u_{10\%}$ (m/s) x 10^{-4}
Sepharose 6 Fast Flow (6FF)	GE Healthcare (Uppsala, Sweden)	15.70
Sepharose 4 Fast Flow (4FF)	GE Healthcare (Uppsala, Sweden)	12.45
10% ABT Agarose-CL (10CL)	ABT (Tampa, FL, US)	3.72
Sepharose 6 Cross Linked (6CL)	GE Healthcare (Uppsala, Sweden)	7.50

3.5.4 Bed Compression

At each incremental increase in flow rate, the fluid drag on packed bed particles increases, causing bed compression (λ) and a decrease in the packed bed height. Bed compression is defined as:

$$\lambda = \frac{L_0 - L}{L_0} \qquad (3.4)$$

The critical level of bed compression (λ_{crit}) is defined as the level of bed compression achieved at the critical velocity. With reference to Table 3.2, λ_{crit} did not vary appreciably with aspect ratio. Neither did it vary across all four of the resins used in this study, with values consistently falling between 0.16 and 0.19. The average λ_{crit} was found to be 0.17 with a relative standard deviation of 5%.

3.5.5 Effects of Mobile Phase Viscosity

The effect of mobile phase viscosity in the range 0.001kg/ms < μ< 0.011kg/ms was examined for the four resins. The results presented in Figure 3.5, show pressure-flow profiles as a function of mobile phase viscosity for Sepharose 6FF and Sepharose 4FF. As expected increases in mobile phase viscosity caused a shift in the pressure-flow profiles to lower flow rates as compression of the resin is facilitated by an increase in the viscous stresses created by the fluid flow through the column.

Table 3.2. Critical compression of packed beds at different column aspect ratios. The λ_{crit} values shown are averages of the values found for the entire range of packing buffer viscosities which were tested at the column dimensions specified. The relative standard deviation (RSD) is that which was found across the viscosity range

Resin	Column Diameter (m) x 10^{-2}	Gravity Settled Bed Height (m)	Critical Compression (λ_{crit})	RSD
Sepharose 6FF	1.6	0.12	0.16	7%
	2.6	0.12	0.17	7%
	10	0.09	0.18	6%
Sepharose 4FF	1.6	0.12	0.17	6%
	2.6	0.12	0.17	9%
	5.0	0.12	0.18	3%
Sepharose 10CL	1.6	0.12	0.16	2%
	1.6	0.05	0.16	4%
	2.6	0.12	0.17	6%
Sepharose CL-6B	1.6	0.12	0.17	10%
	2.6	0.12	0.19	7%
	10	0.08	0.16	6%

Figure 3.6 illustrates the relationship between feed viscosity and the resultant critical velocity for varying column diameters and resin types. Again for ease of comparison, these plots have been normalised for different bed lengths by multiplying the critical velocity (u_{crit}) by the gravity settled bed height (L_0). As predicted, an inverse relationship exists between the critical velocity of a chromatographic system and the mobile phase viscosity. Figure 3.6 also illustrates the effect of diminishing wall support, with a shift to lower critical velocities with increasing column diameter. Interestingly, an approximately 92% drop in the normalised critical velocity ($u_{crit}L_0$) was observed across the viscosity range tested regardless of the column diameter or the resin rigidity.

Comparison of Figure 3.6(a) and (b), shows how the wall support phenomenon is affected by resin rigidity. It can be seen that the negative shift in critical velocity with increasing column diameter is amplified with increased resin rigidity. The impact of wall support phenomenon is correlated to the resin rigidity. This implies that the scale-up issues associated with the loss of wall support when increasing column diameter, are reduced when using more compressible resins.

3.6 Formulation of empirical correlation for the prediction of the critical velocity

It has been found (Stickel *et al.*, 2001) that u_{crit} can be correlated to the bed height and diameter in a straight forward manner, giving rise to the following empirical relationship:

$$u_{crit} L_0 = m\left(\frac{L_0}{D}\right) + b \qquad \textbf{(3.5)}$$

where m and b are empirical constants determined by linear regression, L_0 is the gravity settled bed height and D is the column diameter. Plots of u_{crit} L_0 vs. L_0/D are useful to compare the compressibility of different resins. It has been reported (Stickel *et al.*, 2001) that b is the value of $u_{cri}L_0$ for an infinite diameter column and thus provides a numerical indication of the compressibility of a medium at given

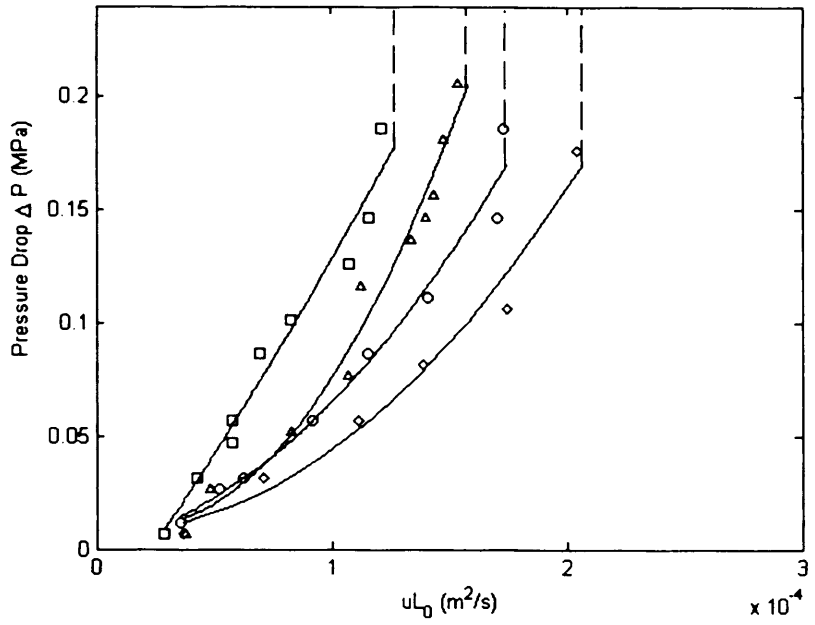

(a)

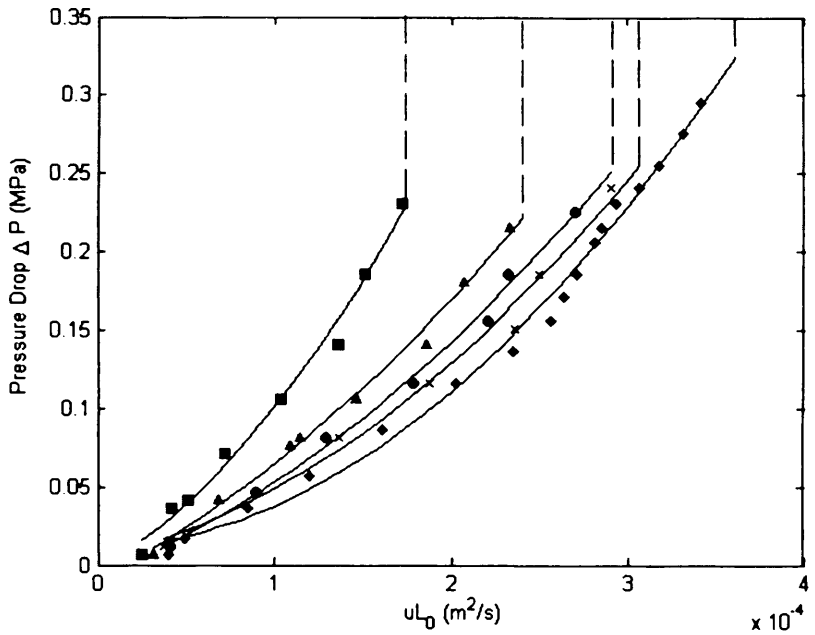

(b)

Figure 3.5 Pressure-flow profiles for different resins over a range of mobile phase viscosities. Bed dimensions were D=0.016m, L_0~0.13m. Superficial fluid velocities have been normalized for differences in bed height. **(a)** Sepharose 4FF (□) 20% Glycerol v/v; (Δ)10% Glycerol v/v; (○) 5% Glycerol v/v, (◊) PBS;. **(b)** Sepharose 6FF ; (■) 20% Glycerol v/v; (▲) 10% Glycerol v/v; (●) 5% Glycerol v/v; (x) 2.5% Glycerol v/v, PBS (♦).

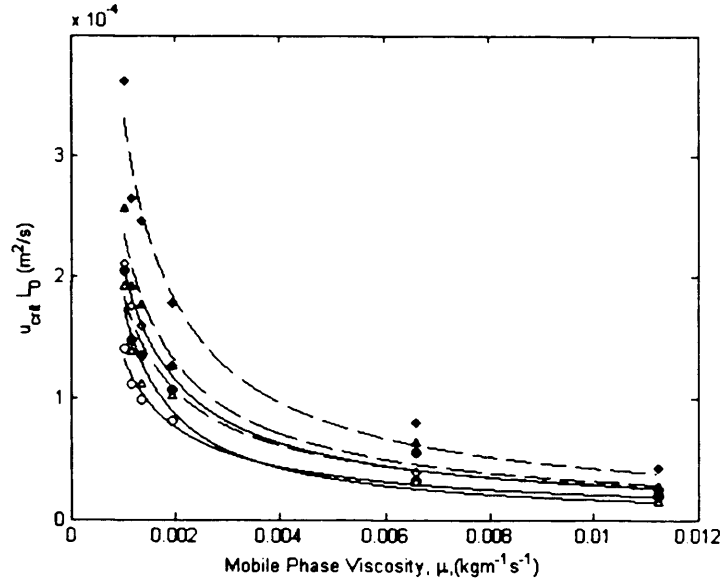

(a)

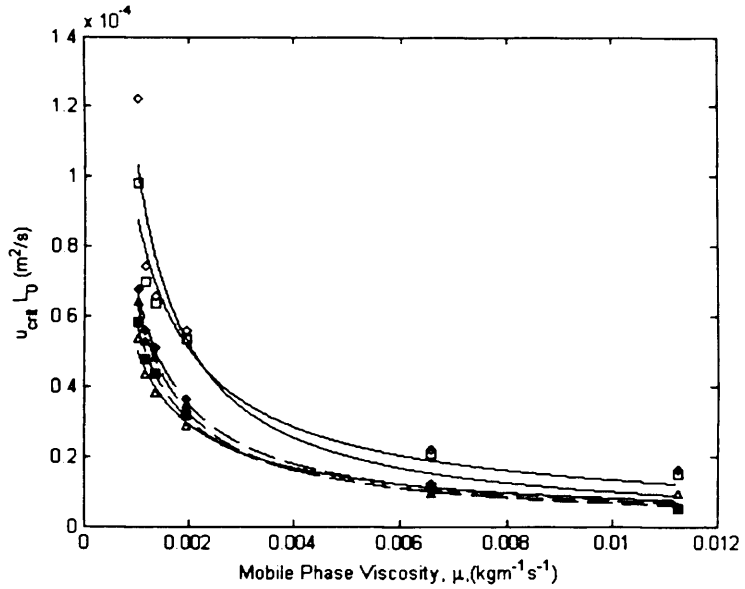

(b)

Figure 3.6 Curve profiles showing variation in critical velocity with packing buffer viscosity for different resins. Superficial fluid velocities have been normalized for differences in bed height. Lines have been added to show trend in data points. **(a)** Sepharose 4FF (solid lines) at bed heights of approximately 0.13m and column diameters of: (◊) 0.016m; (Δ) 0.026m; (○) 0.05m. Sepharose 6FF (dashed lines) at bed heights of approximately 0.13m and column diameters of: (♦) 0.016m; (▲) 0.026m; (●) 0.10m. **(b)** Sepharose CL-6B (solid lines) at column dimensions of: (◊) D=0.016m L_0=0.13m; (□) D=0.026m L_0=0.13m; (Δ) D=0.1m L_0=0.08m. Sepharose 10CL (dashed lines) at column dimensions of: (♦) D=0.016m L_0=0.13m; (■) D=0.016m L_0=0.05m; (▲) D=0.026m L_0=0.12m.

operating conditions. The slope, m, is indicative of the changing wall support with scale. Due to the presence of constants m and b, significant experimentation is required before the correlation can be used to predict the critical velocity of a chromatographic system. The aim here was to use this empirical correlation as a basis and to incorporate terms describing resin rigidity and mobile phase viscosity, in order to reduce the level of chromatographic experimentation required.

Charts of $u_{crit}L_0$ against L_0/D were initially plotted using the data generated from this study shown in Figure 3.7. Table 3.3 summarises values obtained for the constants m and b for the four resins used in this study at varying viscosities. From this table the system dependency of b is clearly discernible and it is observed to decrease as feed viscosity increases and as resin rigidity decreases. However, surprisingly the variation in m with feed viscosity and resin rigidity follows a similar trend to that of b albeit rather weakly. This indicates that it too is also system specific and may not be just a function of column geometry as reported in the literature (Stickel *et al.*, 2001).

The diminishing impact of wall support upon critical velocity with decreasing resin rigidity can be seen by comparing the m values of the 4 different resins used in this study. The m value for Sepharose CL-6B is less than 2% of that found for Sepharose 6FF. This reinforces the observation that the critical velocity is not significantly affected by increasing column diameter when using relatively soft resins (i.e. those with $u_{10\%}$ less than 1.3×10^{-4}m/s).

Figure 3.8 shows the relationship between m, b and resin rigidity over a range of different viscosities. Resin rigidity is expressed in terms of $u_{10\%}$ (see Table 3.1). Figure 3.8 (a) shows m increases with resin rigidity in a linear fashion that can be described by Equation (3.6). The m value determined for the Sepharose 4FF resin in this work was within 17% of the value quoted by Stickel. The b value was within 3%. The reason for the discrepancy in the values for m and b was attributed to the use of differing column dimensions to attain an estimation of the u_{crit} point leading to a slight variation in the linear approximation of the relationship between u_{crit} and column aspect ratio.

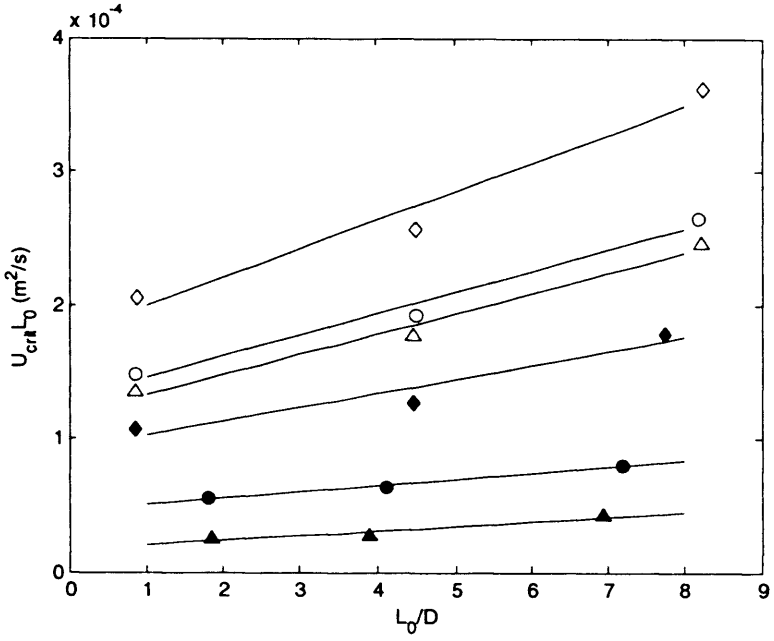

(a)

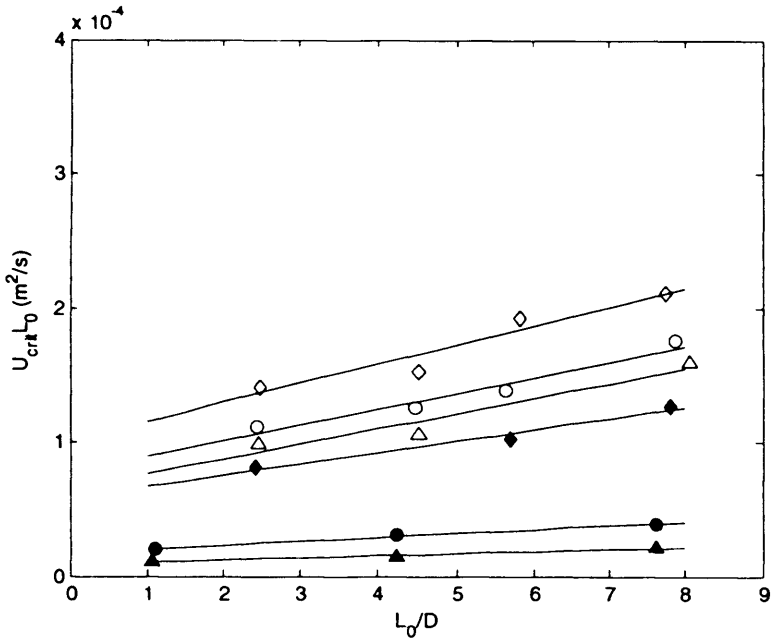

(b)

Figure 3.7 (a- b) Plots of $u_{crit}L_0$ vs. L_0/D, with linear trend lines added with packing buffers of different viscosities, (◊) 0.00102 kg/ms; (○) 0.00107 kg/ms; (Δ) 0.00137kg/ms; (□) 0.00193 kg/ms; (♦) 0.0194 kg/ms; (●) 0.00661 kg/ms; (▲) 0.0112 kg/ms, for **(a)** Sepharose 6FF and **(b)** Sepharose 4FF.

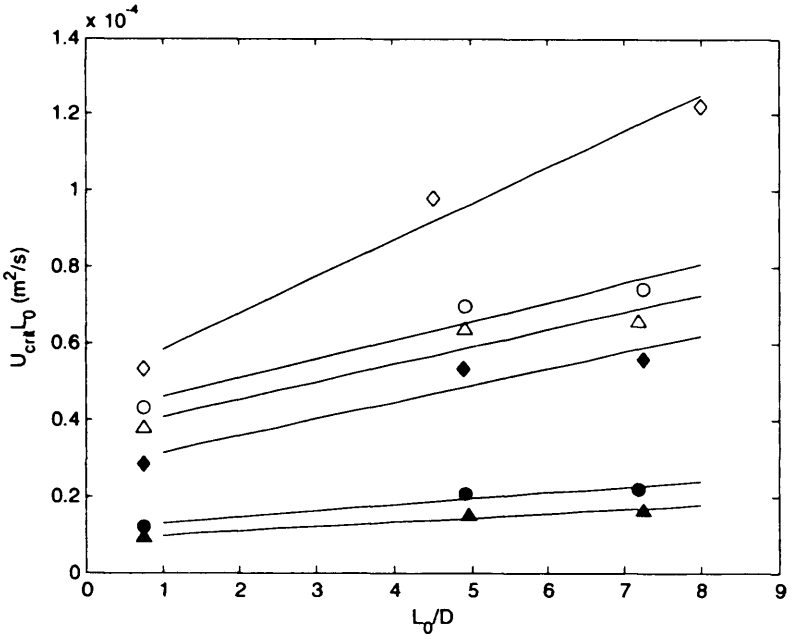

(c)

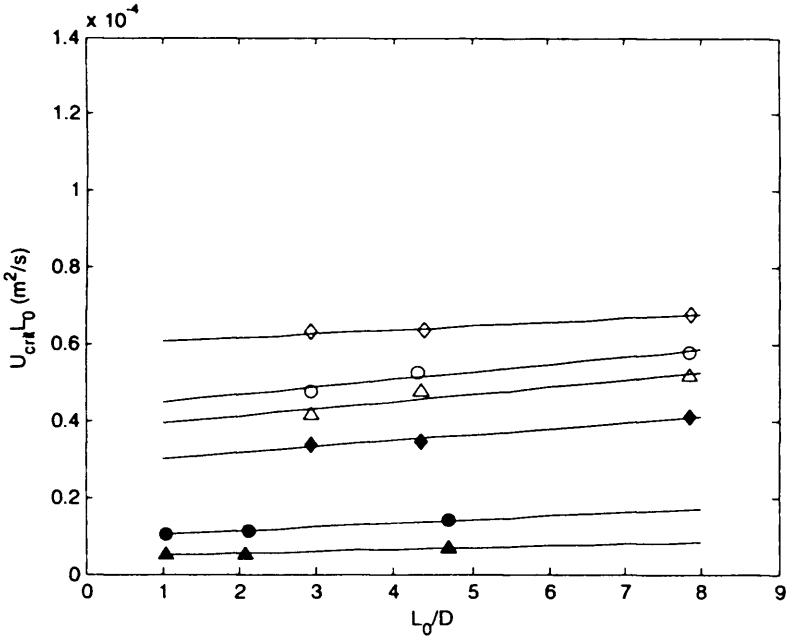

(d)

Figure 3.7 (c- d) Plots of $u_{crit}L_0$ vs. L_0/D, with linear trend lines added with packing buffers of different viscosities, (◊) 0.00102 kg/ms; (○) 0.00107 kg/ms; (Δ) 0.00137kg/ms; (□) 0.00193 kg/ms; (♦) 0.0194 kg/ms; (●) 0.00661 kg/ms; (▲) 0.0112 kg/ms, for **(c)** Sepharose CL-6B and **(d)** Sepharose 10-CL.

Table 3.3 Summary of constants *m* (gradient) and *b* (y-intercept) found from plots of $u_{crit}L_0$ vs. L_0/D, as described by Equation (3.5), for each of the resins used in this study, over a range of mobile phase viscosities.

Resin	Packing Buffer (% Glycerol v/v)	Packing Buffer Viscosity (kg/ms) x 10^{-3}	Gradient, *m* (m^2/s) x 10^{-5}	y-intercept, *b* (m^2/s) x 10^{-5}
Sepharose 6FF	PBS	1.02	2.13	17.81
	5	1.17	1.59	13.00
	10	1.38	1.51	11.76
	20	1.94	1.04	9.21
	50	6.61	0.47	4.58
	60	11.23	0.34	1.72
Sepharose 4FF	PBS	1.02	1.42	10.15
	5	1.17	1.18	7.73
	10	1.38	1.12	6.51
	20	1.94	0.84	5.86
	50	6.61	0.29	1.74
	60	11.23	0.16	0.91
Sepharose 10CL	PBS	1.02	0.18	5.46
	5	1.17	0.15	4.46
	10	1.38	0.13	4.16
	20	1.94	0.09	2.97
	50	6.61	0.06	0.92
	60	11.23	0.01	0.50
Sepharose CL-6B	PBS	1.02	0.95	4.89
	5	1.17	0.50	4.10
	10	1.38	0.46	3.62
	20	1.94	0.44	2.70
	50	6.61	0.16	1.15
	60	11.23	0.11	0.87

$$m = (m' u_{10\%} - m'') \tag{3.6}$$

Table 3.4 summarises the values of m' and m'' found over the range of mobile phase viscosities tested. Equation (3.6) predicts that at sufficiently low resin rigidities the value of m will become negative, as shown by the negative y-intercept values found for the linear trend lines in Figure 3.8(a). This in turn implies that resins displaying sufficiently low rigidities will experience increased critical velocities with increasing column diameters, assuming that bed height is maintained. Whilst this effect was not observed, the diminishing impact of wall support with decreasing resin rigidity was seen. It is probable that m actually tends to zero for very soft resins. The critical velocity will therefore remain constant regardless of column aspect ratio and will be purely dependent upon other factors such as resin rigidity and mobile phase viscosity. The m'' values as summarised in Table 3.4 are relatively small and as such Equation (3.6) can be seen to give a good approximation of the diminishing impact of wall support upon critical velocity with decreasing resin rigidity.

The variation in b with resin rigidity can be seen with reference to Figure 3.8(b). Since b is a system-specific constant, it varies significantly with changing rigidity and the values of b are relatively large compared to those of m. Figure 3.8 (b) also shows a non-linear relationship between b and $u_{10\%}$. A least squares curve fitting algorithm using the MATLAB (The Mathworks Inc., Natick, MA, USA, 2004) routine FMINSEARCH was used to generate equations to describe accurately the trends seen in Figure 3.8(b). An exponential structure described by Equation (3.7) gave the best fit to the experimental data.

$$b = b' e^{b'' u_{10\%}} \tag{3.7}$$

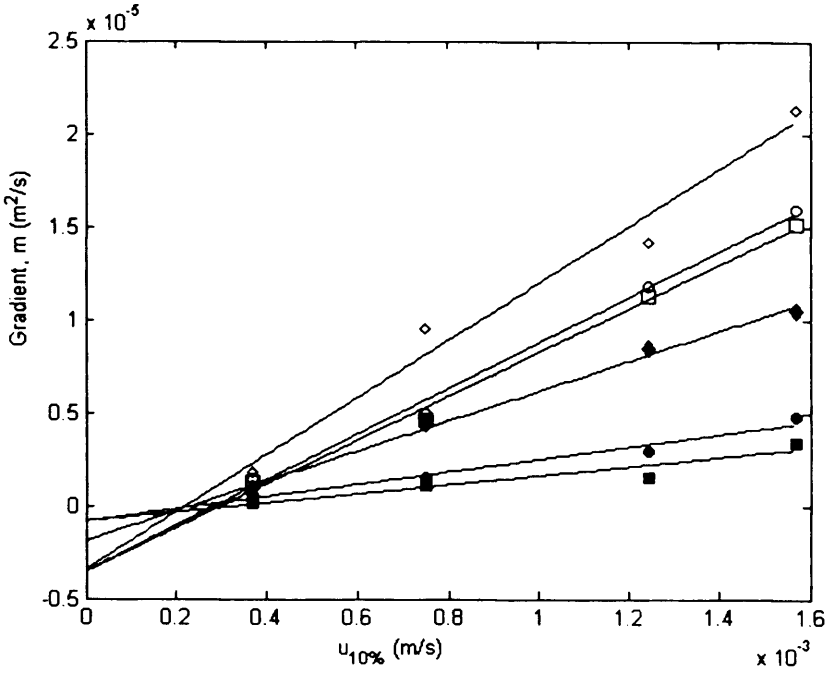

(a)

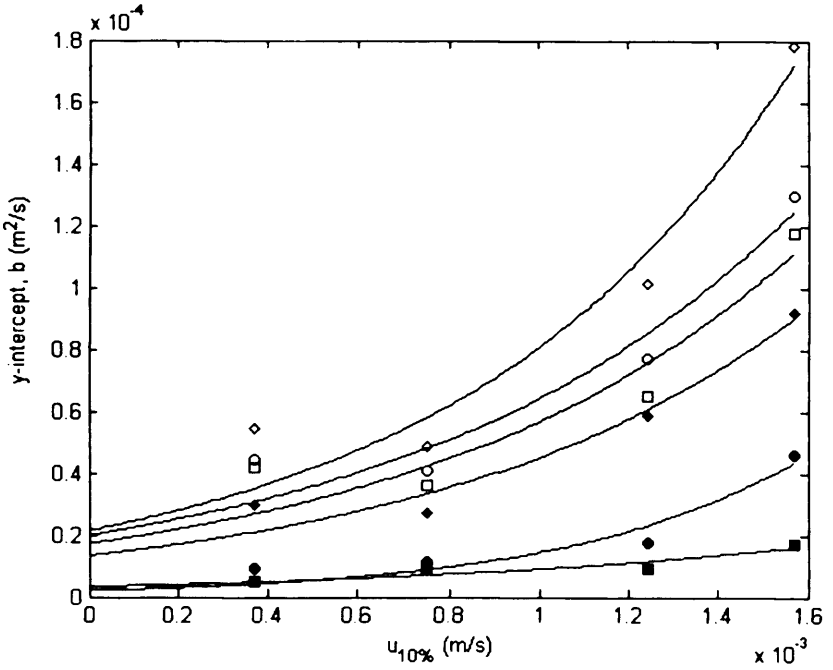

(b)

Figure 3.8 (a) Plots of empirical constant *m* vs. resin rigidity, expressed as $u_{10\%}$ at different mobile phase viscosities. **(b)** Plots of empirical constant *b* vs. resin rigidity, expressed as $u_{10\%}$ at different mobile phase viscosities. (◊) 0.00102 kg/ms; (○) 0.00107 kg/ms; (Δ) 0.00137kg/ms; (□) 0.00193 kg/ms; (♦) 0.0194 kg/ms; (●) 0.00661 kg/ms; (▲) 0.0112 kg/ms. Trend lines show model predictions.

The values of *b'* and *b''* found over the range of mobile phase viscosities tested are summarised in Table 3.4.

Table 3.4 Summary of *m'*, *m''*, *b'* and *b''* values derived from Figure 3.6 across a range of mobile phase viscosities.

Packing Buffer (% Glycerol v/v)	Viscosity, μ (kg/ms) x 10^{-3}	m-value Chart		b-value Chart	
		m' (m) x 10^{-2}	m'' (m^2/s) x 10^{-6}	b' (m^2/s) x 10^{-5}	b''
PBS	1.02	1.53	3.40	2.15	1325
5	1.17	1.23	3.50	2.00	1167
10	1.38	1.18	3.54	1.73	1186
20	1.94	0.80	1.88	1.34	1213
50	6.61	0.33	0.83	0.21	1942
60	11.23	0.24	0.82	0.34	994

Figure 3.9 shows the relationship between *m'*, *m''*, *b'* and the viscosity of the mobile phase. It can be seen from these three plots, that *m'*, *m'' and b'* all have an inverse relationship with μ which may reflect the diminishing effect viscosity has on the critical velocity of a chromatographic system. Again, a least squares curve fitting algorithm using the MATLAB (The Mathworks Inc., Natick, MA, USA, 2004) routine FMINSEARCH was used to generate equations to describe accurately the trends seen in Figure 3.9. These relationships are described in Equations (3.8) - (3.10).

$$m' = \left(4.76 \times 10^{-5}\right)\mu^{-0.83} \qquad \textbf{(3.8)}$$

$$m'' = \left(2.32 \times 10^{-8}\right)\mu^{-0.74} \qquad \textbf{(3.9)}$$

$$b' = \left(4.22 \times 10^{-8}\right)\mu^{-0.91} \qquad \textbf{(3.10)}$$

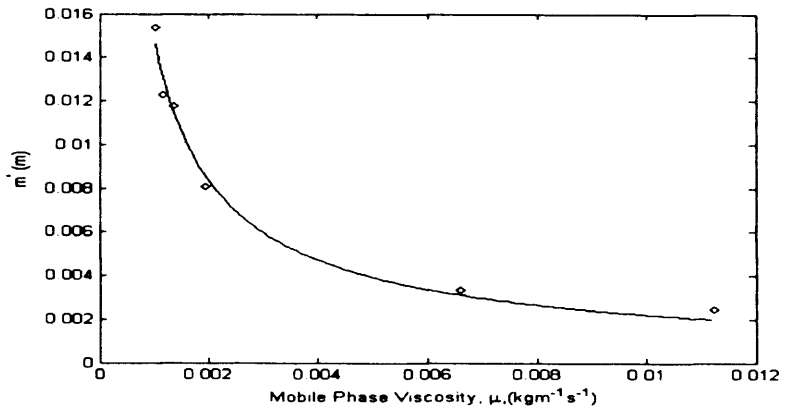

(a)

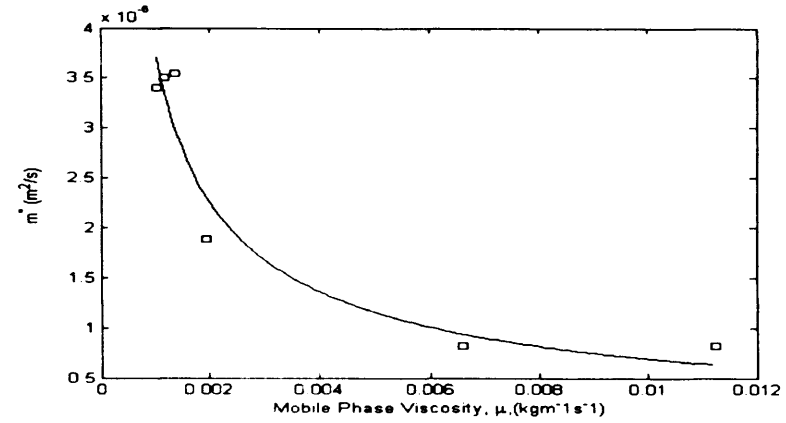

(b)

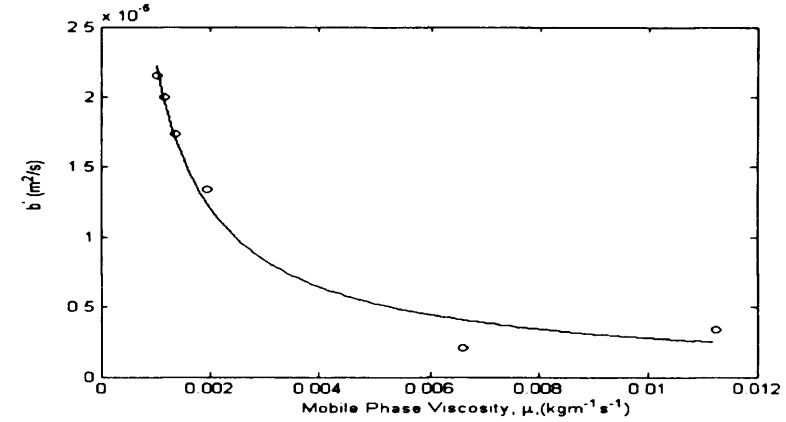

(c)

Figure 3.9 **(a)** Plots of *m'* vs. mobile phase viscosity. **(b)** Plots of *m''* vs. mobile phase viscosity. **(c)** Plots of *b'* vs. mobile phase viscosity. Trend lines show model predictions.

It can be seen from Table 3.4, that the value of b'' does not vary significantly with changes in mobile phase viscosity and that there appears to be no clear trend between b'' and μ. The empirical constant b'' has an average value of 1304 with a relative standard deviation of approximately 20% across the entire viscosity series tested. Therefore in order to simplify the correlation, b'' was deemed to have a constant value, independent of the mobile phase viscosity.

Substitution of Equations (3.6) - (3.10) into Equation (3.5) enables an empirical correlation to be formed which allows the prediction of the critical velocity (u_{crit}) of any chromatographic system, shown in Equation (3.11).

$$u_{crit}L_0 = \left(\left(4.76\times10^{-5}\right)\mu^{-0.83}u_{10\%} - \left(2.32\times10^{-8}\right)\mu^{-0.74}\left(\frac{L_0}{D}\right) + \left(\left(4.22\times10^{-8}\right)\mu^{-0.91}e^{1304u_{10\%}}\right)\right) \qquad \textbf{(3.11)}$$

In order to use this correlation to predict the critical velocity of a chromatographic system employing a new resin, only one experiment needs to be performed; to determine the value of $u_{10\%}$. Once the $u_{10\%}$ value has been determined, and provided the viscosity of the mobile phase is known, the various parameters of the system simply need to be inputted into the above correlation which will then allow the critical velocity of that system to be determined.

Figure 3.10 shows how the model predicted u_{crit} values vary with those determined experimentally for resin with different rigidities and mobile phase with varying viscosities. The model predictions are in good agreement with the experimental data for all sizes of columns tested with an average percentage error of approximately ±2%.

As a more exacting test of the correlation Equation (3.11) was also used to predict the critical velocity of two large production scale packed bed systems which

were not present in the experimental series used to generate the correlation. The critical velocities of columns packed with Sepharose 4 Fast Flow at dimensions of L_0 = 0.194m, D = 1m and L_0 =0.25m, D = 0.45m were predicted using Equation (3.11). The experimentally determined critical velocities of these two systems were obtained from a previously published work (Stickel *et al.*, 2001). The predictions using Equation (3.11) were compared with the experimentally obtained results, as shown in Table 3.5, which indicated that the correlation is capable of predicting the critical velocity of large scale chromatography system, packed with compressible media to a high degree of accuracy, with at worst an error of 17% for the most extreme combination of bed dimensions and buffer used.

Table 3.5 Comparison of predicted and experimentally obtained critical velocities (u_{crit}) for Sepharose 4FF packed at two different aspect ratios.

Buffer Viscosity, μ (kg/ms) x 10^{-3}	D (m)	L_0 (m)	u_{crit} (m/s) x 10^{-4} Experimental (Stickel *et al.*, 2001)	Predicted	Deviation
1.0	1.00	0.190	6.38	6.10	-4%
1.0	1.00	0.130	1.24	1.20	2%
1.5	0.30	0.196	78.51	86.69	-10%
1.5	0.45	0.250	2.94	3.43	17%

The empirical approach taken does neglect two physical phenomena of bed compression: axial compression gradients (Ostergren *et al.*, 1998) and particle deformation (Danilov *et al.*, 1997). These effects likely play a more important role in the vicinity of the critical velocity. Since this empirical model does not attempt to describe flow at u_{crit} but instead uses the critical point as a boundary limit, we believe it is adequate for industrial application.

A further limitation of the correlation is that its applicability can only be ensured for agarose based resins, with rigidities which fall within the range explored in this study. This limitation is mainly brought about by the use of the $u_{10\%}$ term to measure resin compressibility. The structure and behaviour during deformation of other types of resins, such as ceramic based resins, may be significantly different

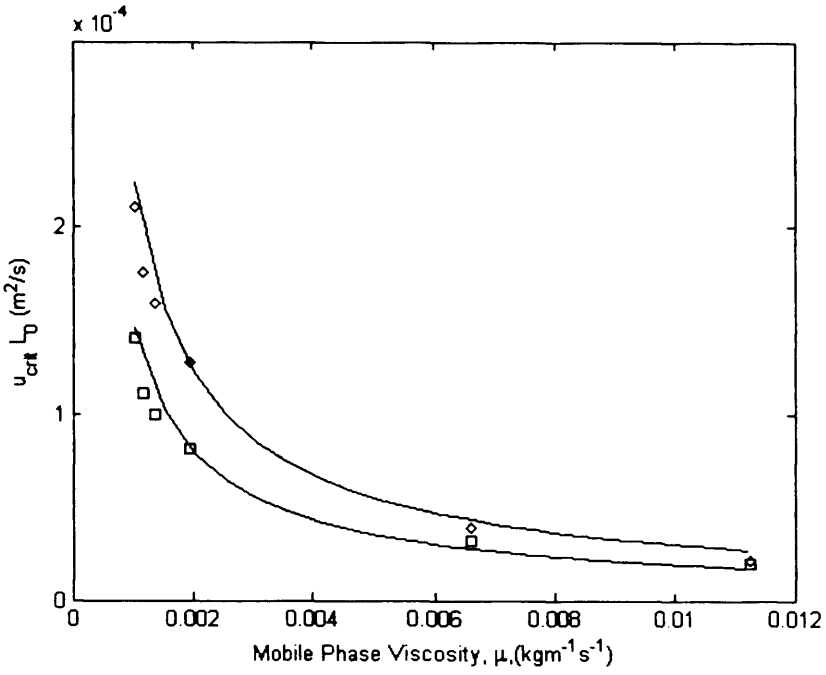

(a)

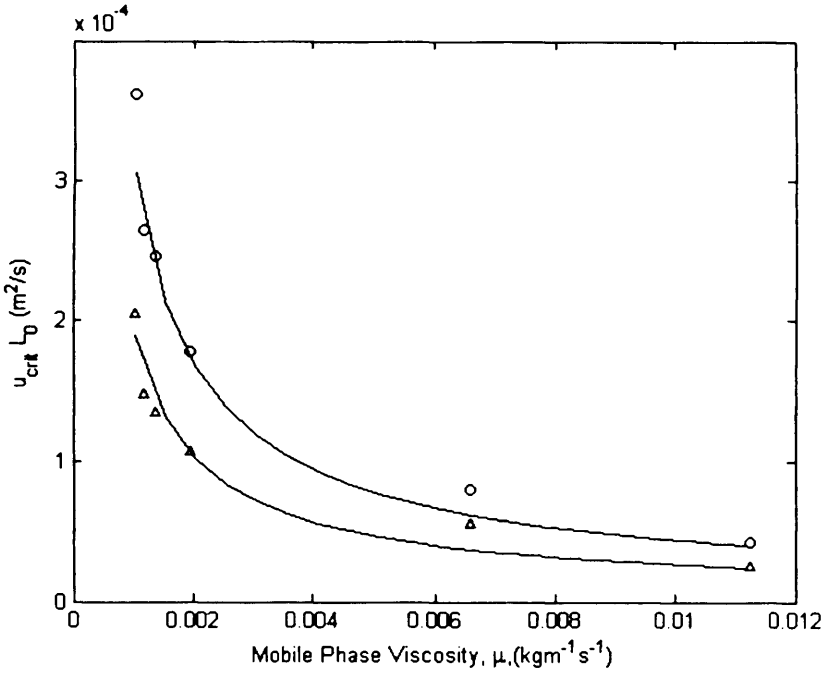

(b)

Figure 3.10 Experimental data points and model predictions showing the variation in critical velocity with packing buffer viscosity for: **(a)** Sepharose 4FF at different column aspect ratios. (◊) D=0.016m L_0=0.12m; (□) D=0.05m L_0=0.12m; **(b)** Sepharose 6FF at different column aspect ratios. (○) D=0.016m L_0=0.12m; (Δ) D=0.10m L_0=0.09m.

from those observed for the Sepharose resins used in this study. Further to this, the compressive properties of resins will change depending on whether they had a functional ligand attached or not. The behaviour of resins with functional groups is the subject of on-going studies. The reason $u_{10\%}$ was chosen as a measurement for resin rigidity as opposed to more conventional measurements, such as through the use of Young's Modulus, was due to the simplicity of the experiment required in order to determine its value. The use of Young's Modulus (Bird *et al.*, 1960) as a measure of resin rigidity may have given a more universally applicable correlation; however, the experiments required are complicated and require specialist equipment. By contrast, the experiment to measure $u_{10\%}$ only requires a lab-scale chromatography column and the use of a straightforward experimental procedure. Furthermore the majority of modern chromatographic processes utilise agarose based resins, with resin rigidities within the range tested in this study. The use of $u_{10\%}$ as a rigidity measurement represents an appropriate trade-off between simplicity and applicability.

3.7 Conclusions

An empirical model has been developed in this chapter (Section 3.6) which allows accurate prediction of the critical velocity of any chromatographic system, utilising a compressible agarose based resin, at varying column scales and mobile phase viscosities. In order to predict the critical velocity of a chromatography system, the model requires more information regarding the column diameter (D), gravity settled bed height (L_0), mobile phase viscosity (μ) and the resin rigidity ($u_{10\%}$). The use of variables to describe system specific parameters serves to limit the number of experiments required prior to application of the model to one; to determine the value of the resin rigidity via a simple experimental protocol, $u_{10\%}$. Since $u_{10\%}$ will be constant for any particular resin, it is possible, through further experiments, to generate a reference table listing the $u_{10\%}$ values for a variety of commonly used resins, in which case, if a chromatography system utilizes a resin which is listed in the table, the need for any experimentation will be completely eliminated (assuming that the viscosity of the mobile phase is known).

The critical velocities as calculated by the correlation generated in this study have been seen to be comparable to values obtained experimentally (± 2%) and are also able to provide relatively accurate predictions (±17%) of critical velocity for large scale chromatography systems detailed in previously published works (Stickel *et al.*, 2001). The correlation can be used prior to, and during, process development in order to determine the change in critical velocity with scale. This will ensure that the fluid flow rates used at a small scale are selected appropriately in order that data that is of relevance for use at process scale is generated.

Investigation into the variation of the critical velocity has so far focused on the physical effects on the critical velocity, however, during chromatographic operation resins are exposed to a range of differing physicochemical effects. This will be examined in the next chapter of the study, using the Stickel model (Stickel *et al.*, 2001) to investigate the impact on packed bed integrity and critical velocity caused by the variations in pH that occur during a chromatographic cycle with a particular emphasis on the role of CIP protocols.

4 EVALUATION OF THE PHYSICOCHEMICAL EFFECTS DURING LARGE-SCALE CHROMATOGRAPHIC OPERATION

4.1 Introduction

As previous chapters have outlined, affinity chromatography is the industry-wide standard for the direct capture and purification of antibodies from cell culture fluid. As explained in Chapter 2, a primary concern when using this unit operation in an industrial purification process is productivity. Therefore, the maximum operable flow through such a chromatographic system is a key design variable. Chapter 3 outlined the limits that column scale and hydrodynamics, place on flow velocity. However the flow velocity can depend on other factors of operation as well.

In many affinity separation systems both ligands and products are bio-molecules of high molecular weight. As such, their three-dimensional structures and activities are very susceptible to changes in environmental conditions, such as temperature, pH and / or ionic strength. During immobilisation of ligands onto resins, the natural conformation of the ligand changes, and the extent of change differs in each system or each molecule in a given chromatographic system. The degree of susceptibility also varies with different support resins and methods of immobilisation onto the support (Kang *et al.*, 1991). The purpose of this chapter is to use the techniques and practices developed in the previous chapter to examine and discuss the effects of changes in pH on bed compression in large scale chromatographic systems. This is especially important in the case of affinity based systems due to the extremes of pH that this processing step uses in the purification of biological entities.

This chapter is divided as follows. Section 4.2 outlines the extremes of pH likely to be encountered during an affinity separation process. Section 4.3 describes the results of ionic interactions that can occur between a chromatography resin and mobile phases of varying pHs. Section 4.4 describes the experimental techniques and analyses that will be used, whilst Section 4.5 illustrates the findings of the study. The final section provides a summary of the main findings and implications of the study.

4.2 The extremes of the affinity purification process

As outlined in Chapter 2, the basic protocol for affinity chromatography is relatively straight forward: bind at neutral pH and elute at acidic pH (Fahrner *et al.*, 2001). Even an un-optimised Protein A step can yield a highly purified antibody. The ease and simplicity of method development of this mode of chromatography has been a key reason for its widespread use in the purification of monoclonal antibodies.

However, an important step in the development of any process for biopharmaceuticals production is comprehensive attention to good manufacturing practices (GMP). This includes the development of robust and effective clean-in-place procedures (CIP) which are inherent in multi-cycle chromatographic operations (Burgoyne *et al.*, 1994). Frequency of column cleaning will be partly determined by the quality of the feed, which in turn is dependent on the stage of the process. The impact of such steps on chromatographic performance is therefore of particular concern in the initial capture mode of operation (Tejeda-Mansir *et al.*, 1997). Highly alkaline sodium hydroxide solutions are commonly used for chromatographic system sanitisation and cleaning, typically, as this represents a cheap and effective buffer solution (Sofer *et al.*, 1989). It is clear that the affinity process utilises extremes of pH during operation.

A common disadvantage of these CIP treatments, however, is that they cause capacity loss due to denaturation of the adsorbent ligands (Tejeda-Mansir *et al.*, 1997; Hale *et al.*, 1994; Boschetti, 1994). Therefore, this type of adsorbent has a finite life defined in terms of the maximum number of possible re-uses. The cost of Protein A affinity resins often necessitates their use for a number of consecutive cycles in order to operate the process in an economic manner and therefore, the lifetime of a resin is an important parameter to the overall process cost (Tejeda-Mansir *et al.*, 1997).

Despite the significant advantages of Protein A chromatography (outlined in Chapter 2), its high cost, together with the susceptibility of the Protein A ligand to denaturation and leaching, has led to recent developments in alternatives to these resins (Kabir, 2002; Verdoliva *et al.*; 2002; Guerrier *et al.*, 2000; Li *et al.*, 1998).

Using techniques such as molecular modelling, protein engineering and phage display, several small protein domains have been constructed based on the IgG binding domain of Protein A (Kabir, 2002; Li *et al.*, 1998). Fassina *et al.* (1996) have identified a Protein A mimetic peptide through synthesis and screening of synthetic multi-meric peptide libraries composed of randomised synthetic molecules with a tetradendate lysine core (Fassina *et al.*, 1996, 1998, 2001). Another approach has employed a combination of molecular modelling and synthetic chemistry to design small molecule ligands that can mimic Fc-Protein A interaction (Lowe *et al.*, 1992; Curling, 2004).

Affinity sorbents based on synthetic affinity ligands offer a number of advantages to compounds derived from biological substances, in particular robustness, relatively low cost, ease of sanitisation with respect to ligand denaturisation, and potential lack of biological contamination (Newcombe *et al.*, 2005). As such these adsorbents significantly increase the number of possible re-uses of the column as capacity degradation is negligible (Newcombe *et al.*, 2005).

Resin lifetime however, is also a function of mechanical stability (Muller *et al.*, 2005). Micro-spherical polymers are widely used as packing materials for chromatography and a variety of other applications. The pore structure and surface area of these beads play an important role in ion-exchange and affinity chromatography. The 'function' of the polymer is based essentially on specific functional residues (or reactive sites). In either case, the size of the micro-beads, the swelling behaviour and the chemical structure of the polymer backbone strongly influence the overall performance of the resin (Arshady, 1991). Usually, a mechanically stable resin is easy to pack and does not shrink or swell during the chromatographic cycle. These requirements are nearly perfectly achieved by silica based resins but not resins based on the prevalent agarose or other polymeric materials (Muller *et al.*, 2005).

4.3 Effects of physicochemical interactions

Resin swelling and shrinking is predominantly observed in ion-exchange resins as they change ionic form with mobile phase, posing potential problems of

significant bed stresses (Zenz *et al.*, 1960; Marra *et al.*, 1973; Kunin, 1976; Muller, 2005). The cause of stress to column based systems is manifold; the pH, solvent, salt, protein content and viscosity change periodically many times. Studies into these phenomena however, predominantly investigate the impact of such effects on mass transfer and adsorption with no reference to bed stability. Recently, Shadday (2006) reported increases in pressure drop of a packed bed system during column regeneration of an ion-exchange resin due to bed swelling. A one-dimensional numerical system was proposed to model transient flow through a swelling packed bed with the aim of describing the influence of friction between the particles and the column walls on the breakthrough curves and the integrity of the bed. Several other models exist that provide a numerical quantification of bed swelling and shrinking (Marra *et al.*, 1973; Sainio *et al.*, 2007). However, these works are complicated and give very limited predictions as to the impact of these phenomena at production scale.

Less work has been reported into the effects on affinity chromatography systems (Muller *et al.*, 2005). Further to this, there is very little in the literature on the impact of multiple cycles of operation on the long-term behaviour of beds under compression. Muller *et al.* (2005) investigated the long term mechanical stability of chromatographic supports. Their investigation however, focused on single chromatographic particles and not the overall packed bed. Although this gives useful data in terms of how resin particle stability varies during operation, the impact of such changes are only put into context when examining their effects on bed homogeneity as a whole.

This chapter investigates the mechanical stability of a chromatographic bed under the differing physicochemical conditions typical of those experienced within a separation cycle. Stability is assessed through insights into the limits of packed bed operation, by evaluation of the critical velocity (u_{crit}) of these systems. Small-scale, as well as pilot scale experiments were used to predict behaviour at production scale under these varying conditions. Individual physicochemical effects were considered along with the periodic changes and interactions that are inherent during large-scale chromatographic operation. Synthetic Protein A affinity resins, each with different

backbone characteristics but the same functionalities, were investigated in order to understand and predict their stability in production-scale packed bed systems.

4.4 Materials and Methods

4.4.1 Chromatography Media

Resins X_{ApA}, X, Z_{ApA} and Z were used in this study. X_{ApA} is a commercially available resin with an artificial-Protein A (*ApA*) ligand attached. Resin X is the underivatised agarose base from which X_{ApA} is synthesised. It is based on a cross-linked 6% agarose bead. Resin Z_{ApA} is a prototype resin which is currently being developed as a commercial successor to the X_{ApA}. Z_{ApA} differs from X_{ApA} in two key areas. The cross-linking is more extensive and regular which allows greater permeability and the spacer –arm is extended. Z therefore, is the underivatised agarose base from which Z_{ApA} is derived. All of the chromatographic media used had an average particle size of 100 +/- 25 μm. Table 4.1 gives a summary of the physical characteristics of the resins investigated in this study.

Table 4.1 Properties of resins used in this study.

Resin name	Base resin	Modification
X	6% cross-linked agarose	none
X_{ApA}	6% cross-linked agarose	*-ApA*
Z	6% highly cross-linked agarose	none
Z_{ApA}	6% highly cross-linked agarose	*-ApA*

4.4.2 Experimental Equipment

The experimental set-up was the same as that shown in Figure 3.1. Two bench-scale columns with adjustable column lengths and inner diameters of 0.016 m

and 0.026 m (models XK16, XK26, GE Healthcare, Uppsala, Sweden) were used, in addition to two pilot/production-scale columns (BPG-100/500, BPG-200/500, GE Healthcare, Uppsala, Sweden) with an internal column diameter of 0.1 m and 0.2 m respectively and adjustable length.

Due to the differences in the volumetric flowrates required in order to reach critical velocity for the different combinations of columns and resins tested, three different feed delivery and pressure measurement systems were used. The AKTA Explorer system (GE Healthcare, Uppsala, Sweden) was used in experiments involving the XK16 and the XK26 columns with the X, X_{ApA} and Z resins. A Dynamax Model SD-1 Solvent Delivery System (Rainin Instrument Co. Inc., Oakland, CA, US) was utilised for XK16 and XK26 columns involving the Z_{ApA} resin. For the BPG-100 and BPG-200 pilot scale columns, a 605Di Peristaltic Pump (Watson Marlow, Wilmington, MA, US) was used for feed delivery.

Column pressure drops (ΔP) were measured using either internal pressure measurement devices present in the feed delivery systems (in the case of the AKTA Explorer) or needle pressure gauges inserted into the column inlet line (in the case of the pilot-scale system). The volumetric flowrate through the columns during all of the experiments was measured manually by collecting the column output in a graduated cylinder for a timed period. In all cases, in order to reduce the extra-column pressure drop, column inlets were connected directly to injection valves whilst column outlet lines were fed directly into a waste collecting container, as opposed to a fraction collector.

Particle size distributions were measured using a Malvern Mastersizer 2000 laser sizer (Malvern Instruments, Worcestershire, UK). The instrument uses a Low Angle Laser Light Scattering (LALLS) method to measure particles in the range of 0.1 to 2,000 μm. The samples were diluted and dispersed in RO water to achieve an obscuration of approximately 10-12%. The data of interest obtained from the instrument was the d_{50}, which is defined as the point within the particle distribution where 50% of the particles, by volume, are smaller than the stated diameter.

4.4.3 Experimental Procedure

To simulate the varying physical properties of feed streams found in industry, a range of different buffers were used. Feed streams of different pH were replicated by titration of phosphate buffer (20mM sodium phosphate) with appropriate amounts sodium hydroxide and hydrochloric acid. Buffer solutions with a neutral pH (pH 7) and an acidic pH (pH 3) were produced to mimic the load, wash and elution pHs observed during a typical MAb binding to Protein A capture step. A solution of 1M sodium hydroxide (NaOH, pH 13.3) was further used to simulate conditions of a Clean-in-Place (CIP) protocol.

4.4.3.1 Pressure-flow procedure

To begin packing, a measured volume of slurry was poured into the column and allowed to gravity settle overnight. The top plate of the column was lowered into the supernatant and flow was started. For experiments involving XK columns, the packing buffers were initially pumped through the columns at 0.5 mL/min for 30 minutes in order to flow pack the resin. The feed flowrate was then increased to 1mL/min for 15mins in order to equilibrate the packing. With the BPG-100 and 200 columns, the feed solution was initially pumped through the column at 340 mL/min for 30 minutes. Following this, the top adaptor of the column was lowered to the top of the bed, and measurements of the initial pressure drop and bed height were taken.

The flowrate of packing buffer through the column was gradually increased until a 35kPa increase in the pressure drop (ΔP) was seen, at which point measurements of bed height and fluid flowrate were taken. This procedure was repeated until the pressure measured did not settle on a particular value, but instead continued to increase without any further increase in delivered flowrate. It was deemed at this point that the critical velocity for the column had been reached. To ensure an accurate measurement of the critical velocity; when the critical point was approached, the volumetric flowrate out of the column was measured. The critical velocity was deemed to be the point at which any further increase in pump speed yielded a negligible change in the flowrate measured from the outlet of the column.

4.4.3.2 Cycling studies

Resins were packed into beds of dimensions D = 0.016cm and L_0 ~ 13cm with a velocity of 1.11 x 10^{-3} m/s. Packing buffer was phosphate buffer titrated to pH 7. Packing took place in accordance with vendor instructions and only beds that had passed the minimum recommended column efficiencies and asymmetries stated were used. These quality attributes were evaluated from a pulsed input from which the height equivalent of a theoretical plate (HETP) and asymmetry (As) was measured (see Appendix A). Loading proceeded at 3.33 x 10^{-4} m/s.

The steps of a chromatographic cycle were performed using blank buffer runs. Equilibration was simulated using phosphate buffer at pH 7 (4CV). Loading buffer was assumed to have the same pH as equilibration. It was felt that this step would not impact the analysis of physiochemical interaction with the resin and was not included in the cycle. Equilibration was followed by elution with phosphate buffer at pH 3 (4CV). Following this, the column was flushed with pH 7 buffer after which sanitisation was performed with 1M NaOH (4CV). Typically, chromatographic performance is monitored through the evaluation of HETP and As. During operation, this was evaluated through transition analysis, the theory of which is outlined in Appendix A. The transition took the form of step change in conductivity during the pH 3 wash. 1M sodium chloride (NaCl) was added to the pH 3 phosphate buffer solution to produce the step.

4.5 Results and Discussion

4.5.1 Pressure-flow analysis

Figure 4.1(a) shows the pressure-flow profiles for increasing mobile phase pH when using the X_{APA} resin. On addition of the sodium hydroxide solution, the value of the critical velocity decreased by approximately 80%, when compared to that found when u_{crit} was evaluated under acidic conditions. To understand this, the microscopic state of the column was investigated. The mean particle diameter (d_{50}) of the resin particles was measured after treatment with a specified volume of each buffer. Figure 4.1(b) shows that on addition of the pH 3 buffer there is a slight shrinking in the particle diameter compared to under neutral conditions. However, when resin particles were exposed to caustic conditions the mean particle diameter of

the bed increased significantly by greater than 3% of its value under neutral conditions.

Many studies have reported that the greatest bed stresses experienced by compressible packed bed systems occur in the bottom region of the bed (Mohammed *et al.*, 1992; Koh *et al.*, 1998; Stickel *et al.*, 2001; Keener *et al.*, 2004; Shadday, 2006). Resin particles at the bottom of the bed are exposed to both the gravitational stresses from the weight of the particles above them as well as the viscous drag from the mobile phase flowing through the column (Mohammed *et al.*, 1992). High bed stresses distort the shape of the particles which reduces the local bed porosity (Shadday, 2006). When porosity is reduced to a minimum, pressure-drops start to increase. The flowrate at which this occurs is the critical velocity. This provides an explanation as to the increased stresses experienced by the swelling of the X_{ApA} resin.

A consequence of the swelling experienced by X_{ApA}, is that the density of the resin particles decreases; particle volume increases, whilst molar mass remains constant. Density decreases reduce the rigidity of the resin particle allowing easier deformation than when not in their swelled state. Particles at the lower part of the column cannot accommodate swelling by expanding axially due to the compressive stresses imposed on it by fluid flow and, therefore, the stresses required to reach u_{crit} under conditions of resin expansion are attained earlier. Under the same reasoning the slight decrease in particle size experienced on addition of the low pH buffer increases the rigidity of the resin bead as particle density increases. Therefore, u_{crit} is attained later than at neutral conditions.

The cause of the swelling of the resins beads was addressed next. Pressure-flow tests were conducted on resin X, the agarose backbone of X_{ApA}. Figure 4.2(a) shows the pressure profiles resulting from tests using a variety of buffers. The critical velocity of the resin decreased when experiments were conducted using 1M sodium hydroxide solution. However, the decrease compared to the value attained when testing with pH 3 buffer was approximately 30% and represents a considerable reduction in the compressive effect. There was only a decrease of 3% between the u_{crit} of the bed when compressed with pH 3 buffer compared to when the pH 7 buffer

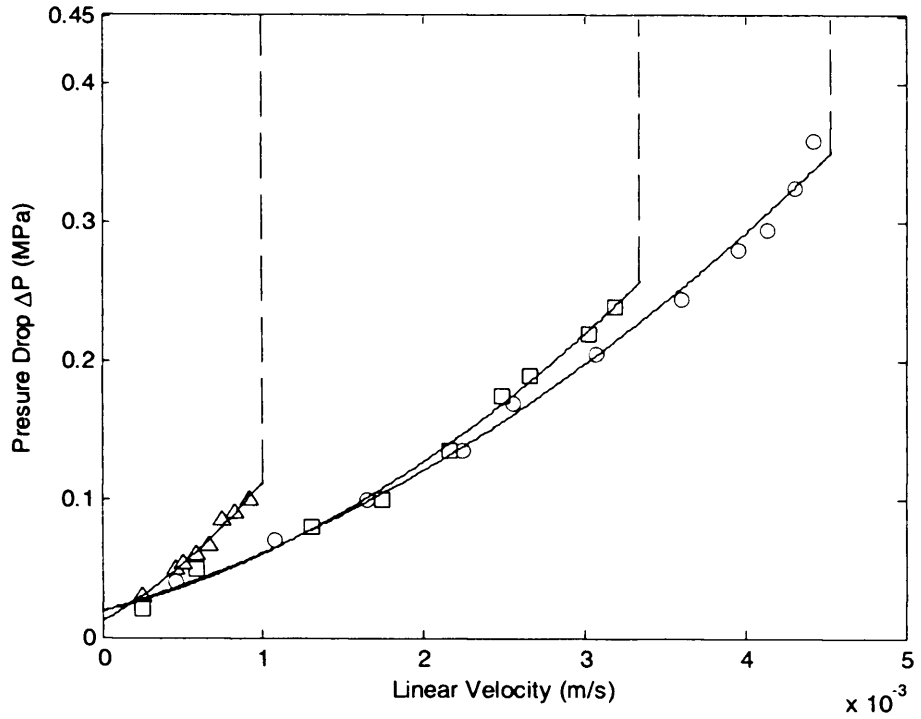

(a)

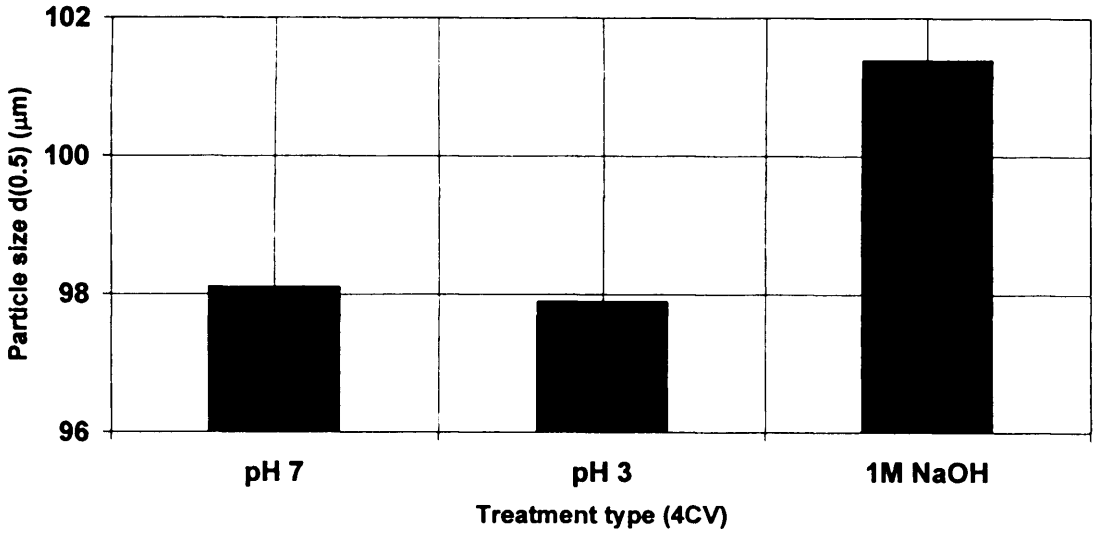

(b)

Figure 4.1 (a) Pressure-flow profiles for the X_{ApA} resin over a range of mobile phase pHs. Bed dimensions were D=0.016m, L_0~0.13m. Superficial fluid velocities have been normalized for differences in bed height; (○) pH 3, (□) pH 7, (Δ) 1M NaOH (pH 13.3). **(b)** Mean particle size (d_{50}) measurements of resin X_{ApA} after treatment of 4CV over a range of mobile phase pHs.

was used. It was deemed that the level of decrease was sufficient to assume the bed compresses in the same manner for these two buffer solutions. (The standard deviation in the u_{crit} measurements was 2-5% in all cases.) Examination of the d_{50} of the resin particles of X in Figure 4.2(b) showed no variation in particle size on exposure to different pH buffers. The reduction in u_{crit} on addition of the hydroxide solution cannot therefore, be attributed to particle deformation as was the case for the X_{ApA}. Measurement of the viscosities of the buffer solutions used in this study (Table 4.2) showed that the 1M NaOH solution was approximately 4% greater than the pH 7 and pH 3 buffer solutions. The drop in u_{crit} observed in Figure 4.2(a) on addition of hydroxide solution, can therefore be attributed to the increased viscosity of this feed. (The reasoning behind decreases in critical velocity with high viscosity solutions is described in Section 3.3.)

Further to this however, it has been reported (De Koning *et al.*, 1984) that the mechanical strength of resins decrease when alkaline concentration increases. This is due to the hyrolysis of the agarose structure under such conditions. The extent of this effect forms part of future studies and was not quantified specifically in this work.

It can be concluded that the swelling of the particles experienced by the X_{ApA} resin is not due to the interaction between hydroxide solution and its agarose backbone. However, the higher viscosity of the hydroxide buffer does contribute to the reduction in the ucrit of this resin. Particle swelling is therefore a result of the interaction between the hydroxide solution and the *ApA* ligand attached to the resin base. Investigation into the chemistry of the ligand, shown in Figure 4.3, provides an explanation for swelling phenomena observed.

Figure 4.3 shows that the *ApA* ligand contains phenolic groups. Previous studies have found that phenolic groups tend to have a pKa value of around 10.2 (Ferris *et al.*, 2002). The pH of the hydroxide solution added to the column is approximately 13.3. Theory states that de-protonation will occur under these conditions, leaving the *ApA* ligand in the form portrayed in Figure 4.3(b) (Solomons, 1996). The net negative charge on each phenolic group causes repulsion between the two groups that result in an expansion of the agarose bead as the bead is pulled in

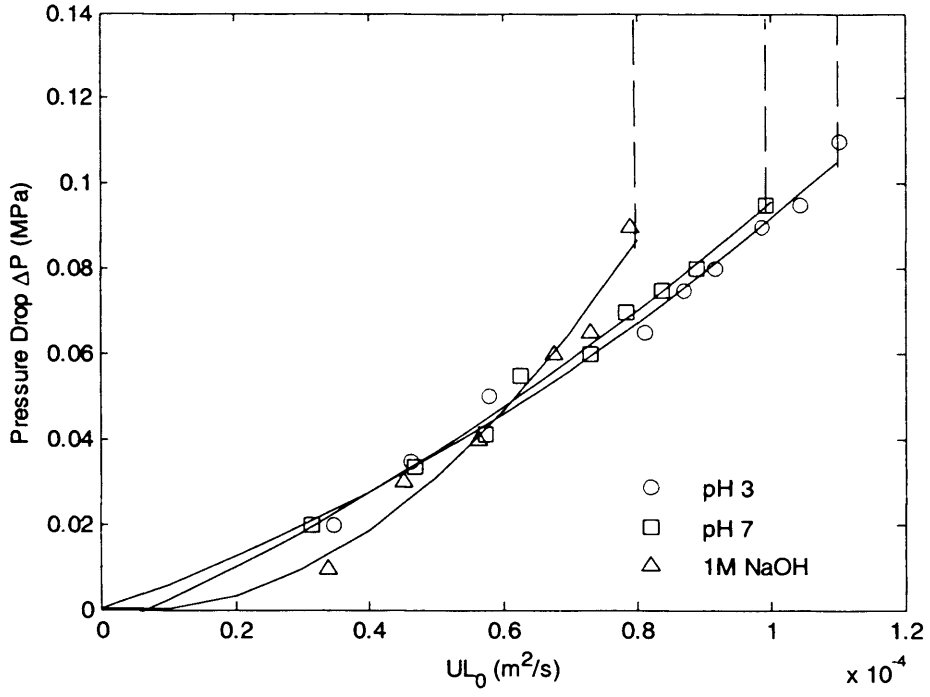

(a)

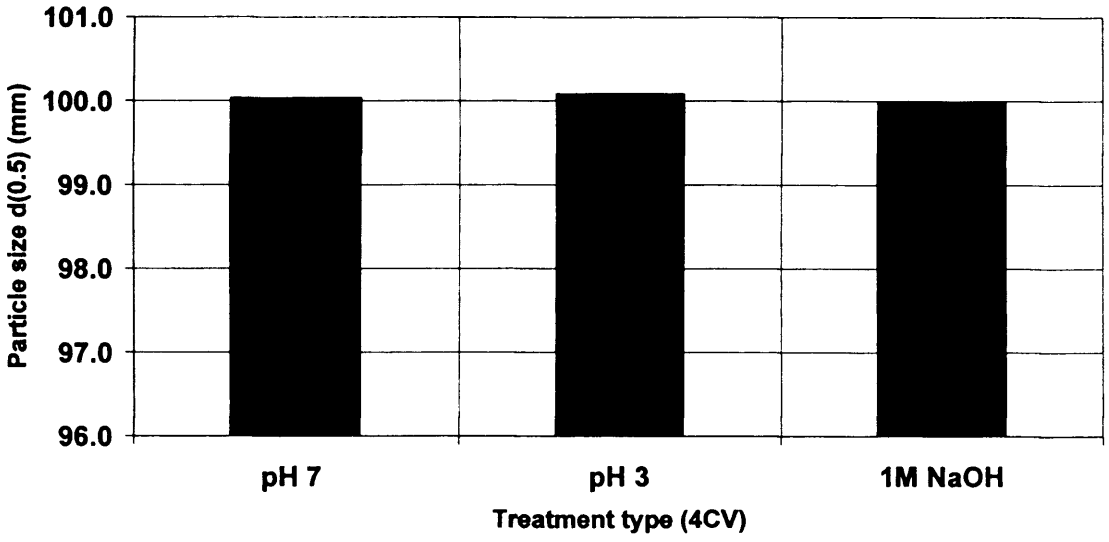

(b)

Figure 4.2 (a) Pressure-flow profiles for the underivatised X resin over a range of mobile phase pHs. Bed dimensions were D=0.016m, L_0~0.13m. Superficial fluid velocities have been normalized for differences in bed height; (○) pH 3 , (□) pH 7, (Δ) 1M NaOH (pH 13.3). **(b)** Mean particle size (d_{50}) measurements of resin X after treatment of 4CV over a range of mobile phase pHs.

Table 4.2 Summary of the mobile phase viscosities of the buffer solutions employed in this study.

Packing buffer	Packing buffer viscosity(kg/ms) x 10^{-3}
Phosphate buffer (pH 3)	1.02
Phosphate buffer (pH 7)	1.02
1M NaOH (pH 13.3)	1.06

opposing directions. It is this particle expansion caused by the introduction of the sodium hydroxide into the bed, together with the increased viscosity of this solution that causes the collapse of the X_{ApA} resin observed at lower flowrates.

The flowrate that can be applied to packed bed systems at process scale is essential when considering issues of productivity and facility throughput. Consequently, the investigation proceeded to measure the impact of the effects of column sanitisation with NaOH at production scale. The model proposed by Stickel *et al.* (2001) illustrated in Equation (4.1) and described in detail in Section 3.6 was used to estimate the critical velocities of production scale columns.

$$u_{crit} L_0 = m\left(\frac{L_0}{D}\right) + b \qquad \textbf{(4.1)}$$

It was determined that plots of u_{crit} L_0 vs. L_0/D were useful to compare the compressibility of resins under different processing conditions. Critical velocity was determined for a variety of different bed lengths using the columns with diameters described in Section 4.3. Figure 4.4 shows a chart of $u_{crit}L_0$ against L_0/D using the data generated from this study. The influence of NaOH is clearly discernible as there is a downward shift in the function to lower flowrates. As has been discussed previously in Section 3.6, m in Equation (4.1) quantifies the contribution of wall-

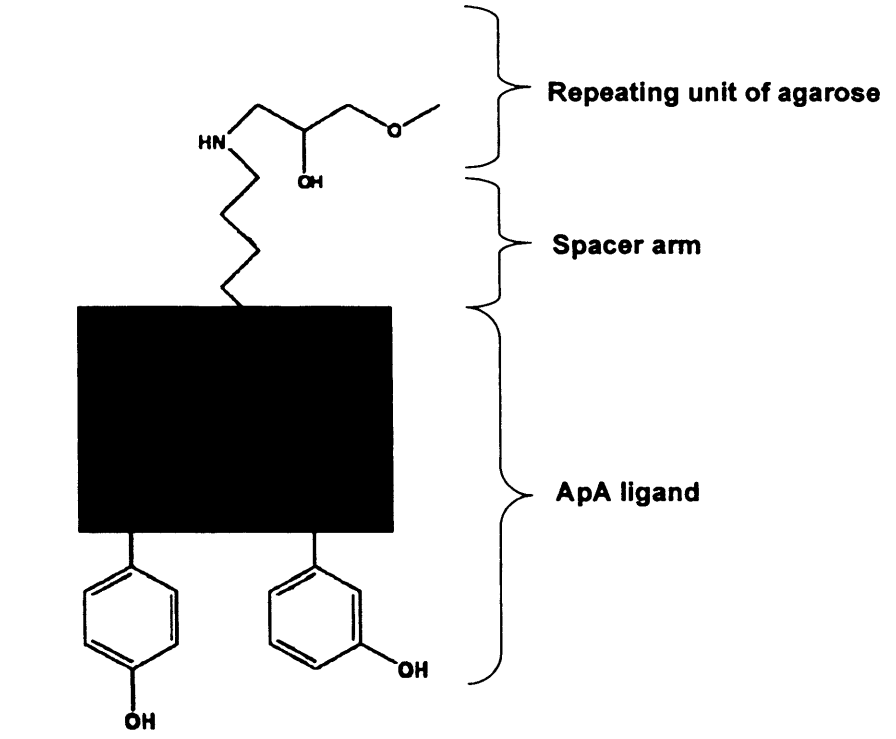

(a)

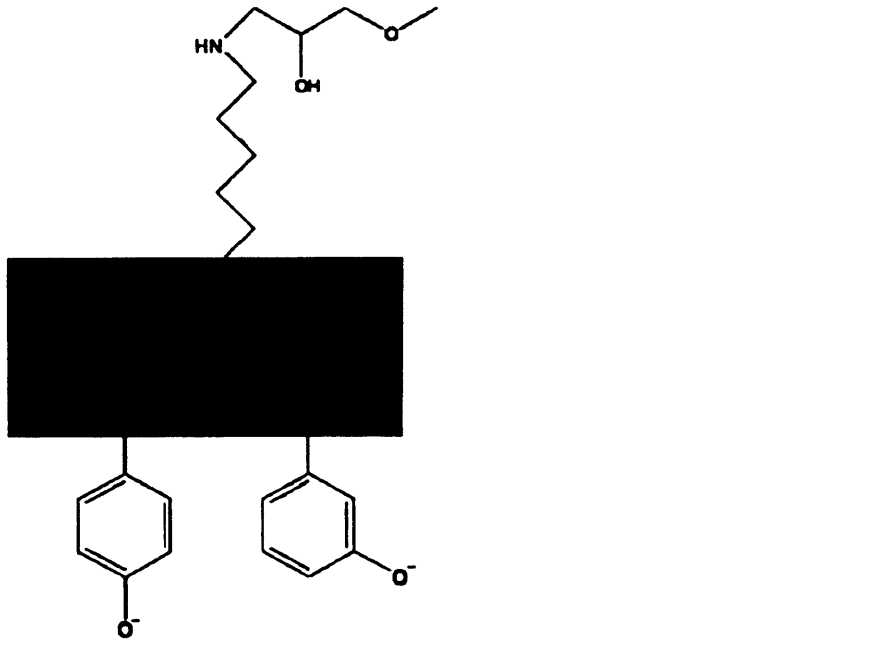

(b)

Figure 4.3 Planar chemical structure for ApA ligand used in both X_{ApA} and Z_{ApA} under **(a)** neutral buffer conditions and **(b)** under highly alkaline conditions.

support to the compressive process. b is the value of $u_{cri}L_0$ for an infinite diameter column and thus, provides a numerical indication of the compressibility of a medium at given operating conditions. Operating conditions for all experiments were kept constant with the exception of the variation in buffer pH. Therefore, the parameter 'b' gives a quantifiable indication as to the impact of buffer properties on the compressive strength of the resin.

Table 4.3 shows the m and b values of the Stickel plots seen in Figure 4.4. The system specificity of b is clearly evident. There is approximately a nine-fold decrease in the value of b calculated when experiments were performed with the pH 3 buffer compared to those performed with 1M NaOH. There is also a sharp decrease in the m value on addition of the sanitisation buffer. The shallow gradient on the Stickel function under caustic conditions follows similar observations found earlier (Figure 3.8 (a) of Section 3.6) where is was shown that as resin rigidity decreased there was an associated decrease in the effect of column wall-support. It was hypothesised that m would tend to zero for very soft resins. The reduced rigidity of the X_{ApA} resin under high pH conditions causes this decrease in the m.

Table 4.3 Summary of constants m (gradient) and b (y-intercept) found from plots of $u_{cri}L_0$ vs. L_0/D, as described by Equation (4.1), for the X_{ApA} resin used in this study, over a range of mobile phase pHs.

Packing buffer	m **(m^2/s) x 10^{-4}**	b **(m^2/s) x 10^{-4}**
Phosphate buffer (pH 3)	0.53	1.3
Phosphate buffer (pH 7)	0.43	1.2
1M NaOH (pH 13.3)	0.01	0.2

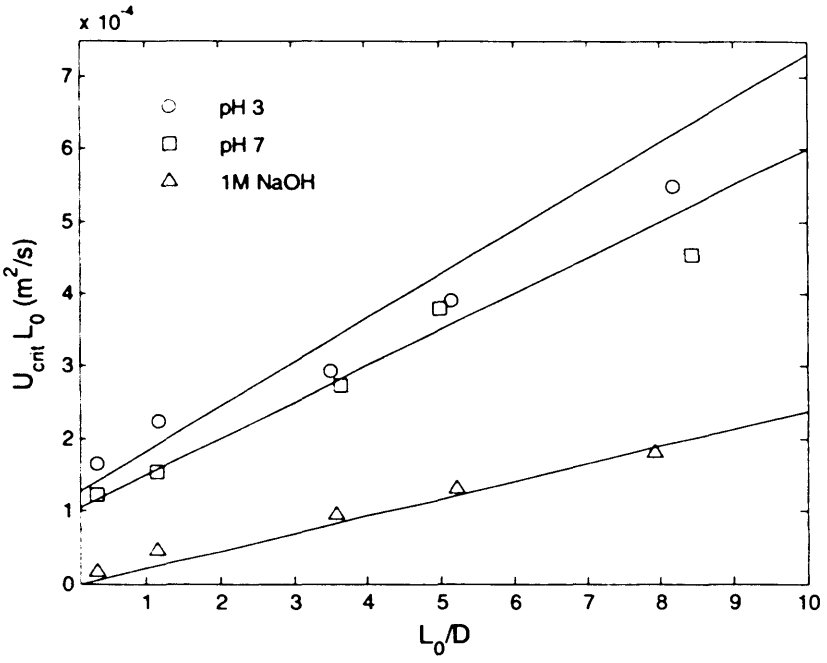

Figure 4.4 Plot of $u_{cnt}L_0$ vs. L_0/D for X_{ApA} resin, with linear trend lines added with packing buffers of different pH, (○) pH 3; (□) pH 7, (Δ)1M NaOH (pH 13.3).

4.5.2 Effect of increasing resin rigidity

Resin swelling in a given solvent is a multifaceted property, reflecting the chemical structure of the polymer backbone, degree of cross-linking and the architecture of the polymer matrix (Arshady *et al.*, 1991). When a low cross-linked resin swells in a solvent, the resin particles expand and a certain degree of short range re-organisation of the loose and tight polymer chain segments may take place. Long range conformational changes are, however, prohibited by the cross-link bridges between the chains. Therefore, extensive cross-linking may restrict even the short-range mobility of the chain segments, minimising the extent of swelling (Arshady, 1991). As such, it has been shown that the extent of resin particle swelling decreases as the nominal degree of cross-linking increases (Brough *et al*, 1978). Through this reasoning, resin Z_{ApA} was produced based on a highly cross-linked agarose backbone to overcome the potential limitations in flowrate of the X_{ApA} resin. A technique for the quantification of resin rigidity through flow compression of a defined column system was described in Section 3.5.3, where the $u_{10\%}$ term was measured. Linear relationships were again obtained when plotting superficial fluid

velocity against bed height, demonstrating the elastic nature of agarose based resins. $u_{10\%}$ was measured for all the resins investigated in this study, with the results presented in Table 4.4.

The impact of cross-linking upon the rigidity of a resin can be observed by comparing the $u_{10\%}$ of resin X to that of Z, since these have the same agarose content but a different extent of cross-linking. This comparison shows over an eight-fold increase in $u_{10\%}$, with the greater level of cross-linking. Interestingly, the attachment

Table 4.4 Rigidity of resins used in the study, expressed in terms of $u_{10\%}$, determined by linear regression of data obtained from bed compression experiments.

Resin	Resin Rigidity, $u_{10\%}$ (m/s) x 10^{-4}	Mean particle diameter under neutral conditions, d_{50} (μm)
X	4	100
X_{ApA}	15	98
Z	35	94
Z_{ApA}	102	93

of ligands to the X and Z resins also produced an increase in the rigidity of the resulting functionalised resins compared with their underivatised forms. Further to this, a decrease in the d_{50} of the resin particles was also observed in X_{ApA} and Z_{ApA} compared to their respective agarose bases. The functionalisation of agarose or other polysaccharide resin support is accomplished through activation and further derivatisation of the hyroxy groups inherent in these polymers. It has been shown that the system of reaction pathways connecting agarose to a functional ligand generally leads to extensive intra-resin cross-linking (Arshady, 1990), which increases resin rigidity. Increasing the extent of cross-linking decreases the particle size as the intra- particle bonds pull the polymer arrangement closer together, forming a more compact bead structure.

Pressure-flow measurements were conducted on the Z_{ApA} with varying buffers and the results are displayed in Figure 4.5 (a). The variation in the critical velocity under the varying pH conditions is much less pronounced. There is only a 20% reduction in u_{crit} when tests were conducted with sodium hydroxide compared to that of the pH 3 buffer. Examination of the mean particle diameter of this resin under different conditions in Figure 4.5 (b) shows there is still a degree of particle expansion with sodium hydroxide. However, there is only a 0.3% increase in the particle size compared to the 3% increase observed in the X_{ApA} resin. This shows that the increased level of cross-linking of the Z_{ApA} resin has considerably mitigated the swelling of the resin beads caused by the ionisation of the *ApA* ligand. Figure 4.6 shows plots of $u_{crit}L_0$ against L_0/D for Z_{ApA}. It can be seen that there is a significant increase in critical velocities that can be attained at larger scales. Table 4.5 shows that under high pH conditions, the b parameter has only decreased by four-fold compared to when the pH 3 buffer was used. The gradient m is seen not to vary significantly under the conditions tested. The reduction in the magnitude of particle swelling under caustic conditions has therefore increased the viability of the use of this resin on scale-up.

4.5.3 Effect of column cycling

Having evaluated the impact of individual buffers on packed bed stability, the effects of column cycling were then investigated. Chromatographic cycles are multifaceted operations involving a variety of different buffers. As such, physicochemical interactions between buffer pH and resin chemistry are not only singular but also combinatorial. Figure 4.7(a) shows the pressure profile for two cycles of operation when operating with resin X_{ApA}. Pressure-drop across the packed bed system is observed to spike on the introduction of the sodium hydroxide solution. As resin particles reduce in rigidity, the bed compresses during operation and pressure-drop increases. Pressure-drop reduces after washing with 4CV of pH 7 buffer after sanitisation but stabilises at a higher pressure than previously. On subsequent introduction of the sanitisation buffer during the second cycle of operation the pressure-drop increased to infinity as the packed bed collapsed.

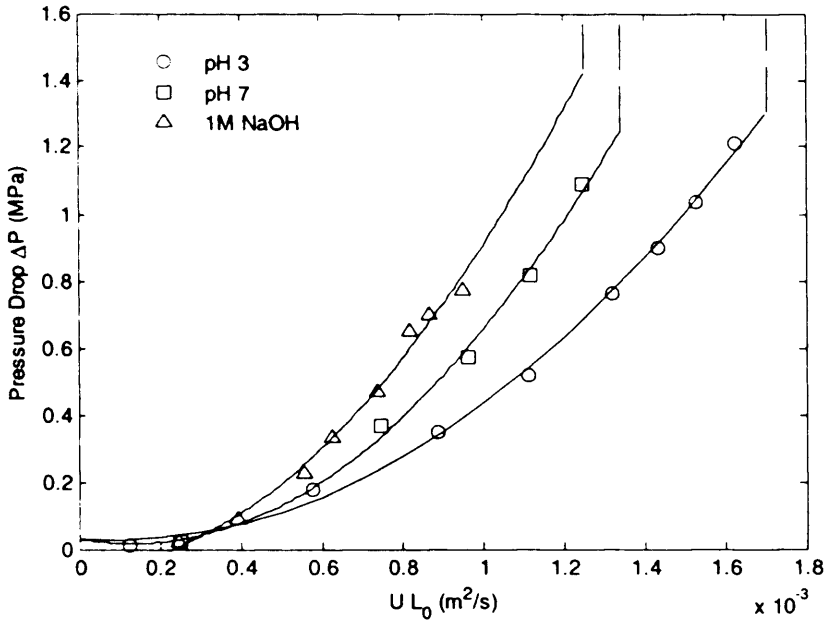

(a)

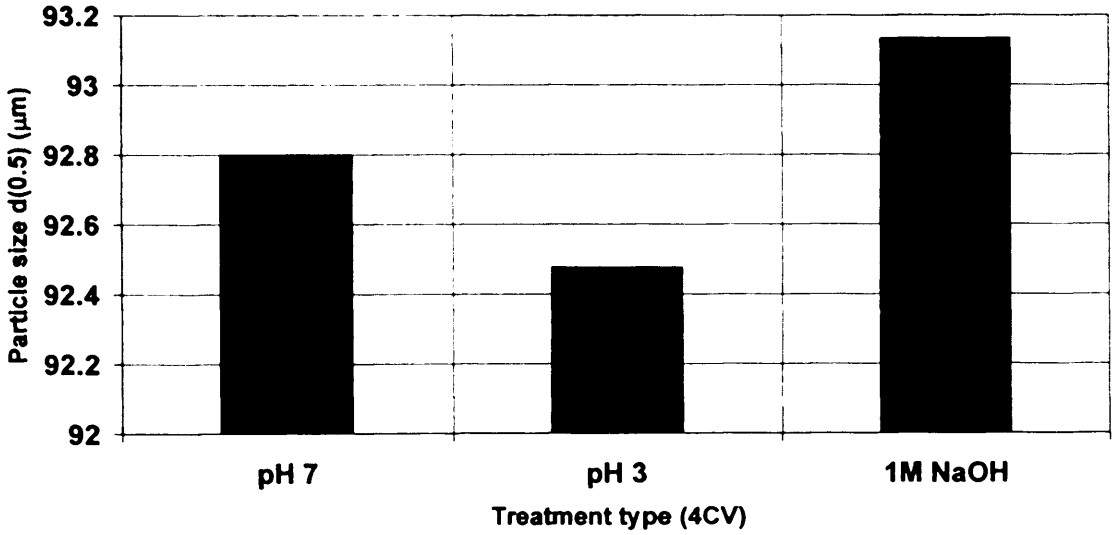

(b)

Figure 4.5 (a) Pressure-flow profiles for the Z_{ApA} resin over a range of mobile phase pHs. Bed dimensions were D=0.016m, L_0~0.13m. Superficial fluid velocities have been normalized for differences in bed height; (○) pH 3 , (□) pH 7, (Δ) 1M NaOH (pH 13.3). **(b)** Mean particle size (d_{50}) measurements of resin Z_{ApA} after treatment of 4CV over a range of mobile phase pHs.

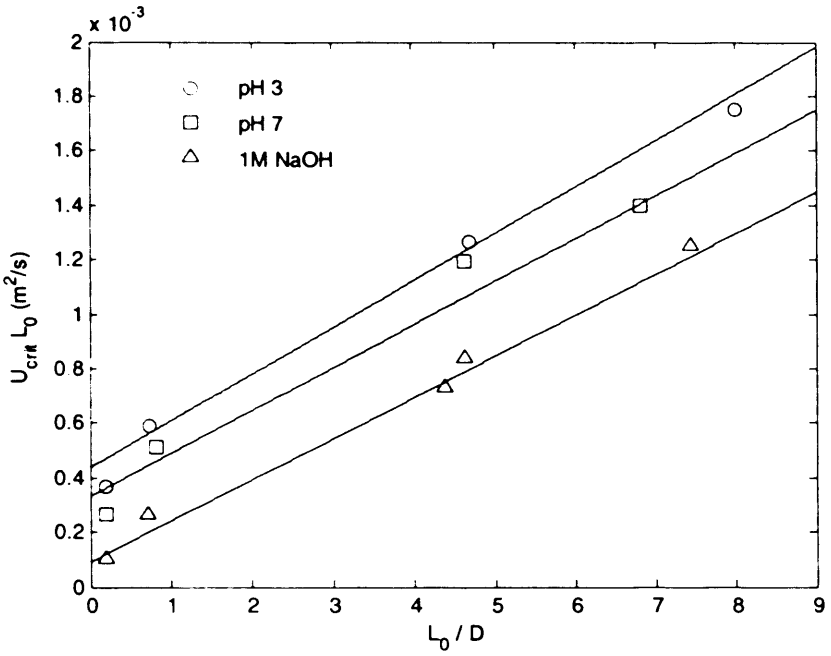

Figure 4.6 Plot of $u_{crit}L_0$ vs. L_0/D for Z_{ApA} resin, with linear trend lines added with packing buffers of different pH, (○) pH 3; (□) pH 7, (Δ)1M NaOH (pH 13.3).

Table 4.5 Summary of constants *m* (gradient) and *b* (y-intercept) found from plots of $u_{crit}L_0$ vs. L_0/D, as described by Equation (4.1), for the Z_{ApA} resin used in this study, over a range of mobile phase pHs.

Packing buffer	*m* (m^2/s) x 10^{-3}	*b* (m^2/s) x 10^{-3}
Phosphate buffer (pH 3)	0.17	0.42
Phosphate buffer (pH 7)	0.17	0.34
1M NaOH (pH 13.3)	0.15	0.13

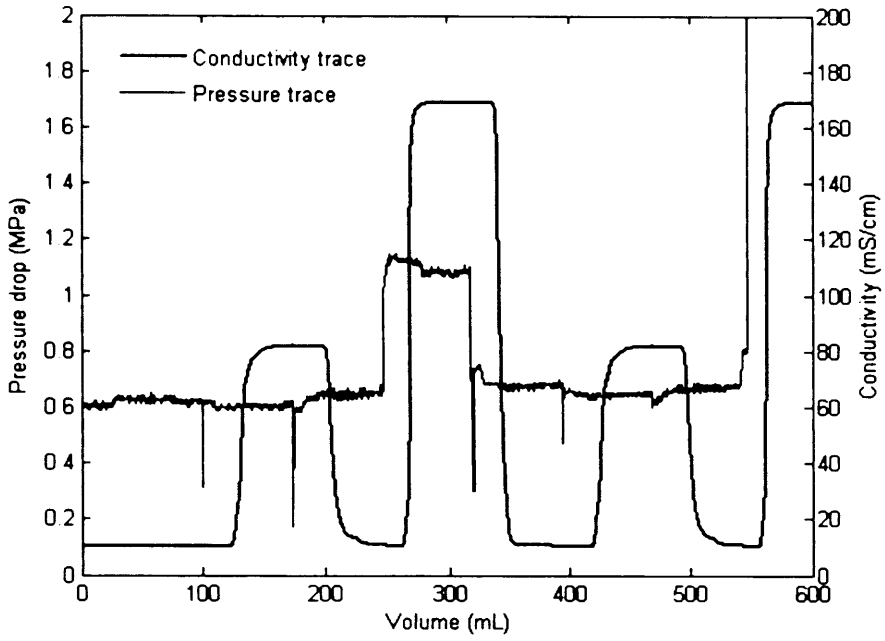

(a)

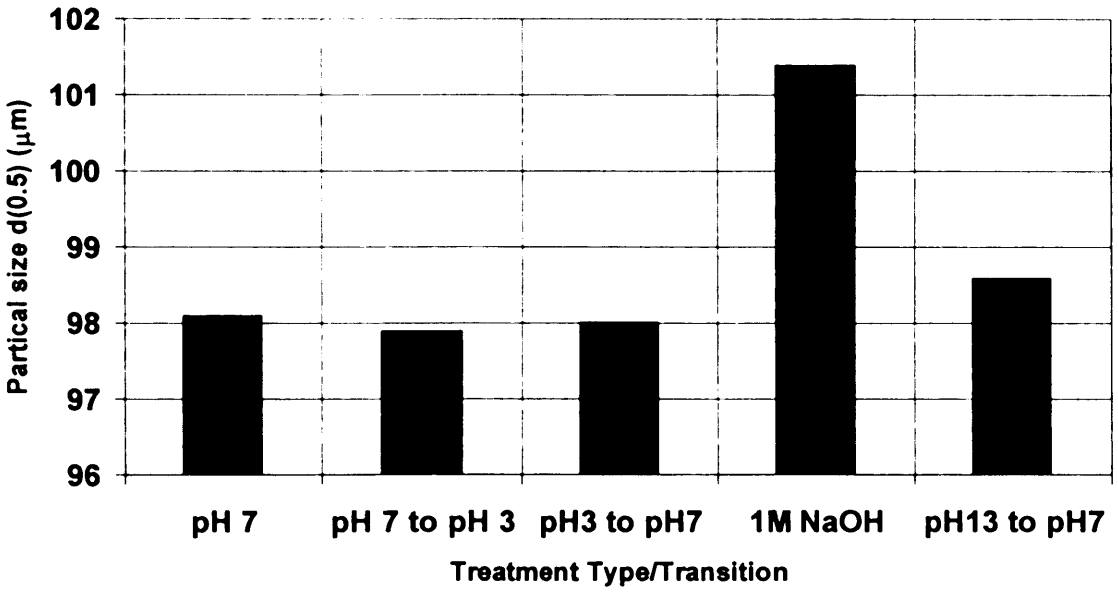

(b)

Figure 4.7 (a) Pressure and conductivity traces for blank buffer runs during typical chromatographic operation when using resin X_{Ap4}. One cycle consisted of (4CV pH 7 buffer, 4CV pH 3 (+ 1M NaCl) buffer, 4CV pH 7 buffer, 4CV 1M NaOH). **(b)** Particle size (d_{50}) measurements of resin X_{Ap4} during one cycle of operation.

The cause of this can be understood by examination of Figure 4.7 (b). Here, the variation in the d_{50} of the resin beads during one cycle of operation is shown. As expected the particle size increases on contact with the hydroxide solution due to the ionisation of the *ApA* ligand. Washing with a further 4 CV of pH 7 buffer reduced the particle size as the ionisation effect was diminished with the introduction of lower pH conditions. However, the particle diameter did not return to its initial size as the phenol groups on the *ApA* ligand were still partially charged, causing the resin beads to retain a degree of swelling. The bed therefore, had a reduced mechanical stability compared with that at the start of the cycling process. On introduction of the second caustic wash, the extent of swelling experienced by the beads was cumulative. As such, bed rigidity fell significantly and the resin collapsed during operation. Complete neutralisation of the ionising *ApA* ligand with a long, low pH wash after column sanitisation, would have extended operation. However, the introduction of an extra step in the chromatographic cycle would increase process time and buffer consumption, which would impact on the productivity and cost of the process.

The pressure trace during operation with the prototype Z_{ApA} resin is presented in Figure 4.8(a). The pressure-drop is much more stable, with no significant increases in pressure on introduction of the sanitisation buffer. Examination of the variation in the particle diameters in Figure 4.8 (b) shows that there is still an increase in bead diameter when washing with sodium hydroxide. However, the increase is small due to the greater rigidity of the resin particles and therefore, the bed maintains its mechanical stability during operation at the specified flowrate. Particle swelling was reduced to such an extent that the use of the pH 7 re-equilibration buffer was sufficient to neutralise the ionised *ApA* ligand and allow the particle size to contract to its original level.

Figure 4.9 (a) illustrates the use of transition analysis (Larson *et al.*, 2003) to calculate non-Gaussian HETP and asymmetry values for the Z_{ApA} resin and its base, resin Z, over 50 cycles of operation. The Z_{ApA} resin was compared to its underivatised form to investigate if there is any loss in performance during operation due to ionisation associated with the use of this ligand. As such, resin Z represents a control,

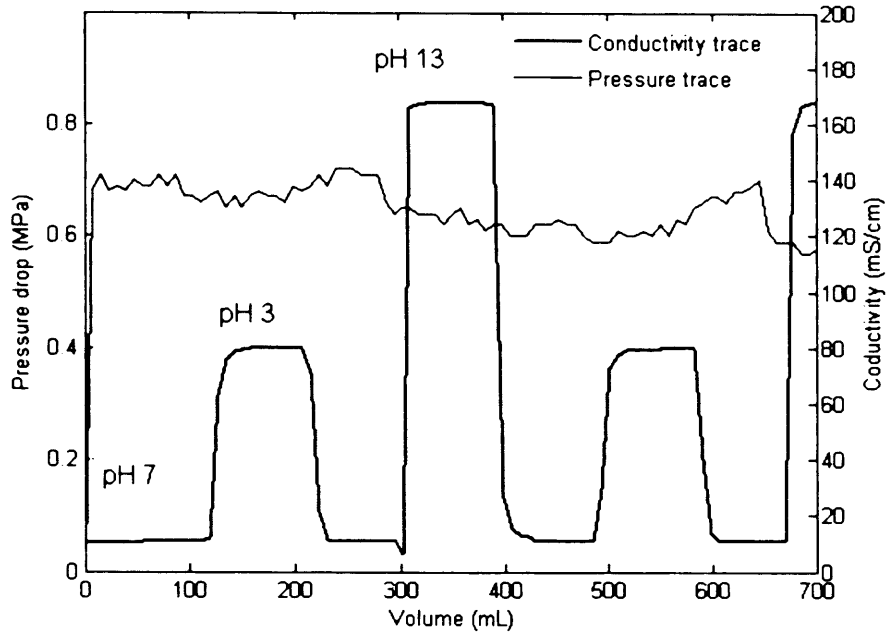

(a)

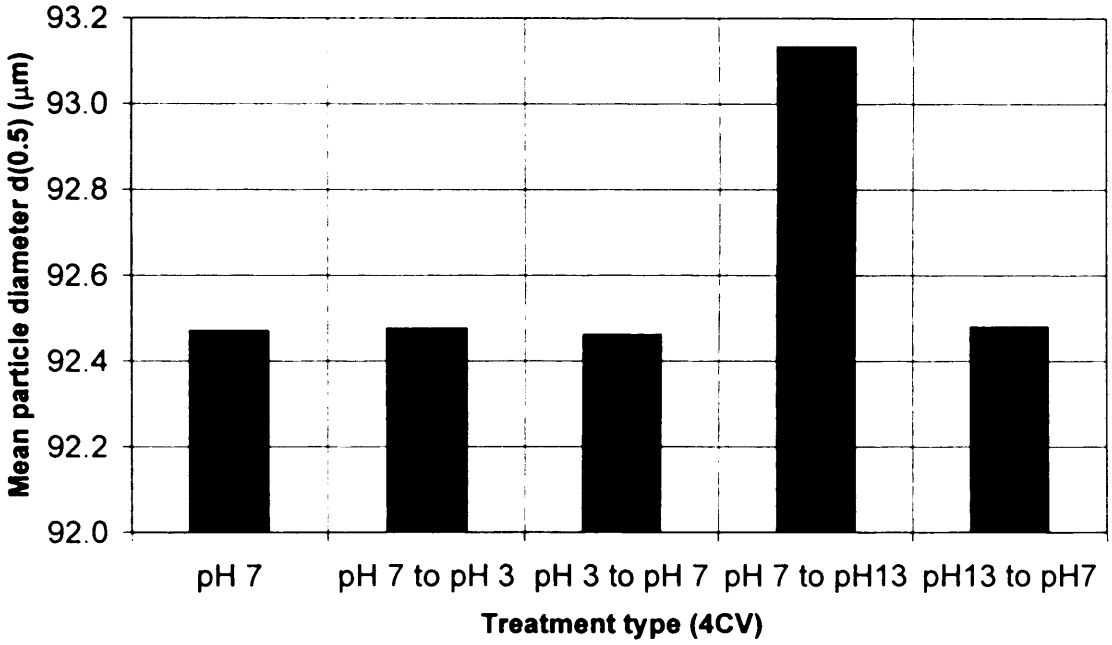

(b)

Figure 4.8 (a) Pressure and conductivity traces for blank buffer runs during typical chromatographic operation when using resin Z_{Ap4}. One cycle consisted of (4CV pH 7 buffer, 4CV pH 3 (+ 1M NaCl) buffer, 4CV pH 7 buffer, 4CV 1M NaOH). **(b)** Particle size (d_{50}) measurements of resin Z_{Ap4} during one cycle of operation.

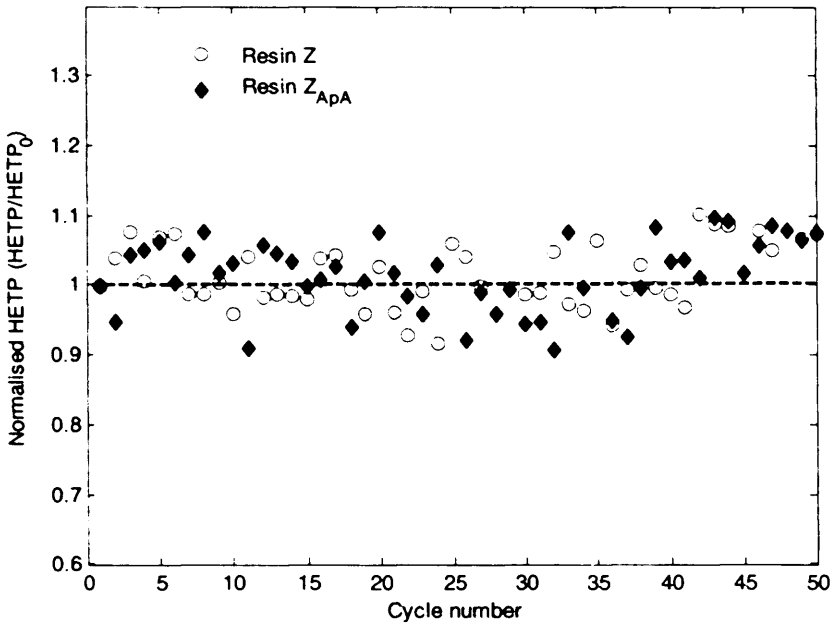

(a)

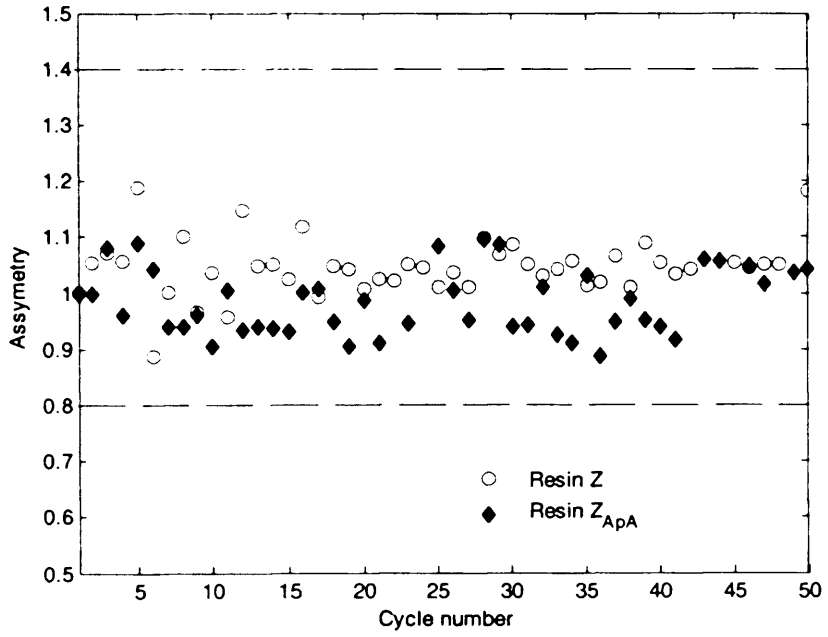

(b)

Figure 4.9 (a) HETP and **(b)** asymmetry values for the Z_{ApA} resin over 50 continuous cycles of operation. Bed dimensions were D=0.016m, L_{packed} ~0.11m. Flowrate of operation was 3.33x 10^{-4} m/s. Bold dashed line in **(a)** shows initial HETP value of a fresh bed after packing. Dashed lines in **(b)** are to demonstrate the maximum and minimum requirements of asymmetry outlined by the vendor.

as it has already been demonstrated that there is negligible particle distortion of the agarose base with any of the buffer types used in this study. The presence of the *ApA* ligand reduces bead porosity and therefore retards the flow of unretained NaCl molecules that provided for the step change used in the evaluation of HETP (Section 4.3).

The HETP levels that can be achieved with the derivatised resin are much lower than those that can be attained by the base resin. Therefore, variation in HETP throughout operation was normalised against its value from the first cycle of operation so as to provide for a better comparison in performance between the two resins tested. It can be seen that the HETP values of both resins remain fairly consistent over the runs shown, indicating that there is no degradation in column efficiency over multiple uses. Asymmetry values shown in Figure 4.9 (b) are also quite stable and well within the vendor specified limits, as indicated by the dashed horizontal lines. Figure 4.10, however, shows variability in particle diameter of beds tested after a number of cycles. While there was no trend in the variation of particle diameter with operation time, it was reasoned that the constant change in bead structure could impact the mechanical stability of the resin. Packed bed systems were cycled to varying degrees, after which the resins were then un-packed and re-suspended. The re-suspended slurries were then gravity packed into columns and the u_{crit} of the resulting beds were tested. Figure 4.11 shows the results of this analysis.

It can be observed that the critical velocity of both resins decreased with operation time. The critical velocity of resin Z decreased by less than 1% of its original value after operation with 20 cycles. u_{crit} did not drop further despite longer operation. The drop suggests some degradation in mechanical stability over time. u_{crit} for Z_{ApA} was observed to drop by the same degree after 20 cycles. However, u_{crit} continued to decrease further with increasing cycles of operation and dropped by almost 5% after 50 cycles of operation. This suggests that continuous variation in particle size caused by physicochemical interactions impacts on the structure and hence mechanical stability of the packed bed.

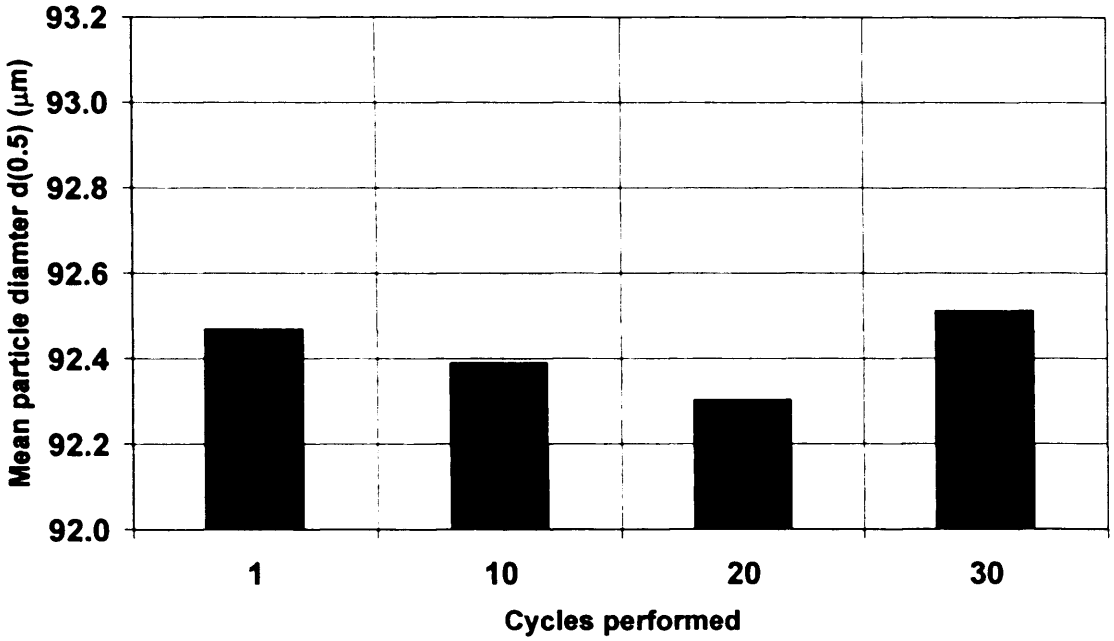

Figure 4.10 Mean particle size (d_{50}) measurements of resin Z_{ApA} after completion of a specified number of cycles of operation. Bed dimensions were D=0.016m, L_{packed}~0.11m. Flow velocity of operation was 3.33x 10^{-4} ms^{-1}.

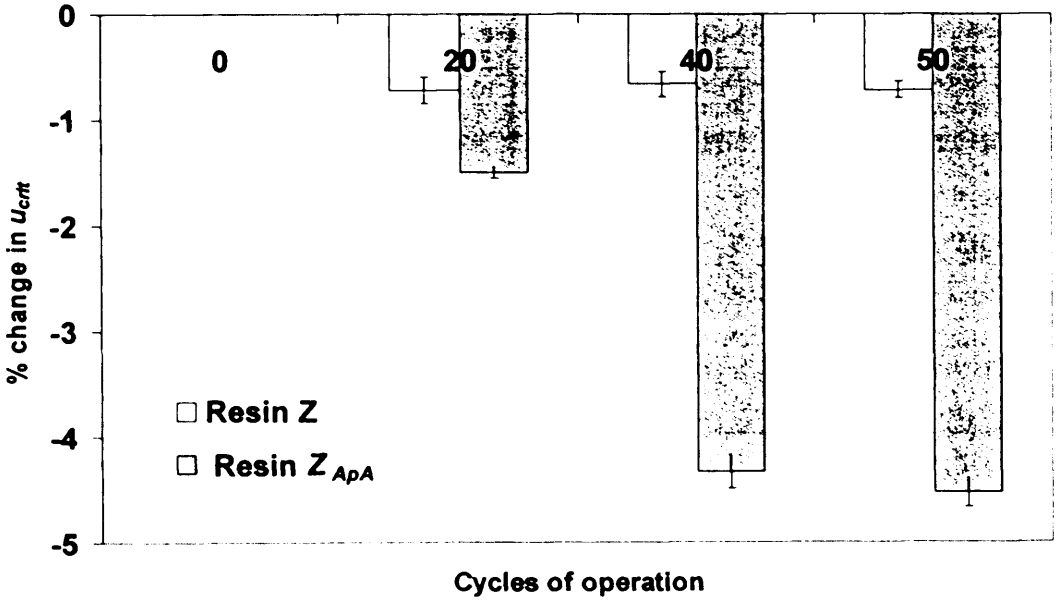

Figure 4.11 Variation in the critical velocity after a specified number of cycles of operation for resin Z and Z_{ApA}. Mobile phase used was phosphate buffer at pH 7. Results showed a relative standard deviation of 10-15%.

4.6 Conclusion

The impact of physicochemical interactions on the mechanical stability of a series of synthetic Protein A resins has been investigated. For the X_{ApA} resin critical velocity was reached much earlier during sanitisation using sodium hydroxide (NaOH) compared to when phosphate buffer at low and neutral pH was used. The reason for this was two-fold: (1) the increased viscosity of the hydroxide solution and (2) the ionisation of the artificial- Protein-A (*ApA*) ligand which caused resin particles to swell. The swelling reduced the rigidity of the bed significantly, particularly during scale-up. A second resin, Z_{ApA}, was developed based on a more rigid agarose base. Rigidity of Z_{ApA} was found to be approximately 7 times greater than that of X_{ApA}. The increased resin rigidity diminished particle expansion and, as such, produced a six-fold increase in packed bed compressive strength under highly alkaline conditions. Rigidity increases also allowed for more extensive cycling with this resin without pressure-drop becoming excessive. Traditional monitoring during column operation of height equivalent to a theoretical plate (HETP) and asymmetry (As) yielded no significant variations over 50 cycles of operation. However, it was found that resin particle diameter continuously changed throughout operation. Testing the mechanical stability of the bed after several cycles of operation showed a continuous drop in the critical velocity. This indicates a decrease in the rigidity of the resin particles which was not ascertained through HETP and As testing. This work demonstrates the importance of testing chromatographic bed stability with all the buffers types used during operation. It has also shown that the mechanical stability of the bed should be validated for the number of cycles that it must process, as bed rigidity reduces with time.

Clearly limitations of rigidity and bed stability on scale-up will impact both the economics and throughput of chromatographic systems. The next chapter outlines a framework which integrates these factors, providing for a model which will help the designer select the most productive and economic chromatographic design for a specified process duty.

5 THE DEVELOPMENT OF AN INTEGRATED FRAMEWORK FOR ASSESSING THE SOLUTIONS IN CHROMATOGRAPHIC PROCESS DESIGN IN LARGE SCALE MANUFACTURE

5.1 Introduction

The investigation and discussion to this point has revolved around the limits of initial capture chromatography operation. Chapters 3 and 4 have described how column hydrodynamics and physicochemical effects on resin structure can limit the maximum productivity that can be attained in some large-scale chromatographic systems. However, productivity is often not the sole concern at process scale. Protein A stationary phase media are almost a magnitude more expensive as compared to traditional chromatographic media with non-proteinaceous ligands (Ghose *et al.*, 2006). Furthermore, requirements for efficient cleaning and lack of alkaline stability place additional constraints on the Protein A system, requiring an integrated approach to designing such a process.

This chapter demonstrates a framework for the design and analysis of chromatographic steps. Particular focus is placed on addressing issues of scale-up, column sizing as well as overall process concerns such as scheduling and product degradation. The functionalities are illustrated by application to a Protein A separation where the effects of column diameter, bed length and linear flow rate on cost of goods (COG/g) and productivity (g/h) are investigated so as to identify the optimal operating strategy. The scope of the framework is indicated in Section 5.2. Section 5.3 describes the approaches undertaken in simulating the chromatographic data to be used. Section 5.4-5.5 details the productivity and cost models developed in this study. Section 5.6 describes how resin degradation is to be modeled and how this translates into a finite resin lifetime. The key features and components of the simulation tool are identified in Sections 5.7-5.10. A general overview of the tool structure is presented in Section 5.11. Finally a summary is provided in Section 5.12.

5.2 Scope of framework

Historically most chromatographic purification processes tend to be optimised empirically. Strategies used for the selection of column size chiefly utilise the experience of the design engineer combined with a few simple scale up rules (Gu *et al.*, 2003). Separation media and running conditions are selected according to the expertise of the person responsible (Geisow, 1992). Such approaches tend not to be systematic and can prove very time consuming, relying heavily on the use of expensive pilot-plant facilities in which to test out proposed new processes. As production technologies for new drugs become progressively more complex, rapid process development will be needed to enhance manufacturing operations by shortening time lines and reducing the cost of goods. Computer-aided tools can help to facilitate this.

Excellent models exist to describe the behaviour of small-scale chromatographic systems that account for the dynamics of column behaviour during the column loading, washing and eluting stages (Gu, 1995; Gu *et al.*, 2003; Guiochon *et al.*, 2003; Karlsson *et al.*, 2004). However the performance and chromatographic efficiency of small scale columns can be significantly different from production scale leading to complicated and uncertain scale up. A key issue for columns packed with deformable materials is media compression (Keener *et al.*, 2002, 2004a, 2004b), which can compromise chromatographic resolution. Furthermore, bed compression limits the maximum operational flowrate (Chapter 3). Current chromatographic separation models fail to account for this.

Significant effort has been devoted in the past towards optimisation of the chromatographic unit operation (Cowan *et al.*, 1989; Felinger *et al.*, 1994; Mao *et al.*, 1996; Fahrner *et al.*, 1999a; Larson *et al.*, 2003; Karlsson *et al.*, 2004; Ghose *et al.*, 2004; Keener *et al.*, 2002, 2004a, 2004b) where assumptions on resin characteristics and column properties were often made. Results from such studies are limited to solutions for particular aspects of the chromatographic process. To achieve high overall process efficiency requires a more integrated approach to design. This is because the process performance of a column will be altered by the interactions that exist between parameters in the chromatographic process and the other unit

operations within a sequence. Little work has been published on the use of chromatographic models in such an overall process design. Previous work has focused more on the optimisation of a single cycle chromatographic step and consideration of the individual concerns relating to chromatographic scale-up. Nevertheless a few attempts to tackle particular characteristics of chromatographic process design and operation have been made, of which a few interesting examples are given below.

Work has focused on column optimisation in terms of productivity, usually through the use of differing loading strategies (Ghose *et al.*, 2004). Since chromatography media tend to be expensive, rather than designing a column to be large enough to process a batch in a single cycle, use of a smaller column for several cycles to purify a single batch is often made. Such cycling tends to increase the total purification time and decreases the productivity (Felinger *et al.*, 1994; Fahrner *et al.*, 1999a) but makes better use of expensive media.

Fahrner *et al.* (1999a) discuss the importance of locating the optimal flowrate and bed length for chromatography and suggest that higher flow rates will reduce process times. However, as noted above, with large scale processes the permissible flowrate and bed length is considerably constrained by the effect of media compression. Especially for the case of mammalian cell cultivation with extended culture protocols of 5 to 15 days, it may be more viable to select small diameter chromatography columns which are cycled frequently and hence used intensively to process a single batch. This has the additional virtue of avoiding extensive periods of downtime when the column is idle. Adopting such a strategy emphasises the importance of column scheduling in order to realise the greatest gains and productivity. Unlike fermentation which, due to the nature of cell growth, is run constantly for 24 hours a day until the desired end point is reached, downstream processing are often scheduled to fit with shift patterns so that they can be monitored. Cycles of chromatographic operation must therefore be fully completed within the allocated DSP period available in each working day. The exception is column clean-in-place (CIP) procedures and sanitization which can be left unsupervised overnight.

To complicate the design issue still further, binding capacity degradation and ligand leakage can have a profound affect upon the performance of matrices, especially immunoadsorbant systems such as Protein A (Hunt *et al.*, 2001). To fulfill regulatory guidelines whilst working in a multi-cycle environment, CIP procedures become part of the master method for chromatographic column operations (Burgoyne *et al.*, 1993). These CIP treatments intrinsically cause capacity loss in the adsorbents (Boschetti, 1994) which therefore have finite lifetimes defined in term of the maximum number of possible re-uses. It is the binding capacity of the adsorbent over its entire working life that defines the true operating cost and which must be considered in any economic evaluation. With the complexity inherent in overall chromatographic process design, model-based computational tools become indispensable.

This section describes an integrated framework based on the use of a verified mathematical model for characterising a chromatographic step both in terms of its process and economic performance so as to address issues of scale-up, column sizing and column scheduling.

5.3 Simulating chromatographic data

Mathematical models for description of the chromatographic separation process have been around since the early 1940s (Wilson, 1940; Martin *et al.*, 1941; DeVault, 1943). They are now considered to be beneficial for the design and optimisation of purification steps. The general rate model solved by Gu and co-workers (Gu *et al.*, 1995) was chosen to provide the chromatographic data to be studied and offers a compromise between model complexity and ease of use (Chase, 1984; Guiochon *et al.*, 2003). The model uses two mass balance equations; one in the mobile phase outside the resin particles of the stationary phase and the other in the stagnant mobile phase inside the resin particles. These can be derived from the equations of continuity given by Bird *et al.* (1960). Also there are two kinetic equations, one relating the two mobile phase concentrations (mass transfer kinetics), the other relating the stagnant mobile phase and the stationary phase concentrations (kinetics of adsorption – desorption).

5.3.1 Formulation of Up-take kinetics

The transport of a solute within a spherical particle was described by a pore diffusion model (Arve *et al.*, 1987; Weaver *et al.*, 1996; McCue *et al.*, 2003) in this study. According to this model, mass transfer is assumed to be affected by two resistances in series: the external film resistance and the intraparticle mass transfer resistance (Tsou *et al.*, 1959; Arve *et al.*, 1988; Horstman *et al.*, 1989; Skidmore *et al.*, 1990; Tongta *et al.*, 1994; Weaver *et al.*, 1996; Hunter *et al.*, 2000; Quinones-Garcia *et al.*, 2001). For the case of Protein A media, it has been shown that intraparticle diffusion and film mass transfer govern the overall mass transfer resistance, while contribution from reaction kinetics is not significant (Horstman *et al.*, 1989; McCue *et al.*, 2003). The following conservation equation can be written to relate these two transport resistances:

$$(1-\varepsilon_p)\frac{\partial q_s}{\partial t}+\varepsilon_p\frac{\partial C_p}{\partial t}-\varepsilon_p D_{eff}\left[\frac{1}{R^2}\frac{\partial}{\partial R}\left(R^2\frac{\partial C_p}{\partial R}\right)\right]=0 \qquad \textbf{(5.1)}$$

where q_s is the solute concentration in the particle's solid (on a pore-free volume basis), a function of both radial position (R) and time (t). C_p is the solute concentration in the pore fluid, ε_p is the particle porosity and D_{eff} is the effective diffusivity.

5.3.1.1 Solid phase concentration profile

The average concentration in the stationary phase, C_p for a spherical particle can be defined through a mass balance as:

$$C_p=\frac{3}{R_p^{\,3}}\int_0^{R_p}C_p\,\varepsilon_p\,dr \qquad \textbf{(5.2)}$$

where R_p is the distance from the centre of the particle to its boundary. In this model it is assumed that intra-particle mass transfer occurs by diffusion in liquid-filled pores with a driving force expressed in terms of the pore fluid concentration gradient.

The adsorbed protein is assumed to be in equilibrium with that in the pore fluid at each radial position within the particle (Weaver *et al.*, 1996).

Equilibrium between the pore fluid and the solid phase concentrations in affinity systems can be modelled using a Langmuir isotherm (Chase, 1984; Ghose *et al.*, 2004) which is expressed by:

$$q_s = \frac{Q_{max}\, C_p}{K_d + C_p} \qquad \textbf{(5.3)}$$

where Q_{max} is the monolayer capacity and K_d is the Langmuir equilibrium dissociation constant. The above equations can be solved subject to initial and boundary conditions. The initial concentration in the particle's core is given by:

$$\text{At } R = 0, \qquad \frac{\partial C_p}{\partial R} = 0 \qquad \textbf{(5.4)},$$

$$\text{At } t = 0, \qquad C_p\,(0,R) = 0 \qquad \textbf{(5.5)}$$

At the boundary of the particle, R_p, taking a balance of mass flux at the particle interface gives:

$$\text{At } R = R_p, \quad \frac{\partial C_p}{\partial R} = \frac{k_f}{\varepsilon_p D_{eff}}\left(C_b - C_{p,R=R_p}\right) \qquad \textbf{(5.6)}$$

5.3.2 Column Behaviour

The differential mass balance equation over the packed bed column can be written as:

$$-D_b \frac{\partial^2 C_b}{\partial Z^2} + v\frac{\partial C_b}{\partial Z} + \frac{\partial C_b}{\partial t} + \frac{3k_f(1-\varepsilon_b)}{\varepsilon_b R_p}\left(C_b - C_{p,R=R_p}\right) = 0 \qquad \textbf{(5.7)}$$

where, C_b is the solute concentration within the bulk fluid phase and is a function of axial position, Z and time t. ε_b is the void fraction of the bed, D_b is the axial diffusivity and v is the interstitial velocity. The various terms in Equation (5.7) account for axial dispersion, convective transfer of the solute, accumulation in the interstitial spaces and solute uptake in the porous beads respectively. Assuming there is no protein in the column in the beginning, the initial conditions can be written as follows:

At $t = 0$, $\qquad C_b = C_b(0, Z)$ **(5.8 (a))**

$$C_p = C_p(0, R, Z) \qquad \textbf{(5.8 (b))}$$

In order to include axial dispersion at the inlet of the column and mixing at the exit of the column, the Danckwerts' (Danckwerts, 1953) boundary conditions are used:

$$Z = 0, \quad \frac{\partial C_b}{\partial Z} = \frac{v}{D_b}\left(C_b - C_0(t)\right) \qquad \textbf{(5.9)}$$

$$Z = L, \quad \frac{\partial C_b}{\partial Z} = 0 \qquad \textbf{(5.10).}$$

In general, axial dispersion should be considered at the entrance of the column because a steep first order spatial gradient exists there (Sridhar *et al.*, 1994). When axial dispersion is insignificant, Equation (5.8a) reduced to $C = C_0$ at the entrance, which is the case of a step input.

Formulation of the model is subject to the following basic assumptions: (1) the column is isothermal, (2) the packing particles are considered spherical and possess the same size, (3) the diffusion in the radial direction is negligible, (4) there is no convective flow inside particle macro pores, (5) the packing density is even along the column length, and (6) the mass transfer and kinetic parameters are constant.

The shape of the chromatographic profile is thus determined by the equilibrium isotherm (Equation 5.3), transport within the particle (Equation 5.1), film mass transfer (Equation 5.6) and deviations from plug-flow in the column (Equation 5.7). The solution of the equations for the model was achieved via orthogonal collocation on finite elements (Gu, 1995). Figure 5.1 shows a schematic of the strategy of the numerical method used to solve the PDE system in the model. The bulk fluid phase particle phase equations are first discretised using the finite elements and orthogonal collocation methods respectively. Following discretisation, the resulting system of differential equations was numerically integrated using the MATLAB (The Mathworks Inc., Natick, MA, USA, 2004) routine ODE15s. This routine uses a quasi-constant step size implementation of numerical differentiation formulas in terms of backward differences. The model describes the change of adsorbate concentration with time in the mobile phase, which is a function of the flowrate at which the mobile phase is pumped through the column.

5.3.3 Parameter estimation for the rate model

Experimental data from process-scale chromatographic beds are not often reported in the literature because of issues of commercial sensitivity. Therefore, the adsorption behaviour of large-scale columns has historically been studied largely from model simulations based on data acquired using small-scale laboratory columns. Parameters for a chromatography model may be divided into two types. Physical dimensions such as column length and diameter can be easily measured with precision. Binding parameters, bed void volume fraction and particle porosity are not readily available but may be determined experimentally. In this work existing

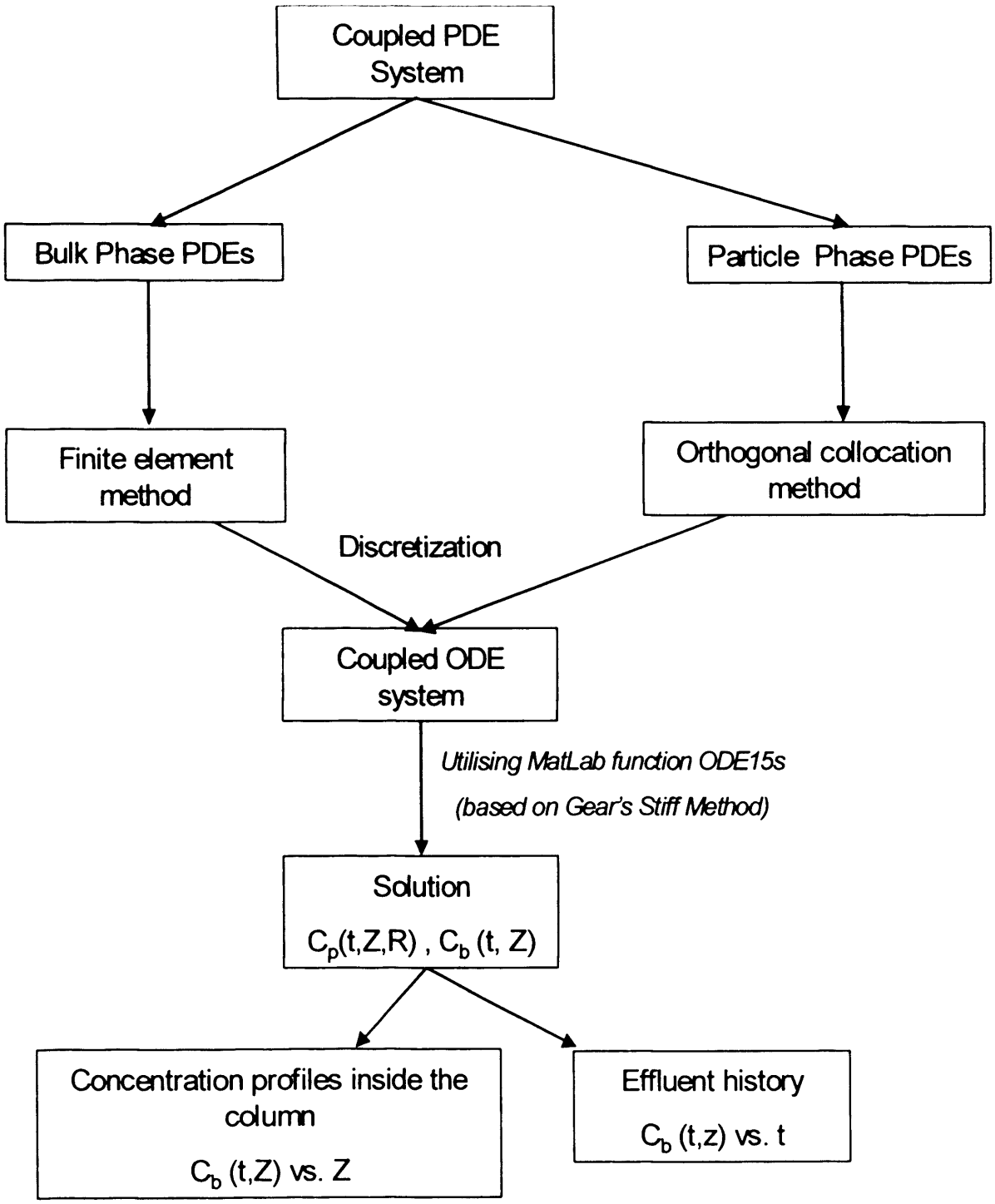

Figure 5.1 Schematic flowchart showing the solution methodology used to solve the General Rate model.

correlations and previously published data were used to determine the values of the latter group of parameters. The correlations used in the model are listed in Table 5.1. The comparison of calculated and experimental breakthrough can be used in the validation of mathematical models and in extracting system parameters for further simulation (Chase, 1984). Mass transfer and some physical parameters were estimated through the fitting of this data to the general rate model using a nonlinear unconstrained optimisation routine FMINSEARCH in the MATLAB (The Mathworks Inc., Natick, MA, USA, 2004) programming environment. (Literature and fitted data for the adsorptions described in this thesis can be found in Appendix B.)

The results of the parameter estimation for the resins used throughout this study are given in the Tables 5.2-5.4 below. The value of effective diffusivity (D_{eff}) obtained from the model fittings was approximately 4-5 x 10^{-8} cm^2/s for the agarose based resins, rProtein A Sepharose FF™ and MabSelect™. This is of the same order of magnitude found by experimental work performed by Ghose *et al.*, (2004) and Tscheliessnig *et al.*, (2004) who found D_{eff} to be approximately 4-8 x 10^{-8} cm^2/s for MAb and Fc-fusion proteins binding onto the MabSelect™. Furthermore, the fitted values were even closer to those found by Hahn *et al.* (2005) who reported values between 3-5 x 10^{-8} cm^2/s for concentrations of IgG in between 1-3g/L binding onto MabSelect™. D_{eff} for the controlled pore glass (CPG) based resin, Prosep vA® Ultra, was found to be approximately 5.7 x 10^{-8} cm^2/s. This value is in the same range as reported by other authors (McCue *et al.*, 2003) who have reported D_{eff} values in the range of 0.3-5.0 x $10^{-9}cm^2/s$ for IgG binding to porous glass based Protein-A media.

The film mass transfer coefficient (k_f) at different linear flow velocities was found to be between 7 – 15 x 10^{-4} cm/s for all media depending on the value of linear velocity chosen (50-500 cm/h). These values agree well with those of Hahn *et al.* (2005) who found k_f to be between 2-2.5 x 10^{-3} cm/s from shallow bed experiments when IgG solutions were passed through both agarose and CPG columns at a velocity of 1250 cm/h. However, these values are an order of magnitude larger than those reported (Ghose *et al.*, 2004; Hahn *et al.*, 2005) from experiments conducted in batch systems.

Table 5.1 Correlations used to determine process parameters used in the general rate model.

Parameter	Correlation	Reference
Q, Volumetric flowrate	$\frac{v.CV.\varepsilon_b}{L}$ (CV denotes column volume)	Gu *et al.*, (2003)
D_{eff}, Effective intraparticle diffusivity	$\frac{D_m(1-2.104\lambda+2.09\lambda^3-0.95\lambda^5)}{\tau_{tor}}$	Yau *et al.*, (1979)
λ	d/dp (d_p is the particle pore diameter).	Yau *et al.*, (1979)
τ_{tor}, Tortuosity factor	Lies between 2-6	Gu *et al.*, (1995)
d, molecular diameter of the solute	$1.44MW^{1/3}$	Gu *et al.*, (1999)
D_m, molecular diffusivity	$2.74\times10^{-5}MW^{-1/3}$	Gu *et al.*, (2003)
k_f, film mass transfer coefficient	$0.687v^{1/3}\left(\frac{\varepsilon_b R_p}{D_m}\right)^{-2/3}$	Wilson *et al.*, (1966)

rProtein A Sepharose FF™

Table 5.2 Model parameter values for the adsorption of a MAb to the rProtein A Sepharose FF™ resin.

Parameter	General data	IgG	Reference
Resin particle radius, r_p (cm)	0.0045		rProtein A Sepharose FF data sheet found at www.gelifesciences.com , (2004)
Pore diameter, d_p (A)	300		fitted
MW (g/mol)		150000	Persson *et al.* (2004)
ε_b	0.42		Gu *et al.* (2003)
$\varepsilon_{p\ effective}$	0.6		Gu *et al.* (2003)
External film mass transfer, k_f (cm/s)		0.0015	fitted
Effective diffusivity, D_{eff} (cm^2/s)		4×10^{-8}	fitted
Dissociation constant, K_d (g/L)		0.2	Hahn *et al.* (2003)
Saturation capacity, Q_{max} (g/L)		50.2	Hahn *et al.* (2003)

MabSelect ™

Table 5.3 Model parameter values for the adsorption of a MAb to the rProtein A MabSelect™ resin.

Parameter	General data	IgG	Reference
Resin particle radius, r_p (cm)	0.00425		MabSelect data sheet found at www.gelifesciences.com, (2005)
Pore diameter, d_p (A)	440		estimated [a]
MW (g/mol)		150000	Persson *et al.* (2004)
ε_b	0.41		Gu *et al.* (2003)
$\varepsilon_{p\ effective}$	0.52		Hahn *et al.* (2005)
External film mass transfer, k_f (cm/s)		0.0016	fitted
Effective diffusivity, D_{eff} (cm^2/s)		5×10^{-8}	fitted
Dissociation constant, K_d (g/L)		0.12	Hahn *et al.* (2005)
Saturation capacity, Q_{max} (g/L)		61.2	Hahn *et al.* (2005)

[a] based on discussions with K. Lacki, GE Healthcare Biosciences, Uppsala, Sweden, 2006.

Prosep vA Ultra®

Table 5.4 Model parameter values for the adsorption of a MAb to the Prosep vA Ultra® resin.

Parameter	General data	IgG	Reference
Resin particle radius, r_p (cm)	0.005		Hahn *et al.* (2005)
Pore diameter, d_p (A)	700		http://www.millipore.com/catalogue.nsf/docs/C7842 (2006)
MW (g/mol)		150000	Persson *et al.* (2004)
ε_b	0.43		Hahn *et al.* (2005)
$\varepsilon_{p\ effective}$	0.46		Hahn *et al.* (2005)
External film mass transfer, k_f (cm/s)		0.0014	Fitted
Effective diffusivity, D_{eff} (cm^2/s)		5.7×10^{-8}	Fitted
Dissociation constant, K_d (g/L)		0.116	Hahn *et al.* (2005)
Saturation capacity, Q_{max} (g/L)		62.8	Hahn *et al.* (2005)

5.4 Productivity model

The general rate model was used to simulate the loading and washing stages of a chromatographic process at varying loading volumes. A mass balance was performed around the column in order to calculate the amount of protein bound, lost and recovered. The number of cycles required to process an assumed quantity of material can be calculated.

The number of cycles required to process a batch of material is a function of the dynamic binding capacity and is given by:

$$N = \frac{Mass\ to\ process}{DBC.CV} \qquad \textbf{(5.11)}$$

where N is the number of cycles, DBC is the dynamic binding capacity in (g/L) and CV is the column volume in (L).

The productivity, P, of the column can be defined as the mass of protein retained on the column after washing per volume of the adsorbent per unit processing time:

$$P = \frac{Yield \cdot (C_0 \cdot V_{load} - M) \cdot N}{T} \qquad \textbf{(5.12)}$$

the *Yield* or recovery ratio was defined as the mass of protein retained by the column after post-load washing as a percentage of the total mass of protein loaded:

$$Yield(\%) = \frac{Mass\ bound\ post\ wash}{Mass\ loaded\ onto\ column} \cdot 100 \qquad \textbf{(5.13)}$$

C_0 (g/L) is the protein concentration in the sample, V_{load} (L) is the volume of sample at the point where the specified breakthrough level is achieved. M (g) is the quantity of protein discarded before the breakthrough volume and T (h), is the time for which the column is in operation, where:

$$T = Nt_c \qquad \textbf{(5.14)}$$

N denotes the number of cycles taken to process a given amount of material and t_c is the cycle time. t_c incorporates the sum of the times for (i) the equilibration stage, (ii) the loading stage, (iii) the washing stage, (iv) the elution stage and (v) the CIP stage (Yamamoto *et al.*, 1992).

Column CIP was assumed to take place after every cycle. Column sanitisation was also assumed to take place overnight after every processed batch of material. In addition to this, column process time usually includes a fixed overhead associated with preparation and completion of the operation, hence:

$$T = Nt_c + t_P + t_F \qquad \textbf{(5.15)}$$

where t_p is the preparation time before the first load and t_F is the clean up time after the final cycle.

Purity of the eluate was calculated based on a step elution assuming negligible losses. Purity was estimated through:

$$Purity\ (\%) = \frac{Mass\ product\ recovered}{Mass\ product\ recovered + Mass\ contaminant\ recovered} \cdot 100$$

(5.16 a)

$$Impurity\ (ppm) = \frac{Mass\ contaminant\ recovered\ (mg)}{Mass\ product\ recovered\ (kg)} \qquad \textbf{(5.16b).}$$

5.5 Cost models

5.5.1 Fixed capital investment

Multiplying the total equipment purchase cost by a factor, usually termed the 'Lang Factor', provided a rapid order-of magnitude estimate of the fixed capital cost. A cost equation summarising this technique is given as:

$$C_{\$\,Col+rig} = f_L\, C_{\$\,E} \qquad \textbf{(5.17)}$$

where, $C_{\$\,Col+rig}$ is the total cost of the chromatography column and skid, $C_{\$\,E}$ is the equipment cost and f_L is the Lang factor. In addition to equipment cost, the Lang factor accounted for cost factors relating to items such as piping, instrumentation, electrical work, buildings, utilities and site preparation as well as design and engineering costs and contractors fees. The value of the factor depends on the type of plant. For chemical engineering facilities, values in the range of 3-5 are often recommended (Peters *et al.*, 1991; Sinnot, 1993). Examples of capital cost breakdowns in the literature (Hamers, 1993; Osborne, 1997; Nelson, 1998) have suggested factors in the range of 6-7 as more typical for biopharmaceutical plants. In addition, discussions with industrial experts have indicated that factors in the range of 4-7 are more suitable for the biopharmaceutical sector (A. Sinclair, BioPharm Services, Bucks, UK, personal communication).

A key stage in calculating the capital investment for a production plant is determining the total equipment purchase cost ($C_{\$\,E}$). An estimate of the cost of new equipment can be obtained from a known cost for that type of equipment and the ratio of their capacities raised to an index value. The cost is related to the capacity by the following equation:

$$C_2 = C_1\left(\frac{Q_2}{Q_1}\right)^n \qquad \textbf{(5.18)}$$

where n = index value,

C_2 = cost of equipment with capacity Q_2,

C_1 = cost of equipment with capacity Q_1.

Process engineers often use the well known six-tenths rule, where the value of n is traditionally taken as 0.6 (Sinnott, 1993). However, Remer and Idrovo (1991) warned against blind use of such exponent value and indicated exponential scaling factors for 58 different types of bioprocess equipment. This exponential method was used to provide an estimate of the investment likely to be required. The exponential index value used together with the purchase cost of known resources are tabulated in Table 5.5. The cost inputs together with the index value were determined from industrial experts and vendor sources (e.g. BioPharm Services, Prometic Biosciences, GE Healthcare). The costs of related resources in subsequent case studies were calculated based on these cost estimation factors.

Table 5.5 Base cost data for fixed capital investments. (Costs were estimated based on discussions A. Sinclair, BioPharm Services, Bucks, UK.)

Equipment	*n* (index value)	Base cost, C_1 ($)	Base capacity, Q_1
Stainless-steel column	0.7	20000	45 L
Chromatography skid	0.07	180000	3 L/min

5.5.2 Cost of goods model

As has been stated in Chapter 1, a significant percentage of the total manufacturing cost of therapeutic antibodies is incurred during purification (Myers, 2002). When used, Protein A dominates this and can account for up to 10% of the

overall cost of goods per gram (COG/g) for a given bioprocess (Rouf *et al.*, 2001). The chromatographic costs alone can therefore reflect how the process-wide COG/g fluctuates depending on the column strategy chosen and a suitable estimate for the overall cost of a MAb production process. It would be useful to be able to estimate the exact COG/g associated with different processing strategies. For this study COG/g was calculated as a function of the chromatographic step alone and is therefore referred to as a COG/g $_{specific}$.

The cost of goods was defined as the manufacturing cost, thus excluding general expenses such as sales and administration costs. The direct and indirect/fixed overheads were derived as a function of the capital investment for the column together with its assembly in the plant. The direct costs were computed based on the utilisation of resources such as materials, utilities and staff. Since the tool was intended for evaluating the effects of different production strategies it was found to be more useful to base labour costs on their utilisation over the production campaign rather than considering them as a fixed annual salary-based cost. Costs for quality staff was increased compared to those assumed to work in production, to reflect the higher burden on quality control activities in the biopharmaceutical industries.

According to Sinnott (1997), the annual cost of laboratory analyses required for process monitoring and quality control (Qc/Qa) is roughly 20-40% of the operating labour cost. For this analysis, it was assumed that Qc/Qa represented 40% of the cost of operating labour. Buffer costs were determined as a function of volume used per cycle over the production campaign. Table 5.6 outlines the base cost data for the direct resources used in the subsequent case studies. As such the COG/g $_{specific}$ was defined by:

$$COG/g_{specific} = \frac{T \cdot c_{\$time} + c_{\$Col+rig\,dep} + [N_{cycles} \cdot c_{\$buffer} + \frac{c_{\$resin}}{N_{life}}] \cdot CV}{Mass\ of\ product\ recovered} \qquad \textbf{(5.19)},$$

where $C_{\$\ time}$, is the cost per hour of labour which is a function of column operator costs and Qc/Qa personnel costs. $C_{\$\ buffer}$ is the cost per litre of buffer solution used

and $C_{\$\ resin}$ is the cost per litre of resin used during processing. N_{life} is the resin lifetime in terms of maximum number of reuses. $C_{\$Col+rig\ dep}$ is the depreciation cost of the column skid and rig calculated as a percentage of the initial fixed cost outlay of the stainless steel chromatography column and skid ($C_{\$\ col+rig}$) (Farid, 2001; Lim, 2004) .

5.6 Resin degradation

One of the factors that impacts greatly on the cost of the affinity process is the functional lifetime of the resin. The initial cash outlay for a Protein A chromatographic resin can represent a substantial investment. If the resin can be recycled the costs per gram of final product will decrease (Sofer, 1987). Resin life can be maximized through conscientious maintenance. Sample preparation to remove particulates, use of proper equipment and steps to maintain system hygiene can all lead to lifetimes of hundreds of cycles. CIP procedures for a packed bed column are usually performed through washing with a solution of sodium hydroxide to solubilise lipids or precipitated proteins which remain bound to the resin. However, often as a consequence of the CIP conditions required to regenerate a column, binding capacity decreases during multi-cycle processes. This is generally attributed to ligand leakage or inactivation caused by the harsh high pH cleaning protocols. The choice of CIP protocol used is dependent on the extent of resin fouling introduced through the feed material loaded.

The results of an extensive cleaning cycle study of the rProtein A media MAbSelect (Johansson *et al.*, 2002) was used to develop a resin degradation function. The degradation function was derived through the assumption that the maximum saturation capacity of the resin, $Q_{max,}$ decreases during the CIP procedure as binding sites becomes unavailable. The dissociation coefficient, K_D was assumed to remain unaffected during the cleaning process. It is the number of potential binding sites that is affected by the hydroxide solution and not the affinity of the Protein A ligand. The rate model was modified to account for this diminishing Q_{max}

Table 5.6 Cost input data for all the direct resources used in the subsequent case studies; (b) data found from GEHealthcare Biosciences product catalogue (**www.gelifesciences.com**, 2007); (c) data found from Millipore Inc., product catalogue (**www.millipore.com/catalogue.nsf/home**, 2007); (d) data extrapolated from Sigma Aldrich product catalogue (**www.sigmaaldrich.com**, 2007).

Resource	Cost ($)	Reference
Materials		
rProtein A Sepharose Fast Flow resin	7459.60/L	(b)
MabSelect resin	8895.60/L	(b)
MabSelect SURE resin	12500/L	(b)
Prosep vA Ultra resin	14606/L	(c)
Pseudo resin (Chapter 7)	10000/L	(Assumed)
Chemicals		
Equilibration/Load/wash/elution buffer (100mM Sodium Phosphate)	0.152 + WFI/L	(d)
CIP buffer – agarose based resins (250mM Sodium hydorixde + 1M NaCl)	0.28+ WFI/L	(d)
CIP buffer – CPG based resins (0.1M HNO_3)	1.8+WFI/L	(d)
CIP/Sanitisation buffer (6M Guanidine)	19+WFI/L	(d)
Sanitisation buffer (0.1 M acetic acid)	0.5+WFI/L	(d)
Staff		
Operator	25/h	Farid (2001)
Qc/Qa	40/h	Farid (2001)
Utilities		
WFI	3/L	Zhou *et al.* (2006)

through estimation of the rate of loss of binding capacity using a fitted equation of the form:

$$Q_N - Q_0 = \Delta Q = -\Phi N \qquad \textbf{(5.20)}$$

where Q_N represents the dynamic binding capacity of the system after N cycles in g/L, Q_0 denotes the initial binding capacity of the resin before use and Φ is the degradation coefficient found through least mean squared fit. Φ was determined from studies performed by Johansson *et al.*, (2002) in HR 5/10 columns packed with MabSelect. Loading proceeded to 10% breakthrough with a velocity of 336 cm/h. CIP buffer was 250mM NaOH + 1M NaCl. The experimental data used and subsequent fits can be found in Appendix B. (Equation (5.20) is probably not generic and more work would be needed to establish the form of the degradation function for any new resin and CIP procedure being examined but it is adequate for the stated purpose of developing an overall methodology.)

Further to the issue of resin degradation, flowrate also plays an important role in the determination of dynamic binding capacity (Fahrner *et al.*, 1999a, 1999d) and the overall time of chromatographic operation. In most chromatographic operations CIP flowrate is fixed to achieve a required residence time in the column; so that the column is exposed to the necessary level of cleaning to meet regulatory standards. In this work CIP procedures were assumed to have been carried out with a contact time of 15 minutes. (Johansson *et al.*, 2002).

5.6.1 Estimation of resin lifetime

Decreasing binding capacity caused by degradation, increases the cost of good per gram of processed product (COG/g) as less product is being adsorbed per cycle. Reusing the resin over an extended operational life may not be the most cost effective strategy to follow. It would be useful to be able to estimate the exact COG/g associated with different processing strategies.

The functional lifetime of a resin is determined by its ability over a given number of uses to produce material of acceptable quality and yield. The actual lifetime of a resin can be defined in many ways is largely dependent on the needs of the particular bio-manufacturing firm. The useful lifetime can be determined by such business decisions as resin cost, campaign length, storage cost, labour to pack columns, process downtime during packing and lost production if a new column is required in the middle of a campaign (O'Leary *et al.*, 2001). Clearly, understanding the relationship between resin lifetime and cost is very useful in the decision-making process and provides an indication as to when the resin should be replaced.

To acquire and accurate estimation as to the cost incurred during each cycle of operation, the operational COG/g per cycle was calculated through Equation (5.21):

$$COG/g_{specific}\ per\ cycle = \frac{c_{\$time_N} + c_{\$buffer_N} + (c_{\$resin} \cdot CV) + c_{\$Col+rig\ dep}}{Mass\ of\ product\ recovered_N} \qquad \textbf{(5.21),}$$

where $c_{\$\ time}$, is the cost per hour of labour, $c_{\$\ buffer}$ is the cost per litre of buffer solution used, $c_{\$\ resin}$ is the cost per litre of resin used during processing and N is the cycle number. A bio-manufacturing firm would find it useful to be able to estimate the exact specific costs that they are willing to incur for different processing strategies. Equation (5.21) should give an indication as to how the specific operational COG/g per cycle varies.

The costing approach described above can be further extended to evaluate the economic potential of reusing a resin. Economic potential can be described through an equation of the form:

$$Economic\ potential_N = (MAb_{recovered\ N} \cdot \$_{MAb}) - (Overall\ manufacturing\ \ cost_N + (MAb_{lost\ N} \cdot \$_{MAb})) \qquad \textbf{(5.22 a)}$$

where,

$$Overall\ manufacturing\ cost_N = \frac{COG_{specific}\ per\ cycle}{\%\ contribution\ of\ \text{Protein A}\ to\ the\ overall\ process\ cost}$$

(5.22 b),

$$COG_{specific}\ per\ cycle = c_{\$time_N} + c_{\$buffer_N} + (c_{\$resin} \cdot CV) + c_{\$Col+rig\ dep}$$

(5.22 c),

where $\$_{MAb}$ is the MAb selling price and N represents the cycle number.

The assumption here is that there is sufficient demand that all MAb recovered is sold providing for an estimate of potential revenues in an ideal setting. Therefore, a pseudo profit, represented by the economic potential, can be calculated through the estimation of total manufacturing process cost. If it is assumed that the costs of Protein A chromatography represents 8 % of the overall manufacturing process cost, then a suitable estimate can be made in terms of this quantity. Further to this, an additional penalty cost is added to the equation representing the potential losses in revenue caused by a low yielding process. Yields were assumed to be constant for the process train with the exception of the Protein A step and these assumptions are listed in Table 5.7. Equation (5.22a) should give an indication as to number of reuses which will provide the most economic potential to a firm and therefore provides an estimate of resin lifetime.

$\$_{MAb}$ in Equation (5.22a) refers to an estimate of the price of a typical monoclonal antibody ($/g) which is commercially available. $\$_{MAb}$ however, is not taken to be the full market price of the MAb. The market prices will reflect costs due to marketing, intellectual property, development costs as well as the cost of manufacture (Moscho *et al.*, 2003). Added to these is a suitable profit margin. The economic potential function (Equation 5.22a) however, is only representative of manufacturing costs and therefore, choice of selling price must also reflect this scenario to gain a more accurate insight into the profitability of the processing strategy. Moscho *et al.* (2003) state that for biotechnology companies, manufacturing costs are generally equal to 15% of sales with profit margins typically between 10-30% of sales. Selling price in this analysis was taken to represent the costs of

manufacturing in addition to profit margin. Therefore, $\$_{MAb}$ was assumed to be 25% of the commercial price of a typical monoclonal antibody. Calculation of commercial selling price was based on the patient dosage and costs of treatment.

For the cancer drug Avastin™, the cost of treatment to the patient on an annual basis was estimated to be $55,000 (www.nytimes.com, 2006). Patient dosage requirements are 5mg/kg fortnightly[c]. Assuming a typical patient body weight a commercial price estimate was calculated as $5300/g. Consequently, $\$_{MAb}$ was taken to be $1325/g.

5.7 Addition of an ultra-filtration step

The case study described in Chapter 6 shows how a change in the process flowsheet can impact the design and operation of the initial capture step. The study focuses on the integration of an ultra-filtration (UF) pre-concentrating step prior to initial capture. Most large-scale UF devices use tangential flow filtration (TFF), also referred to as a cross-flow configuration, in which the feed flow is parallel to the membrane and thus perpendicular to the filtrate flow (Blatt *et al.*, 1970). This allows retained species to be swept along the membrane surface and out the device exit, significantly increasing the process flux compared to that obtained with dead-end operation. A concentration boundary layer consisting of a high concentration of retained solutes typically develops at the upstream surface of the membrane. This highly concentrated region reduces the effective pressure driving force and can cause extensive membrane fouling from protein adsorption, denaturation, precipitation, or aggregation. The performance of many TFF systems is determined almost entirely by the rate or flux at which these retained solutes are transported away from the membrane and back into the bulk solution, a phenomenon referred to as concentration polarization.

Typical process fluxes in UF range from 25 to 250 $L/m^2/h$ (Van Reis *et al.*, 1999). In a TFF unit operation, filtrate flux increases with increasing pressure applied from the feed to the filtrate side of the membrane or trans-membrane

[c] (does taken from product labels available on www.fda.gov and www.emea.eu.it)

pressure (TMP). This increase proceeds up to a point and then it levels off. The initial increase can be attributed to fouled membrane resistance. The second regime, when flux begins to level with increasing TMP is caused by the concentration of protein at the membrane surface being high and therefore a significant portion of the applied pressure is working against the protein osmotic pressure. As protein concentration increases or feed flow rate decreases, the TMP at which the flux plateaus decreases. Therefore, for a standard UF process, the optimum flux at which to run a process is at the knee of the flux vs. TMP curve, where nearly the highest flux is achieved without exerting excessive pressure or reaching exceedingly high protein wall concentrations.

After determining the process flux and assuming that the total volume to be processed is known, the membrane area required for the final unit operation can be determined. However, since flux is filtrate flow rate divided by both area and time, the membrane area is also a function of the total process time. Choosing a longer process time leads to lower membrane area requirements. This is beneficial because membrane and capital costs are reduced. In addition, unrecoverable hold-up volume is lower in smaller unit operations, minimising yield losses. However, excessively long process times put the product at risk for quality degradation and/or bio burden contamination.

A cross-flow filtration model was required for concentration operations and is given through a simple mass balance across the unit operation shown in Equation (5.23):

$$CF = \frac{Mass\,to\,process}{Mass\,to\,process - \left(t_{filtration} \cdot flux \cdot A_m\right)} \qquad \textbf{(5.23)},$$

where, flux describes the rate at which solution flowed through the membrane. It is commonly measured in litres of permeate per square metre per hour (L/m^2 h). $t_{filtration}$

Table 5.7 Assumed process yields and processing times for unit operations in the assumed process train.

Unit operation	Process time	Yield (%)	Reference
Fed –batch culture	15 days	100	Assumed
Centrifugation	4 h	95	Farid (2001)
Dead-end filtration / Ultrafiltration	3 h / 6h	95	Farid (2001)
Affinity chromatography	Calculated	Calculated	
Virus inactivation	-	95	Taken from 'Virus clearance selection guide, Millipore Technical library, www.millipore.com/publications.nsf (2007)
Diafiltration 1	-	95	Farid (2001)
Ion exchange chromatography	-	95	Taken from Capto S data sheet found at www.gelifesciences.com (2007)
Virus removal filtration	-	95	Taken from 'Virus clearance selection guide', Millipore Technical library, www.millipore.com/publications.nsf (2007)
Diafiltration 2	-	95	Farid (2001)
Ion exchange/ Gel-filtration chromatography	-	95	Taken from Capto Q data sheet found at www.gelifesciences.com , (2007)
Final filtration	-	95	(Assumed)

is the process time for filtration to take place and A_m is the membrane area. For a specific membrane, performance could be rated in terms of the concentration factor (CF) achieved for the processing time ($t_{filtration}$) required; alternatively the membrane area (A_m) required to achieve a desired concentration factor within a set time could be found. Thus Equation (5.23) can be used to estimate equipment size in terms of rig and membrane area required to achieve a given level of performance. The costs associated with this unit operation are described in Table 5.8.

Membrane fouling is a critical factor in almost all UF processes. Fouling can occur because of protein adsorption, deposition, precipitation, denaturation, and aggregation, all of which affect membrane performance as well as product yield and quality (van Reis *et al.*, 1999). The rate and extent of fouling are determined by the morphological and chemical characteristics of the membrane, fluid mechanics in the module and buffer chemistry (Belfort *et al.*, 1994). Membrane cleaning or regeneration is performed whenever the flux or selectivity drop below some minimally acceptable level. In addition, membrane disinfection and sterilisation must be performed between process runs even in the absence of significant fouling. Chemical cleaning is performed using appropriate detergents, acids, alkalis, enzymes or chelating compounds. Alkali cleaners (NaOH) are particularly effective for removing biological foulant (Tragardh, 1989).

Filtration membranes in this study were assumed to be regenerated after each batch using a sodium hydroxide solution. Membrane lifetime is very much a process specific value however. Here, membranes were assumed to be replaced after every 10kg of product had passed through a square meter of membrane (A. Sinclair, BioPharm Services, Bucks, UK, personal communication). So for example, a filtration unit with a membrane area of $5m^2$ can process 50kg of product before it is discarded.

Measurements, to determine the change in viscosity with titre for varying degrees of pre-concentration were extrapolated from experimental data reported by Pradipasena *et al.*, (1977). The experimental data reported and the function fit used to perform extrapolation can be found in Appendix B.

Table 5.8 Equipment costs for the ultrafiltration, pre-concentrating step.

Equipment	n (index value)	Base cost, C1 ($)	Base capacity, Q1
Ultrafiltration rig	0.04	360000	450 L/min
Ultrafiltration membrane cassettes	-	1935/m^2	-

The addition of the pre-concentrating step was to investigate whether or not such a change to the process would allow the initial capture step to meet a more intensive level of process performance (see Chapter 6). As such, process performance was deemed to represent both the pre-concentrating and initial capture operations. Therefore productivity as defined by Equation (5.12) becomes:

$$P = \frac{R(C_0 V_b - M)N}{T + t_{filtration}} \tag{5.24}$$

and the COG/$g_{specific}$ given by Equation (5.19) becomes:

$$COG / g_{specific} = Equation\ (5.18) + \frac{T_{filtration} \cdot c_{\$time\ filtration} + c_{\$UF\ rig\ dep} + [Q_{cleaning} \cdot c_{\$buffer\ UF} + \frac{c_{\$membrane}}{N_{membrane\ life}}] \cdot A_m}{Mass\ of\ product\ recovered} \tag{5.25}$$

where $C_{\$\ time\ filtration}$, is the cost per hour of labour which is a function of operator costs for the filtration step. $C_{\$\ buffer\ UF}$ is the cost per litre of buffer solution used and $C_{\$\ membrane}$ is the cost per square metre of membrane used during processing. $N_{membrane\ life}$ is the membrane lifetime in terms of maximum number of reuses. $C_{\$UF\ rig\ dep}$ is the depreciation cost and the fixed investment of the filtration skid and rig.

5.8 Compression effects

Large changes in column scale and aspect ratio result in increased resin compression due to loss of wall support. Excessive compression of the adsorbent changes the pressure drop – flowrate characteristics of the column and can result in severe flow instability (Mohammed *et al.*, 1992) , thus placing a practical limit on the flowrate through a given packed bed system. The theory behind such phenomena is detailed in Chapter 3, where an empirical model for compressible packed bed columns is proposed. This has been evaluated at scale and provides a quantitative prediction of the critical velocity (u_{crit}), the maximum practical operational velocity. Equation (3.11) correlates u_{crit} with column aspect ratio, resin rigidity and mobile phase viscosity and is presented as Equation (5.26):

$$u_{crit}L_0 = \left(\left(4.76\times10^{-5}\right)\mu^{-0.83}u_{10\%} - \left(2.32\times10^{-8}\right)\mu^{-0.74}\left(\frac{L_0}{D}\right) + \left(\left(4.22\times10^{-8}\right)\mu^{-0.91}e^{1304u_{10\%}}\right)\right) \quad \textbf{(5.26)}$$

5.9 Column utilisation

To process a given batch of antibody using small columns requires that each is run for several cycles. The extent of column utilisation was defined as the ratio of the amount of time the column is in active process use to the maximum time available for that particular quantity of material to be processed. For the overall campaign the column utilisation can be defined as:

$$Column\ Utilisation\ (\%) = \frac{Time\ in\ operation}{Total\ available\ production\ time} \times 100 \quad \textbf{(5.27)}$$

Total available production time was based on process times of the unit operations upstream of the initial capture step. Assumed values are reported in Table 5.7. Cycling of columns increases the total time for purification and thus decreases the production rate. For some combinations of column size and flowrate it will not be

possible to achieve a production rate sufficient to process a given amount of material in the time required. In such cases a level of utilisation greater than 100% would be indicated by application of Equation (5.27). This is clearly not feasible.

The length of the DSP operating shift assumed restricts the number of times a column can be cycled during a day. Furthermore the last cycle of chromatographic separation must be fully completed in a DSP shift. This places an additional constraint on the flowrates available to those whereby the column can be cycled sufficiently rapidly that the column is cycled up to the product collection step during a production day, whilst CIP and column sanitisation before subsequent batches are run overnight. Operating at flowrates below this level leads to cycle times that exceed the shift constraint.

5.10 Product degradation

Prior to purification across the Protein A column the product protein is typically present in a very complex media containing host cell proteins from cell culture and is at its most susceptible to enzymatic degradation. Therefore, a further design constraint would be to process the load on the column as soon as possible after harvest. For example, though monoclonal antibodies (MAbs), can be held in storage at 2-8 ^{0}C for up to 7 days without loss in activity (James Savery, Biopharm Services, Bucks,UK, 06/06/2005), this may still be significant, given the constraints in DSP shift operation. For a process batch, the maximum allowable time to process the given load before product starts to degrade can be defined as:

$$Product\ Degradation\ Limit = \frac{Time\ in\ operation\ per\ batch}{Hold\ time\ limit} \qquad \textbf{(5.28)}$$

Column options which indicate operation at a level below this constraint are clearly not feasible if product degradation is to be avoided.

5.11 Integrated Modelling Approach

A structured simulation tool programmed using MATLAB (The Mathworks Inc., Natick, MA, USA, 2004) was developed so as to assist in the decision-making process for the design and operation of initial capture chromatography. The framework integrates various key aspects of column operation at large-scale: resin compression, resin degradation, material specific separation and column scheduling. The productivity as a measure of process efficiency and the cost of goods as a measure of process economics are chosen as the design constraints. Extra constraints at large –scale and from process scheduling have also been incorporated into the framework. The effects of these factors were represented through 'Windows of Operation' which enable the engineer to visualise rapidly the variable region in which it is possible to achieve a specified level of process performance. The window can also be employed to investigate the effects of altering key operating variables on the overall process behaviour. The methodology is demonstrated through a case study outlined in subsequent chapters.

The procedure used in this work to construct the windows of operation consists of a series of steps as shown in Figure 5.2, each of which are outlined in detail below:

Step 1. Data from the parameter estimation techniques (outlined in Appendix B) describing the adsorption and mass transfer properties of the chromatographic separation are identified and input into the model. These include the physical make-up of the stationary phase e.g. the particle porosity, pore size and bed voidage as well as the mass transfer and adsorptive data associated with the product species to be adsorbed.

Step 2. Once the separation has been characterised in Step 1, user-defined parameters are now input. These variables include the titre, loading flowrate, column diameter (Dc), bed length (L), the load volume (i.e. Safety Factor, SF, see Chapter 7) and the number of batches to be processed. The parameters are typically varied to examine their impact on the separation and overall chromatographic process.

Step 3. In the third step, the option of whether or not to include and pre-concentrating ultrafiltration (UF) step is offered. If such a process is to be modelled, then definition of the membrane area and concentrating time of the UF step is required. From the mass balance described in Equation (5.23) a concentrating factor provided by the UF step is calculated. If no pre-concentration is required to be modelled then the model is directed to Step 4.

Step 4. In the next step, the opportunity to model the post-load wash stage is provided. If it is desired to model this step then further parameter data is required as described by Step 5. If post-load washing is to be assumed and not explicitly modelled then the model is directed to Step 9.

Step 5. In the fifth step parameter data is required to define a contaminant quantity in the feed stream entering the column. Typically in this study contaminant components are considered a lumped term and modelled as a single component based in host cell protein (HCP) data. Within this research, contaminant data was referenced from literature sources, however experimental or parameter estimated data can also be input at this point.

Step 6. In this step, a decision must be made as to the type of post-load washing to be modelled (Chapter 7). If there is significant adsorption of contaminant to the Protein A resin then a two-stage washing strategy utilising and intermediate wash buffer may be required. If contaminant binding is not significant then a more traditional equilibration wash may be sufficient. If this is the case then the model proceeds to Step 8.

Step 7. If an intermediate wash buffer is required then adsorption and mass transfer data must be provided to model the interaction of the contaminant and product species with this intermediate wash buffer. In this study literature sources together with parameter estimation were used to determine these quantities.

Step 8. Here, the linear velocity of the post-load washing (v_{wash}) can be defined by the user.

Step 9. Sufficient data has now been provided and therefore the general rate model programmed in the MatLab environment can be run.

Step 10. The tenth step provides the model outputs in terms of either data points or plots of the concentration of the modelled species coming out of the column (C_b) vs. time or volume.

Step 11. From the data provided in Step 10, Equation (5.16b) is then used to calculate the impurity level in the output stream from the column.

Step 12. The twelfth step involves the calculation through Equation (5.26) of the maximum linear velocity that can be attained through the column given the user determined values of column geometry, flowrates and titre.

Step 13. The next step involves calculating the column utilisation based on Equation (5.27). Here the quantity of time required to process a batch of material before the next successive batch is ready to be processed is calculated. This step thus provides an indication whether a column option is feasible or not for processing multiple batch campaigns.

Step 14. Similarly to Step 13, Equation (5.28) calculates the product degradation limit. This step examines is a column option will be able to process a batch of material before product degradation starts to occur.

Step 15. Based on the user defined number of batches to be processed (Step 2), Equation (5.11) is used to calculate the number of cycles required for the process.

Step 16. In this step the lifetime of the resin is determined through the procedure outlined in Section 5.6.1. Once calculated this in input to the model.

Step 17. A check is made to determine is the required number of cycles is equal to the number of cycles simulated ($N_{simulate}$). If more cycles are required the model flow

proceeds to Step 18. If no further cycles are required to be simulated then the model proceeds to Step 20.

Step 18. In this step a further check is made to examine if the number cycles simulated, $N_{simulate}$ exceeds the resin lifetime. If $N_{simulate}$ is greater than the resin lifetime, $N_{simulate}$ is re-set to zero indicating cycle 1 of a new resin and the resin counter N_R is updated. If the resin life has not been exceeded then model proceeds to Step 19.

Step 19. Here, Equation (5.20) is used to degrade the adsorptive capacity of the resin signifying the degradation observed in resins over multiple cycles when sodium hydroxide solutions are used as cleaning agents.

Step 20. In the twentieth step, the productivity of the process is calculated through Equation (5.12) or (5.24) depending on whether a UF step was modelled within the process. The calculated data is then stored.

Step 21. The next step evaluates the COG/g based on Equation (5.19) or (5.25) depending on whether the modelled process contained a pre-concentrating step and the calculated data is then stored.

Step 22. Here, the option of evaluating different parameters is given. If the impact of a varying the column geometry and loading velocity on the productivity and cost of the process is required then model flow proceeds to Step 2, where the new data can be input.

Step 23. In this step, the linear washing flowrate can be varied if required. If a new washing velocity is to be investigated the model flow proceeds to Step 8.

Step 24. The model outputs in two forms. The first is if only one set of data was evaluated then a single data output for productivity and COG/g is given. Further to this, the constraint data of maximal flowrate, column utilisation and product degradation data will also be given. If several variables or parameters were estimated

then the model has the option of displaying such results in the Windows of Operation format whereby contours of productivity and COG/g can be displayed. Here also suitable contours of constraints can be displayed (as outlined in Chapter 6) which show clearly the feasible regions of operation.

5.12 Conclusion

In this chapter the development of a prototype tool to model the trade-offs in chromatography processing is presented. The modelling approach developed and adopted allows modellers to capture both the process and business knowledge of the chromatographic manufacturing process. Such a tool is useful for process management, resource utilisation, cost analysis and process efficiency assessments, all of which together bear on the examination of column size and operation for different process options. The application and implementation of the methodology proposed will now be described through a series of case studies in the following chapters (Chapters 6 and 7). Through this, the utility of the approaches will be established and the nature of the process insights gained from such methods can be demonstrated.

Initially, the approach is applied in the selection of column dimension and loading strategy in a given processing scenario (Chapter 6). The analysis is taken further in Chapter 7 where column operating conditions are examined in more detail. Here load volume and post load washing are investigated, as is the impact on $COG/g_{specific}$ and productivity. Chapter 7 also examines the relative advantages and disadvantages of operating with incompressible chromatography media compared to the use of compressible agarose media.

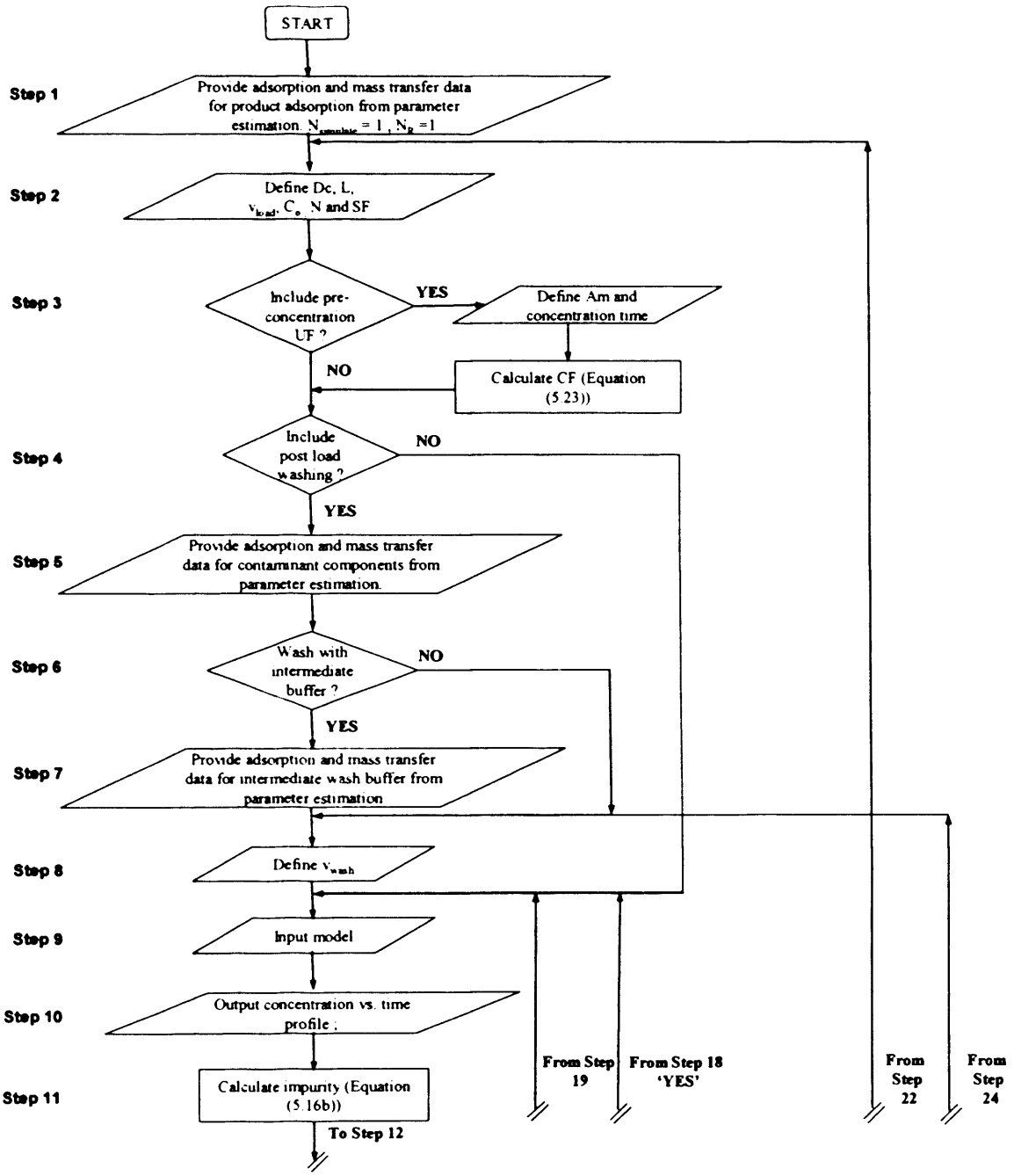

Figure 5.2 Process flowchart of integrated model for design and operation of a chromatographic step (continued on next page).

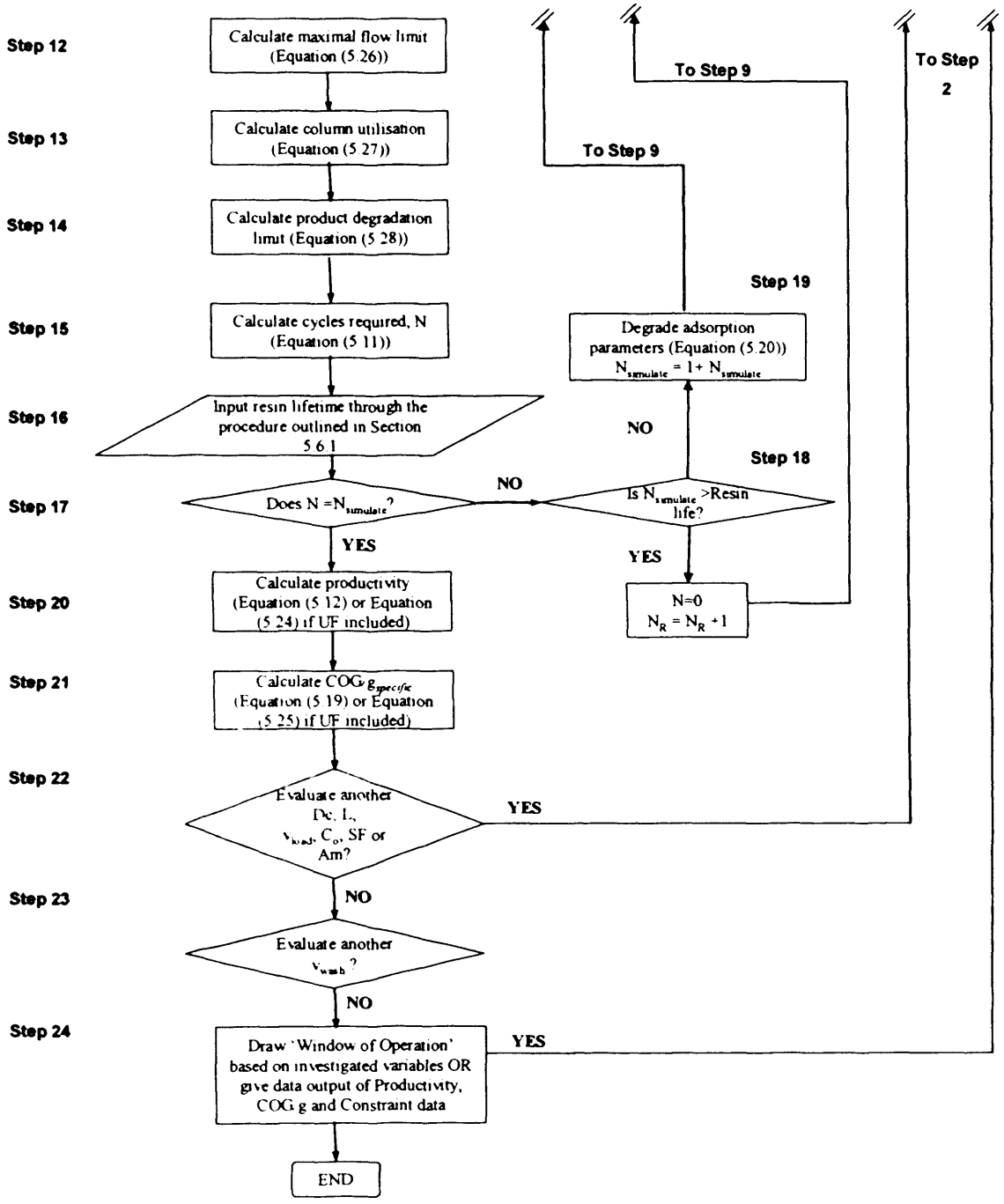

Figure 5.2 (conti) Process flowchart of integrated model for design and operation of a chromatographic step.

6 APPLICATION OF FRAMEWORK FOR ASSESSING THE SOLUTIONS IN CHROMATOGRAPHIC PROCESS DESIGN AND OPERATION FOR LARGE-SCALE MANUFACTURE

6.1 Introduction

This chapter describes the implementation of the framework presented in the previous chapter as a simulation tool for modelling biopharmaceutical manufacture. In this decision-support tool, emphasis is placed on how a closer integration of chromatographic process data and business modeling can be achieved by capturing common information in an object-orientated environment. The steps to use this tool for addressing the impact of chromatography manufacturing options on strategic technical and business indicators are identified.

The chapter is structured as follows. In Section 6.2 the background to the case study is described which addresses the question of how to select the size and operational velocities of a Protein A initial capture step in a MAb production process. Section 6.3 will focus on what parameters were used for the model process. Section 6.4 investigates alternative methodologies of estimating resin lifetime. In Section 6.5 an examination of how productivity varies with column strategy is presented. A similar analysis in terms of cost of goods is described in Section 6.6. Section 6.7 describes how feasible column strategies can be selected based on product and process specific knowledge. Section 6.8 shows how the model framework can be extended to incorporate changes to the process flowsheet. Finally a summary is provided in Section 6.9.

6.2 Case study based on the production of MAbs

A hypothetical case study that examines the impact of variations in key process parameters on cost of goods and productivity will now be examined. The design, implementation and application of the tool described in Chapter 5 was explored using data for the production of a recombinant humanised monoclonal antibody (IgG) from CHO cells. MAbs have emerged as an important and rapidly

expanding class of drugs for the treatment of human disease. At least 400 monoclonal antibodies are in clinical trial at present (Gura, 2002). As such they provide a representative challenge for the proposed methodology. Antibody titers in the order of 1 -5 g/L have been reported using fed-batch cultures of mammalian cells (Birch *et al.*, 2004; Thommes *et al.*, 2007). Assuming a product titer of 1 g/L and a fixed reactor volume of 10000L, approximately 100kg of MAbs would be produced during plant operation in a year. The preferred method for the capture and purification of MAbs is Protein A chromatography. Affinity chromatography achieves a very high degree of purification of the desired species and often in a single step. The biospecific ligand, Protein A, is however, extremely expensive compared to other chromatographic media and often exhibits poor stability when exposed to vigorous CIP regimes. Since Protein A is often used as the first capture step it may be rate-limiting due to the low protein concentrations and large volume loads associated with such early stage processing (Ghose *et al.*, 2004).

The case study is based around the decision of what size of Protein A chromatography column to use in a given downstream processing (DSP) train. A fixed set of process assumptions, listed in Table 6.1, were made. All simulations were driven by the need to process a defined batch of material from a 10,000L fed-batch reactor. Processing by the affinity column was every 15 days. In all, the reactor was scheduled to output 20 batches in a 48 week production year. An overview of the primary recovery stages of the process used in the case study is illustrated in Figure 6.1. The key performance variables used to assess the various possible process solutions were the level of productivity (g/h) and the cost of goods contribution of the affinity capture step ($COG/g_{specific}$, $/g) to the overall process-wide cost of goods.

6.3 Parameter estimation

Data was taken from the literature (Hahn *et al.*, 2003) and was assumed to follow the adsorption of clarified humanised monoclonal antibody (IgG), produced in Chinese Hamster Ovary (CHO) cells, onto the rProtein A Sepharose Fast Flow™ (GE Healthcare, Uppsala, Sweden) resin used in this study. The resin base, Sepharose 4 Fast Flow, is a highly cross-linked, 4 % agarose derivative with high

chemical and physical stability (see Chapter 3). The values of the main parameters used in the model are listed in Table 5.2.

Table 6.1 Overall process assumptions for the manufacture of a MAb from mammalian cell culture.

Assumption	Input Value	Reference
Plant operating hours	48 weeks a year, 7 days a week, 12 hrs a day	Assumed
Lang factor	6	Sinnot (1993)
Bioreactor size	10000L	Assumed
Batch interval	15 days	Assumed
Centrifugation time	4h	Farid, (2001)
Filtration time	3h	Farid, (2001)
Product degradation time	36 hrs	Assumed

It was assumed that certain parameters were to remain constant in a particular manufacturing environment. These values are listed in Table 6.2; however, the framework presented can be extended for any column length, concentration and buffer volume.

6.4 Evaluation of resin lifetimes

Equation (5.22a) was used to estimate a theoretical economic potential for the process dependent on the chromatographic cost of continuously reusing a given quantity of Protein A resin (Equations (5.22b-c). A manufacturing revenue was estimated through the product of the quantity of MAb recovered from the process and

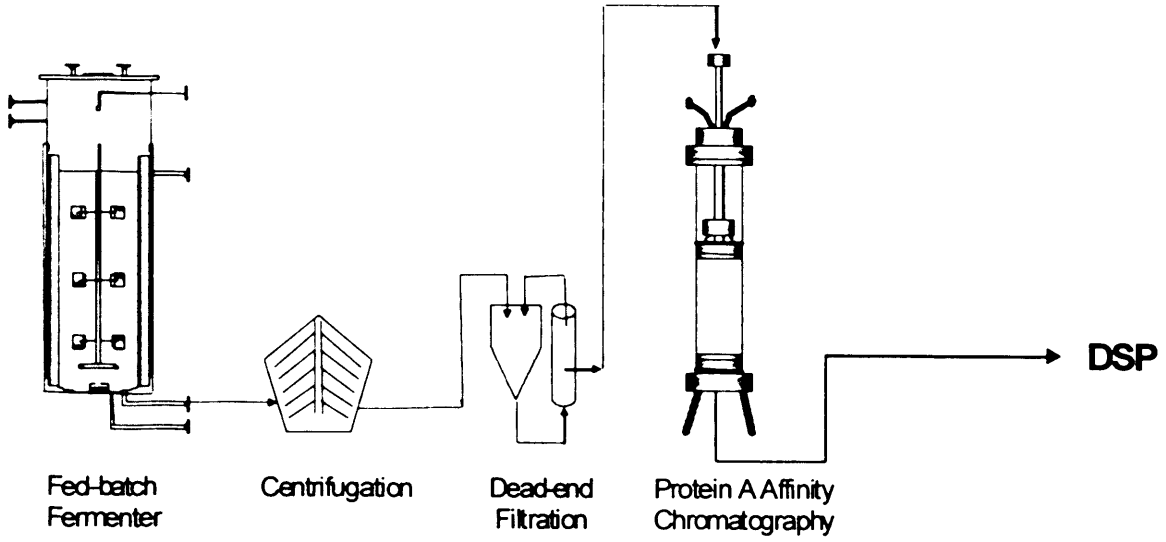

Figure 6.1 Schematic process flow-sheet showing fermentation, primary recovery and initial capture in a typical MAb manufacturing process.

a market selling price based on manufacturing costs alone ($\$_{MAb}$, see Section 5.6.1). The aim was to calculate the theoretical extent to which a resin can be reused and as such it was assumed that there was an unlimited batch of material from which processing could take place. Chromatographic performance was calculated through simulations based on the assumptions outlined in Table 6.1-6.3 together with the degradation caused through extensive cycling described by Equation (5.20). Process yields of the other unit operations used during the manufacturing process post initial capture were outlined in Table 5.7 and were assumed to be approximately 70% collectively. These losses were assumed constant as the investigation was based on observing how the economic potential varied with Protein A reuse alone.

Decreasing binding capacity caused by degradation increases the cost of goods of processed product ($COG/g_{specific}$). Load volume was calculated based on the column capacity of a fresh resin and it was assumed that this level of loading remained constant throughout operation. Therefore, product losses incurred during the loading stage increase as breakthrough is achieved earlier with every cycle. Simulations of the variation in costs with cycle number show a non-linear increase in the $COG/g_{specific}$ per cycle as resin lifetime extends (Figure 6.2 (a)). The cumulative economic potential for varying process strategies are displayed in Figure 6.2 (b).

Table 6.2 Chromatographic process assumptions for the manufacture of a MAb from mammalian cell culture. *CV denotes column volume.

Assumption	Input Value	Reference
Titer, C_0	1 g/L	Assumed
Bed Height, L	15 cm	Assumed
Column yield	98 %	Assumed
Chromatography Equipment depreciation	10 %	Assumed
$u_{10\%}$, constant in Equation (5.26)	12.45 x 10^{-4} m/s	See Chapter 3
Load volume/cycle	Column loaded to 1% of the initial feed concentration.	Assumed
Volume of equilibration buffer used / cycle	4 CV*	Ghose *et al.* (2004)
Volume of wash buffer used / cycle	4 CV	Ghose *et al.* (2004)
Volume of Elution buffer used / cycle	4 CV	Ghose *et al.* (2004)
CIP contact time/ cycle	15 min	Johansson *et al.* (2002)
CIP capacity degradation constant, Φ Eq. (5.20)	0.17	Johansson *et al.* (2002)
Yield of DSP post initial capture	70 %	Estimated from Table 5.7
Chromatography contribution to process cost Eq. (5.22b)	8 %	Assumed
Selling Price MAb, $\$_{MAb}$ Eq. (5.22a)	$1325	See Section 5.6.1

The solid line in Figure 6.2 (b) shows the cumulative operating profit when reusing the resin for an extended period if the column is loaded to 1% breakthrough. Cumulative profit increases initially with cycle number. This is because the revenue earned from the MAb bound to the column over a range of cycles outweighs the costs of production and hence the profitability of such a strategy increases. However there comes a point when the column capacity is degraded to such an extent that product losses per cycle are so great that the cost of running the process becomes more expensive than the returns gained from continued production. An optimal point occurs corresponding to the most profitable number of cycles for which the resin can be re-used. This represents a prediction of the resin lifetime in terms of financial return.

6.4.1 The effect of column diameter on lifetime

Figure 6.2 (b) shows that the larger the column used, the higher the economical potential attained. Larger columns can adsorbed more product per cycle due to their greater overall capacities than smaller columns and therefore the cumulative revenue that can be earned over time is greater. As such, the initial increase in the profitability function grows steeper with increasing column size as revenue is earned at a greater rate. Another consequence of the greater capacity of larger columns is displayed in Figure 6.2 (c), which shows the shape of the function describing how resin lifetime varies with column diameter. It can be seen that the use of smaller columns of diameters 20-40cm are infeasible. The revenue gained per cycle when operating these column strategies is small due to the relatively low column capacity. As such, the cumulative revenue earned never surpasses the costs of the process.

However, increases in capacity, when using larger columns of diameters 60-200cm yield more feasible options. Resin lifetime increases with column size given the greater revenues that can be earned per cycle, despite the higher initial costs associated with the use of large quantities of expensive resin. Figure 6.2 (c) shows that lifetimes start to plateau for very large columns. This is due to the diminishing increases in capacity as columns get larger as shown in Table 6.3.

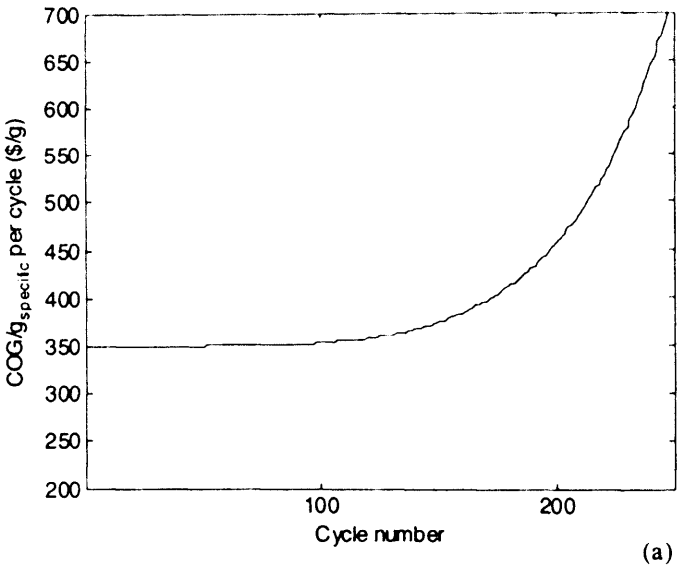

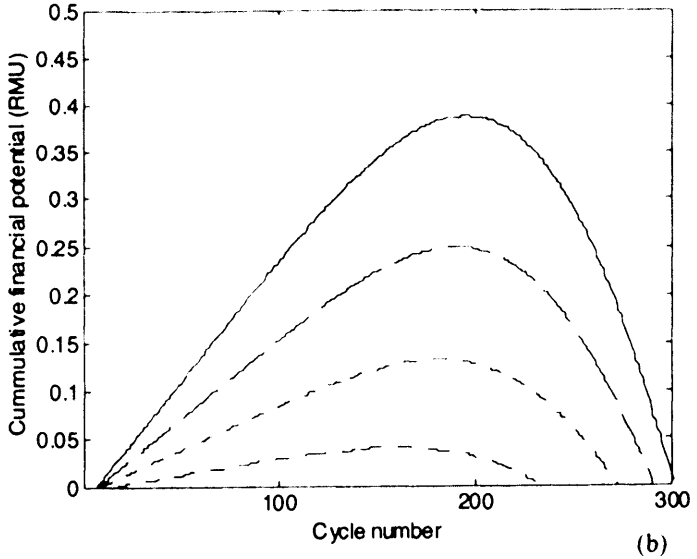

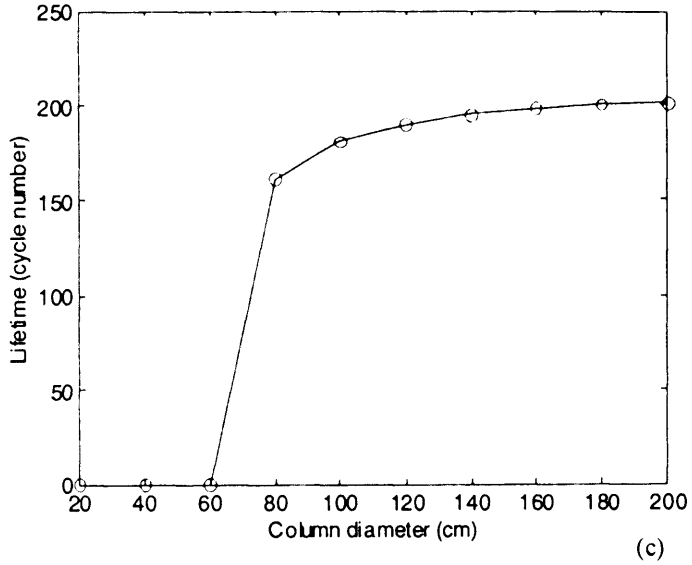

Figure 6.2 (a) Variation of $COG/g_{specific}$ with cycle number for a column of diameter (Dc) 100 cm when loaded at a velocity of 250 cm/h. **(b)** Cumulative operational profit vs. cycle number calculated based on loading velocity of 250 cm/h and a fixed bed height of 15cm for varying column diameters; Dc = 60 cm (— · —); Dc = 80 cm (·····); Dc =100 cm(— — —); Dc = 120 cm (———); **(c)** Resin lifetime as a function of column diameter when loading at 250 cm/h and with a bed height of 15cm.

Table 6.3 Variation of overall column capacities with column diameter. Dynamic binding capacity (DBC) in this case was 23.7 g/L. DBC was calculated based on loading to 1% breakthrough at a velocity of 250cm/h, bed height = 15cm. * denotes, values calculated relative to the preceding column capacity.

Column Diameter, Dc (cm)	CV (L)	Overall capacity, DBC. CV (g)	Increase in overall capacity (%)*
20	5	111	-
40	19	447	302
60	42	1003	124
80	75	1784	78
100	118	2787	56
120	170	4015	44
140	231	5463	36
160	302	7136	31
180	382	9031	27

6.4.2 Effect of loading velocity on lifetime

Figure 6.3 (a) shows how economic potential fluctuates with loading velocity and cycle number. Variation in loading velocity leads to alterations in the ascent gradient of the economic potential function. This mirrors the change in dynamic binding capacity with velocity. For lower flow velocities, dynamic capacity is high as lower velocities allow binding on stationary phase sites which were less accessible when higher velocities are used. As such, more product per cycle can be captured allowing for higher revenues per cycle. This leads to a steeper initial increase in the profitability function than when operating with higher velocities. Despite the higher rate of increase in profitability associated with low loading velocities, Figure 6.3 (b) shows that lifetimes increase with increasing loading velocity, followed by an eventual decrease. The reasons for this can be explained more clearly with reference to Figure 6.4.

Figure 6.4 shows the concentration profiles in the solid phase prevailing on completion of loading to 1% breakthrough. In Figure 6.4 (a) the solid phase concentration profile inside the column is shown when loading at a velocity of 100 cm/h during the 1st operational cycle. When loading at a low velocity MAb has

sufficient time to diffuse fully into the binding sites of the resin making full use of the available column capacity. As a result more product can be loaded onto the column and breakthrough is achieved later. It can be seen that almost all the column capacity is saturated with product. The concentration of product along the bed eventually falls as the majority of the product loaded is adsorbed closer to the top of the bed and therefore less unbound material is available to be adsorbed by the resin particles which are located towards the exit of the column. The dashed line shows the solid phase concentration profile during loading on a column operating its 25th cycle. When column capacity is degraded during operation, the free resin capacity remaining is insufficient to capture the mass of material which is loaded onto the column and consequently there is a large amount of product lost out of the column. Losses in product equate to losses in revenue accounted for in the penalty feature of the economic potential calculation (see Section 5.6.1), which cause the more rapid diminishment of returns when adopting low velocity strategies.

Figure 6.3 (b) shows the same analysis performed for a column when loaded at a velocity of 300 cm/h. It can be observed that resin capacity is relatively under-utilised when high load velocities are used as MAb exits the column before it can diffuse to the stationary phase binding sites, resulting in an earlier breakthrough. There is therefore less material bound to the column and more free capacity throughout the column to capture the material loaded. During the 25th cycle of operation it can be seen that the column is better utilised. Available binding sites have decreased due to the level of degradation the exposed resin has experienced. The resin fails to bind the same quantity of MAb loaded onto the column as during the 1st cycle due to this reduction in capacity and the concentration of MAb in the effluent stream is higher than initially, causing an early breakthrough than experienced with a fresh resin. However, much more of the product that is loaded onto the column in this case is bound, compared to the case of Figure 6.3 (a). The greater free capacity available when using high load flows together with the relatively lower level of mass loaded onto the column reduces the product losses on degradation when compared to when low velocity strategies.

Figure 6.3 (b) shows that increasing loading velocity to levels greater than 400 cm/h leads to a decrease in the resin lifetime. Binding capacity is reduced to such an extent, through the use of such high load velocities that the revenues that can be earned through these strategies are extremely low. Thus, even the relatively meagre losses in product that occur during multi-cycle operation using high load velocities impact upon the revenues attained, causing an early decent of the economic potential curve.

The profiles displayed in Figure 6.3 (a) show variations between the maximum economic potential that can be attained when using a given loading velocity and the lifetime associated with such a strategy. Figure 6.5 shows how the maximum economic potential varies with loading velocity. Initially, the maximum potentials that can be achieved are low when loading with sufficiently moderate velocities. Despite the high binding capacities associated with these strategies, large losses in product caused by the effects of degradation result in low economic potential values. As loading velocity is increased, there exists a trade-off between the reduction in binding capacity caused by an increase in velocity and a reduction in product losses caused by degradation. As velocity is increased from 50-150 cm/h, the drop in capacity is sufficiently moderate that the maximum profitability still increases due to the extended number of cycles these flow strategies allow before revenue losses caused by low yield become significant. Increasing velocities further however lead to reductions in the dynamic capacities and therefore the quantity of product that can be adsorbed per cycle. A consequence of this is a reduction in the revenue that can be earned per cycle. Therefore an optimum velocity exists if the highest economic potential is to be achieved for a given column size.

6.5 Productivity Analysis

Breakthrough curves were simulated for a variety of different loading velocities and column sizes. Typically, process scale columns vary in size from column diameters of 10 cm up to 200cm (personal communication, customer

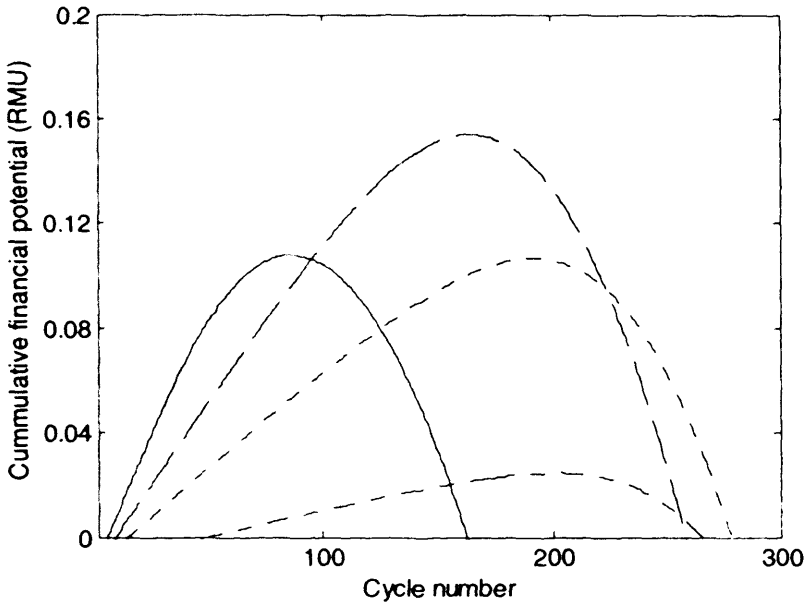

(a)

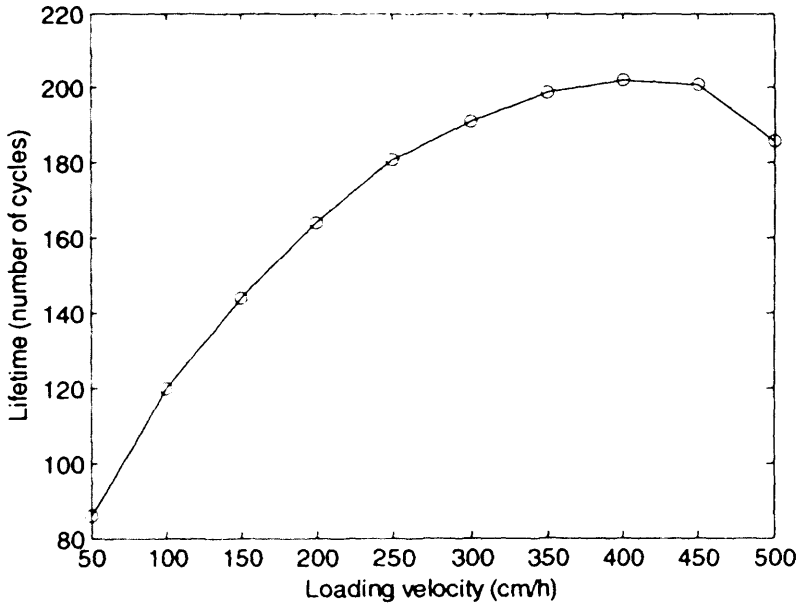

(b)

Figure 6.3 (a) Cumulative economic potential produced for a number of cycles for a 100cm diameter column with varying loading velocity, 50 cm/h (———), 200 cm/h (— — —), 300 cm/h (·····), 450 cm/h (— · —); **(b)** Variation of resin lifetime with loading velocity.

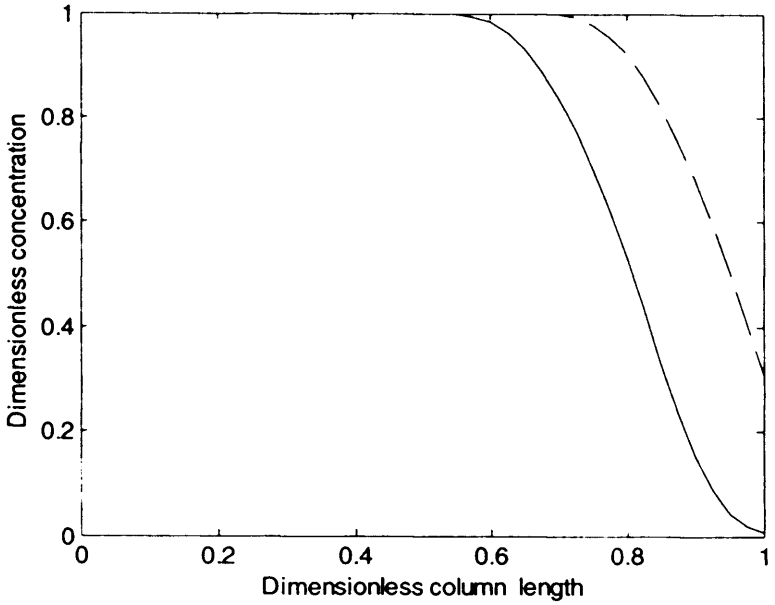

(a)

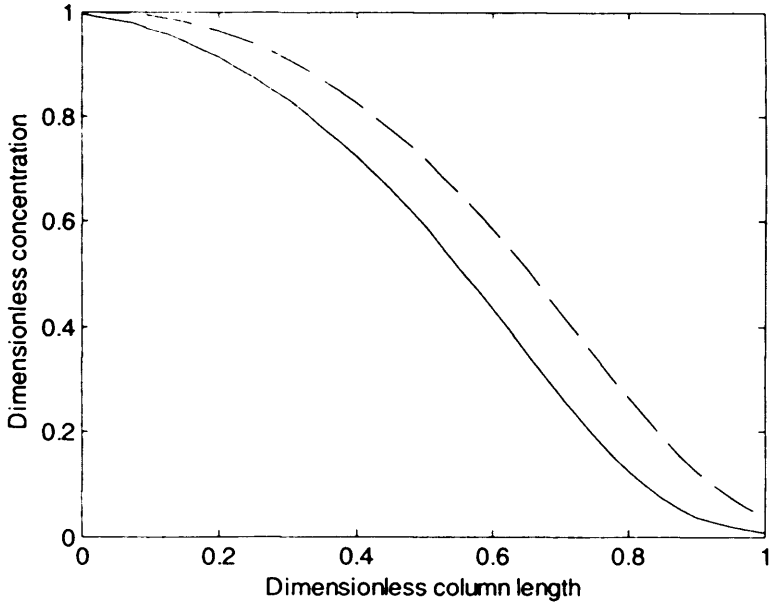

(b)

Figure 6.4 Concentration profiles in the solid phase at the end of loading to 1 % breakthrough after the 1st operational cycle (———) and the 25th operational cycle (— — —) when loading with a loading velocity of **(a)** 100cm/h and **(b)** 300 cm/h.

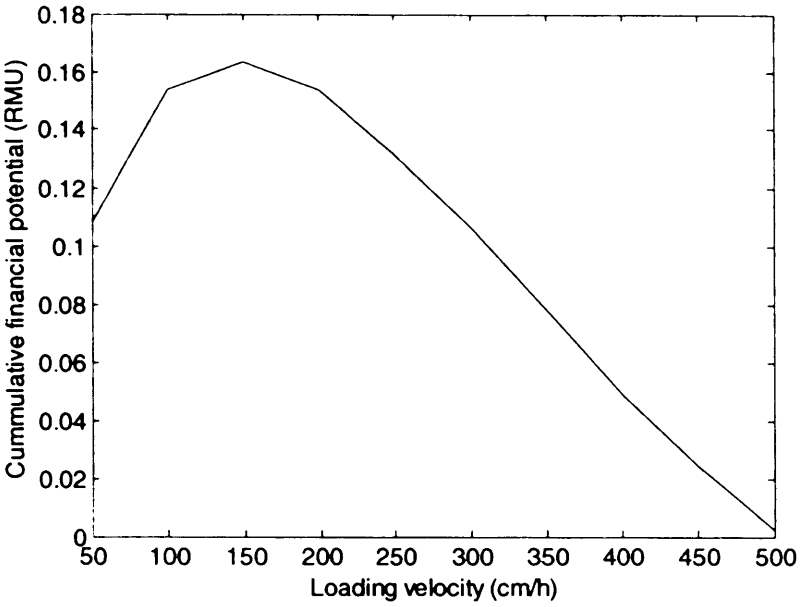

Figure 6.5 Maximum cumulative economic potential reached when varying loading velocity for a column of 100cm diameter and a bed height of 15cm.

services, Pall Corporation, Portsmouth, Hants, UK). Equation (5.12) was then used to determine the effect of varying the linear loading velocities and column sizes on the production rate, which is demonstrated in Figure 6.6 (a). High column productivity can be achieved with large diameter columns run at relatively low velocities. The contour lines representing productivities of 500g/h and higher, display pronounced fluctuations. This effect is most evident in the case of larger column sizes and is a consequence of an inability to utilise the full capacity of these columns during operation.

Productivity is defined by the amount of product the column processes and the time taken to process this material. The process time is a function of the number of cycles each column option requires to process the given material. The amount of material to be processed per batch was fixed at 10000g of antibody. Table 6.4 shows the number of cycles required to process this quantity of material for a selection of column options. As velocity is increased the number of cycles required also increases because column breakthrough is achieved more rapidly at higher velocities.

Table 6.4 The number of cycles required to process one batch of material for a sample selection of column options available.

Loading velocity (cm/h)	Column diameter (cm)						
	20	**40**	**60**	**80**	**100**	**120**	**140**
50	45	12	5	3	2	2	1
100	52	13	6	4	3	2	2
150	60	15	7	4	3	2	2
200	69	18	8	5	3	2	2
250	81	21	9	6	4	3	2
300	93	24	11	6	4	3	2
350	108	27	12	7	5	3	3
400	126	32	14	8	6	4	3
450	145	37	17	10	6	5	3
500	166	42	19	11	7	5	4

A consequence of attaining faster breakthrough is the reduced quantity of material that can be loaded onto the column in this period. Loading at faster velocities will therefore require a greater number of cycles of operation be used to process a given batch of material. At the end of processing the batch the last column cycle will usually operate with a load that will not achieve the full loading capacity of the column. This under-utilises the expensive resin and increases the column process time for comparatively little gain. The integer nature of this effect is the intrinsic cause of the fluctuations seen in the productivity contours at rates of greater than 500 g/h seen in Figure 6.6 (a).

The impact of under-utilising columns can be seen more clearly with reference to Figure 6.6 (b). Here the variation in productivity with velocity for column diameters of 40cm and 100cm is shown. For the 100cm column, after an initial increase in productivity with loading velocity, there is a sudden decrease in productivity followed again by a further increase with velocity. Referring to Table 6.4, it is apparent that the decrease in productivity seen for the 100cm column corresponds to an increase in cycle number that occurs at a velocity of 150 cm/h and again at 400cm/h. The step increase in cycle number, and hence cycle time, is sufficient that it leads to a decrease in productivity. Productivity increases in-line with velocity for the 40cm column as expected. Table 6.4 shows the increase in cycle number with velocity for this column. Because of the relatively small capacity of the

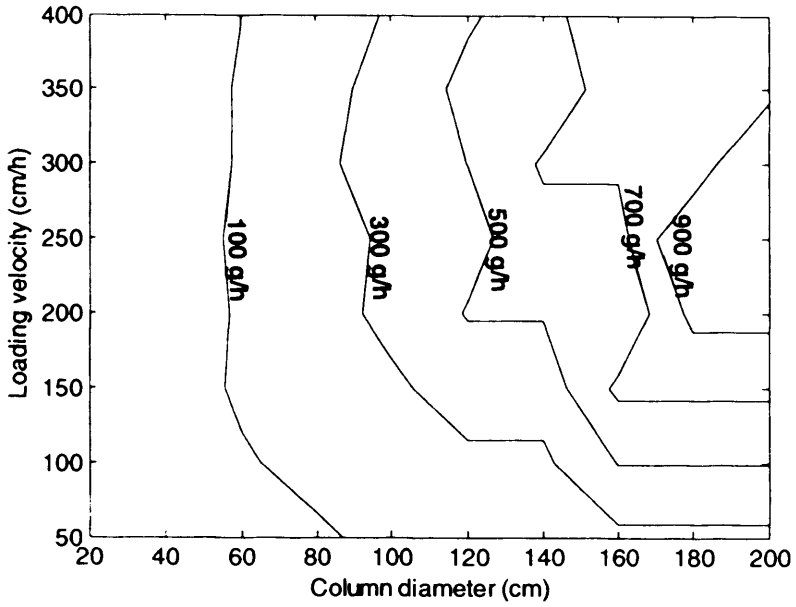

(a)

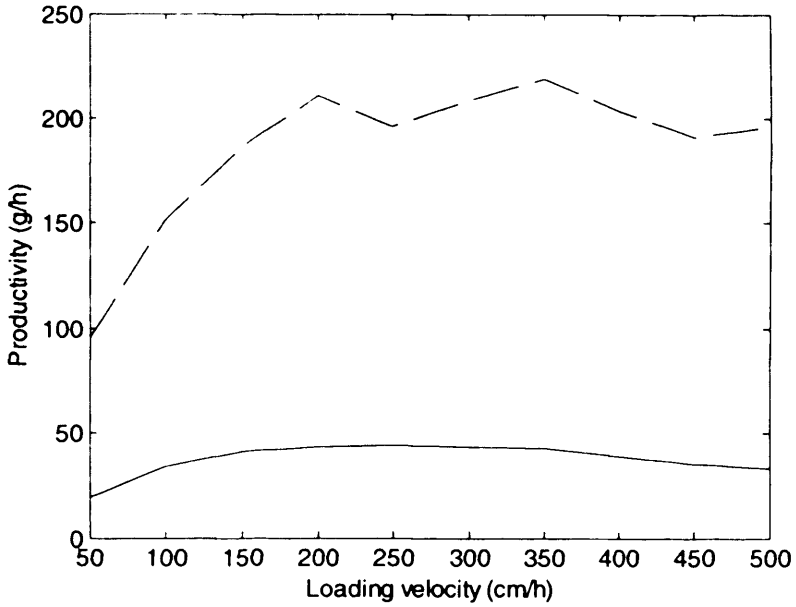

(b)

Figure 6.6 (a) Productivity contours for differing column sizes and velocities **(b)** The variation of productivity for a variety of velocities for a 40cm and 160 cm column diameter.

40 cm column it tends to be better utilised compared to its larger counterpart. These variations in productivity for differing column diameters at various velocities cause the contour fluctuations observed in Figure 6.6 (a). Due to these effects it is common practice in industry to split a batch equally across all cycles on a chromatography column. This results in a lower resin binding capacity and hence productivity but ensures consistent chromatographic performance across all cycles. (Such an analysis is presented in Chapter 7.)

A window of operation for chromatographic operation may be defined by the application of a series of constraints. The first of these relates to loading velocity which is limited by the effects of compression. Application of this constraint is shown in Figure 6.7 (a). Above this constraint operation is infeasible. Figure 6.7 (b) shows the application of a 100% utilisation constraint. Application of this constraint which accounts for both filtration and centrifugation process time restricts the size of chromatography columns which can be used. Beyond this constraint operation is infeasible as column options will fail to meet the required production level. Operating at a column utilisation level of 100% is undesirable as this means that the column would have to run without respite for the whole production campaign in order to meet the specified production rate targets, with no allowance for downtime. This is clearly not a robust operating strategy.

Figure 6.7 (c) shows the imposition of a further constraint corresponding to the available column strategies which allow operation within the DSP scheduling restrictions. This serves to restrict the minimum flow rate of the columns. The region below this constraint is infeasible. Figure 6.7 (c) therefore examines the impact of large scale limitations on the column options available to designers for a given process duty. The window shows the feasible region of operation allowing for the effects of compression, resin degradation, column scheduling and the limitations of imposed by assumed DSP working patterns. The window shows the maximum theoretical range of operating strategies available for the process. This is not a robust solution since operation is defined by the very extremes available e.g. u_{crit} and 100% utilisation. Figures 6.8 (a) and 6.8 (b) demonstrate how the window of operation may be impacted by the need to operate away from the very limits of the system. In

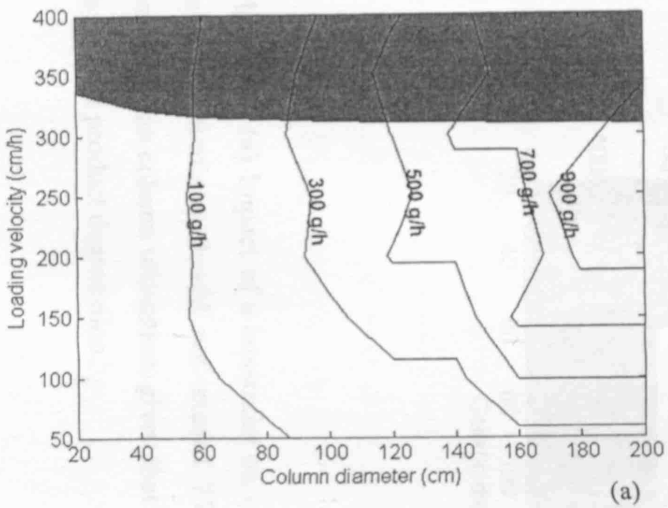

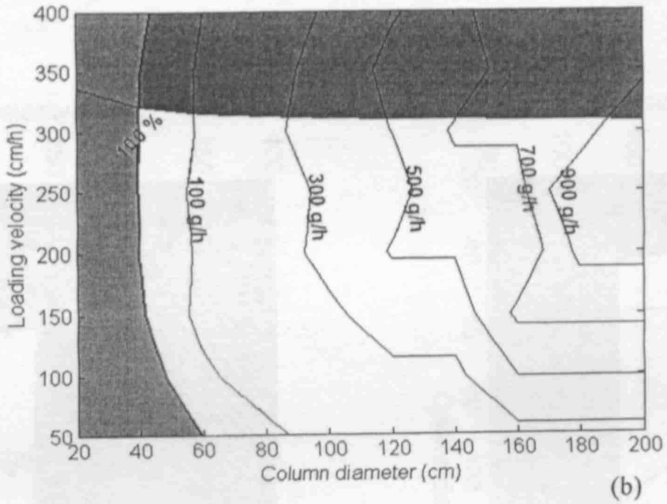

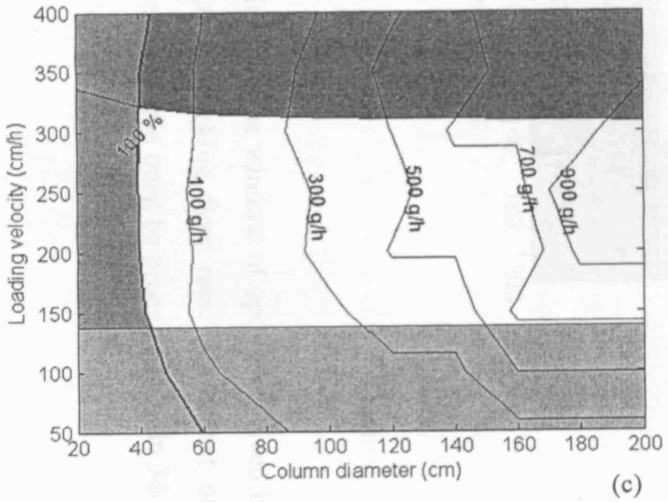

Figure 6.7 The development of a graphical representation of the feasible operating strategies using the integrated framework. (a) The implementation of a compression constraint on the loading velocity for a bed height of 15cm. (b) The implementation of a column usage constraint whereby columns operating below this limit were unable to process the required product in the time available. (c) The implementation of a scheduling constraint whereby a minimum of one complete cycle has to be concluded in a day.

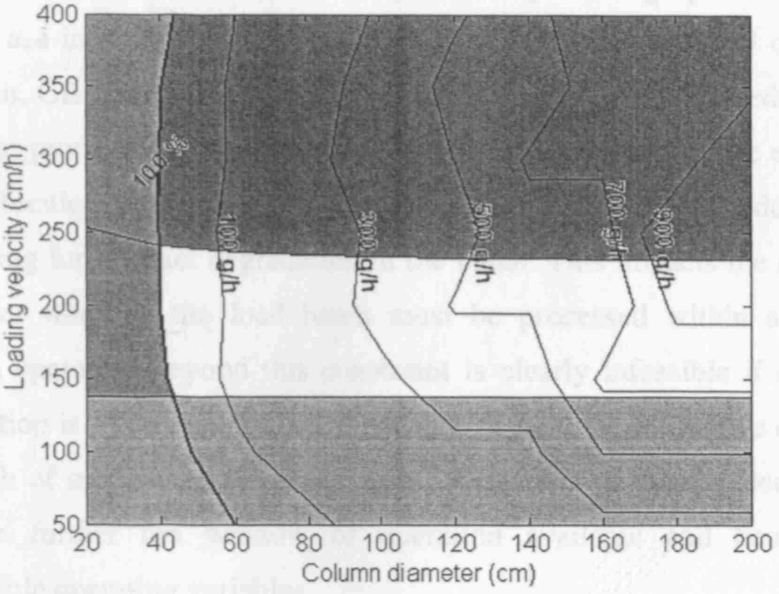

(a)

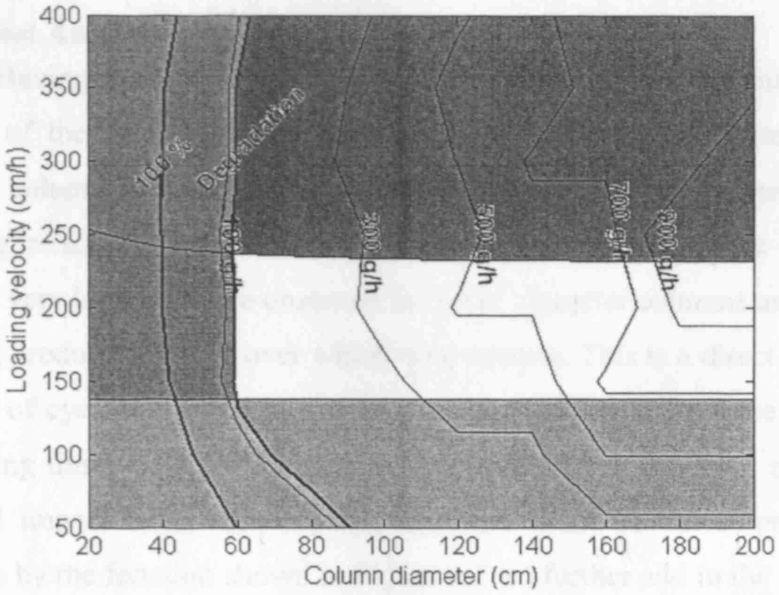

(b)

Figure 6.8 (a) Impact of a constraint on velocities on the window of operation, given that column operations should not exceed 75% of the packing flow rate. **(b)** Impact of a constraint on column utilisation, given that harvested media must be processed within 36 hrs to prevent product degradation.

Figure 6.8 (a) the need to avoid compression by limiting operation to no more than 75% of u_{crit} in order to avoid any compressive effects (personal communication, J. Svensson, GE Healthcare, NJ, US, 11/04/2005) is shown. This reduction reflects the particular properties of typical agarose- based matrices which are easily deformed at high velocities. Figure 6.8 (b) shows the imposition of an additional constraint accounting for product degradation in the batch. This impacts the column utilisation constraint whereby the load batch must be processed within a 36 hour period. Column operation beyond this constraint is clearly infeasible if excessive product degradation is to be avoided. Column options must be productive enough to process the batch of material in the given time. The effect of these added restrictions is to decrease further the window of operation available and hence the range of permissible operating variables.

6.6 Cost Analysis

Having evaluated the process performance we now examine the economic aspects of the process. Figure 6.9 shows the $COG/g_{specific}$ contours produced for varying column diameters and loading velocities. Unlike the productivity contour plot, Figure 6.6 (a), there is more variability in the trends of the $COG/g_{specific}$ data. Initially very high costs are observed for small diameter columns as a consequence of the long production times over which they operate. This is a direct result of the large number of cycles required to process the given material by these columns. Longer processing times will also impact on staff costs, while the large numbers of cycles required impact resin consumption. The low resin lifetimes' predicted for these columns by the function shown in Figure 6.2 (c) further add to the already high resin consumption. All of these contribute to the $COG/g_{specific}$. The effects can be more clearly observed by reference to Figure 6.10, where the $COG/g_{specific}$ breakdown for a constant loading velocity equivalent to 75% of the critical velocity is presented.

There is a dramatic decrease in going from column diameters of 40 -80 cm which again, mirrors the resin lifetime function, Figure 6.2 (c). Here between column diameters of 40 -80 cm the function experiences a steep increase, which follows the

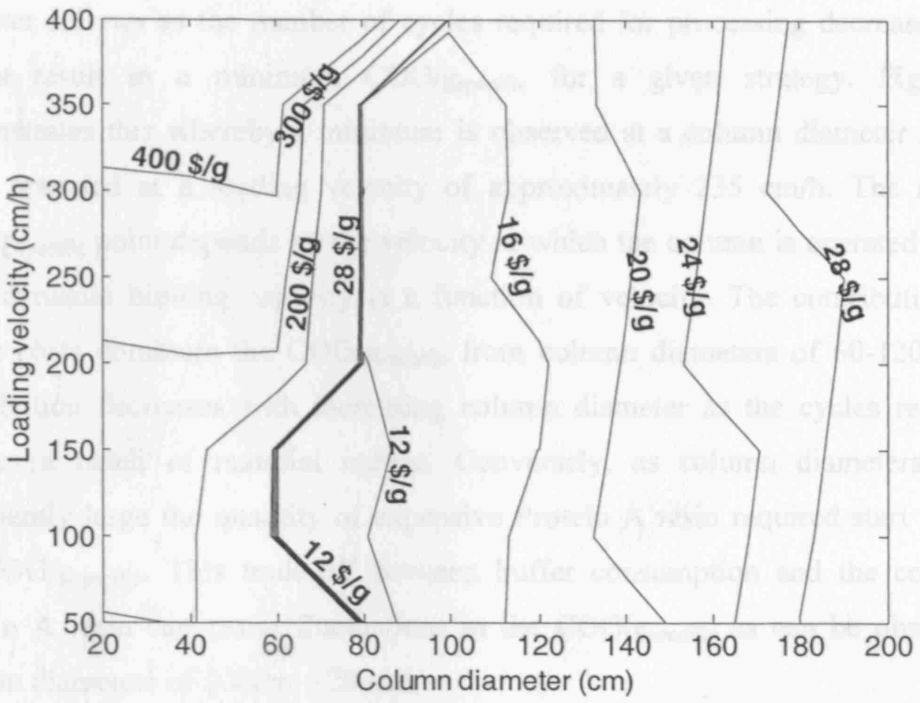

Figure 6.9 Contour plot representing the variation in $COG/g_{specific}$ ($/g) with column diameter and loading velocity.

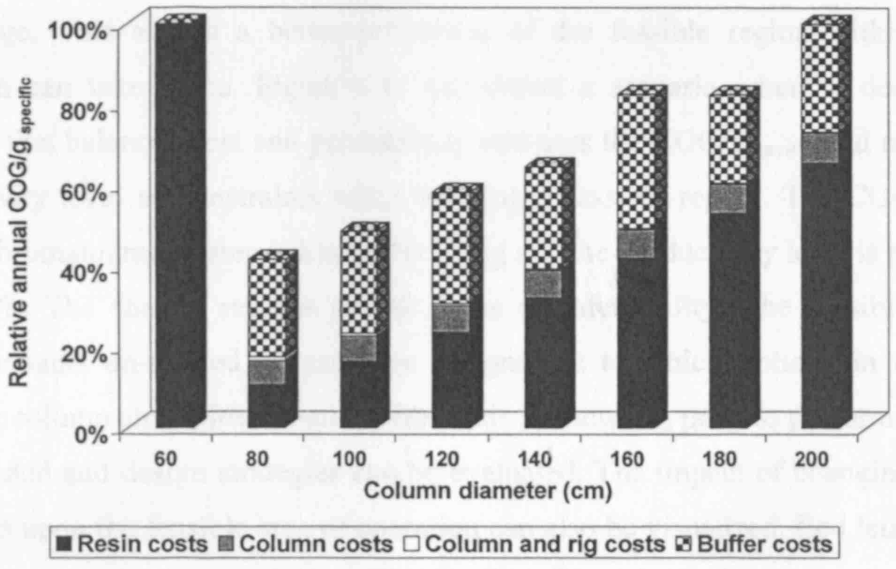

Figure 6.10 Breakdown of annual $COG/g_{specific}$ for different sizes of columns run at 75% of their maximum velocity.

sharp rise in resin lifetime in this region. Decreases in costs with increased column diameter follows as the number of cycles required for processing decreases. These effects result in a minimum $COG/g_{specific}$ for a given strategy. Figure 6.10 demonstrates this whereby a minimum is observed at a column diameter of 80 cm when operated at a loading velocity of approximately 235 cm/h. The minimum $COG/g_{specific}$ point depends on the velocity at which the column is operated since the resin dynamic binding capacity is a function of velocity. The contributions from buffer costs dominate the $COG/g_{specific}$ from column diameters of 60-120cm. This contribution decreases with increasing column diameter as the cycles required to process a batch of material reduce. Conversely, as column diameters become sufficiently large the quantity of expensive Protein A resin required start to dictate the $COG/g_{specific}$. This trade-off between buffer consumption and the cost of the Protein A resin can cause fluctuations in the $COG/g_{specific}$ as can be observed for column diameters of 160cm – 200cm.

6.7 Window of Operation

The utility of the kind of analysis presented in this chapter is that it allows the designer to customise limiting constraints based on product and process-specific knowledge. This allows a better prediction of the feasible region within which operation can take place. Figure 6.11 (a) shows a scenario where a decision is required that balances cost and productivity and uses the $COG/g_{specific}$ and minimum productivity level as constraints when defining a feasible region. The $COG/g_{specific}$ for the chromatography step is limited to \$15/g and the productivity level is restricted to 200g/h. The shaded regions denote areas of infeasibility. The feasible region which remains un-shaded informs the designer as to which options in terms of differing column strategies remain. Within this framework, process performance can be predicted and design strategies can be evaluated. The impact of changing design strategies upon the feasible area of operation can also be visualized. Bed length is an important factor in process design. Figures 6.11 (b) and (c) show how the feasible regions defined by productivity and cost, change with bed length. Figure 6.11 (b) shows that a larger feasible area is produced for a length of 10cm than that for the base case length of 15cm as seen in Figure 6.8 (a). A shorter bed length provides for

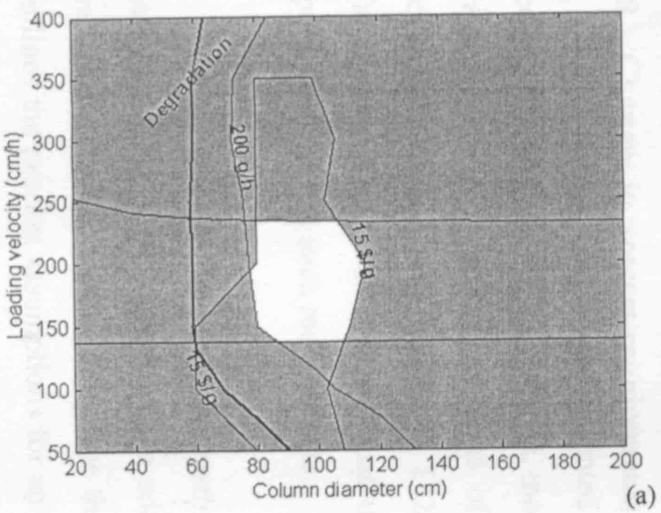

(a)

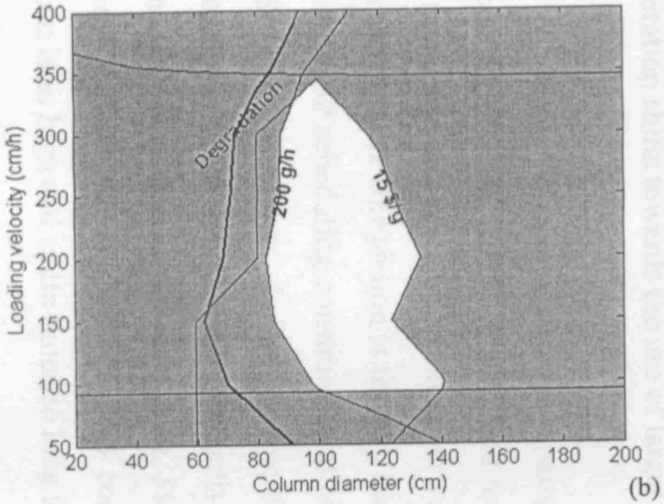

(b)

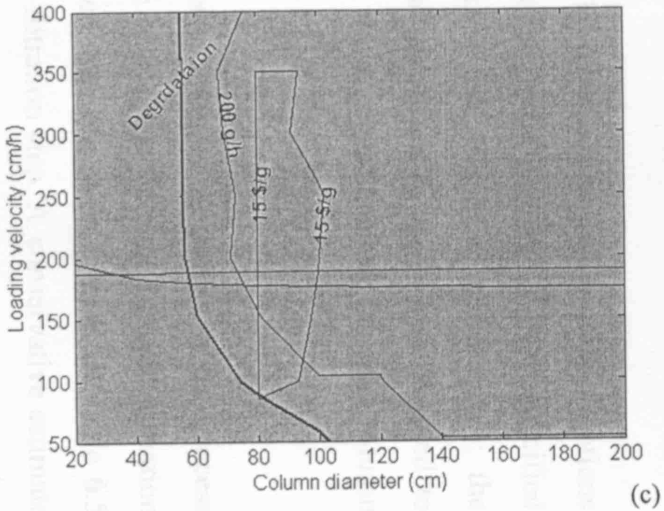

(c)

Figure 6.11 Windows of operation produced when constraining both cost at 15$/g and productivity at 200g/h for column lengths of **(a)** 18, **(b)** 10, **(c)** 20 and **(d)** 30cm.

a shorter residence time in the column and usually faster cycle times and a reduction in the shift constraint, as cycles can be completed within a day at lower velocities. Shorter beds are more rigid allowing for operation of column options at higher velocities. Finally, a reduction in bed length reduces the overall column volume and decreases column productivity, as noted in Figure 6.6 (a). The feasible region of operation shifts towards the use of larger diameter columns.

Figure 6.11 (c) shows that a reduction in the feasible area of operation occurs when the column length is increased to 20cm. Longer columns are more prone to compression and must be run at lower velocities than for a shorter column. The time taken for cycle completion is thereby increased and this necessitates an upward shift in the DSP scheduling constraint to allow full completion of column cycles within a DSP shift. However, due to the increase in column volume associated with an increase in bed length, column productivity and cost contours shift towards the use of smaller diameter columns. However, Figure 6.11 (c) shows that all column options become infeasible for the specified constraints; the compressive force felt by the resin is so high and cycle times so long that no options are sustainable.

6.8 Changes in process requirements

The model framework presented can be used to investigate various options open to the designer. If for example, more intensive constraints than those specified previously, were required in terms of process and economic performance; the required $COG/g_{specific}$ is limited to \$12/g and the productivity level is limited to 300g/h then Figure 6.12 shows that under these conditions no feasible column options can sustain such requirements.

One solution to overcome such an issue may be a change in the process flowsheet. One option could be the addition of a pre-concentrating ultra-filtration step prior to initial capture to reduce the batch volumes to be processed. Table 6.5 outlines the process assumptions for an ultra-filtration step. A conservative estimate for flux of 25 $L/m^2/h$ was assumed so that output solutions provide for a 'worst case' scenario for the designer. Further to this, filtration time was assumed to take place for 6 h, based on modelling data used by Farid (2001) when designing an

ultrafiltration step as pre-concentration prior to initial capture in their work. As detailed in Section 5.7, a long filtration time reduces the requirements for large amounts of membrane area.

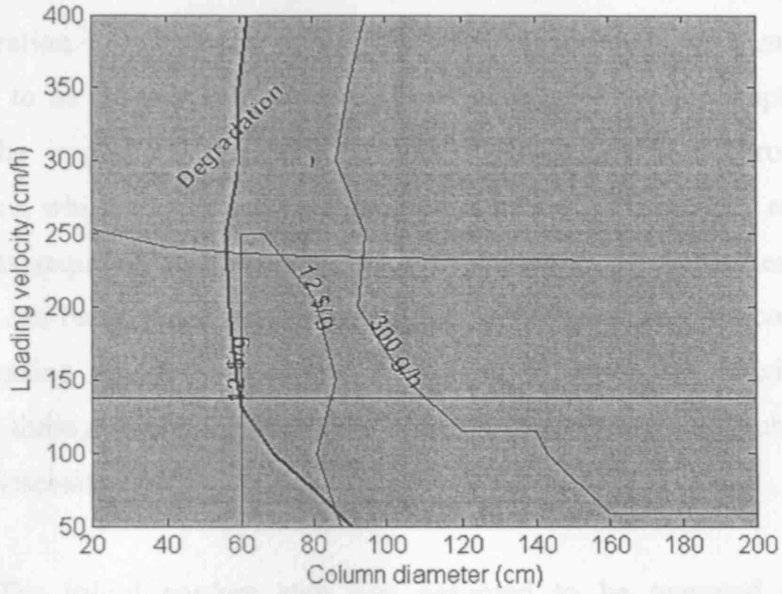

Figure 6.12 Window of operation showing no feasible column solutions when more intensive process constraints are required. Here, productivity is increased to 300 g/h and the required COG/$g_{specific}$ is reduced to 12$/g.

Table 6.5 Process assumptions for ultra-filtration step prior to initial capture chromatography. (Data based on discussions with J.Lim, BioPharm Services, Bucks, UK).

Assumption	Input Value
Filtration time (h)	6
Flux (L/m^2/h)	25

Equation (5.23) was used to calculate the extent of concentration attained based on the selection of the quantity of membrane used in the filtration step. The use of large quantities of membrane area has a bearing on cost, as the direct cost of the process increases the greater the membrane. However, Equation (5.23) shows that increasing membrane area leads to greater concentration factors which in turn mean greater reductions in process batch volume. Unfortunately, increasing the concentration of the batch to be processed corresponds to a more viscous feed solution to be processed by the initial chromatography step. Chapter 3 described in detail the impact of viscosity on the compression of a chromatography bed. Therefore, whilst the inclusion of the pre-concentrating step, may reduce the number of cycles required to process a batch of material, the velocities with which the column can be operated will be restricted. Table 6.6 shows the concentrating effect of increasing membrane use and the extent to which the maximum operational velocity through a column decreases brought about through the subsequent increases in feed viscosity.

The initial capture step was assumed to be operated at the maximum practicable operating velocity, taken to be 75% of the critical velocity and calculated through Equation (5.26) for the various column geometries and feed viscosities. Fixing the chromatographic velocity, allows the designer to visualise how the process performance criteria vary with column diameter and varying filtration membrane area. Figure 6.13 (a) shows how productivity changes with these design variables. A membrane area of 0 m^2 denotes no application of ultra-filtration and therefore provides a reference point as to the effect of this concentrating step.

As expected, productivity increases with increasing membrane area as well as column diameter. In both instances the increase in productivity is a consequence of the reduction in the number of cycles required for processing a batch of material. A reduction in the chromatographic cycles necessary reduces the total processing time. Figure 6.13 (b) shows how costs vary. Costs trends follow that of Figure 6.9 where, initially high costs are generated when operating with smaller columns due to high resin and buffer consumptions caused by long processing times. However, costs reduce with the application of the concentrating step as the number of cycles required

to process a batch of material decreases with increasing membrane area used. In fact a minimum COG/$g_{specific}$ is found for a column diameter of 80 cm when using a membrane area of approximately 30 m^2.

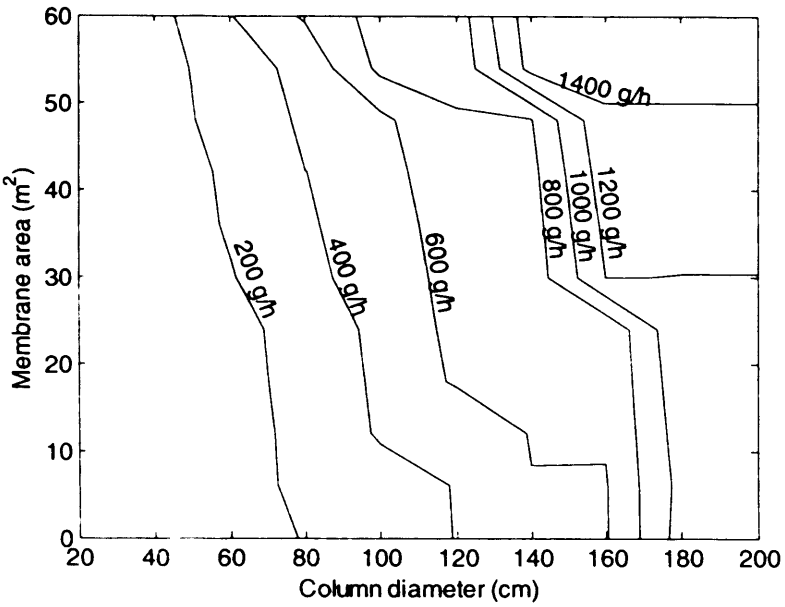

(a)

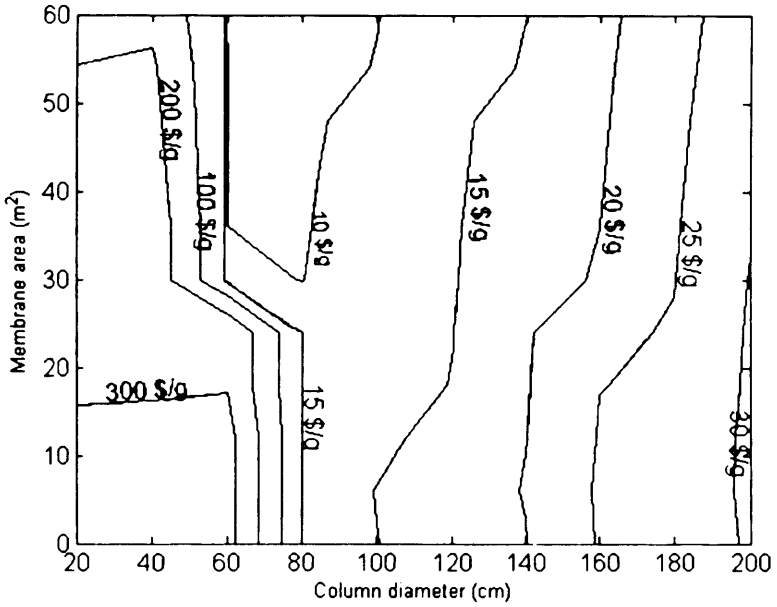

(b)

Figure 6.13 (a) Productivity contours for differing column sizes and membrane areas. **(b)** COG/$g_{specific}$ contours for varying column diameter and membrane area. Column loading velocity was fixed at 75% of the u_{crit}.

Table 6.6 Titres of load solutions achieved after applying varying degrees of pre-concentration and the maximal operating velocities calculated through Equation (5.26). * u_{crit} was calculated for a column of diameter 100cm and a bed height of 15cm.

Membrane area (m^2)	Titre (g/L)	Viscosity of loading buffer (x 10^{-4} kg/ms)	Max operational velocity 75% of u_{crit}* (cm/h)	Dynamic Binding Capacity (g/L)
0	1	8.05	234	23.7
10	1.2	8.09	233	25.6
20	1.4	8.17	230	27.4
30	1.8	8.29	227	30.2
40	2.5	8.49	222	33.0
50	4	8.94	212	37.3
60	10	11.13	174	46.2

Figure 6.14 (a) shows the application of the intensive performance criteria specified in Section 6.8. It shows that with the application of the pre-concentrating step, feasible column options become available to the designer to meet these targets. Typically most membrane units are produced in modular form, to allow easy replacement and scale-up (van Reis *et al.*, 1999). This means that there are only discrete quantities of membrane area available commercially. Similarly, column diameters are commonly only commercially available in discrete sizes. Millipore Corp. produce membrane modules available in cassettes providing a surface area of 2 m^2 [a]. GE Healthcare Biosciences manufacture column diameters varying in increments of 20cm[b] . Assuming that the filtration modules and chromatography columns are purchased from these commercial entities, Figure 6.14 (b) shows how the feasible region of operation is further reduced based on the discrete design options available. The intersection of the grid lines shows the points of available operation within the window of operation.

[a] www.millipore.com/catalogue.nsf/docs/C7840, accessed 2007
[b] ChromaFlow™ found in product catalogue within www.gelifesciences.com, 2007

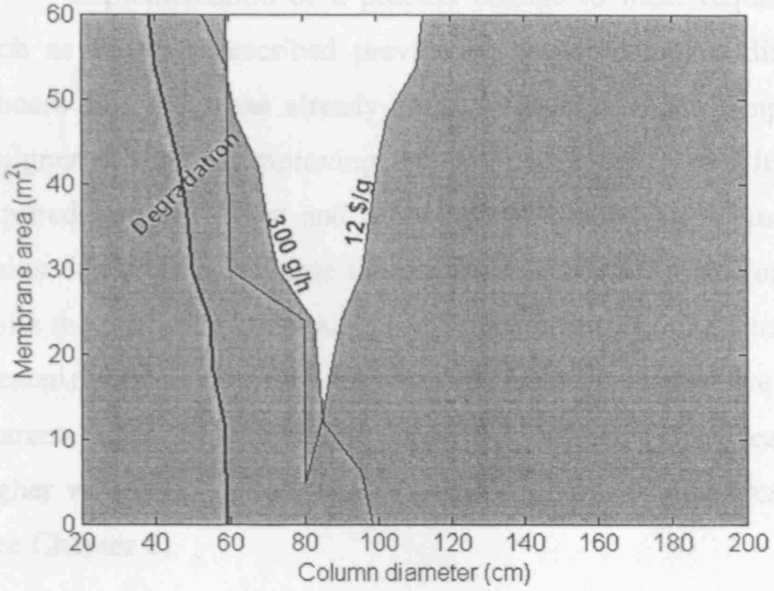

(a)

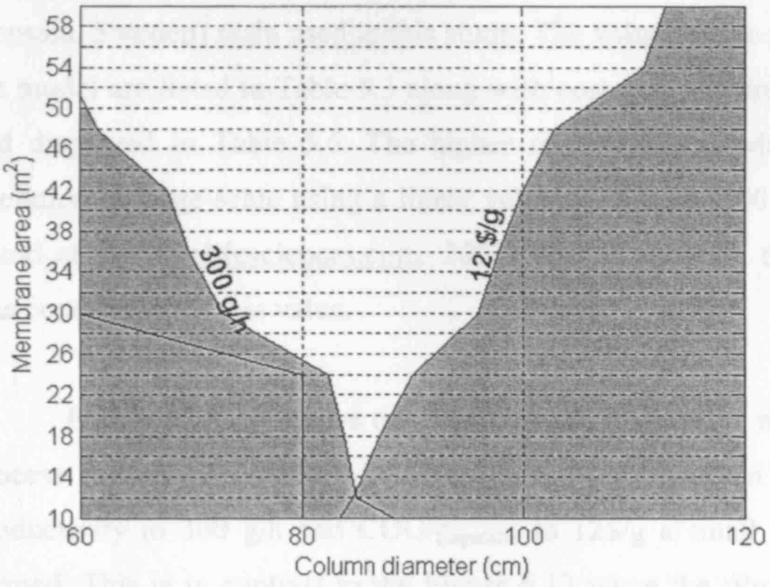

(b)

Figure 6.14 (a) Window of operation produced when constraining both cost at 12$/g and productivity at 300 g/h for varying membrane areas and column diameters. **(b)** Magnification of the window produced in (a) showing the discrete membrane and column options (denoted by grid intersections) commercially available to the designer.

6.8.1 Alteration of resin choice

Implementation of a process change to meet required performance targets such as the one described previously, is sometimes a difficult procedure if the process flowsheet has already been defined. A much simpler option open to the designer is that of improving the chromatographic step itself so as to attain the required targets of cost and productivity. The advent of more rigid agarose based resins designed to mitigate the problem of bed compression (see Chapter 2), have shifts the operating constraints and improved processing performance. In addition to greater rigidity, this new generation of Protein A resins have improved mass transfer characteristics and adsorptive capacities, allowing for greater capture of MAb at higher velocities. However, the penalty for use of these resins is their greater cost (see Chapter 2).

Data was taken from commercial literature[c] and was assumed to follow the adsorption of clarified humanised monoclonal antibody (IgG), produced in Chinese Hamster Ovary (CHO) cells, onto the rProtein A MabSelect^{TM} (GE Healthcare, Uppsala, Sweden) resin used in this study. The values of the main parameters used in the model are listed in Table 5.3 along with cost data acquired from the same source and displayed in Table 5.6. The higher rigidity of the MabSelect^{TM} resin allows operation at large-scale using a linear velocity of up to 500 cm/h (product data file found at www.gelifesciences.com, *2007*). It was assumed that operational velocity was constrained at this value.

Figure 6.15 (a) shows the effect of employing this new resin in the original process flowsheet described in Figure 6.1. It can be seen that when constraining productivity to 300 g/h and $COG/g_{specific}$ to 12$/g a small window of operation is formed. This is in contrast to the Figure 6.12 when the rProtein A Sepharose FF^{TM} was used. The greater velocities that can be attained using the MabSelect^{TM} resin ensure faster cycle times thus increasing the productivity of the overall process. Further to this, the enhanced mass transfer and adsorption kinetics (see Table 5.3) produce higher dynamic binding capacities at all the velocities tested when compared with the Sepharose FF^{TM} resin. Increases in the amount of product that can be bound

[c] MabSelect product data file found at www.gelifesciences.com, *2007*

reduce the number of cycles required to process a given batch. This in turn leads to a reduction in the $COG/g_{specific}$ despite the higher initial capital cost of the resin.

Figure 6.15 (b) shows the window of operation that is formed when using the MabSelect™ resin on application of a concentrating step prior to the Protein A chromatography. Loading velocity in this scenario was fixed at 500 cm/h for all column options investigated. It was assumed that the resin was sufficiently rigid to allow operation at this velocity despite the increases in the feed viscosity associated with the use of large membrane areas. (Equation (5.23) was not used to determine u_{crit} values due to resource limitations which prevented the estimation of $u_{10\%}$.) It can be observed that a larger number of column options are available to the designer through use of this strategy. Table 6.7 shows a summary of the feasible design options available to attain the specified performance criteria for both resins studied. Interestingly, application of the concentrating step yields no difference in the feasible column sizes available in both resin cases despite the feasible area of operation being larger when the MabSelect™ resin is used. This is a symptom of the discrete nature of the chromatography column sizes and membrane areas which limits the options available to the designer. Overall, use of the MabSelect™ resin offers greater operational flexibility, leading to more feasible process options as it does not require pre-concentration to meet process needs.

6.9 Conclusion

The development and implementation of a prototype tool to model the trade-offs in chromatography processing has been presented. Such a tool is useful for process management, resource utilisation, cost analysis and process efficiency assessments, all of which together bear on the examination and selection of column size and operation for different process options. This tool has been used to construct a series of 'windows of operation' which enable the designer to account for the

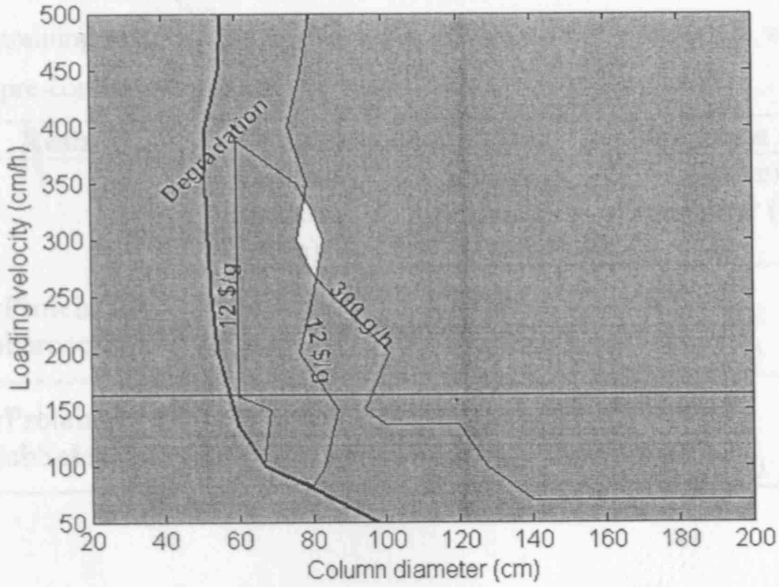

(a)

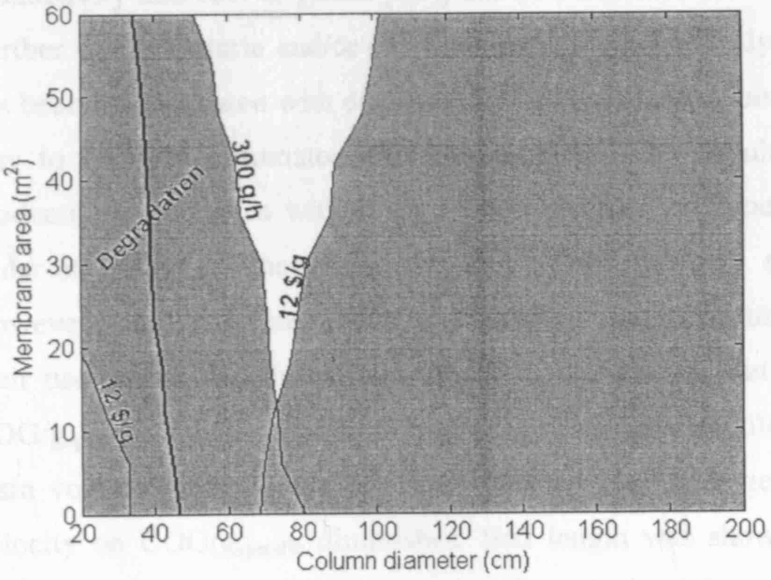

(b)

Figure 6.15 Window of operation produced when operating with the rProtein A MabSelect™ resin for **(a)** with no pre-concentrating step and **(b)** with application of a pre-concentrating step. $COG/g_{specific}$ is constrained to 12$/g and productivity to 300g/h.

Table 6.7 Summary of the discrete feasible column and membrane solutions available when constraining both $COG/g_{specific}$ to 12$/g and productivity to 300g/h with and without the use of a pre-concentrating step.

Resin	No pre-concentration		Inclusion of pre-concentration	
	Column diameter (cm)	Loading velocity (cm/h)	Column diameter (cm)	Membrane area (m^2)
rProtein A Sepharose FF™	**No solutions**		60	52-60
			80	26-60
			100	42-60
rProtein A MabSelect™	80	270-340	60	44-60
			80	26-60
			100	54-60

influence of compression, media degradation and column utilisation on the performance of a chromatography step and to quantify their effects in term of productivity and cost of goods per gram ($COG/g_{specific}$) for the chromatography step. Further design criteria and/or extra constraints can be easily added on. The method has been demonstrated with data from a Protein A separation and offers a convenient way to quantify chromatography performance. The simulation results show that productivity fluctuates with linear velocity for large diameter columns due to the under-utilisation of these large columns when they are not loaded to capacity. However, small diameter columns can suffer from over-utilisation which restricts their use due to scheduling constraints. It was shown that the minimum value of $COG/g_{specific}$ varies according to the velocity used for smaller columns. However as resin volume start to dominate costs with the use of larger columns the effect of velocity on $COG/g_{specific}$ diminishes. Bed length was shown to have a significant effect on the maximum flow allowable through the column. This in turn influences cycle times which effect column scheduling to fit DSP shift patterns. The results drawn from the case study provide a valuable insight into the feasible process strategies which can be used.

The window of operation was further shown to reflect the particular flowsheet selected. This was exemplified with a case study involving the addition of a concentrating step prior to initial capture. The tool was used to select design criteria

for both the chromatography and concentrating effect and it was shown that reducing the batch volume to be processed provided for a design solution when the cost and productivity of the Protein A step alone were infeasible. Further to this, the model provided a suitable platform for investigating the use of the new generation of Protein A resins as another design alternative. It is envisaged that such a tool can be used in the early stages of process development hence contributing to planning and project management decisions, enabling different designs and operational options to be explored rapidly.

Having investigated column design and operation in terms of column sizing and loading velocity, Chapter 7 now addresses an already sized and scheduled Protein A step. The investigation moves on to show how the framework described in Chapter 5 can be used to examine the operation of the Protein A step in more detail in terms of the chromatographic cycle itself. The impact and interactions that occur during the load, wash and CIP portions of the process are examined as well as the varying challenges that the designer has to address when selecting the appropriate Protein A resin for a particular process.

7 APPLICATION OF THE MODELLING FRAMEWORK TO ASSESS THE IMPACT OF OPERATING STRATEGY ON INITIAL CAPTURE CHROMATOGRAPHY IN LARGE SCALE MANUFACTURE.

7.1 Introduction

As has been described, the large-scale, economic purification of proteins is an increasingly important problem for the biotechnology industry. For a large number of protein-ligand systems, the adsorption of protein molecules to the adsorbent is sufficiently weak that during the post- load washing stage, some protein which has already been adsorbed onto the solid phase will re-enter the liquid phase and may be carried out of the column. Such product loss can have a significant effect on the economics of biopharmaceutical production.

In the previous chapter, the modelling framework described in Chapter 5 was used to size columns based on scheduling and process requirements. The effects on column size through changes in the process flowsheet as well as resin choice were also demonstrated. This chapter focuses on an already sized column. Whereas previously, yields were taken as an assumed value here the framework is used for determining the optimum operating parameters in order to help mitigate potential yield losses. The effects of loading velocity, loading volume and the post-load washing strategy on cost of goods (COG/g) and productivity (g/h) are investigated so as to identify the optimal operating strategy. Section 7.2 describes the importance of the post-load washing stage as well as the implications of its use for Protein A resins with differing backbone materials. Section 7.3 describes the modelling approach undertaken in this work when describing post-load washing. Section 7.4 outlines the case study which exemplifies the use of the framework in this analysis. Section 7.5 provides the results and discussions of the analysis whilst Section 7.6 shows how the windows of operation approach may be used in design decisions. Finally Section 7.7 provides a brief summary of this chapter.

7.2 The importance of the post-load wash stage

Protein A affinity chromatography is the predominant capture step for the purification of MAbs. A chromatographic cycle on a Protein A column comprises several steps including CIP stages which not only restore capacity but are also crucial to assure prolonged usage of the chromatography resin. The popularity of the Protein A step is mainly due to its high selectivity which leads to a high purification potential (Johansson *et al.*, 2003). However, these advantages are traded off against a relatively high cost per litre associated with this type of chromatographic resin. Several published works have been devoted to various techniques and developments for the optimal usage of Protein A resins. Generally optimisation in terms of operating strategies has revolved around the loading stage (Yamamoto *et al.*, 1992; Farhrner *et al.*, 1999; Johansson *et al.*, 2003; McCue *et al.*, 2003; Ghose *et al.*, 2004) given that this is frequently the rate determining step in a chromatographic cycle. There have also been many advances in understanding the science and application behind optimising the conditions in isocratic elution, gradient elution and displacement chromatography (Jacobson *et al.*, 1992; Felinger *et al.*, 1996, 1998). However, there are only limited references in the literature which describe the impact of the post-load washing stage (Arve *et al.*, 1987; Levison *et al.*, 1992; Mao *et al.*, 1996; Millipore Technical Brief, TB1026EN00, 2006[a]).

The biological raw material from which the MAb is to be purified usually contains a range of contaminating compounds including endotoxins, DNA and host cell proteins (HCP) which are often present in quantities far exceeding the amount of the desired product (Arve *et al.*, 1987). On loading, Protein A resins as with all chromatography media, can exhibit a degree of non-specific binding, which is typically characterised by co-elution of HCPs together with the desired product MAb. A wash step between loading and elution to disrupt the interactions that occur between the contaminants and the resins, without prematurely eluting the product MAb could increase the levels of HCP removal (Arve *et al.*, 1987). Such a step is traditionally used as part of a chromatographic cycle in manufacturing.

[a] http://www.millipore.com/publications.nsf/docs/tb1026en00

Given the specificity of the Protein A ligand this non-specific binding is usually due to either ionic or hydrophobic interactions with the resin backbone or immobilization chemistry (Millipore Technical Brief, TB1026EN00, 2006[a]). As a consequence, the degree of non-specific contaminant binding is also a function of the material from which the resin backbone is synthesised. The most prevalent resins available on the market today have either an agarose backbone with various degrees of cross-linking or are made of a controlled pore glass (CPG) matrix. CPG is quite hydrophobic as compared to agarose and thus exhibits significantly higher levels of non-specific interactions (Ghose, 2005).

For most applications post load washing is carried out using a buffer at neutral pH, usually the equilibration buffer. Hahn *et al.* (2006) found that host cell protein content in eluates was approximately 10 times higher when washing a CPG resin with a neutral buffer when compared to an agarose based resin. Operating strategies with several wash steps have been developed for CPG resins to address specifically this issue (Blank. 1997; Breece *et al.*, 2005; Lebreton *et al.*, 2006). One such strategy is a two step washing strategy (Lebreton *et al.*, 2006) aimed at selecting conditions for an intermediate wash buffer which will elute greater levels of HCP and other contaminants. Subsequent elution of the MAb will result in a higher purity product pool. Typically, the first stage of this washing strategy will take the form of equilibrating the column after loading (Lebreton *et al.*, 2006). This also serves to help wash out any unbound contaminants which have diffused into the pores of the resin. The subsequent second stage involves washing with a buffer whose pH is selected between that of the loading and elution buffers (Millipore Technical Brief, TB1026EN00, 2006[a]) to elute any non-specifically bound contaminants. Washing with a low pH buffer however may run the risk of initiating premature elution of the product MAb, impacting on the overall yield of the process.

Mao *et al.* (1996) have shown that product losses resulting from post-load washing impact on the productivity of the chromatography step as a whole. It was also shown that product yield may be improved by under-utilising the total column capacity so that breakthrough does not occur before the loading stage is terminated. Through this action, the adsorbent particles of the column stationary phase close to

the outlet of the bed have vacant ligands as the resin is under-utilised. During the wash, product can be re-adsorbed as they flow through the column. Historically, this practice has been used commercially and is referred to as using a 'safety factor'. Typically, safety factors are within the range of 5-20 % below the breakthrough load volume (Lyer *et al.*, 2002). Operating with a safety factor of 80 therefore indicates loading a volume onto the column that is 20 % below the breakthrough load volume. Operating with a safety factor of 100 equates to loading to breakthrough which in this study was assumed to be to 1% of the concentration of product in the feed. Loading strategies which make use of safety factors may compromise productivity of the chromatography step as less material per cycle is loaded onto the column. Therefore, the more conservative the strategy, the longer the time it will take to process a batch of material. This however, can be traded-off against lower losses in product. Little modelling work has been done to examine the production economics of a chromatography step operating with a safety factor in place. Further to this there has been no analysis as to how to determine the optimum safety factor for a given process.

To complicate issues further to fulfill current regulatory criteria, clean-in-place (CIP) procedures have become part of the master method for chromatographic operation (Burgoyne *et al.*, 1993). Sodium hydroxide solutions are commonly used for chromatographic system sanitisation and cleaning (Sofer *et al.*, 1989). It has been shown that this type of treatment causes a capacity loss in adsorbents (Boschetti, 1994), which therefore have finite lifetimes defined in terms of the maximum number of possible re-uses. It is the binding capacity of the adsorbent over its entire working life that defines the true operating cost and which must be considered in any economic evaluation. Resin lifetimes are an important consideration in the economics of a Protein A capture step. This is because rather than using a large column to process a batch of antibody in a single cycle, typical bioprocess applications run a smaller Protein A affinity column for several cycles to process a single batch. This reduces the risk of lost capital costs if the column is compromised during operation and also brings the column diameter into a practical range. Despite optimised cleaning procedures resins experience a gradual loss in capacity. These loses can be minimised using a more alkali stable ligand.

Resins possessing a CPG backbone however do not typically include hydroxide solutions in their cleaning protocols. This is because CPG becomes unstable in highly alkaline conditions causing a rapid increase in column back-pressure during operation (Lute *et al.*, 2005). Therefore, in these instances cleaning involves the use of phosphoric acid and guanidine based solutions (Millipore technical Brief, DS4241EN00, 2007[b]). Despite the greater expense of these buffers, capacity losses are greatly reduced during multi-cycle operation as compared to the use of hydroxide solutions (Lute *et al.*, 2005), with resin lifetimes reaching up to 300 cycles of operation (Fahrner *et al.*, 2001; Millipore technical Brief, DS4241EN00, 2007[b]).

The application of safety factors becomes important when considering losses in resin capacity during operation. Under-utilising the capacity of the resin ensures a constant level of chromatographic performance for a longer length of time before degradation causes a reduction in binding performance. This chapter utilises the framework proposed in Chapter 5 for characterising the operation of a chromatographic step in terms of both its process and economic performance. In this case the tool is used to provide a basis for the selection of operating strategy in terms of loading and subsequent washing of initial capture chromatography in a manufacturing environment. Typically in industry, the choice of Protein A resin is application specific and depends on achieving the best compromise between capacity, product purity and flow characteristics (which contribute to throughput). Therefore, to demonstrate the full functionalities of the tool developed, the methodology is demonstrated through a case study involving a theoretical Protein A resin whose properties represent an industry average. This pseudo-resin displays characteristics of a CPG resin backbone, whereby non-specific binding is relatively high. Further to this, the resin also demonstrates capacity degradation rates which are similar to those found on agarose based resins cleaned with hydroxide solutions. Outputs are presented via readily interpreted graphical formats for the easy visualisation of process trade-offs. The objective was to achieve a maximum

[b] http://www.millipore.com/publications.nsf/docs/ds1013en00

production rate and minimum cost for a Protein A affinity process whilst ensuring that the basic requirements of product purity and yield were met.

7.3 Modelling Approach

With the complexity involved in overall chromatographic process design, model based computational tools are indispensable. The general rate model developed by Gu and co-workers (1995) and described in Section 5.3 was chosen to provide the chromatographic data to be studied and offers a compromise between model complexity and ease of use.

7.3.1 Parameter Determination for the general rate model

The physical and chemical properties of the pseudo-resin were taken as averaged values of those quoted in literature for commercially available CPG and agarose based Protein A resins used in the separation of humanised monoclonal antibody (IgG), produced in Chinese Hamster Ovary (CHO) cells (McCue *et al.*, 2003; Hahn *et al.*, 2005). The pseudo-resin parameter values, taken as the average between the values for the MabSelect™ resin described in Table 5.3 and the Prosep vA® Ultra resin described in Table 5.4 are listed below in Table 7.1. It was assumed that the equilibrium between the IgG and the solid phase concentrations in affinity systems can be modelled using a Langmuir isotherm.

Feed stream contaminants were modelled as a single lumped component term. The contaminant adsorption was also assumed to exhibit Langmuirian behaviour. This is because of the relatively high level of non-specific binding assumed to be associated with the resin used in this analysis. Adsorption parameters for the contaminant were modelled through fitting Langmuir parameters to attain typical adsorption and desorption behaviour of HCPs observed in initial capture operation in an industrial process (Hahn *et al.*, 2006). The feed concentration of the contaminant component was taken to be 5 times larger than that of the MAb, which reflects values observed in a typical antibody production process (Lebreton *et al.*,

Table 7.1 Assumed parameter values representative of a pseudo-resin possessing intermediate properties between commercially available the agarose resin MabSelect (Table 5.3) and the CPG based resin Prosep vA Ultra® (Table 5.4) for the adsorption of MAb from CHO cells to Protein A.

Parameter	General data	IgG	HCP
r_p (cm)	0.0046		
d_p (A)	570		
MW (g/mol)		150000	20000
ε_b	0.41		
$\varepsilon_{p\ effective}$	0.49		
External film mass transfer, k_f (cm/s)		0.0015	0.0023
Effective diffusivity, D_{eff} (cm^2/s)		4.7×10^{-8}	8.6×10^{-8}
Dissociation constant, K_d (g/L)		0.118	2
Saturation capacity, Q_{max} (g/L)		61.5	13
After intermediate washing			
Dissociation constant, K_d (g/L)		0.177	4
Saturation capacity, Q_{max} (g/L)		58.4	11.7

2006). The values of the main parameters describing the separation are listed in Table 7.1.

7.3.2 Washing Strategy

In this work a two step post-load washing strategy was investigated. The first step, which occurs directly after loading, was assumed to be fixed. This consisted of the column being washed with 3 column volumes (CV) of neutral equilibration buffer at a constant velocity of 500 cm/h. The values of the model parameters in this wash stage were taken to be the same as during adsorption (see Table 7.1).

The second wash step was assumed to involve a buffer whose pH was intermediate between that of the load and elution buffers; hence the interaction mechanisms during the adsorption stage are not valid here. The model parameters for this low pH wash buffer were obtained by fitting the model to literature values reported for similar conditions. Mann *et al.* (Millipore Technical Brief, TB1024EN00, 2007[c]) state that there is a greater than 75 % reduction in levels of HCP when washing with an intermediate wash buffer as opposed to the equilibration buffer. Further to this, Sada *et al.* (1986) have shown decreases in adsorption capacity in immuno-affinity chromatography with pH. In some cases this decrease is up to 10 % when washing with buffers of pH 4-5. The values of the model parameters in this wash stage are given in Table 7.1.

The assumed change in adsorption equilibrium during intermediate washing for both the contaminant and product binding to Protein A is shown in Figure 7.1. A linear mixing rule was used when modelling the front between the equilibration buffer used in the first wash and the intermediate pH buffer on commencement of the second stage of washing.

The elution stage of the chromatographic cycle was not modelled specifically but was assumed to take a step-wise approach (Fahrner *et al.*, 1999) with negligible losses in product. All other stages of the chromatographic cycle, with the exception

[c] http://www.priorartdatabase.com/IPCOM/000127319/

of loading and the second intermediate wash step, were assumed to be operated at a linear velocity of 500 cm/h taken as corresponding to the maximum operational column pressure drop. Adopting such a strategy emphasises the importance of column scheduling in order to realise the greatest gains in productivity. Unlike fermentation which, owing to the nature of cell growth, is run 24 h a day until the desired end point is reached, downstream processing operations are often scheduled to fit with shift patterns so as to ensure constant monitoring. Cycles of chromatographic operation must therefore be fully completed within the allocated downstream processing period available in each working day (discussed in more detail in Chapter 5, Section 5.9).

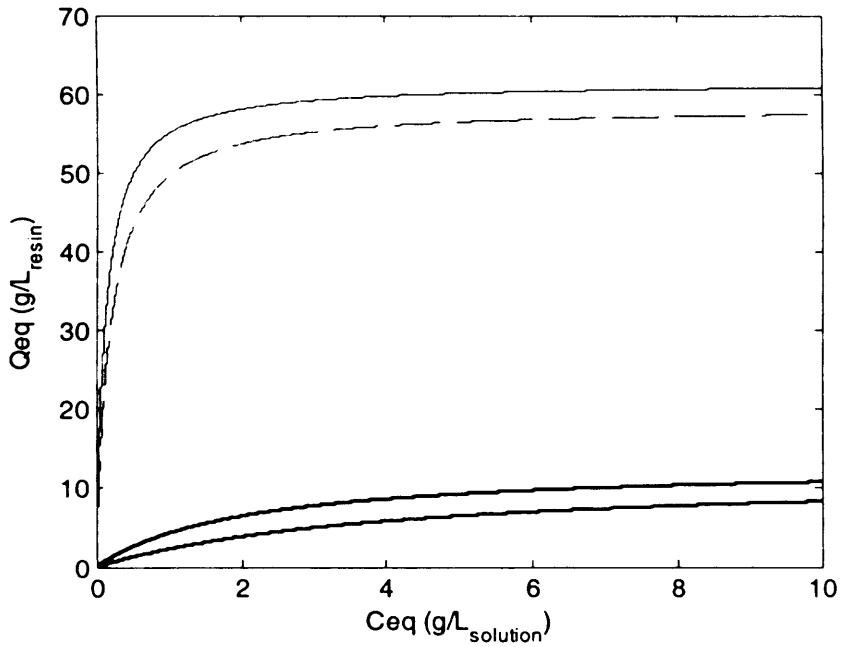

Figure 7.1 Adsorption equilibrium data for **(a)** MAb binding to Protein A on conditions of a neutral pH buffer (———) and under conditions of an intermediate wash buffer (— — —); Lumped contaminant term binding to resin backbone on conditions of a neutral pH buffer (▫▫▫) and under conditions of an intermediate wash buffer (▫ ▫ ▫).

7.3.3 Resin Degradation

One of the factors that impacts greatly on the cost of the affinity process is the functional lifetime of the resin. The degradation of the pseudo-resin was assumed to follow a degradation function of the form described in Equation 5.20 shown in Section 5.6. The rate of degradation was assumed to follow the results of an extensive cleaning cycle study of the rProtein A media MabSelect^{TM} (Johansson *et al.*, 2002).

7.4 Case Study based on the Production of MAbs

The design, implementation and application of the framework were explored using data for the production of recombinant humanised monoclonal antibody from CHO cells. Cell culture titres for protein, particularly MAbs, have increased over the recent years from tenths of a gram per liter to 10 g/L (Thommes *et al.*, 2007). To reflect the typical titres used today a product titer of 3 g/L was assumed. A fixed reactor volume of 10,000 L was also assumed in this case, meaning that approximately 400 kg of MAb would be produced during plant operation in a year. The case study focuses on the Protein A initial capture stage in this process. It was assumed that the column had already been sized and a fixed set of process assumptions, listed in Table 7.2, were made. All simulations were driven by the need to process a defined batch of material from a 10,000 L fed-batch reactor. The reactor was scheduled to output 20 batches in a 48 week production year. We sought to determine what is the best loading and washing strategy to use so as to ensure a desired level of product purity and yield. The relative merits and limitations of differing washing and loading strategies are explored with the help of technical and financial indicators: $COG/g_{specific}$ and the productivity of the capture step (g/h).

7.5 Results and Discussion

7.5.1 Process Output

Figure 7.2 (a) shows the relationship between eluate purity and yield after various amounts of post-load washing with neutral equilibration buffer. It can be seen that the recovery of product is dependent on the requirement for purity and that yield decreases with increasing wash duration and hence purity. Contaminants

Table 7.2 Overall process assumptions for the manufacture of a MAb from mammalian cell culture. *CV denotes column volume.

Assumption	Input Value	Reference
Lang factor	6	(Assumed)
DSP plant operating hours	48 weeks per year, 7 days per week, 8h per day	
Bioreactor size	10,000L	(Assumed)
Titer, C_0	3 g/L	(Assumed)
L (cm)	20	
D (cm)	100	
Chromatography Equipment depreciation	10%	(Assumed)
Volume of equilibration buffer used / cycle	4 CV*	Ghose *et al.* (2004)
Volume of Elution buffer used / cycle	4 CV	Ghose *et al.* (2004)
CIP contact time/ cycle	15 min	Johansson *et al.*, (2002)
CIP capacity degradation constant, Φ Eq. (5.20)	0.17	Johansson *et al.*, (2002)
Yield of DSP post initial capture	70%	Calculated, Table 5.7
Chromatography contribution to process cost	8%	(Assumed)
Selling Price MAb, MP_{MAb}	$1325	(Assumed)

entering the column through the feed stream form a relatively weak equilibrium with the backbone of the pseudo-resin and therefore the resin exhibits a degree of non-specific binding. As post-load washing commences, the equilibrium binding conditions inside the column are altered for both the contaminant and the product. While the disruption to the binding equilibrium of contaminants to resin is a favourable process, as the intensity of washing increases, more MAb is eluted from the column (Figure 7.2 (a)) and process yield decreases.

Generally, purity levels required post Protein A purification needs to be greater than 98%. Fahrner *et al.* (2001) reports that in a typical antibody recovery process, HCP levels in the eluate pool after Protein A purification should be in the range of 200-3000ppm. Figure 7.2 (b) shows the eluate purity and yield relationship when a two stage washing strategy is implemented. Here, the first stage of washing was performed with 3CV of equilibration buffer whilst the subsequent second stage comprised 4CV of washing with an intermediate buffer. The addition of the intermediate wash buffer disrupts the interactions between the HCP contaminants and the resin backbone but also induces premature elution of the MAb product. Product yield decreases more rapidly in comparison to washing with a neutral pH buffer. The rate of product loss between 2CV and 4CV of washing is greater than the yield losses between 8CV and 10CV of washing. This is because the effluent concentration profile at high wash volumes starts to decrease as the concentration of MAb inside the solid phase of the resin has reduced.

The specific mechanisms active during post-load washing can be observed through examination of the concentration profiles of the product MAb in the solid phase along the length of the column, during the loading and washing stages. Figure 7.3 (a) shows the concentration profiles in the solid phase prevailing on completion of loading to 1% breakthrough. The concentration of product along the bed falls as the majority of the product loaded is adsorbed near the top of the bed and therefore less unbound material is available to be re-adsorbed by the resin particles which are located towards the exit of the column. Figure 7.3 (b) shows how the concentration profile changes if a two wash step strategy is implemented. During the first stage of washing, the MAb-ligand complexes formed at the top of the bed are disrupted by

the wash buffer leading to a reduction in the product concentration in the solid phase and an increase in the concentration in the bulk fluid phase. After a period of time a concentration gradient is established between the parts of the column which are not fully saturated with MAb and the bulk fluid phase, which results in the transport of MAb from the bulk fluid back into the stationary phase in a similar manner as during the loading stage. Therefore MAb which was unbound becomes re-adsorbed to available ligands sites causing the increase in concentration that is observed further down the bed. By this time however, there may be a degree of product loss as MAb exits the column through the effluent stream.

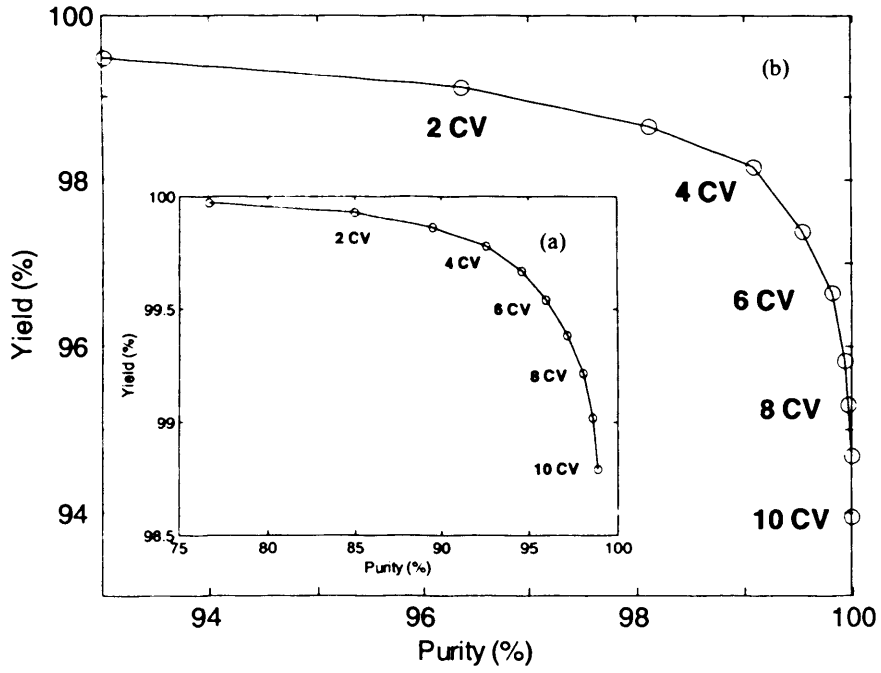

Figure 7.2 Yield as a function of final purity after various levels of washing in a Protein A affinity column after loading to 1% breakthrough for (a) single stage washing with equilibration buffer and (b) two stage washing with 3CV of equilibration followed by various amounts of intermediate wash buffer. The numbers on the curves represent the number of column volumes (CV) of wash buffer passed through the column at a velocity of 500cm/h.

Washing with a further 4CV of intermediate wash buffer shifts the concentration profile further down towards the end of the bed. The harsher washing conditions cause more product to elute so that there is a greater quantity of MAb flowing towards the exit of the column. However, as can be observed in Figure 7.3 (b), the concentration of product at the column exit is higher than that after the neutral pH wash. This is due to the fact that not all the available MAb is re-bound to the column as available binding sites become saturated. Any unbound MAb exits the column.

The dashed lines in Figure 7.3 represent solid phase concentration profiles when loading to below the effluent breakthrough level, in this case with a safety factor of 80. Loading to below the breakthrough level indicates that the quantity of product loaded was insufficient to utilise the breakthrough capacity of the bed as can be seen in Figure 7.3 (a). The unused capacity represents vacant ligands which are available to capture any product which becomes unbound during the wash stage. Therefore, there is a greater chance of product re-capture during washing. Since the area under the loading and washing profiles are nearly the same, almost no product loss during the first wash step is observed under these conditions. A reduction in the product losses during the second wash step is also observed (Figure 7.3 (b)).

It can be concluded that performance in terms of process yield can be improved by under-utilising the column during the loading stage whereby a safe margin of vacant ligands is provided which can re-adsorb any product which becomes detached during post-load washing. In order to investigate this further, simulations were carried out for a variety of different load and wash volumes at a constant velocity, the results of which are shown in Figure 7.4. The first wash step was assumed to be constant and carried out at 500 cm/h and for 3 CV. Wash volumes quoted from this section onwards will therefore refer to the second intermediate wash step only.

Figure 7.4 (a) shows contours of product yield for varying safety factors and levels of post-load washing. For a given volume of washing, yield decreases with increasing safety factor. The lower the safety factor or load volume, the greater the

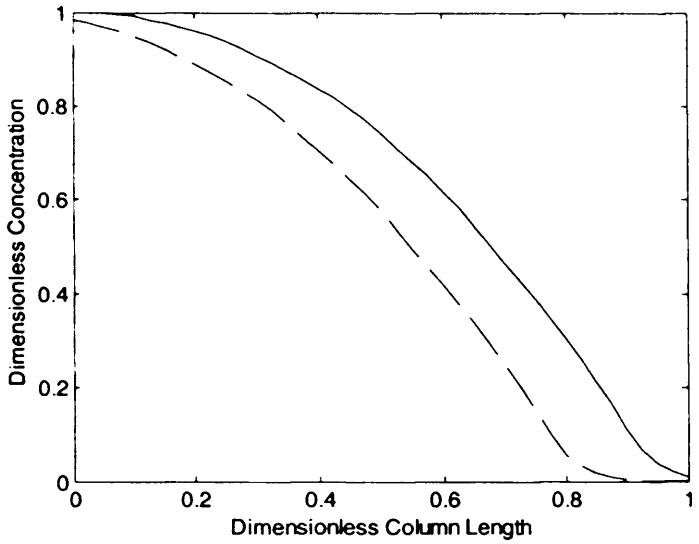

(a)

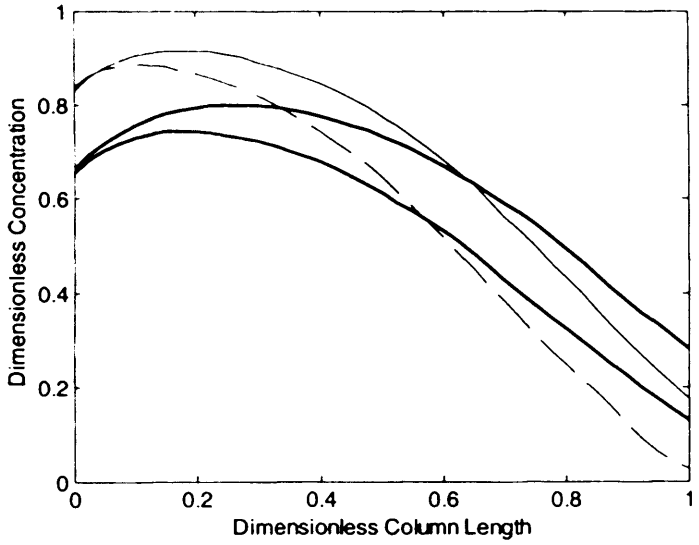

(b)

Figure 7.3 Concentration profiles in the solid phase at **(a)** the end of loading to 1% breakthrough (———) and at the end of loading to 80% of the breakthrough load volume (— — —). **(b)** Concentration profiles in the solid phase at the end of the first wash stage when washing with 3CV of equilibration buffer after loading to 1% breakthrough (———), the end of washing with 3CV of equilibration buffer after loading to 80% of the breakthrough volume (— — —); and concentration profiles in the solid phase at the end of the second wash stage when washing with 4CV of low pH buffer after loading to 1% breakthrough (———) , the end of the second wash step when washing with 4CV of low pH buffer after loading to 80% of the breakthrough volume (— — —).

quantity of vacant ligands available to rebind any MAb that has been desorbed during intermediate washing.

Figure 7.4 (b) shows contours of product purity for varying levels of washing and loading. The greater the level of washing, the higher the eluate product purity. However, for a given wash volume, product purity is observed to increase with decreasing safety factor. This effect is seen most clearly when washing with low volumes of buffer. The trend can be attributed to the higher contaminant to product ratio in the column at low load volumes. Generally, due to the contaminants' lack of affinity to the Protein A ligand, the concentration of contaminant will have approached closely the equilibrium levels at all positions in the column before the loading stage is terminated and hence the smaller load volumes which also equate to low safety factors correspond to a smaller mass of product loaded onto the stationary phase. Consequently a greater proportion of contaminant is present in the column when using load volumes closer to that required to achieve breakthrough. This trend is however, fairly weak when the quantity of wash buffer is high. In these instances contaminant levels are reduced greatly compared with that of the MAb, whose yield is a function of the safety factor applied.

7.5.2 Impact of column cycling

As discussed earlier, binding capacity decreases during multi-cycle operation. Figure 7.5 (a) shows the effect that such degradation has on the mass of product lost as a percentage of the mass loaded onto the column over a number of cycles of operation. Total product losses, meaning losses that occur during the loading and washing stages, can be observed to increase continuously with the number of cycles of operation. Here, the column was washed with 6 CV of wash buffer at a velocity of 500 cm/h and loaded to breakthrough as well as with a safety factor of 80. The results show the mass of product lost that is attributable to the wash stage alone. Wash losses increase with increasing reuse of the resin for a certain number of cycles. As washing commences and MAb becomes prematurely desorbed from the Protein A ligands, capacity losses reduce the amount of product that can be re-bound through the column. Greater amounts of MAb are lost in the effluent stream from the column the more the resin is degraded.

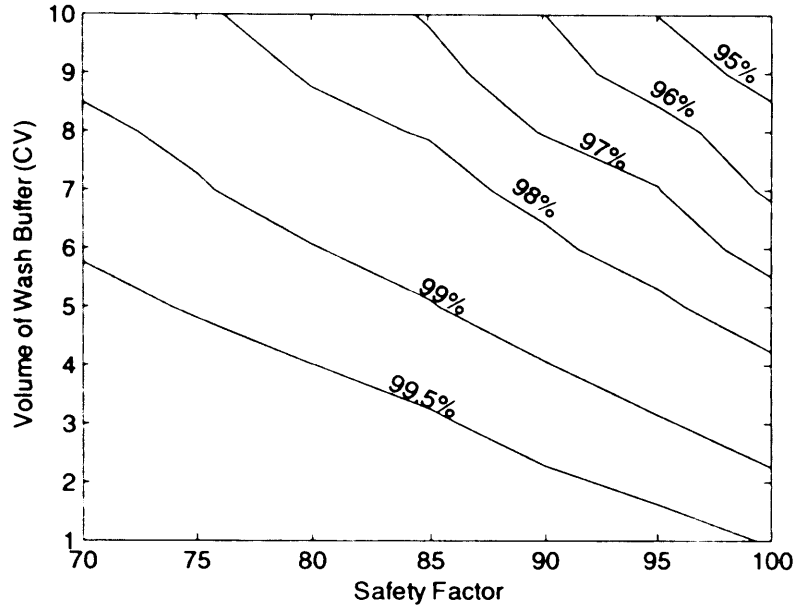

(a)

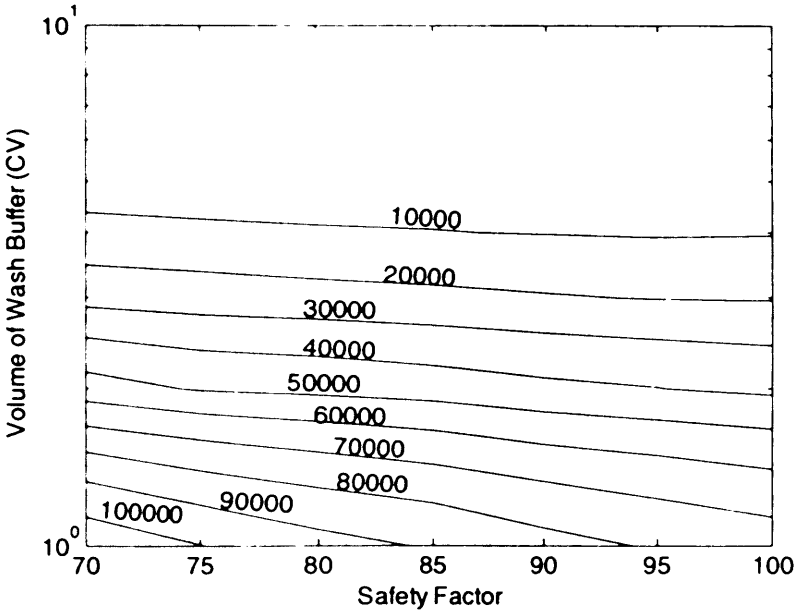

(b)

Figure 7.4 Contours of yield **(a)** and purity **(b)** for differing wash volumes of intermediate buffer and safety factors for a loading velocity of 500cm/h and washing velocity of 500cm/h.

The mass lost during the wash closely follows that of the total product losses for approximately 75 cycles when loading to breakthrough and for 125 cycles on implementation of a safety factor of 80. This indicates that the majority of yield losses up to these points can be attributable to wash losses. Subsequent reuse of the resin however is then characterised by product loss attributed to the loading phase as breakthrough is achieved earlier whilst wash losses level off. The combined product losses continue to increase. Eventually decreases in wash losses result from reduced levels of binding that occur on severely degraded resins during the adsorption stage. Typically however, such extended cycling is not encountered in industry where lifetimes of 100-200 cycles will be more than economically sufficient (Johansson *et al.*, 2002).

Figure 7.5(b) shows the solid phase concentration profiles during loading and washing on a column operating its 200th cycle. It can be seen that the column is almost fully saturated as available binding sites are approaching a minimum due to the significant level of degradation the exposed resin has experienced. The resin fails to bind the quantity of MAb loaded onto the column and the concentration of MAb in the effluent stream is high, reflecting early breakthrough. As washing commences the concentration peak exits the column rapidly and after washing with 6 CV of buffer, the concentration peak has moved out of the column and the effluent concentration of MAb declines. Therefore, actual product loss during the washing stage is reduced in comparison to that seen during the initial cycles of operation.

The application of a safety factor of 80 decreases the level of product loss during washing as compared to a safety factor of 100. The impact of the reduction in capacity when reusing the resin is diminished as the available capacity of the resin is greater than if loading had proceeded to breakthrough. Consequently, it takes more cycles to achieve the same levels of product losses as when loading with no safety factor. After running the column for approximately 230 cycles the fraction of the product lost during the wash stage to that loaded onto the column is greater than when loading to breakthrough. A consequence of implementing a safety factor is that less material is loaded onto the column and therefore as the level of degradation

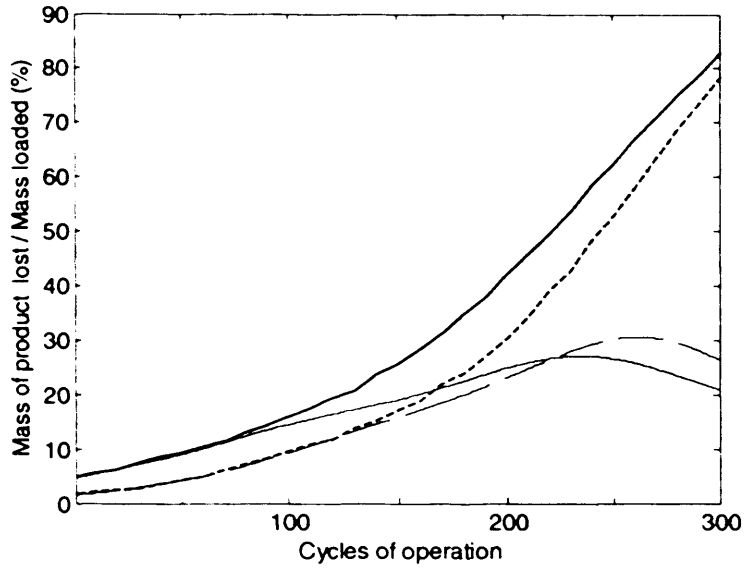

(a)

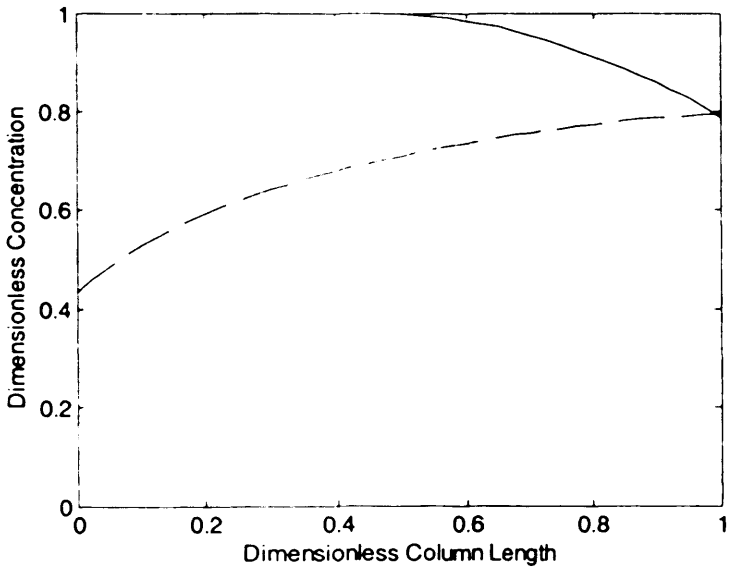

(b)

Figure 7.5 (a) Mass of product lost during intermediate washing with 6CV of buffer as a proportion of mass loaded onto the column when operating with a safety factor of 80 (— — —) and 100 (———); grey lines show the total losses in product for both washing and loading stages, over an extended number of cycles of operation; **(b)** Concentration in the solid phase during the 200th process cycle, at the end of loading (———) and at the end of washing with 6CV of wash buffer (— — —). Loading and washing took place at a velocity of 500cm/h.

increases so the proportion of product loss in the wash and load stages, as a percentage of the mass loaded onto the column increases at a greater rate than for higher load volumes (no safety factor).

7.5.3 Impact of loading velocity on washing

Figure 7.6 (a) shows the impact of varying the loading velocity on the losses that are incurred during column washing as a function of the number of cycles. For operation up to approximately 220 cycles, loading at the lower velocity increases the product loss. Beyond this point product losses in the wash are greater when adopting a higher loading velocity is used. The reasoning behind such trends may be explained with reference to Figure 7.6 (b).

Figure 7.6 (b) shows the impact of varying the loading velocity on the solid phase concentration profiles inside the column after loading and washing during the first cycle of operation. When loading at a low velocity MAb has sufficient time to diffuse fully into the binding sites of the resin making full use of the column capacity. When washing begins the free resin capacity remaining is insufficient to capture the mass of material desorbed during the wash and consequently product is lost out of the column. Conversely resin capacity is relatively under-utilised when high load velocities are used. There is therefore less material bound to the column and more free capacity throughout the column to capture any material desorbed during the washing stage. Figure 7.6 (a) shows that after approximately 200 cycles product losses caused by the wash are greater when loading with a velocity of 500 cm/h than when loading at 200cm/h. This is a consequence of the greater mass of material captured onto the column when using the lower velocity. Therefore, despite the absolute product losses being higher in the case of loading with a lower velocity, the proportion of product lost compared to that loaded is smaller, than when loading at higher velocities.

7.5.4 Evaluation of resin lifetime

Equation (5.22a) was used to calculate the cumulative economic potential as a function of the extent of resin reuse. The solid line in Figure 7.7 (a) shows the

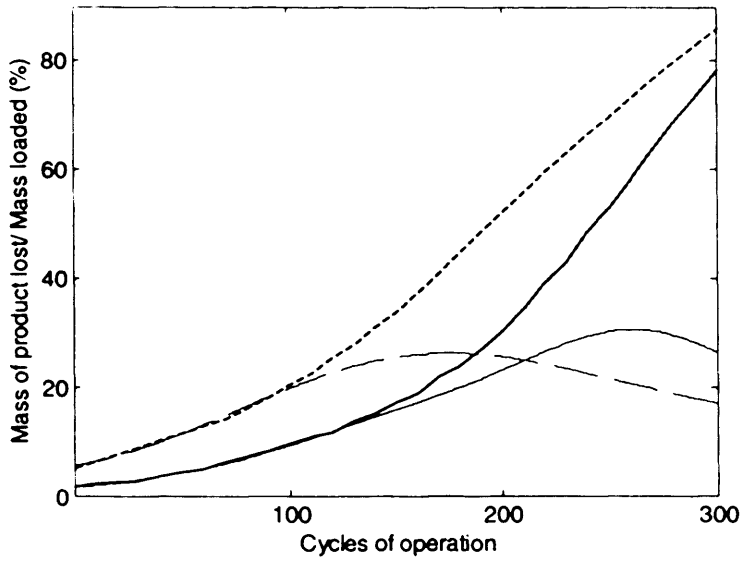

(a)

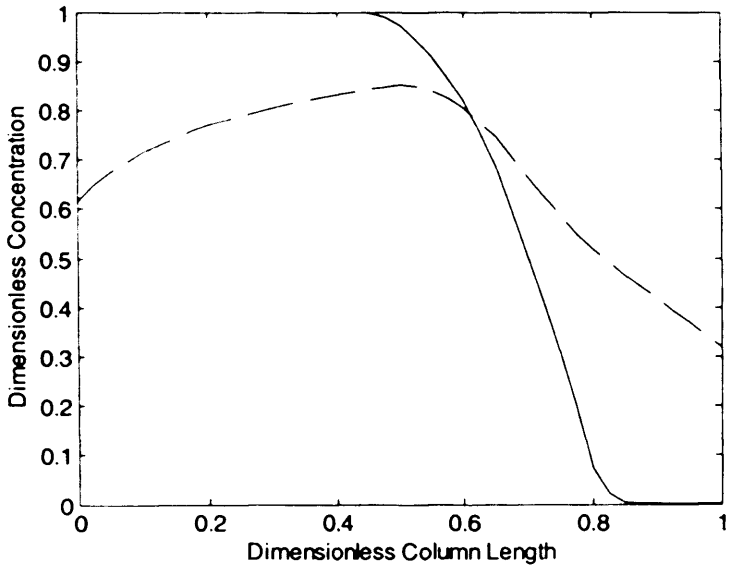

(b)

Figure 7.6 **(a)** Mass of product lost during intermediate washing with 6CV of buffer as a proportion of mass loaded onto the column when operating with a safety factor of 80, for a loading velocity of 500cm/h (———) and 200cm/h (— — —) over an extended number of cycles of operation. Grey lines show the total losses in product for both the washing and loading stages. **(b)** Concentration profiles in the solid phase when after loading at 200cm/h (———) and washing with 6CV of intermediate wash buffer (— — —). Washing proceeded at a velocity of 500cm/h.

cumulative economic potential when reusing the resin for an extended period if the column is loaded to 1% breakthrough. Cumulative potential increases initially with cycle number. This is because the revenue earned from the MAb bound to the column over a range of cycles outweighs the costs of production and hence the economic gains of such a strategy increases. There comes a point when the column capacity is degraded to such an extent that product losses per cycle are so great that the cost of running the process outweighs the returns gained from continued production. An optimal point occurs corresponding to the most profitable number of cycles for which the resin can be re-used and is in effect a prediction of the resin lifetime based upon a financial metric. It was assumed that the loading strategy would remain constant during operation. Load volume was calculated based on the column capacity of an unused resin. The decrease in economic potential is abrupt and reflects the fact that product losses incurred during the loading stage increase exponentially (see Section 6.4.1) as breakthrough is achieved earlier with every cycle.

The dashed lines in Figure 7.7 (a) show the cumulative economic potential of the same column but accounting for post-load washing. As the level of washing increases the rate of the increase in profitability diminishes. Increasing the levels of column washing reduces product yield and since the mass bound to the column per cycle after washing reduces, revenues fall. Economic potential levels off as costs start to outweigh gains at an earlier stage in operation and resin operating lifetime decreases. Therefore, the maximum extent of column re-use is a function of the washing strategy used. The calculated resin lifetimes accounting for washing strategy show a significant decrease in the lifetimes than those estimated solely on the basis of loading. It is clearly important therefore that the effects of column washing are incorporated into any economic analysis if a realistic insight of process performance is to be achieved.

Figure 7.7 (b) shows the effect that loading with a safety factor has on the resin optimum lifetime. Examination of the gradients of the initial increases in the profitability curves in Figure 7.7 (b) show a slight reduction in the profitability when operating with a low safety factor over the first 100 cycles. Operation with

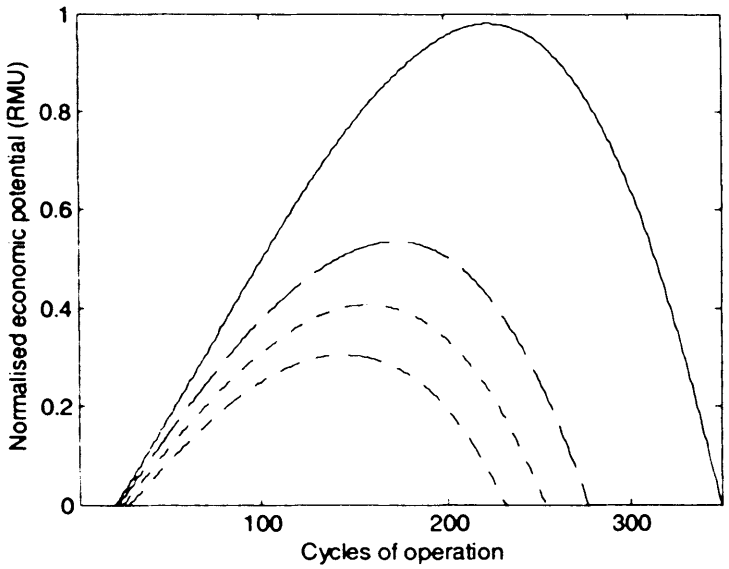

(a)

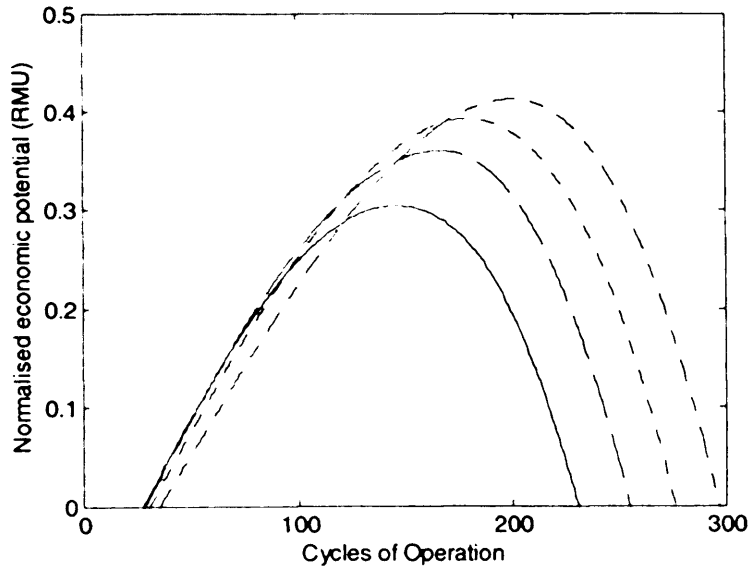

(b)

Figure 7.7 (a) Cumulative operational profit vs. cycle number calculated based on a safety factor of 80 for various lengths of post-load washing; after loading (———), after 2 CV of washing (— — —), after 4 CV of washing (·····) and after 6 CV of washing (— · —). **(b)** Cumulative operating profit vs. cycle number calculated based on washing for 6CV for various safety factors (SF); SF = 70 (— · —), SF = 80 (·····), SF = 90 (— — —) and SF = 100 (———).

low safety factors is indicative of a reduced quantity of mass loaded onto the column. Therefore, initially during the early cycles of operation there is a reduction in the profitability per cycle when compared to operation with higher safety factors as less mass is recovered per cycle. However as resin reuse increases, product losses due to degradation in resin capacity become more significant the higher the safety factor used. Here, operation with low safety factors become more profitable since resins may be reused more extensively. Conversely though, for processing a given quantity of product the use of low safety factors necessitates the reuse of the resin more often relative to strategies which involve the use of high safety factors.

7.5.5 Impact on product purity

Sometimes in manufacturing operation it may not be prudent to operate at the point of highest profitability alone and other factors have to be considered in the determination of the best operating strategy. It can be seen from Figure 7.8 that product purity decreases with cycle number. As a result of capacity losses caused by CIP procedures, less product is bound per cycle. Since the resin's propensity for binding contaminants is largely unaffected by the CIP procedures adopted and remains constant whilst the amount of product bound decreases with cycle number, product purity decreases with cycle number. Complete antibody recovery processes often contain both anion and cation exchange chromatography columns downstream of the Protein A step which together provide significant clearance of host-cell proteins (Fahrner *et al.*, 1998). However, failure to purify the cell culture to a high level of eluate purity during the initial capture phase will place extra burdens on the purification steps downstream. A bio-manufacturing firm would be able to estimate the exact purity that they are willing to incur through the running of a single Protein A resin and therefore can specify limiting criteria based on such analysis.

7.5.6 Productivity Analysis

7.5.6.1 Loading strategy

Selection of an appropriate loading velocity is dependent on the requirements of the process and the objectives of the designer, but are usually defined by

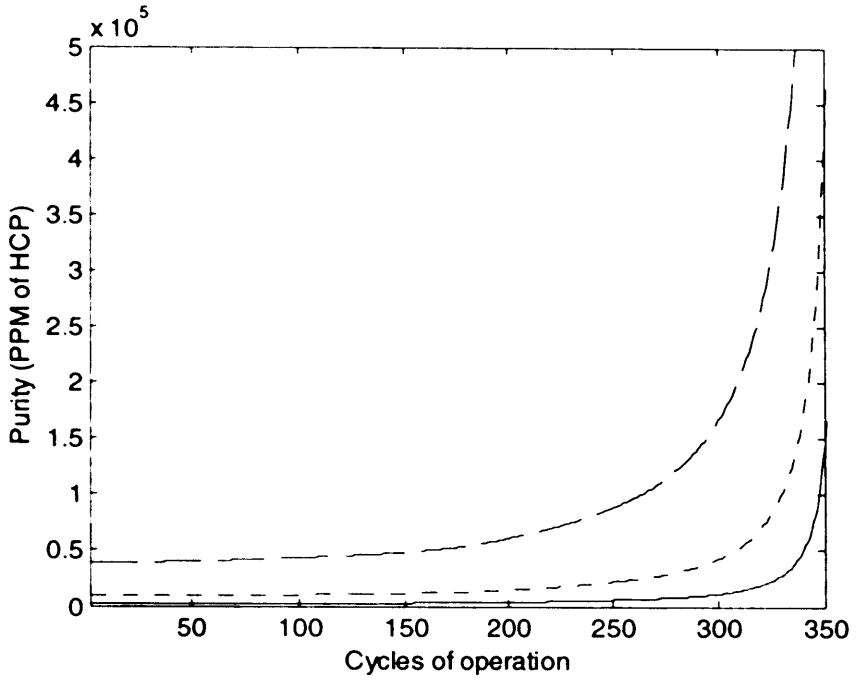

Figure 7.8 Variation in product purity for various level of column washing over a number of cycles when loading to 1% breakthrough with a velocity of 500cm/h; after 2 CV of washing (— — —), after 4CV of washing (·····) and after 6 CV of washing (———).

productivity and cost considerations. Simulations were carried out for a variety of loading velocities to determine its effect on the productivity of the process over 20 batches of operation; the results of which are seen in Figure 7.9. The equilibration, post-load washing, elution and regeneration steps were assumed to operate at the maximum possible velocity within the column pressure-drop limits. Figure 7.9 shows that as load velocity is increased productivity increases because process time reduces. At a particular low binding capacity (high load velocities) losses in yield (Equation (5.13)) are so great that productivity starts to diminish with increasing velocity. In practice however, productivity is not a continuous function of loading velocity as velocities are adjusted to ensure that a batch of material is split equally across all cycles on the column to avoid problems of under-loading on the last cycle. The vertical dashed lines shown in Figure 7.9 denote the discrete loading velocities available to the designer for this particular case study that allow for consistent column performance over a batch of material.

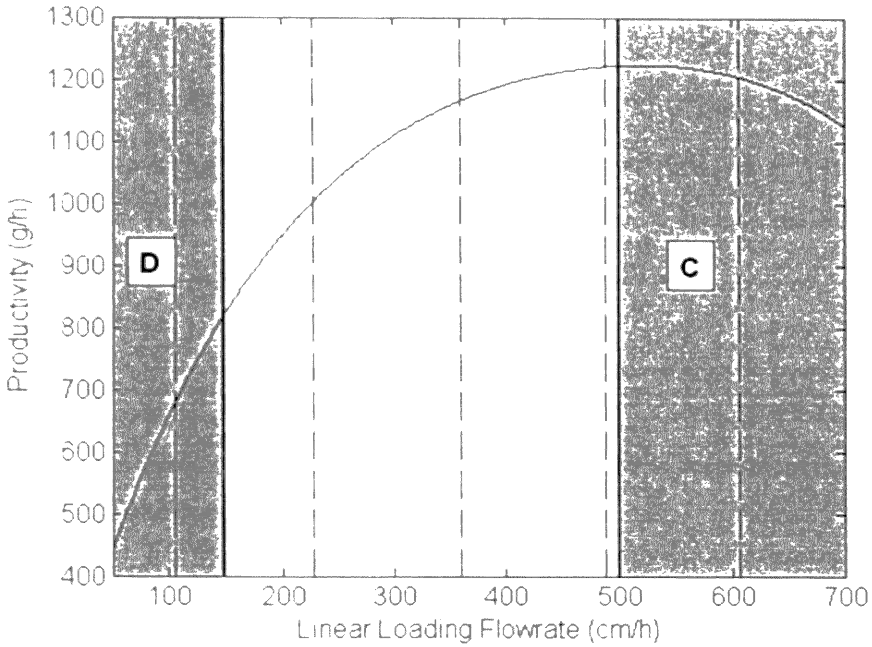

Figure 7.9 Simulated plot of productivity vs. linear loading velocity; adjusted loading velocities required to ensure an equal mass of material is loaded on each cycle during when processing a batch of material (— — —).; Area C denotes an infeasible region of operation based on the implementation of a constraint based on the maximum velocity allowable through a column at this scale of operation; Area D denotes an infeasible region of operation based on the implementation of a scheduling constraint whereby a minimum of one complete cycles has to concluded in a day.

A window of operation for chromatographic operation may be defined by application of a series of constraints on the loading velocity. The shaded area C in Figure 7.9 shows the application of the first of these relating to the maximum velocity achievable when operating the specified column. Operation at velocities above this constraint is infeasible as it would exceed the permissible pressure drop. The shaded area D shows the imposition of a further constraint corresponding to the available loading velocities which allow operation within the DSP scheduling restrictions. This serves to restrict the minimum loading velocity of the column, assuming that the other stages of the cycle are run at the maximum possible velocity

(500 cm/h). In this case there are only three loading velocities available to the designer.

To operate the column at maximum productivity the loading velocity was adjusted to be as close to the maximum allowable velocity value as possible whilst never exceeding it. The equilibration, post-load washing, elution and regeneration steps were also assumed to operate at this maximum velocity. Table 7.3 shows the adjusted loading velocity used for each safety factor investigated as well as the number of cycles required to process a single batch of material.

7.5.6.2 Washing strategy

The washing strategy chosen will also impact on the productivity of the process. As the safety factor is increased the number of cycles required decreases because load volume is greater at higher safety factors. Figure 7.10 (a) shows how contours of productivity vary with safety factor and volume of wash buffer. Productivity increases with safety factor as fewer cycles are required to process a batch of material. Productivity however decreases with increasing volumes of wash buffer used, due to the longer washing times and the increasing yield losses associated with the use of these strategies.

A consequence of using an adjusted loading velocity for differing safety margins is the fluctuations observed in the productivity contours. The reason for these in fluctuations may be more clearly seen with reference to Figure 7.10 (b). Here the variation in yield and productivity with safety factor is shown for a given quantity of wash buffer used. As expected, yield decreases with increasing safety factor. Productivity however, shows more variability and can be directly attributable to the variation in loading velocities required for the differing operating strategies as shown in Table 7.3. Table 7.3 shows that an equivalent number of cycles are required to process a batch of material when loading with either a safety factor of 70 or 75. The increase productivity between these two safety factors observed in Figure 7.10 (b) is caused by the higher loading velocity utilised when loading with a safety factor of 75. Loading with a safety factor of 80 reduces the number of cycles required to process a batch of material. A reduction in the loading velocity coupled with the

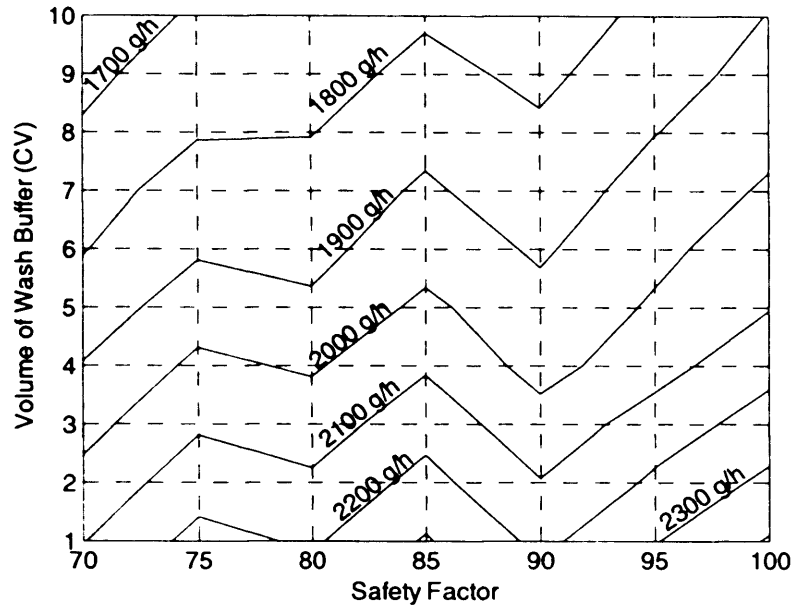

(a)

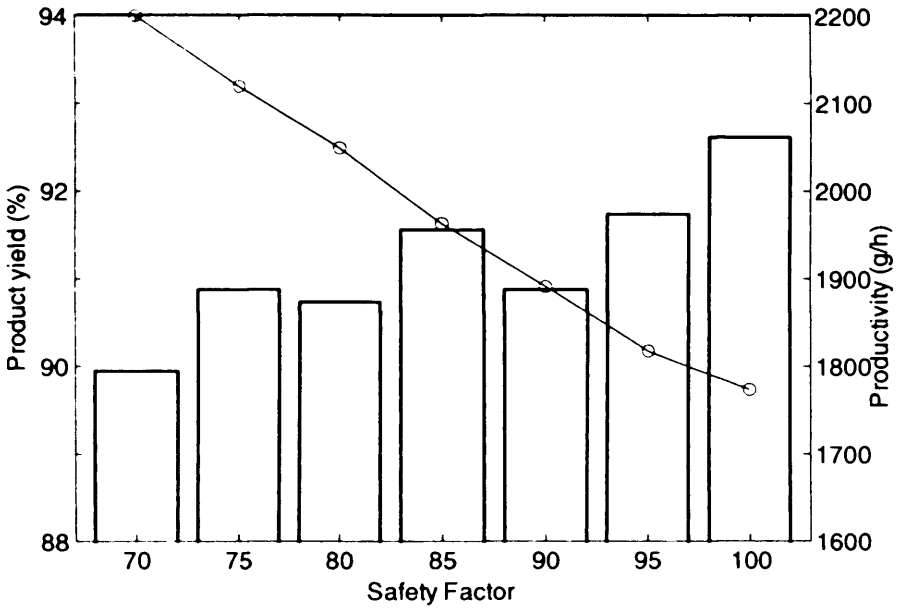

(b)

Figure 7.10 (a) Productivity contours for differing safety factors and volumes of wash buffer; **(b)** Variation in productivity (bars) and yield (——o——) when washing with 6CV of wash buffer.

increased load volume associated with the use of higher safety factors increases the capacity utilisation of the resin allowing for a reduction in the number of cycles required to process a batch. However, as shown in Figure 7.10 (b) productivity can be observed to drop slightly when loading with safety factor of 80. Despite a drop in the total process time associated with a decrease in the required cycles, the use of this strategy requires a low loading velocity which leads to an increase in the product losses during the washing stage, decreasing the yield of the process. The reduction in the product recovered mitigates any increases in productivity which occurs due to processing a batch of material in fewer cycles. Productivity can be observed to increase when operating with safety factor of 90 to 100. Table 7.3 shows that the cycles required for these loading levels are equivalent whilst loading velocity increases with safety factor, reducing processing time.

Table 7.3 Adjusted velocities for equal cycle loading for various load volumes when operating at maximum possible loading velocity during operation (maximum productivity condition).

Safety Factor	Linear loading velocity (cm/h)	Mass of product bound per litre resin (g/L)	Cycles of operation/batch
70	435	24	8
75	486	24	8
80	435	27	7
85	478	27	7
90	410	32	6
95	448	32	6
100	488	32	6

7.5.7 Cost Analysis

7.5.7.1 Loading strategy

Having evaluated the chromatographic performance we now examine their impact on the economic aspects of the process. Table 5.6 displays the cost input data used in the calculation of the $COG/g_{specific}$ (Equation 5.19) for the differing process

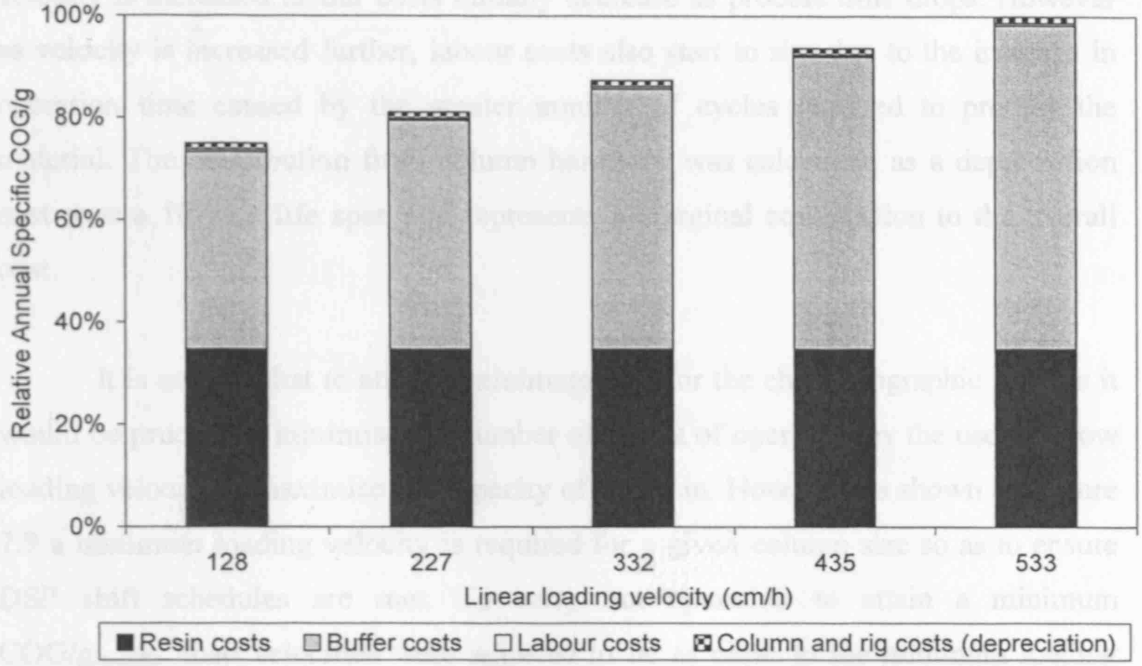

Figure 7.11 Breakdown of annual cost of goods per gram ($COG/g_{specific}$) for varying linear loading velocities when loading with a safety factor 80 and washing with 6CV of buffer.

strategies evaluated. Figure 7.11 shows how the $COG/g_{specific}$ changes with the adjusted loading velocities when the column is loaded with a safety factor of 80 and washed with 6CV of buffer at 500 cm/h. The increase in $COG/g_{specific}$ observed with loading velocity can be explained with reference to the main components that make up the cost of column operation. A consequence of attaining faster breakthrough is a reduced quantity of material that can be loaded onto the column during this period. Loading at a faster velocity will necessitate a greater number of cycles of operation be used to process a given batch of material. The impact of this increase in cycles with flow rate on the $COG/g_{specific}$ can be seen in Figure 7.11. $COG/g_{specific}$ is dominated by the cost of the resin as well as the cost of buffer required for the process. As the number of cycles required for processing increases with velocity, the volume of buffer consumed also increases adding to the process expenditure. At the highest velocities buffer costs begin to dominate the overall cost of the chromatographic step. Labour costs are high for the lowest flow rate investigated as the time taken to complete one cycle of operation is so great that the overall operation time is long, despite needing fewer cycles during the campaign. As

velocity is increased labour costs initially decrease as process time drops. However as velocity is increased further, labour costs also start to rise due to the increase in operation time caused by the greater number of cycles required to process the material. The contribution from column hardware was calculated as a depreciation cost over a 10 year life span and represents a marginal contribution to the overall cost.

It is evident that to attain a minimum cost for the chromatographic process it would be prudent to minimise the number of cycles of operation by the use of a low loading velocity to maximise the capacity of the resin. However, as shown by Figure 7.9 a minimum loading velocity is required for a given column size so as to ensure DSP shift schedules are met. To carry out operation to attain a minimum $COG/g_{specific}$, load velocities were adjusted to be as close to the minimum loading velocity allowable. Table 7.4 shows the adjusted loading velocity used for each safety factor investigated as well as the number of cycles required to process a single batch of material when operating under this strategy.

Table 7.4 Adjusted velocities for equal cycle loading for various load volumes when operating at minimum possible loading velocity during operation (minimum specific cost condition).

Safety Factor	Linear loading velocity (cm/h)	Mass of product bound per litre resin (g/L)	Cycles/Batch
70	162	38	5
75	194	38	5
80	227	38	5
85	259	38	5
90	175	48	4
95	200	48	4
100	227	48	4

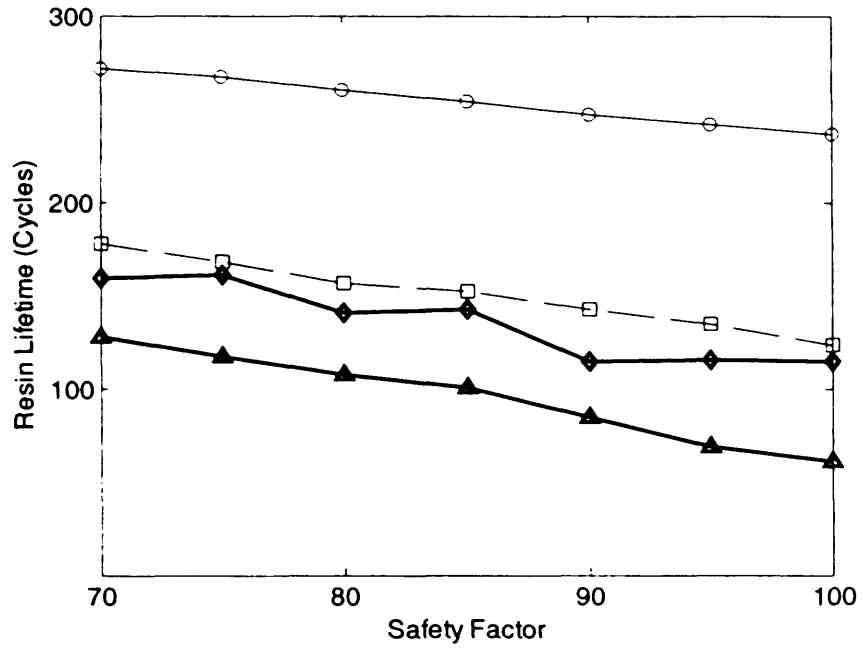

Figure 7.12 Resin optimum lifetimes for various safety factors based on binding capacity data only when loading at 500cm/h (——o——) and on data when loading at 500cm/h is followed by washing for 6CV at 500cm/h (— □ — —); Resin lifetimes for various safety factors operating at the adjusted loading velocities for the maximum productivity operation case displayed in Table 7.3 (····· ◊ ·····) and when operating under the conditions displayed in Table 7.4 (— · —Δ — · —)when washing with 6CV of buffer.

7.5.7.2 Washing strategy

As has been demonstrated, resin costs are a major factor in the $COG/g_{specific}$ and resin lifetime becomes very important in keeping the $COG/g_{specific}$ to a minimum. Figure 7.12 shows that the economic lifetime decreases linearly with safety factor when a constant loading velocity of 500cm/h is used. The linear decrease can be attributed to the linear form of the degradation function assumed in Equation (5.20). The rate of decrease is a direct function of the degradation coefficient. The figure also shows the importance of including post load washing in the calculation of resin lifetime. Lifetimes considered simply from dynamic binding capacity from the loading stage may only yield over- optimistic results.

Equation (5.22a) was used to calculate the resin lifetimes for the adjusted loading velocity used for the case where productivity was maximised (Table 7.3) and

when $COG/g_{specific}$ is minimised (Table 7.4). The results are shown in Figure 7.12. The fluctuations in the profiles mirror the changes in loading velocity with safety factor used, whereby a reduction in loading velocity causes a reduction in the resin lifetime as yield losses increase. Similarly, it can be observed that the minimum $COG/g_{specific}$ case exhibits lower resin lifetimes. This however can be traded-off against the reduction in the number of cycles required during production when using these strategies.

Figure 7.13(a) shows the impact on $COG/g_{specific}$ for varying washing strategies and safety factors when following a loading strategy as described in Table 7.3. Low $COG/g_{specific}$ may be achieved when operating with low levels of column washing. The use of low quantities of wash buffer reduces the risk of premature product elution therefore increasing the process yield. Such strategies however may not produce the required level of product purity. The $COG/g_{specific}$ increases with increasing levels of column washing. $COG/g_{specific}$ however, fluctuates when the safety factor is varied for a given level of column washing and the degree of fluctuation is a strong function of the number of cycles required to process material for the given campaign. When washing with 3CV of wash buffer, initially costs are high for safety factors of 70 to 75. $COG/g_{specific}$ decreases as safety factor increases to 80. This is due to the decrease in number cycles required to process each batch of material. A minimum $COG/g_{specific}$ is attained when a safety factor of 90 is used as this strategy uses the least number of cycles to process the batch. Costs then increase again when using factors of 95-100 as the cycles required to process a batch remain constant when using these strategies, however, yield losses which are symptomatic of high safety factors increase. Therefore, in this scenario a safety factor of 90 represents the best compromise between the costs of processing and product recovery. The trends described follow a similar pattern when higher volumes of wash buffer are used. However, costs also mirror the resin lifetime function. For instance when washing with 4 CV there is a sudden increase in the $COG/g_{specific}$ when operating with safety factors 90 and 95. This reflects the low resin lifetimes associated with these strategies which then require the use of a greater quantity resin over the production time, increasing the cost of the process.

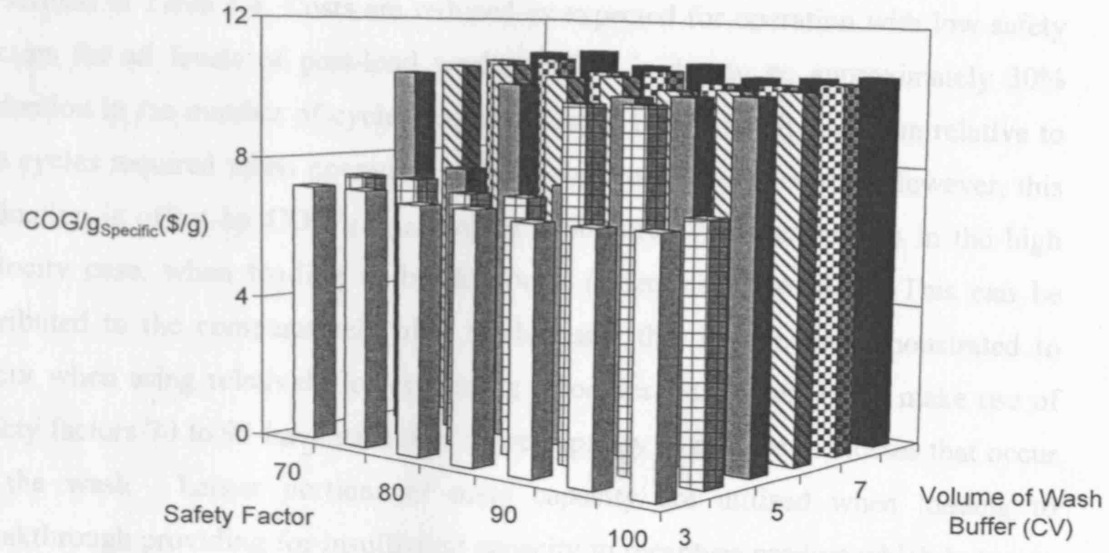

(a)

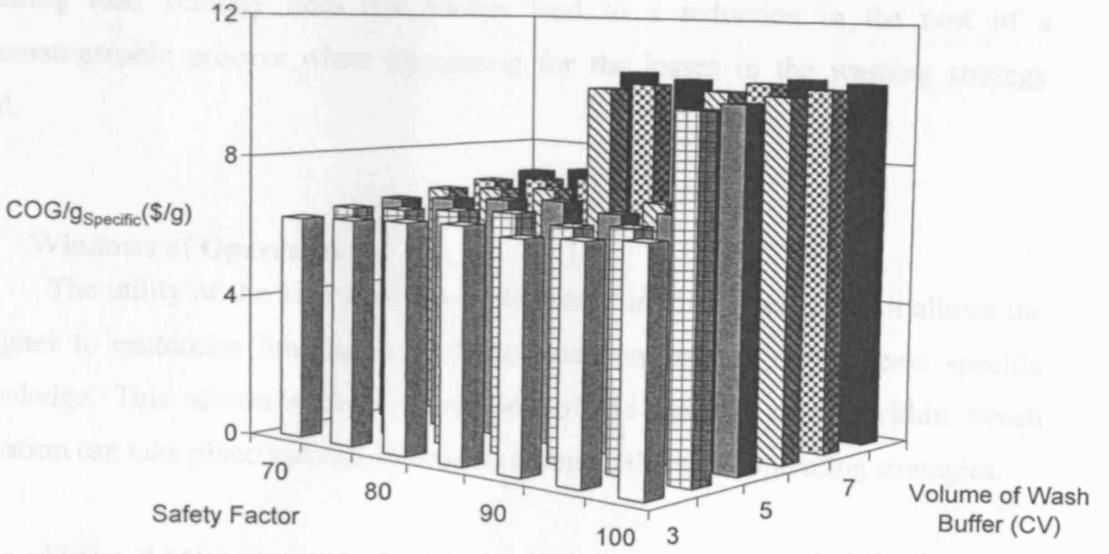

(b)

Figure 7.13 COG/$g_{specific}$ for varying safety factors and volumes of wash buffer for **(a)** when operating at maximum productivity as described in Table 7.3; **(b)** when operating under conditions described in Table 7.4.

Figure 7.13(b) shows the COG/$g_{specific}$ for varying washing strategies and safety factors for the loading strategy using the lowest possible loading velocity as described in Table 7.4. Costs are reduced as expected for operation with low safety factors for all levels of post-load washing. This is due to an approximately 30% reduction in the number of cycles required during the 20 batch operation relative to the cycles required when operating at the highest possible velocities. However, this reduction is offset by COG/$g_{specific}$ values which are even greater than in the high velocity case, when loading to breakthrough (safety factor of 100). This can be attributed to the comparatively high wash losses that have been demonstrated to occur when using relatively lower loading velocities. Strategies which make use of safety factors 70 to 95 have sufficient spare capacity to capture the losses that occur in the wash. Larger portions of resin capacity are utilised when loading to breakthrough providing for insufficient capacity to recapture product which becomes unbound during the wash. This effect is magnified by the use of large quantities of wash buffer where large masses of product become unbound during the washing stage. This leads to high yield losses and increased COG/$g_{specific}$. It is evident that reducing load velocity does not always lead to a reduction in the cost of a chromatographic process when accounting for the losses in the washing strategy used.

7.6 Windows of Operation

The utility of the kind of analysis presented in this paper is that it allows the designer to customise limiting constraints based on product and process specific knowledge. This allows a better prediction of the feasible region within which operation can take place and can be used to compare different operating strategies.

Figure 7.14(a) shows a scenario based on maximising column productivity through the use of the conditions described in Table 7.3. Here, a decision is required that balances cost and productivity and uses COG/$g_{specific}$, minimum productivity and minimum purity levels as constraints when defining a feasible region. COG/$g_{specific}$ is limited to 10.5 $/g, productivity is restricted to 1850 g/h and purity is defined as a minimum level of HCP acceptable in the eluate pool, which in this scenario was assumed to be 3000 ppm (Fahrner *et al.* (2001) report typical eluate impurity levels

to be between approximately 200-3000 ppm HCP). The shaded regions denote areas of infeasibility. The feasible region (un-shaded) informs the designer as to which options remain in terms of differing column strategies. To select an optimum level of operation, the number of column volumes of wash buffer required was assumed to be integer in nature, though this is not always the case in reality. The point shown in Figure 7.14 (a) represent the discrete solution of the number of column volumes and safety factors which are available to the designer, that fulfill the specified criteria. It can be seen that washing with 6 to 7 CV of wash buffer using a safety factors ranging from 80 to 100 meets the process and economic requirements. Table 7.5 shows a breakdown of the productivity and $COG/g_{specific}$ of the feasible column options available. It can be seen that the most economic option would be operation with a safety factor of 90 and washing with 6 CV of buffer, whilst the most productive option would be operation with no safety factor (e.g. 100) when washing with the same quantity of buffer.

Table 7.5 Productivity, $COG/g_{specific}$ and purity of feasible column strategies available to the designer under loading conditions outlined in Table 7.3 and when washing with a velocity of 500cm/h.

Safety Factor	$COG/g_{specific}$ ($/g)	Productivity x 10^3 (g/h)	Impurity, HCP (ppm)
	6CV of wash buffer		
80	10.4	1.87	2450
85	10.5	1.95	2160
90	10.1	1.89	2230
95	10.2	1.97	2200
100	10.3	2.06	2180
	7 CV of wash buffer		
90	10.3	1.85	1070
95	10.3	1.94	870
100	10.4	2.01	990

7.6.1 Effect of Wash velocity

Within this framework, process performance can be predicted and design strategies evaluated. The impact of changing the washing velocity upon the feasible area of operation can also be visualized. Figure 7.14 (a)-(c) show how the feasible

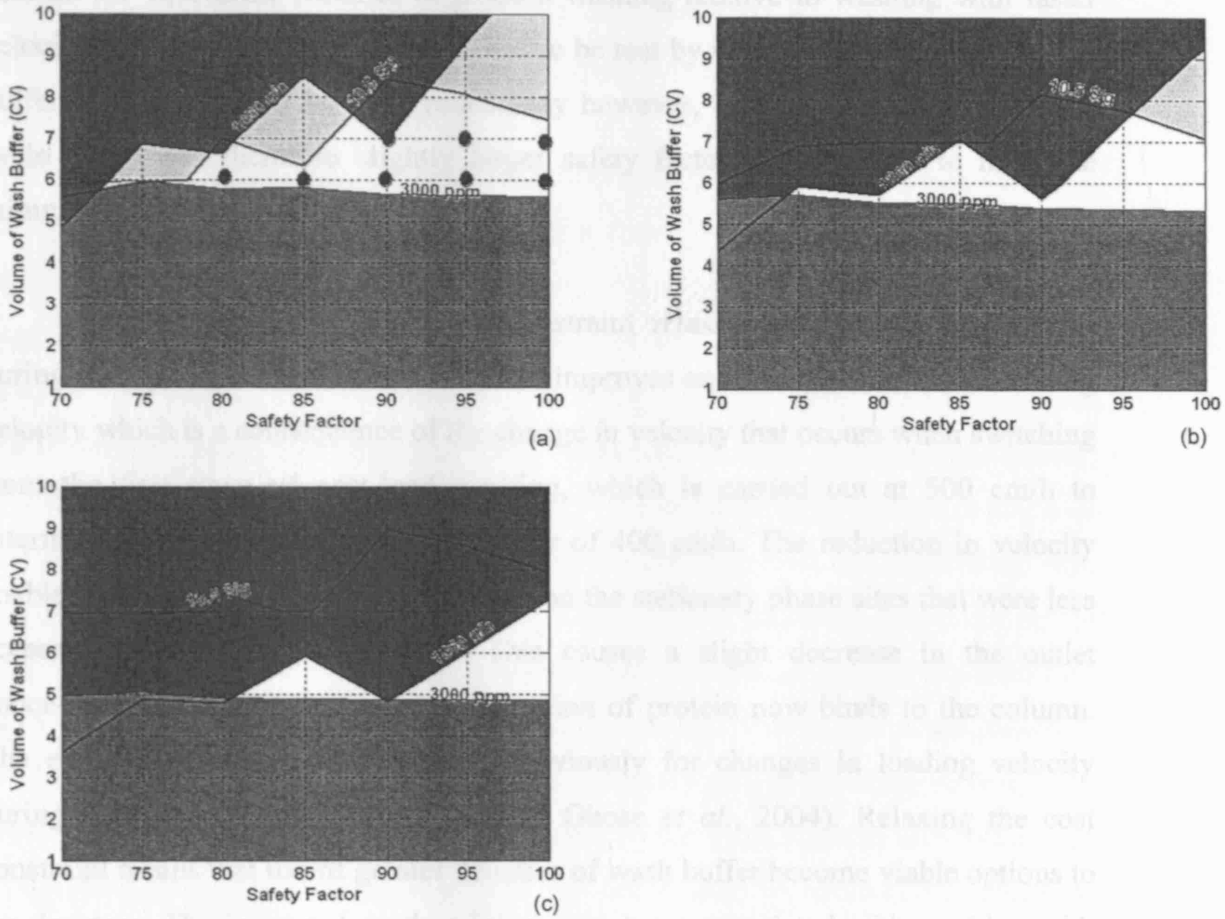

Figure 7.14 The window of operation produced when constraining the productivity at 1850 g/h ■, $COG/g_{specific}$ at 10.5 \$/g ▒ and process impurity ■ at 3000 ppm for **(a)** wash velocity of 500 cm/h, **(b)** the feasible column strategies available to the designer assuming wash volume is a discrete quantity when washing at 500 cm/h **(c)** Window of operation when wash velocity is 400 cm/h, **(d)** window of operation when wash velocity of 300 cm/h.

regions defined by productivity, cost and purity change with wash velocity when trying to maximize productivity under conditions detailed in Table 7.3. Figure 7.14 (b) shows that when a washing velocity of 400 cm/h was used, the feasible area of operation increases as compared with the base case shown in Figure 7.14 (a). A reduction in wash velocity increases the residence time of the wash buffer inside the column for equivalent volumes of column washing relative to washing with faster velocities. Purity requirements can therefore be met by using lower volumes of wash buffer than in Figure 7.14 (a). Productivity however, is reduced due to the longer cycle times, and therefore slightly larger safety factors are required to meet the minimum productivity criteria.

Interestingly, the $COG/g_{specific}$ constraint relaxes slightly, as costs reduce during this operation. This is because yield improves on the reduction of the washing velocity which is a consequence of the change in velocity that occurs when switching from the first stage of post-load washing, which is carried out at 500 cm/h to intermediate washing at a reduced velocity of 400 cm/h. The reduction in velocity enables re-binding, during the wash stage, on the stationary phase sites that were less accessible at the higher velocities. This causes a slight decrease in the outlet concentration of MAb as a greater proportion of protein now binds to the column. The effect is similar to that reported previously for changes in loading velocity during operation (Johansson *et al.*, 2003; Ghose *et al.*, 2004). Relaxing the cost constraint means that use of greater volumes of wash buffer become viable options to the designer. The increased product losses which are associated with washing with large volumes of buffer are diminished through the use of the reduced wash velocity. Washing velocity is reduced further to 300 cm/h in Figure 7.14 (c) and it can be seen that the number of feasible column options within the chosen constraints are reduced slightly compared to the previous case. The reduction in the washing flowrate has made the productivity constraint difficult to attain whilst meeting the required purity when using low safety factors, due to the larger number of cycles that are required with these strategies. Given these results, it may be prudent to operate the post-load wash velocity below the maximum velocity possible. Decreases in velocity do not impact productivity significantly as yields are improved despite an increase in cycle

time. However it does reduce the quantity of wash buffer required to attain a given level of eluate purity as well as increase the product yield of the process.

7.7 Conclusions

The development and implementation of a framework tool to model the trade-offs in chromatography processing has been presented. The method has been demonstrated with data from a Protein A separation utilising a theoretical pseudo-resin which demonstrated properties which are a composite of the most common resins available in industry today. Simulation results show that productivity is a strong function of the washing strategy implemented when operating with a safety factor and that velocities and under-utilisation of the stationary phase can combine to improve yield. As a consequence, a reduction in the loading velocity increases the product losses during post-load washing. It was shown that a minimum $COG/g_{specific}$ can be attained when operating with a low safety factor and a low loading velocity. This is due to the reduction in the number of cycles required to process a batch of material as well as the high yields attained which are characteristic of operation with low safety factors. Conversely, it was also shown that operation with high safety factors when loading at low velocity could increase $COG/g_{specific}$ despite the reduction in the overall number of cycles required for processing. This is due to the losses in yield associated with over utilisation of the stationary phase. Washing velocity was itself shown to have a significant effect on the process yield. This in turn influenced productivity and the COG/g. The tool has been used to construct a series of 'windows of operation' which enable the designer to account for the influence of column loading and washing strategy and to quantity their effects on productivity, cost (COG/g) and purity.

In this next chapter the techniques developed here and in Chapter 6 are implemented in a real case scenario used in evaluating two commercially available Protein A resins, one whose backbone is based on agarose and the other which is based on a CPG base. The objective here is to show how the modeling framework developed can be used from a managerial perspective in the decision of which resin is to be selected for use in a given manufacturing strategy.

8 USE OF FRAMEWORK TO AID COMMERCIAL STRATEGY DECISIONS: A MANAGEMENT CASE STUDY

8.1 Introduction

In the previous chapter the application of a modelling framework in the evaluation of optimal operating strategy for a Protein A resin was demonstrated. The analysis used a hypothetical resin with properties commonly displayed by controlled pore glass (CPG) and agarose materials, thus representing an industry average resin. Through this analysis the full functionality of the model was demonstrated as well as the advantages and limitations of the different resin characteristics. In this chapter the framework is applied to a more realistic case in the evaluation of two commercially available Protein A resins in a process setting; MabSelect^{TM} which poses an agarose backbone and Prosep Ultra$^{®}$ which comprises of a CPG backbone.

The aim in this chapter is to assess these two resins from a business perspective as would be the case in the biopharmaceutical industry. Here, it is assumed that a biopharmaceutical company is developing a therapeutic MAb expressed in mammalian cells for commercial use. It has an already specified process (similar to that specified in Figure 1.2) but faces questions over what Protein A resin should be used in the capture step phase of the process (Figure 6.1) and further to this; what is the best operating strategy to implement with the selected resins?

The decision over resin selection is subject to some intensive limiting constraints. Firstly, existing column hardware must be used for processing and therefore column geometry is fixed. The firm has also specified that the initial capture step should be scheduled to be run under conditions that maximise productivity so as to meet increasing market demand for the therapeutic MAb. From the viewpoint of antibody production in a regulated pharmaceutical environment there are additional criteria for the qualification of an affinity resin besides productivity, which are related to regeneration and impurity clearance (Hahn *et al.*, 2005). Therefore, maximising productivity should be subject to the constraint of a minimum required purity level at the end of the Protein A process. This is important

so as not to impact too greatly on the high resolution steps post initial capture, thus ensuring that the required purity is met at the end of the overall process. Further to this, as always the objective of any firm is to meet these constraints in the most cost effective manner to optimise the profitability of the process.

8.2 Case study set-up

The application of the framework proposed in Chapter 5 was explored using data for the production of recombinant humanised monoclonal antibody from CHO cells. To reflect the typical titres encountered today a product titre of 3 g/L was assumed (Hahn *et al.*, 2006). A fixed reactor volume of 10,000 L was also assumed in this case and the overall production time was one year, meaning that approximately 400 kg of MAb would be produced. A fixed set of process assumptions, listed in Table 8.1, were made. All simulations were driven by the need to process a defined batch of material from a 10,000 L fed-batch reactor. The reactor was scheduled to output 20 batches in a 48 week production year.

In terms of resin selection the firm has limited its decision as to whether or not to undertake the use of an agarose based resin, namely MabSelect™ (GE Healthcare, Uppsala, Sweden) with its limitations in terms of maximum flow velocity and capacity degradation on cleaning. The alternative is the use of the CPG based resin, Prosep vA Ultra® (Millipore Corp, Co Durham, UK) which provides higher limits in terms of flow velocity and does not suffer from capacity degradation during clean-in–place (CIP) procedures. However, as described in Chapter 7, employing a CPG based resin does increase the level of non-specific binding which makes eluate purity a concern.

8.3 Modelling approach

8.3.1 Parameter estimation

The estimated physical and chemical properties of the two resins are listed in Tables 5.3 and 5.4 respectively. Values and fits were based on literature data for the separation of humanised monoclonal antibody (IgG), produced in Chinese Hamster

Table 8.1 Overall process assumptions for the manufacture of a MAb from mammalian cell culture. *CV denotes column volume.

Assumption	Input Value	Reference
Lang factor	6	(Assumed)
DSP plant operating hours	48 weeks per year, 7 days per week, 8h per day	
Bioreactor size	10,000L	(Assumed)
Titer, C_0	3 g/L	(Assumed)
L (cm)	20	
D (cm)	100	
Chromatography Equipment depreciation	10%	(Assumed)
Volume of equilibration buffer used / cycle	4 CV*	Ghose *et al.* (2004)
Volume of Elution buffer used / cycle	4 CV	Ghose *et al.* (2004)
Yield of DSP post initial capture	70%	Calculated, Table 5.7
Chromatography contribution to process cost	8 %	(Assumed)
Selling Price MAb, MP_{MAb}	$1325	(Assumed, Chapter 5)

Ovary (CHO) cells (Hahn *et al.*, 2005). It was assumed that the equilibrium between the IgG and the solid phase concentrations in affinity systems can be modelled using a Langmuir isotherm.

Feed stream contaminants were modelled as a single lumped component term. The contaminant adsorption was also assumed to exhibit Langmuirian behaviour. Adsorption parameters for the contaminant were modelled through fitting Langmuir parameters to attain typical adsorption and desorption behaviour of host cell proteins (HCPs) observed in initial capture operation in an industrial process (Hahn *et al.*, 2006). The feed concentration of the contaminant component was taken to be 5 times larger than that of the MAb, which reflects values observed in a typical antibody production process (Lebreton *et al.*, 2006). The values of the main parameters describing the separation for MabSelect™ and Prosep vA Ultra® are reproduced in Tables 8.2 and 8.3 which now also include the estimated contaminant parameters as well as the impact of intermediate washing on the isotherm profile of the CPG resin. Tables 8.2 and 8.3 show that both resins exhibit similar static capacity levels and uptake kinetics. Simulated plots of binding capacity vs. residence time for both resins are displayed in Figure 8.1 and show that the two reach similar capacity levels at equivalent or closely matched residence times. Therefore, it can be inferred that they both display similar mass transfer characteristics as well.

8.4 MabSelect™ vs. Prosep vA Ultra®: differences in operating strategy

The resins are very similar in terms of their adsorption kinetics and mass transfer properties. The MabSelect™ resin is based on highly cross-linked agarose whereas Prosep vA Ultra® is created from controlled pore glass (CPG). As discussed in Chapter 2 and demonstrated in Chapter 7 the differences in the material from which these resins are synthesised lead to significantly different strategies in their operation.

8.4.1 Loading strategy

Despite the hardened highly cross-linked agarose base of MabSelect™ it still suffers from compression at the largest scales (see Chapter 3). Therefore, the

maximum velocity of this resin is limited to 500 cm/h at production scales[a]. In contrast the porous glass base matrix of Prosep vA Ultra is incompressible, leading to a linear relationship between back pressure and velocity. The response of a Prosep vA Ultra packed column to increased velocity is therefore entirely predictable over different column lengths and diameters. The combination of total rigidity and particle size range allows operation at velocities in excess of 1000 cm/h[b].

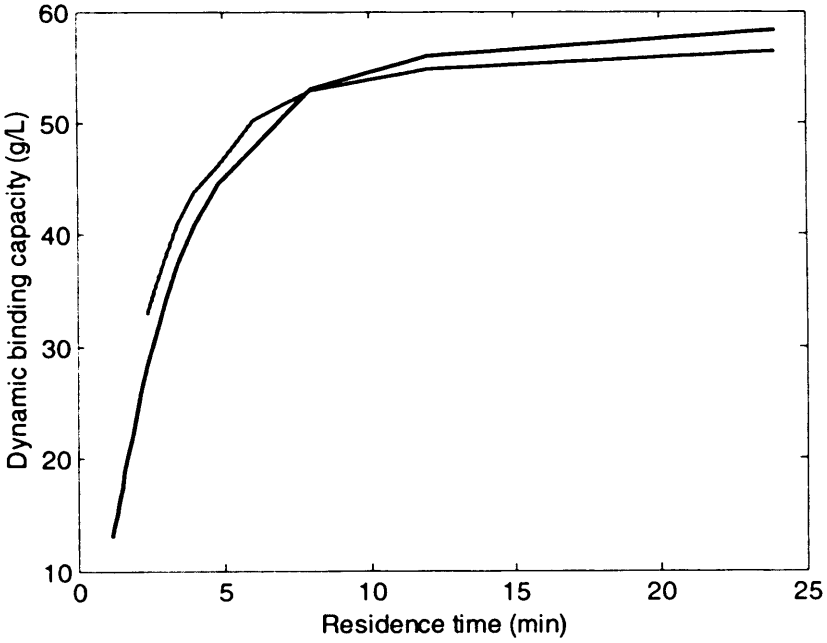

Figure 8.1 Dynamic binding capacity at 1% breakthrough vs. residence time for the MabSelect™ resin (grey line) and Prosep vA Ultra® (black line). Operation of the Prosep resin can be operated with flowrates up to 1000 cm/h (residence times of 1.2 min in a bed of length 20 cm). The operational limit of MabSelect during large-scale operation is a velocity of 500 cm/h (equivalent to a residence time 2.4 min).

[a] MabSelect product data file found at www.gelifesciences.com, accessed 2007.

[b] ProSep vA Ultra product data file, Millipore publication, DS4241EN00, www.millipore.com/publications.nsf/, accessed 2007.

Table 8.2 Model parameter values for the adsorption of a MAb and lumped HCP contaminant to the rProtein A MabSelect^{TM} resin.

Parameter	General data	IgG	HCP
r_p (cm)	0.0043		
d_p (A)	440		
MW (g/mol)		150000	20000
ε_b	0.42		
$\varepsilon_{p\ effective}$	0.52		
External film mass transfer, k_f (cm/s)		0.0016	0.0025
Effective diffusivity, D_{eff} (cm^2/s)		5.0×10^{-8}	8.2×10^{-8}
Dissociation constant, K_d (g/L)		0.12	3.5
Saturation capacity, q_{max} (g/L)		60.2	10

Table 8.3 Model parameter values for the adsorption of a MAb and lumped HCP contaminant to the Prosep vA Ultra® resin.

Parameter	General data	IgG	HCP
r_p (cm)	0.005		
d_p (A)	700		
MW (g/mol)		150000	20000
ε_b	0.43		
$\varepsilon_{p\ effective}$	0.46		
External film mass transfer, k_f (cm/s)		0.0014	0.0022
Effective diffusivity, D_{eff} (cm^2/s)		5.3×10^{-8}	2.2×10^{-7}
Dissociation constant, K_d (g/L)		0.116	1.8
Saturation capacity, q_{max} (g/L)		62.8	12
After intermediate washing			
Dissociation constant, K_d (g/L)		0.174	3.6
Saturation capacity, q_{max} (g/L)		59.66	10.8

8.4.2 Post-load washing

The hydrophobic nature of the CPG resin Prosep vA Ultra® causes an increase in the non-specific interactions that can occur with the resin backbone. This in turn causes a reduction in the purity of the eluate pool. To diminish this effect a two step post-load washing strategy is utilised to ensure that the required purity levels are attained. The first wash step, which occurs directly after loading, was assumed to be fixed. This consisted of the column being washed with 3 column volumes (CV) of neutral equilibration buffer at a constant velocity of 1000 cm/h. The second wash step was assumed to involve an intermediate wash buffer (see Section 7.3). The use of this extra step increases the time requirement and buffer consumption of the chromatographic cycle when this resin is utilised. Further to this, as was demonstrated in Chapter 7, the use of an intermediate wash buffer runs the risk of causing some premature elution of the product MAb bound to the resin during the loading phase. Figure 8.2 (b) shows the assumed change in the Langmuir isotherm profile for the Prosep vA Ultra® resin when an intermediate wash buffer is used. Changes in isotherm values were fitted to reported reductions in product capacity due to changes in buffer pH (Sada *et al.*, 1986) and reductions in impurity levels on use of an intermediate buffer as reported by Mann *et al.* (Millipore Technical Brief, TB1024EN00, 2007).

Agarose based resins such as MabSelect™ are not as hydrophobic in nature as the CPG based resins and therefore exhibit a significantly lower degree of non-specific interaction with feed contaminants. Therefore employing such a resin in a process allows the use of a more traditional post-load washing procedure which makes use a neutral buffer in a single wash step. As such there is no change in the isotherm profile during post-load washing as the wash step proceeds with the loading or start buffer.

8.4.3 Column cleaning

The differences in the typical CIP protocols used for CPG and agarose based resins were outlined in Chapter 7. Typically resins with an agarose base undergo CIP treatments with sodium hydroxide (NaOH) solutions. This has proved a popular

strategy given the effective cleaning properties of NaOH in addition to the relatively low cost of this agent. The conditions of high alkalinity which are inherent in the use of NaOH as a cleaning agent causes bed instability in CPG resins. Thus cleaning procedures for these cases have resorted to the use of highly acidic buffers such as guanidine (GuHCl) and hydrochloric acid (HCl). Due to the hydrophobic nature of the CPG resins, cleaning procedures tend to be longer and more intensive than when agarose resins are used. However, cleaning procedures that undertake the use of these buffers do not cause the resin capacity decreases that are observed when sodium hydroxide solutions are used in the agarose case (Boschetti, 1994). The CIP protocols adopted here were taken from the recommendations as outlined by the respective resin manufacturers. A summary of the protocols is given in Table 8.4.

Table 8.4 Protocols for CIP applied to the different Protein A resins investigated

	MabSelect™	**Prosep vA Ultra®**
CIP	250mM NaOH + 1M NaCl, 15 mins	0.3% (v/v) HCl, pH 1.5, 15 mins; 6M GuHCl, 60mins
Frequency	Every cycle	Every cycle; Every fifth cycle
Degradation coefficient , Φ	0.17	0.04

8.5 Results and discussion

8.5.1 Choice of loading flowrate

The aim here was to select an appropriate loading flowrate which allowed for a strategy of maximum productivity on both resins. Figure 8.2 shows the plots of productivity vs. linear loading velocity for the process over 1 batch of operation. The equilibration, post-load washing, elution and regeneration steps were assumed to operate at the maximum possible velocity within the column pressure-drop limits to maximise productivity. As seen in the figures, productivity at first increases with

increasing loading velocity (due to a reduction in loading time) and then decreases at higher velocities (due to the decrease in column dynamic capacity which outweighs any advantages obtained from the lower loading time). A clear optimum loading velocity exists when trying to attain a maximum productivity for a given system.

The productivity values that can be attained by Prosep vA Ultra® are higher than that produced from MabSelect™ at equivalent loading velocities. This is due to the faster velocities used when running the ancillary chromatographic steps (equilibration, wash, and elution). The same volume of buffer was used for each of these ancillary steps in the case of both resins as it was assumed that these steps are not mass transfer limiting. In both cases however, given the similarity of their binding properties, an optimum productivity can be attained when loading with a velocity of approximately 750 cm/h (a similar optimum flow velocity was found in work performed by Ghose *et al.*, (2004) for the MabSelect™ resin). The shaded regions in the figures denote regions of infeasible operation. In Figure 8.2 (a) area 'C' denotes infeasible operation due to the back pressure constraint caused by resin compression effects that occur in large-scale chromatographic systems (discussed in Chapter 3). In the case of MabSelect™, maximum flow velocity in production scale columns is limited to a maximum velocity of 500 cm/h (GE Healthcare). Area 'D' denotes infeasible operation based on a typical downstream shift schedule, whereby at least one chromatographic cycle constituting load, wash, elution, and CIP must be fully completed before the end of the shift (as discussed in Chapter 5, Section 5.9). It can be seen in Figure 8.2 (a) that the compressive limitations of the agarose based MabSelect™ do not allow its use at the optimum flow velocity.

Conversely, Figure 8.2 (b) shows that feasible operation can be attained when using the optimum loading velocity for Prosep vA Ultra® The incompressible CPG based resin does not suffer from the increases in back pressure at the larger scales. The constraint imposed by area 'C' in this case refers to the pressure limits of the actual resin material itself. Much higher flow velocities can be used with this resin and velocities are limited to 1000 cm/h. A consequence of running the ancillary chromatographic steps at a higher velocity is shown in Figure 8.2 (b) where it can be seen that a slightly lower minimum loading velocity can be used in the case of the

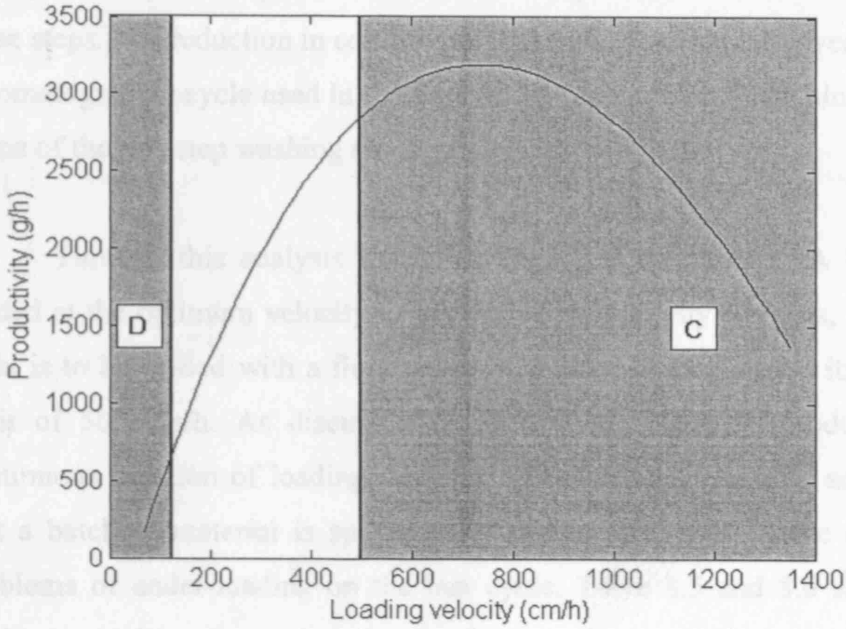

(a)

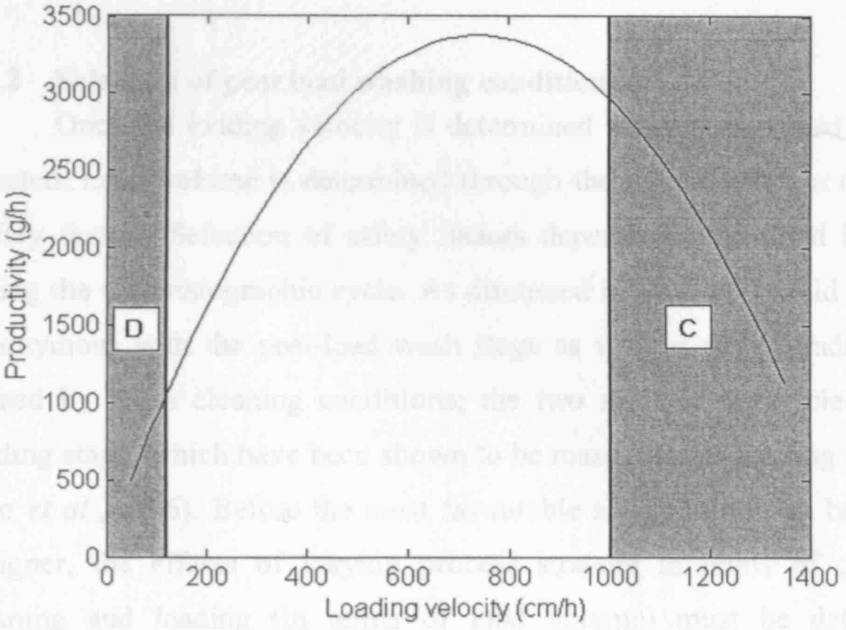

(b)

Figure 8.2 Simulated plot of productivity vs. loading velocity for when loading to 1% breakthrough for **(a)** Mabselect™ and **(b)** Prosep vA Ultra®. The shaded regions are infeasible for column operation in manufacturing. Area C limits the maximal velocity of operation with regards to column back pressure considerations. Area D limits the minimum velocity with regards to the DSP shift schedule, where at least one cycle must be fully completed in a DSP shift.

Prosep vA Ultra® (compared to MabSelect™) given the time saved when processing these steps. The reduction in column process time is only small given the fact that the chromatographic cycle used in the case of Prosep vA Ultra® contains an extra step in terms of the two step washing strategy which is required.

Through this analysis it was deemed that the Prosep vA Ultra® would be loaded at the optimum velocity to maximise productivity whereas, the MabSelect™ resin is to be loaded with a flow velocity as close as possible to its maximum flow limit of 500 cm/h. As discussed in the previous chapter, productivity is not a continuous function of loading velocity. Velocities are typically adjusted to ensure that a batch of material is split equally across all cycles on the column to avoid problems of under-loading on the last cycle. Table 8.5 and 8.6 show the discrete loading velocities for various load volumes when operating at velocities to attain maximum productivity for each resin.

8.5.2 Selection of post load washing conditions.

Once the loading velocity is determined the optimum load volume must be selected. Load volume is determined through the implementation of an appropriate 'safety factor'. Selection of safety factors depends on the yield losses that occur during the chromatographic cycle. As discussed in Chapter 7 yield losses tend to be synonymous with the post-load wash stage as well as the degradation in capacity caused by harsh cleaning conditions; the two steps of the cycle (apart from the loading stage) which have been shown to be mass transfer limiting (Boschetti, 1994, Mao *et al.*, 1996). Before the most favourable safety factor can be selected by the designer, the effects of varying process strategy in terms of column washing, cleaning and loading (in terms of load volume) must be determined on the performance of each resin.

8.5.2.1 Purity analysis

Figure 8.3 shows how eluate purity varies over 20 batches of operation. Figure 8.3 (a) shows that impurity increases over the number of process cycles used for the MabSelect™ resin. This is because the resin's propensity for binding contaminants is

Table 8.5 Adjusted velocities for equal cycle loading for various load volumes when operating at maximum possible loading velocity during operation (maximum productivity condition) for MabSelect™.

Safety Factor	Linear loading velocity (cm/h)	Mass of product bound per litre resin (g/L)	Cycles/Batch
70	445	23.9	8
75	499	23.9	8
80	445	27.3	7
85	492	27.3	7
90	418	31.8	6
95	459	31.8	6
100	499	31.8	6

Table 8.6 Adjusted velocities for equal cycle loading for various load volumes when operating at optimum loading velocity during operation (maximum productivity condition) for Prosep vA Ultra®.

Safety Factor	Linear loading velocity (cm/h)	Mass of product bound per litre resin (g/L)	Cycles/Batch
70	763	13.6	14
75	757	14.7	13
80	746	15.9	12
85	728	17.4	11
90	766	17.4	11
95	739	19.1	10
100	778	19.1	10

largely unaffected by the CIP procedures adopted and remains constant whilst the amount of product bound decreases (due to the capacity degradation of the resin) with cycle number, product purity therefore decreases with cycle number. However, this trend becomes weaker the greater the quantity of wash buffer used. The use of larger volumes of wash buffer minimises the quantity of impurity left bound to the resin, allowing a more constant level of purity to be attained for a longer time.

Figure 8.3 (b) shows how purity varies with the cycles required for the Prosep vA Ultra® resin. The faster flowrate used in the operation of this resin necessitates its use for a greater number of cycles. However, the Prosep resin does not suffer as greatly from capacity losses during operation as does MabSelect™. The result of this is that the level of impurity in the column remains stable for longer periods of time during operation of the column allowing a constant level of operation in terms of eluate purity. This may lead to an easier process validation. Regulatory constraints have forced firms to provide the relevant authorities with data showing a constant level of chromatographic performance over the process life of a quantity of resin (Sofer *et al.*, 1987). Therefore the validation of the Prosep vA Ultra® becomes relatively simple, given the lack of capacity degradation present during operation of such a CPG resin as operation can be proven to be constant for an extended period. However, in terms of MabSelect™, validation becomes more complicated. Due to the increases in impurity levels that occur over time, the use of such a resin would necessitate a detailed knowledge as to the rate of capacity degradation as well as the quantity of impurity fed into the column every batch. Therefore, during a process if there is any batch-to-batch variability in the contaminant concentration or if a quantity of resin behaves slightly differently in terms of its capacity losses than that seen during validation studies, product quality will suffer. Use of MabSelect™ or any other resin impacted by capacity losses during operation would therefore need to be operated with a greater margin for error in terms of evaluation of its number of cycles of feasible operation as well as its acceptable levels of contaminant loading. In this analysis however considerations of validation and associated costs have been omitted due to the lack of realistic input data available.

Figure 8.4 shows how the purity changes with safety factor and volume of wash buffer over the year long operation. It can be seen that the use of an intermediate wash buffer in the case of Prosep vA Ultra® provides for harsher purification conditions allowing the use of a comparatively smaller quantity of wash buffer to attain the same level of purity within the column compared to the use of the more traditional washing protocol on MabSelect™. This is particularly the case for low levels of washing; however, as the volume of wash buffer used is increased the relative purity that can be attained becomes more comparable as fewer contaminants remain in the column after several washes.

8.5.2.2 Productivity analysis

As described previously, to operate the column at maximum productivity the loading velocity was adjusted to be as close to the maximum allowable velocity value as possible whilst never exceeding it. The equilibration, post-load washing, and elution steps were also assumed to operate at this maximum velocity. This should provide an advantage to the incompressible Prosep vA Ultra® whose maximum velocity is double that of MabSelect™ (1000 cm/h as opposed to 500 cm/h). Further to this, Prosep vA Ultra® is loaded at the optimum velocity to maximize productivity. Figure 8.5 shows how productivity contours vary for each resin over the production schedule. The variability in the productivity contours can be attributed to the adjusted loading velocity for differing safety margins displayed in Tables 8.5 and 8.6. Interestingly the gains in productivity that can be attained on use of the incompressible resin are relatively low given the advantages it posses with regards to high flow operation. Figure 8.6 shows the proportion of total process time over the year long production spent on the varying stages on the chromatographic cycle. It can be seen that despite requiring a greater number of cycles to process a batch of material (due to the use of a higher loading velocity, Table 8.6), there is a reduction of approximately 11% in the total processing time when using the Prosep vA Ultra® resin compared to the MabSelect™. The figure shows that a gain in process time can be made during the loading phase and ancillary chromatographic steps (equilibration, wash and elution) due to the higher velocities with which these steps can run. However, the gains in process time are severely diminished by the impact of the

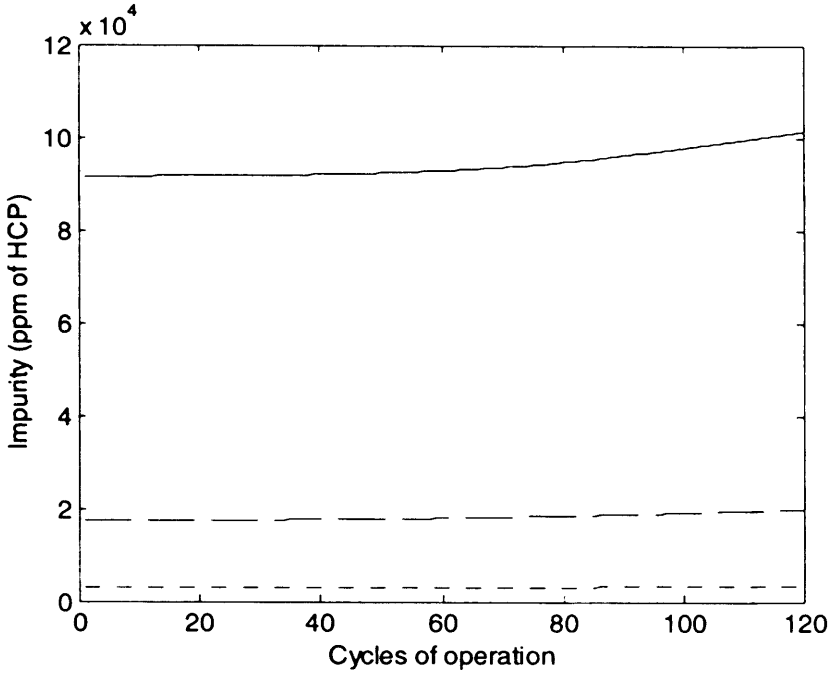

(a)

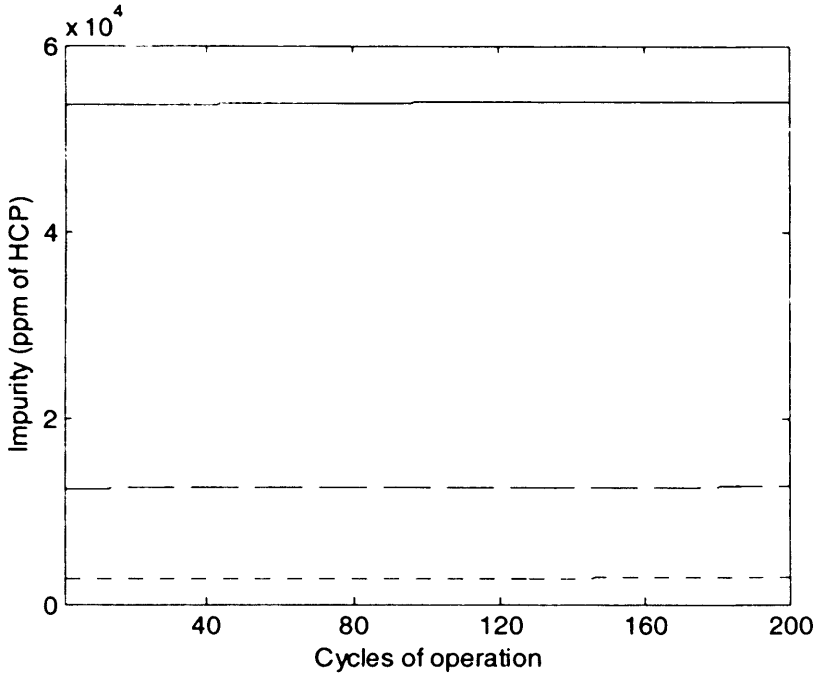

(b)

Figure 8.3 Variation in product purity for various level of column washing over a number of cycles when loading to 1% breakthrough under conditions of maximum productivity for **(a)** MabSelect™ and **(b)** Prosep vA Ultra®; after 2 CV of washing (———), after 4CV of washing (— — —) and after 6 CV of washing (·····).

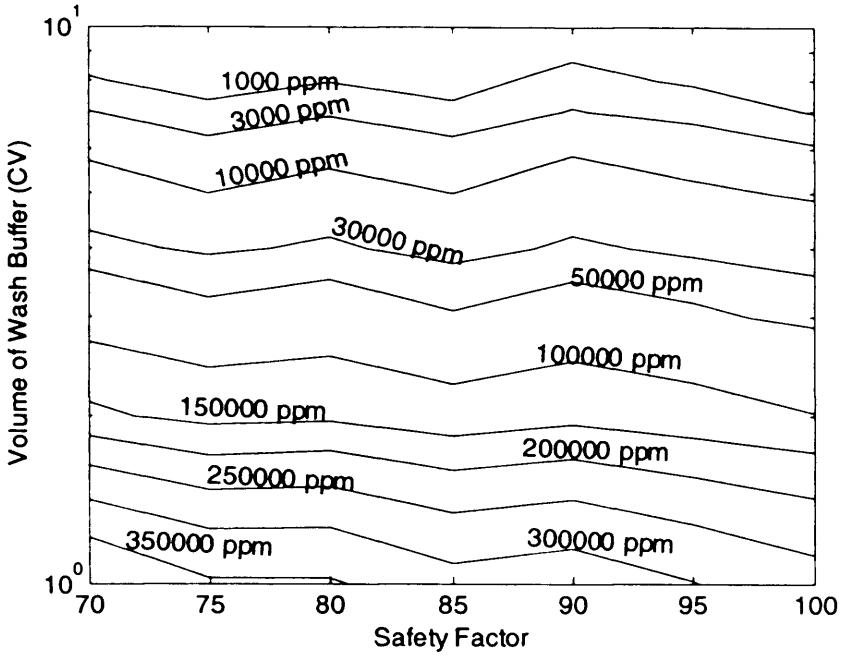

(a)

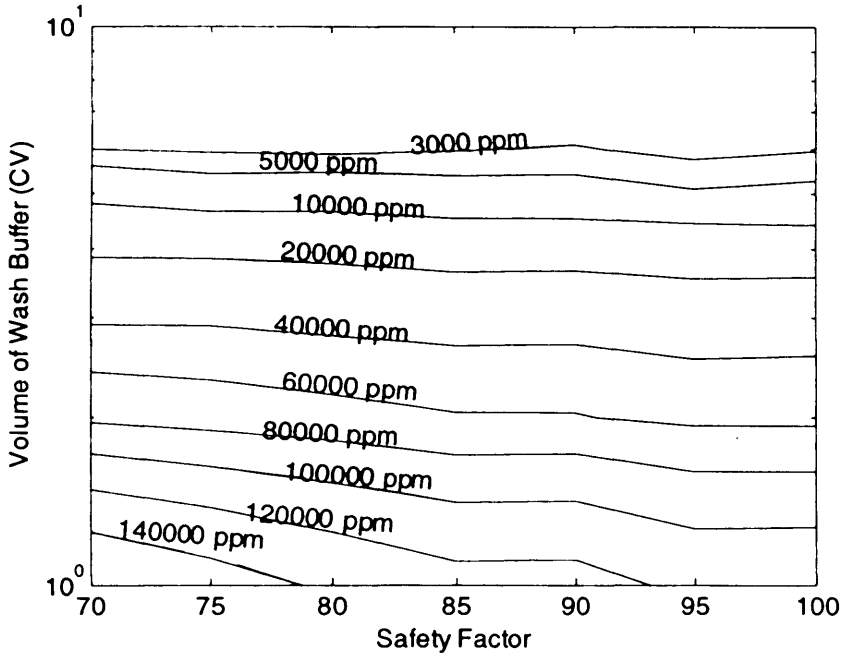

(b)

Figure 8.4 Contours of purity for **(a)** MabSelect™ and **(b)** Prosep vA Ultra® for differing wash volumes and safety factors for a loading velocity over a production year. Loading and washing took place under conditions of maximum productivity.

cleaning (CIP) times necessary in the use of the Prosep resin which are almost three times as long as that used in the case of MabSelect™. Table 8.4 shows the cleaning protocol used for the Prosep resin. Cleaning takes place with the use of an acid wash (HCl) using a contact time of 15mins. However, after every fifth cycle of operation, the resin requires cleaning with an additional guanidine wash utilising a contact time of 60 minutes. Comparatively, a typical process cycle under conditions of maximum productivity using the Prosep resin requires less than 60 minutes of column operation. The necessity of the guanidine based cleaning protocol essentially adds time that is equivalent to processing extra cycles within a given batch, thus diminishing the productivity gains that can be attained through use of a high velocity strategy.

Productivity is not solely based on how fast the process can be run. Process yield is also a defining factor. Figure 8.7 shows contours of yield on both resins that can be attained after 20 batches of operation for a variety of safety factors and volumes of wash buffer. The major cause of yield losses when using MabSelect™ (Figue 8.7 (a)) is that of the degradation in capacity that is brought about through the influence of hydroxide cleaning protocols. Chapter 7 showed that capacity degradation impacts not only the adsorption phase, where product is lost per cycle on loading (assuming load volumes remain constant throughput operation) but also the post-load washing step. A reduction in resin capacity decreases the opportunity for product which becomes unbound during the loading phase to rebind to the resin as it flows through the column. However, capacity degradation is not as great an issue for the Prosep vA Ultra® resin. In this case, product loss can be attributed to the use of an intermediate wash buffer in the two step post-load washing strategy. Use of a wash buffer whose pH is intermediate between that of the load and elution buffer may promote some premature elution of the product MAb during post-load washing. Figure 8.7 shows that the calculated yield losses from both resins are comparative. The results show that there slightly greater losses occur on the Prosep resin through the use of the intermediate wash buffer particularly at lower buffer volumes when compared to the losses incurred on MabSelect™. The relatively similar yields are very much a function of the adverse effects of the degradation

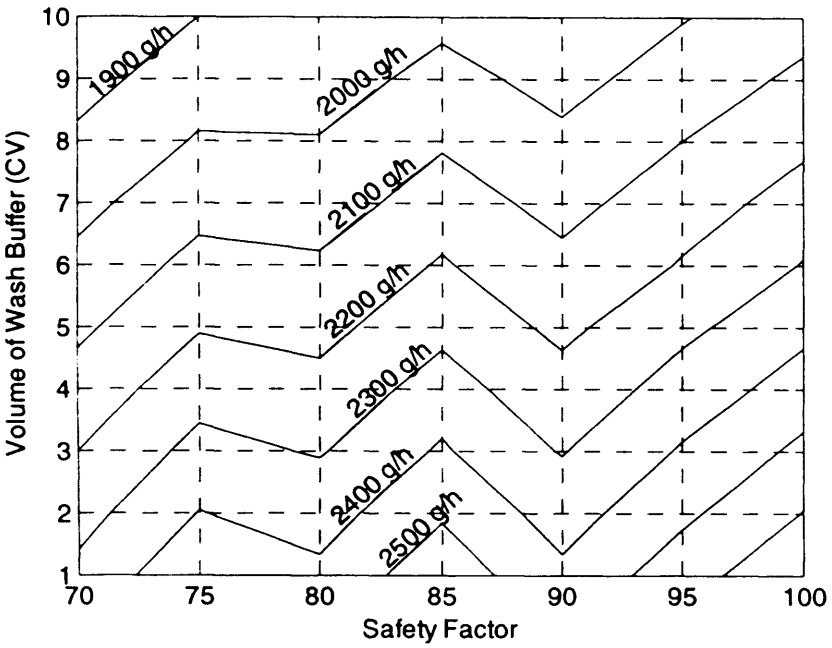
Volume of Wash Buffer (CV)
Safety Factor
1900 g/h
2000 g/h
2100 g/h
2200 g/h
2300 g/h
2400 g/h
2500 g/h
10
9
8
7
6
5
4
3
2
1
70
75
80
85
90
95
100

(a)

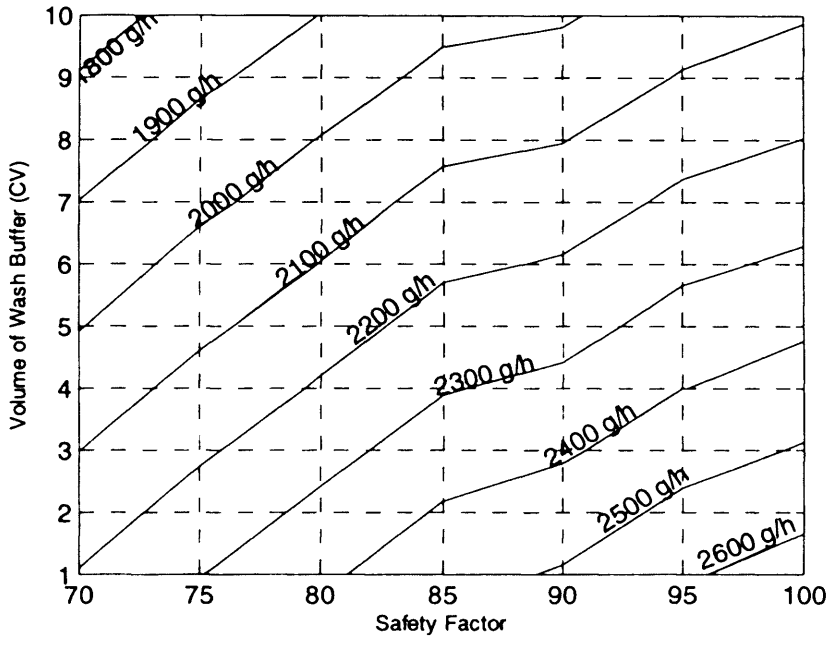
Volume of Wash Buffer (CV)
Safety Factor
1800 g/h
1900 g/h
2000 g/h
2100 g/h
2200 g/h
2300 g/h
2400 g/h
2500 g/h
2600 g/h
10
9
8
7
6
5
4
3
2
1
70
75
80
85
90
95
100

(b)

Figure 8.5 Productivity contours for differing safety factors and volumes of wash buffer for **(a)** MabSelect™ and **(b)** Prosep vA Ultra® under the maximum productivity conditions specified in Tables (8.5 and 8.6 respectively).

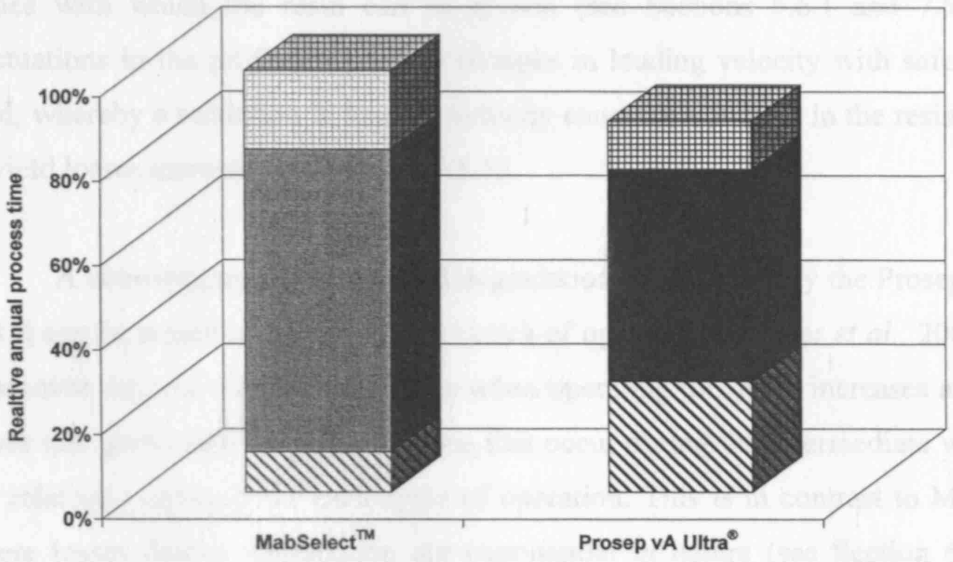

Figure 8.6 Fraction of total process time over a 20 batch period spent on the different stages in a chromatographic process cycle when loading to 1% breakthrough and washing with 7CV of buffer for MabSelect™ (grey scale) and Prosep vA Ultra® (black scale); ■ denotes time spent loading, ▨ represents time spent cleaning and ⊞ denotes time spent on ancillary washes (post-load wash, elution and equilibration).

coefficient in terms of MabSelect™ and the extent to which the intermediate buffer changes the adsorption isotherm in the case of the Prosep resin. In this study both these quantities have been estimated based on empirical data (Johannson *et al.*, 2002; Mann, *et al.*, 2005). Therefore, this data is probably not generic but it is adequate for the stated purpose of developing an overall methodology for the evaluations of each resin.

8.6 Evaluation resin lifetime

Equation 5.22(a) was used to calculate the optimum economic lifetimes of each resin using the adjusted loading velocities used to maximise productivity (Table 8.5 and 8.6). The results of the analysis when performed on the MabSelect^{TM} resin are shown in Figure 8.8. Given the capacity degradation experienced by MabSelect^{TM} the cost of goods per cycle increases and as such there exists a most profitable number of cycles with which the resin can be reused (see Sections 5.6.1 and 7.5.4). The fluctuations in the profile mirror the changes in loading velocity with safety factor used, whereby a reduction in loading velocity causes a reduction in the resin lifetime as yield losses increase (see Section 7.5.3).

A consequence of the reduced degradation experienced by the Prosep resin is that it can be reused in excess of 400 cycles of operation (Farhner *et al.*, 2001). This is because the cost of goods per cycle when operating this resin increases at a much lower rate given that the product losses that occur during the intermediate wash step are relatively constant for each cycle of operation. This is in contrast to MabSelect where losses due to degradation are exponential in nature (see Section 6.4.1). In addition capacity degradation exacerbates product losses that occur during the post-load washing stage. This is because less product that becomes unbound during the wash stage can be rebound to the resin than when a fresh resin is used (Section 7.5.2).

However, due to the difficulties involved in sterilising packed bed systems (one cannot autoclave a packed bed column) microbial contamination or bacterial build-up (contaminants which have not been considered in this analysis) may effect the purity of the product eluate over an extended time (Sofer, 1987). Therefore, regulatory requirements necessitate the replacement of resins and sterilisation of the column before such effects become significant, despite the fact that continued re-use of the column may still be economically feasible. Farhner *et al.* (1999a, 1999b, 2001) and Kemp *et al.* (2002), have shown that Prosep vA Ultra® can be validated under process conditions for up to 300 cycles without significant changes in purity. As such process lifetime for the Prosep vA Ultra® resin was assumed to be a constant value of 300 cycles unless lifetime was evaluated (through the use of Equation

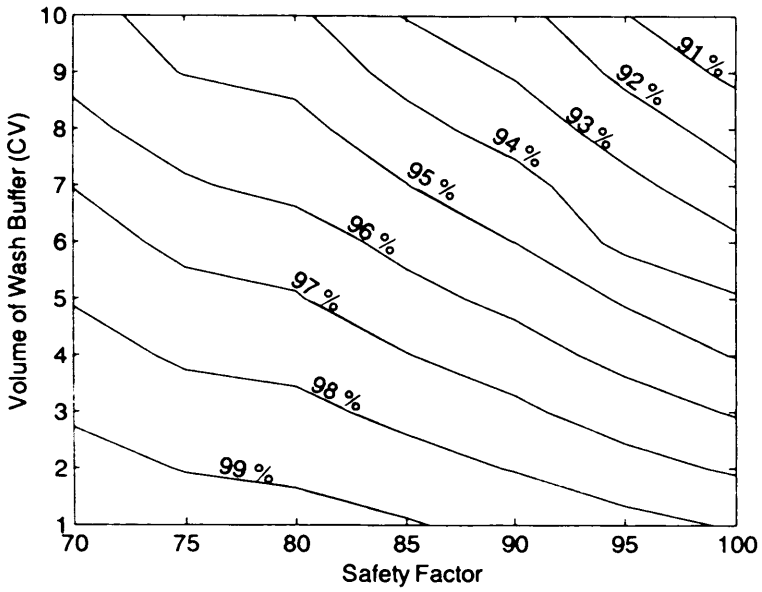

(a)

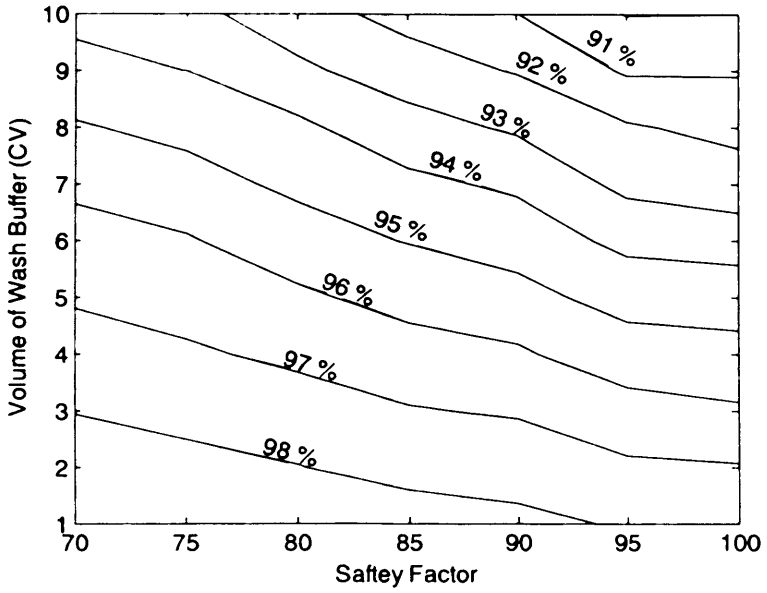

(b)

Figure 8.7 Contours of yield for **(a)** MabSelect™ and **(b)** Prosep vA Ultra® for differing wash volumes and safety factors for a loading velocity over a production year. Loading and washing took place under conditions of maximum productivity.

(5.22a)) to be less than this value. Simulations show that economic based lifetimes for the Prosep resin decrease below the 300 cycle estimation when washing with large quantities of intermediate wash buffer and when using a low loading velocity. The reasons for decreased lifetimes under these conditions have been outlined in Section 7.5.3.

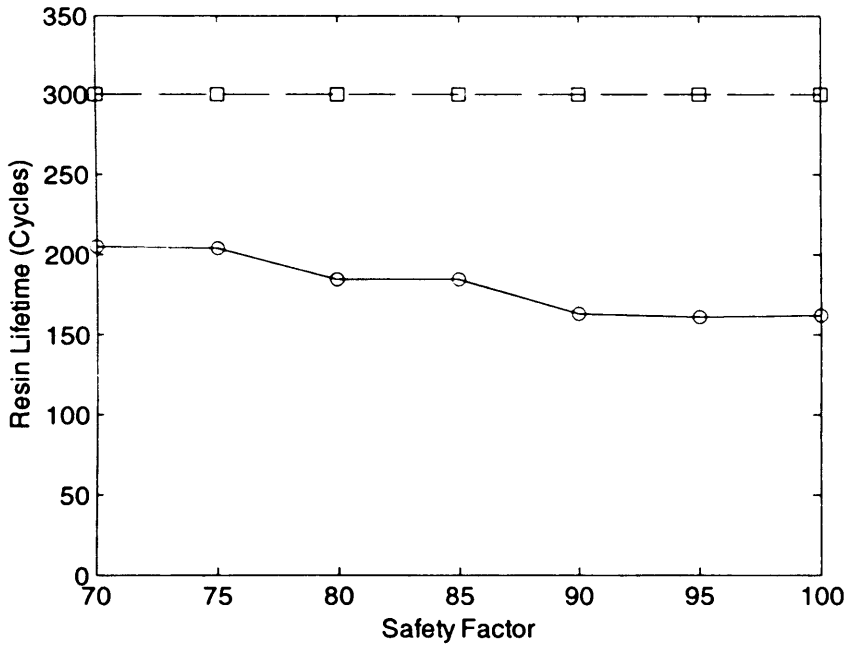

Figure 8.8 Resin lifetimes for various safety factors operating at the adjusted loading velocities for the maximum productivity operation case displayed in Table 8.5 for MabSelect™ when washing with 7 CV of buffer (——○——) and when operating under the conditions displayed in Table 8.6 for Prosep vA Ultra® (— □ — —) when washing with 7CV of buffer.

8.7 Costs analysis

Cost input data detailed in Table 5.6 was used to calculate the annual breakdown of the COG/gspecific for both resins and is displayed in Figure 8.9. COG/gspecific varies with safety factor based on trade-offs that occur through savings in yield (on use of low safety factors) and reduced cycling requirements (on

use of high safety factors, see Section 7.5.7.2). It can be observed that the Prosep costs approximately twice as much as the MabSelect™ resin to run over the 20 batch production schedule. In both cases the contribution of buffer costs dominates the overall COG/gspecific. However, there is a greater buffer utilisation on use of the Prosep resin given the extra wash step used in its operating strategy. Further to this, it can be seen with reference to Table 5.6 that the cleaning buffers used for this resin particularly in the case of the guanidine solution are significantly more expensive than the hydroxide solutions used in the cleaning of the MabSelect™ resin.

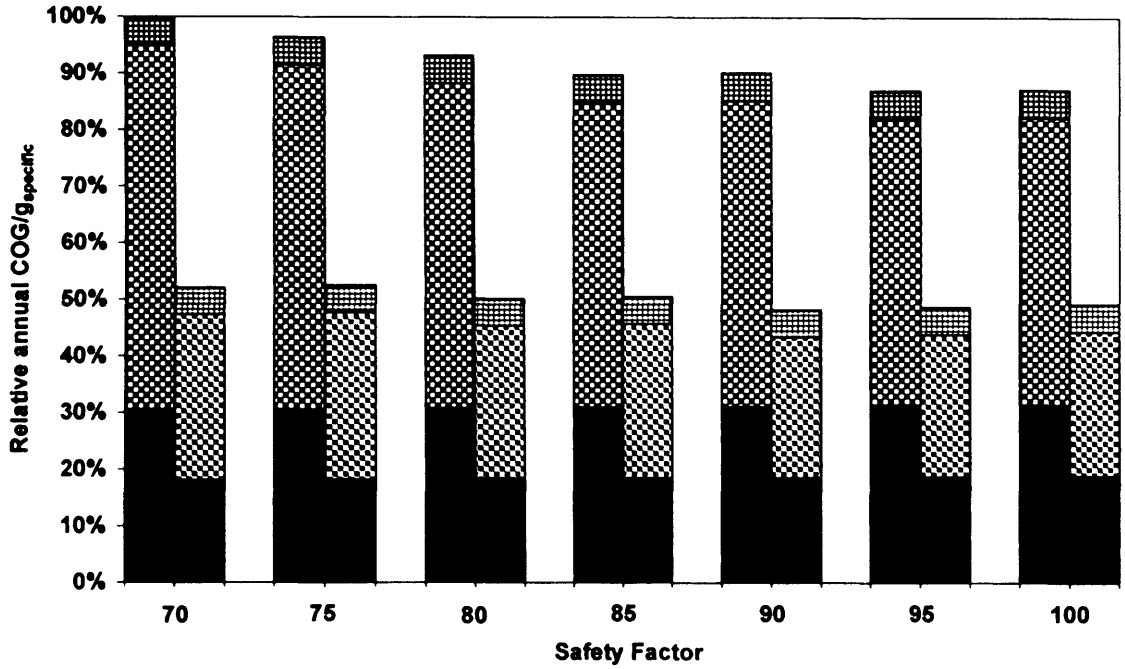

Figure 8.9 Breakdown of annual specific cost of goods per gram ($COG/g_{specific}$) for Prosep vA Ultra® (black) and MabSelect™ (grey) under conditions of maximum productivity (Tables 8.5 and 8.6 respectively) when loading with various safety factors. Prosep vA Ultra® was washed with 6CV of buffer whereas MabSelect™ was washed with 7CV of buffer to ensure an impurity level of 3500ppm; ■ denotes contribution from resin costs to the overall $COG/g_{specific}$, ▩ represents the contribution from buffer costs ▦ represents the contribution from the column and rig (depreciation) costs and □ denotes the contribution from the cost of labour.

Figure 8.10 shows the contribution of cleaning costs to the overall $COG/g_{specific}$ for the year long process. It can be observed that the cost of cleaning the Prosep resin is almost 50% greater than the cost of cleaning MabSelect™. Figure 8.9 shows that resin costs are the next major contributor in the $COG/g_{specific}$. Referring back to Table 5.6, the capital cost per litre of the Prosep resin is nearly twice as expensive as that of MabSelect™. The contributions from the depreciation of the column and rig are constant for both cases as each resin is assumed to be packed into the same column. Labour costs in both cases appear insignificant in comparison to the cost contributors already outlined. It is the increase in the cost of cleaning together with the higher capital cost per litre of the resin that result in the $COG/g_{specific}$ of the Prosep vA Ultra® to dwarf that of the MabSelect™ resin.

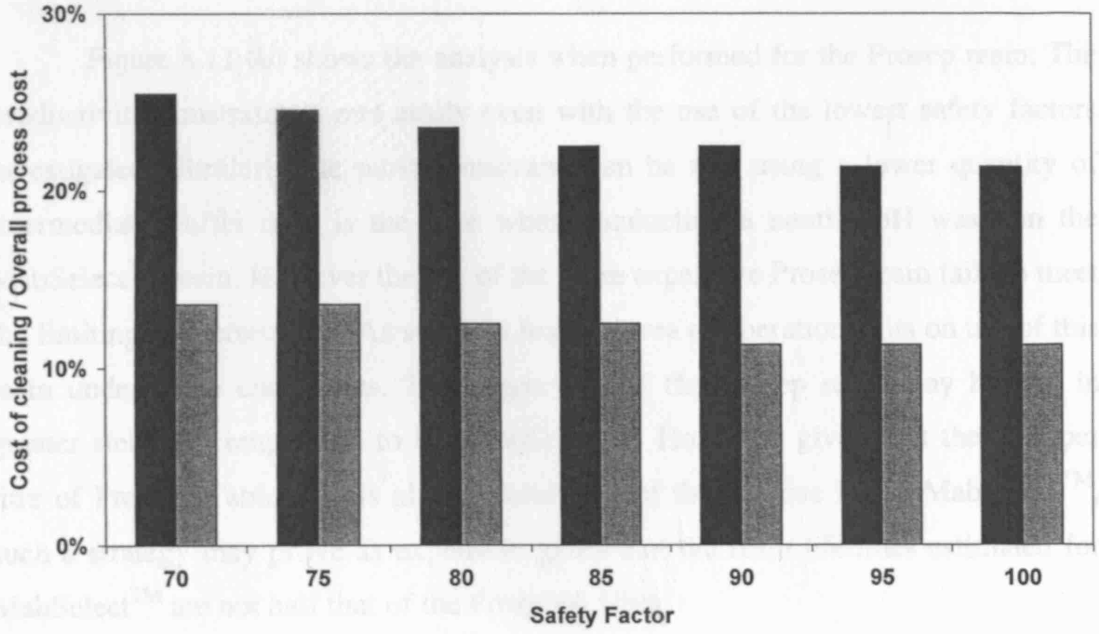

Figure 8.10 Contribution of cleaning costs to the overall $COG/g_{specific}$ for Prosep vA Ultra® (black bars) and MabSelect™ (grey bars).

8.8 Selection of operating strategy

Having investigated the impact of various operating strategies on the use of the two different resins the most advantageous strategies can be selected. A decision

is required that balances cost and productivity and uses specific $COG/g_{specific}$, minimum productivity and minimum purity levels as constraints when defining a feasible options. A window of operation can therefore be defined based on limiting the specific $COG/g_{specific}$ to say 7.5 \$/g, productivity to 2000 g/h and purity, which is defined as a minimum level of HCP acceptable in the eluate pool, to 3500 ppm. Figure 8.11 shows the windows produced based on these limiting constraints for both resins. It can be observed that a variety of strategies are open to the designer when utilising the MabSelect™ resin. Assuming that of the number of column volumes and safety factors which are available to the designer are discrete quantities indicated by the grid lines shown in Figure 8.11 (a), perhaps the most favourable column operating strategy for this resin would be to operate with a safety factor of 90 whilst washing with 7 CV of buffer. This is the most cost effective strategy to follow given the process constraints specified.

Figure 8.11 (b) shows the analysis when performed for the Prosep resin. The productivity constraint is met easily even with the use of the lowest safety factors investigated. Similarly the purity constraint can be met using a lower quantity of intermediate buffer than is the case when conducting a neutral pH wash on the MabSelect™ resin. However the use of the more expensive Prosep resin fails to meet the limiting cost constraint. As such, no feasible area of operation exits on use of this resin under these constraints. The longer life of the Prosep resin may hold it in greater stead in comparison to the MabSelect™. However, given that the cost per litre of Prosep (Table 5.6) is almost twice that of the agarose based MabSelect™, such a strategy may prove as expensive given that the resin lifetimes estimated for MabSelect™ are not half that of the Prosp vA Ultra.

8.8.1 Relaxation of the maximum productivity constraint

Section 7.5.7.1 showed that a decrease in the loading flowrate would enable a lower $COG/g_{specific}$. Such a strategy may be implemented on use of the Prosep resin to reduce its high process costs. Operation at a lower loading velocity reduces the number of cycles required to process a batch of material whilst the ability to operate the ancillary cycles of the chromatographic step at high velocities may enable the productivity constraint to still be met. It was found that lowering the flowrate to the

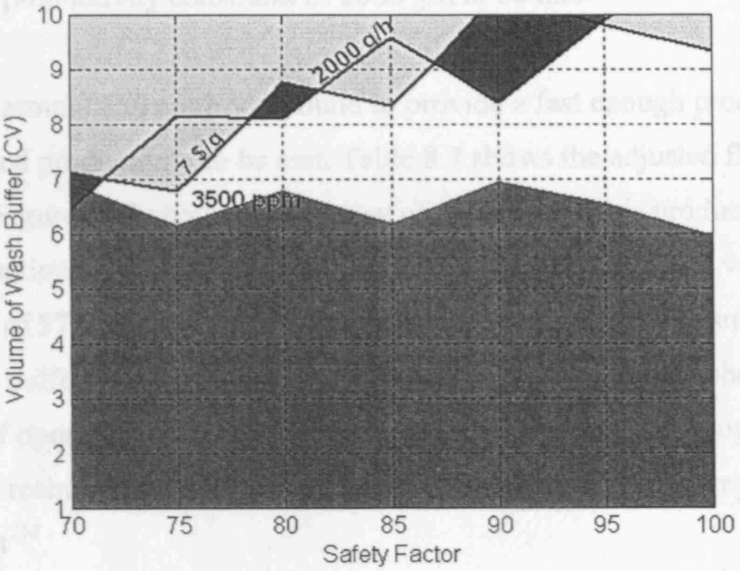

(a)

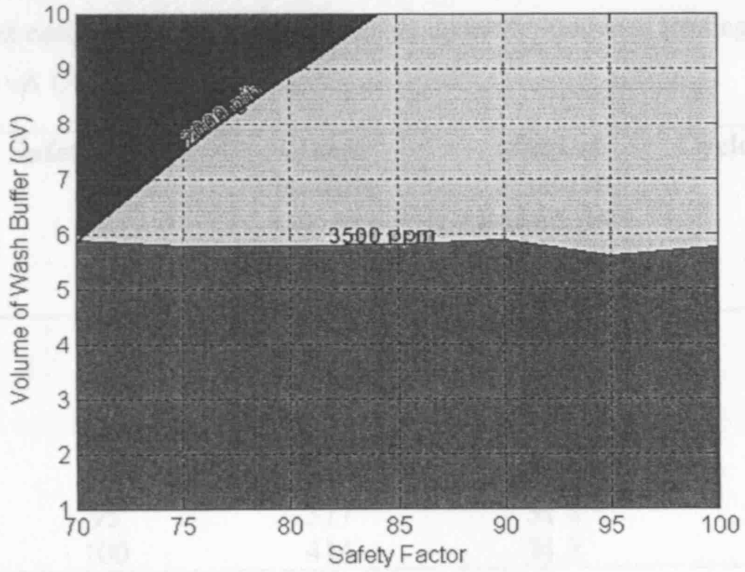

(b)

Figure 8.11 The window of operation produced when constraining the productivity at 2000 g/h ■ and process impurity at 3500ppm ■ and COG/$g_{specific}$ at 7.5 $/g ■ for **(a)** MabSelect™ and **(b)** Prosep vA Ultra®

minimum possible within the DSP constraint specified in Figure 8.2 (b) would not enable the productivity constraint of 2000 g/h to be met.

Operation around 350 cm/h was found to provide a fast enough process time to allow the specified productivity to be met. Table 8.7 shows the adjusted flowrates used for this case. Figure 8.12 shows the window of operation that is produced on implementation of these conditions. Despite the reduction in load velocity the cost constraint of \$7.5/g still cannot be met given the large buffer consumption and expensive buffer and resin costs. A $COG/g_{specific}$ of 10.5 \$/g was shown to provide a window of operation signifying that an extra \$3/g is necessary to operate the Prosep vA Ultra® resin in meeting the specified process criteria when compared to MabSelect™.

Table 8.7 Adjusted velocities for equal cycle loading for various load volumes when operating at optimum loading velocity during operation (reduced loading velocity condition) for Prosep vA Ultra®.

Safety Factor	Linear loading velocity (cm/h)	Mass of product bound per litre resin (g/L)	Cycles/Batch
70	366	23.9	8
75	411	27.3	8
80	366	27.3	7
85	406	31.8	7
90	445	31.8	7
95	377	31.8	6
100	414	31.8	6

8.9 Conclusions

The conclusion to the case study as originally set-up would be operation with the MabSelect™ resin whilst loading with a velocity of 418 cm/h and safety factor of 90. Post load washing would proceed at 500 cm/h for 7CV, although as demonstrated

in Section 7.6.1 a reduction in the washing velocity can reduce buffer consumption and decrease the cost of the process. Such optimisation however is addressed in the future work section of this thesis (Chapter 10).

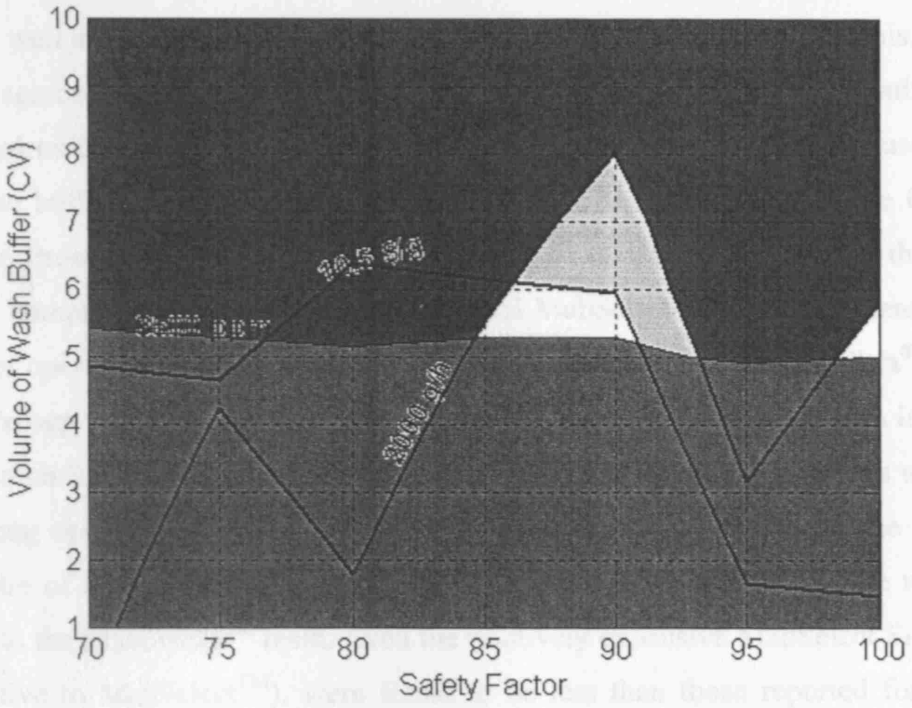

Figure 8.12 The window of operation produced when constraining the productivity at 2000 g/h ■ and process purity at 3500ppm ■ and COG/$g_{specific}$ at 10.5 \$/g ■ for the Prosep vA Ultra resin when loading under conditions denoted by Table 8.7. The initial cost constraint of 7.5 \$/g still could not be met despite the reduction in cycling intensity and buffer utilisation.

It may be that the Prosep vA Ultra® resin has an advantage over MabSelect™ in terms of consistent performance. The comparative lack of degradation during operation allow purity and yield levels to be on average, uniform for a larger number of cycles than in the case of MabSelect™. This may impact the validation studies and costs which are necessary before any chromatographic process can be implemented in a manufacturing scenario. It is noted that these costs have not been applied in this analysis and could be significant in any final conclusions.

However, to solve the degradation problems experienced by MabSelect™ and other agarose based resins, GE Healthcare have recently introduced the MabSelect SuRe® resin onto the market which is resistant to alkaline conditions. The alkaline stability of the ligand puts it on par with the Prosep vA Ultra® in terms of the rate of capacity degradation experienced by the resin thus increasing resin lifetime as well as providing more consistent operational cycles. Further to this, the use of an agarose base allows effective cleaning to take place with the relatively cheaper hydroxide solutions. Furthermore this resin will not require the use of intermediate buffer washes as the agarose base is not as hydrophobic as the CPG base of the Prosep vA Ultra®. The disadvantage of this resin however is that it retains the compressible properties of the original MabSelect™ so that the feasible flowrates of operation remain lower than are possible with the Prosep vA Ultra®. As such, the Prosep vA Ultra® provides a greater flexibility in operation as shown in the case in Section 8.8.1 where operation could proceed at lower loading flowrates while still allowing operation which met the intensive productivity constraint. The high cost per litre of the Prosep resin was found to be the dominate disadvantage when compared to the MabSelect™ resin. Even the relatively expensive MabSelect SuRe® resin (relative to MabSelect™), were found to be less than those reported for the Prosep vA Ultra® resin (see Table 5.6).

Chapter 6-8 have very much focused on the considerations and techniques used in the design of initial capture chromatography. Chapter 9 will switch the focus to that of the various validatory techniques and issues that need to be tackled in any successful integrated design approach to large-scale chromatography.

9 FURTHER CONSIDERATIONS IN AN INTERGRATED DESIGN OF A CHROMATOGRAPHIC SYSTEM: PROCESS VALIDATION

9.1 Introduction

Routine laboratory purification of antibodies has been well described in literature (e.g. Scott, 1987) but the considerations for large-scale production of pharmaceutical grade antibodies are much different than those for laboratory scale. There are extreme purity requirements for pharmaceutical antibodies (Fahrner *et al.*, 2001) and routine large-scale production requires high yield and process reliability (factors which have been outlined in Chapters 7, 6 and 4 respectively). Typically, in order to use a chromatography step in a cGMP manufacturing process for a therapeutic protein, a process validation package which addresses resin cleaning and reuse, step robustness, virus removal studies, and peptide leaching issues is utilised (Kelly *et al.*, 2004). To gain regulatory approval the process must be completely validated to run consistently within specified limits. Therefore process design should be conducted with a view to facilitating validation. Work in this study has yet to consider process validation or qualification, focusing more on the evaluation of process performance. This chapter provides a discussion as to the validation requirements that need to be considered when designing a chromatography step for therapeutic manufacture and how some of the methodologies discussed previously can help in this process.

Validation of all forms of chromatographic processes requires that the equipment be qualified. Chromatographic resins are a critical raw material and acceptance criteria must be established and testing validated (Sofer *et al.*, 1997). Process parameters that must be validated include performance criteria for packed chromatography columns and removal of impurities and any processing additives. Cleaning, sanitisation, and storage routines must also be validated. Three to five consecutive batches must be shown to produce consistent product (demonstration of three consecutive batches is the norm in the USA whereas five is typical in Europe, (Sofer *et al.*, 1997)).

9.2 Column qualification

Column qualification is documentation of work done to ensure that the column and the protocols written to direct operation of the column are appropriate for the purification step intended. Column qualification can be divided into two broad subject areas: column hardware qualification and column protocol qualification (Rathore *et al.*, 2002).

9.2.1 Column hardware qualification

In column hardware qualification, the column size and manufacturing materials need to be documented. The intended packing material needs to be associated with a particular column. Resin qualification and the workflow associated with resin is another topic to be documented. The location in the plant needs to be established. Peripheral equipment, such as tubing and hoses, pressure gauges, clamps, and gaskets needs to be documented. Spare parts must be associated with a particular column as well. A schematic of the column makes the documentation package easier to follow. The construction materials should be verified as part of the overall validation program, and records of those materials need to be kept in the validation record. Leachables and extractables from those materials need to be verified as well. If the column is mobile the process work diagram should show how the column travels, that is, where it is stored, where it is packed, how it is transported, where it is tested, and how it is removed from service and transported out of the operations area.

The schematic diagram shows all the associated lines into and out of the column. The process workflow diagram indicates the tanks that are connected to the inlet side and which tanks are connected to the outlet. Product is collected into one of the tanks on the outlet. People responsible for the process need to know the location and the condition of the product at all times. Qualification of these tanks and fluid path transfers is another part of hardware qualification. Included in the validation package for the column is the engineering drawing of the column. Spare parts are associated with an individual column, and engineers performing the scheduled maintenance on the column can be expected to require access to this part of the

validation record to ensure that the appropriate spare parts are used in maintenance and reordered once they are consumed. Documentation of the gauges used to operate a column should include the calibration record of the gauge as well as the serial numbers or asset number to ensure that the correct gauge is in place during operation.

During process development, the buffers and cleaning solutions are defined for the specific chromatographic step. It is essential also to define acceptable ranges of pH and ionic strength. While it maybe easier to make a buffer of pH 7.4 in the pilot scale, in production quantities the variability may be greater (Sofer *et al.*, 1997). Protocols for the procedures for pH or other variable adjustments should be implemented as well as the acceptable limits of variability.

Column packing methods must be sufficiently defined so that in the event of a change in production personnel, the column will meet the defined performance criteria. Ideally, pressure-flow curves for each lot of chromatographic media should be performed to determine the optimal packing flowrate and pressure. Techniques intended for process design purposes presented in Chapter 3 and 4 may also be implemented as part of the validation protocol for such a reason.

9.2.2 Column protocol qualification

Column protocol or operational qualification includes confirming pump reliability, alarm signal, leakage of liquids and column performance. The function must be verified for alarms, valves, monitors, flow control, air sensors, indicators, pressure transmitters and computer control. Process development work can contribute to the validation of the chromatography step by providing data on the stability of the chromatography resin under equilibration, operating, regenerating, cleaning and sanitizing, and storage conditions (demonstrated in Chapter 4). To operate the column, an associated set of standard operation protocols (SOPs) needs to be written and tested. Regulatory requirements exist to ensure that operators are trained and regularly retrained to maintain their competence in performing the operation.

Any column in the purification process needs to have SOPs for column packing and testing. Once accepted for use, each column needs SOPs for equilibration, running (that is, applying feed to a collection of product), regenerating, and cleaning. SOPs are needed to direct the collection of data for use in ascertaining performance quality, to document how preventive maintenance should be done, and to provide instructions on how material should be stored.

Recent US Food and Drug Administration (FDA) inspections have shown an increased interest in the packing characteristics of process-scale, liquid chromatography columns (Rathore *et al.*, 2002). That is manifested by the agency's emphasis on reproducible packing of chromatography columns by pharmaceutical and biotechnology companies. Although process-scale column packing is still, in many cases, more of an art than a science, the FDA — by its inquiries at inspections — is encouraging companies to move toward a column-packing science. A large part of that science is how a column is characterized or qualified after it is packed.

As discussed in detail in Chapter 3, many variables influence the science of column packing. One factor which wasn't examined was that of the effects of resin slurry concentration. Resin slurry concentration is often overlooked when packing process-scale columns. For poorly understood reasons, resin can pack differently when charged to the column at different concentrations[a]. A slurry concentration that works in one column may not work as well in another manufacturer's column. Resin manufacturers generally have a good idea of what slurry concentration works best with different column technologies. However, perhaps this should be investigated by the end user for optimal performance.

Traditional columns with adjustable upper adaptors can be packed reproducibly with repeated practice. The caveat here is that it may take several attempts to achieve the first optimal pack. Once the technique is determined however, subsequent packing can proceed more efficiently. Newer process-scale column designs, which include dynamic axial compression and self-packing technologies, are generally more user friendly and can be packed successfully on the

[a] personal communication J. Svensson, GE Healthcare, Uppsala, Sweden, 2006

first try. However these columns require more up-front training and the hardware is usually more expensive because it includes additional equipment specially designed to assist in column packing.

Ideally, all resins should be defined before packing, eliminating any small fragments that can be generated by shipping and handling resin. Trace amounts of fines may not have any effect on the actual chromatography, but can eventually lead to occlusion of the bottom screens or frits. Such occlusion would ultimately create increased backpressure, which would require a reduced flow rate. As a result the column would have a reduced throughput. The mobile phase plays an important role in packing process columns. Generally a solvent that packs the resin most tightly is preferred. Placing and securing the upper adaptor directly on the top of the settled bed minimises swelling when the mobile phase is changed. Once a column is packed, a series of standard tests should be conducted to evaluate performance and qualify the column. The results of these tests do not predict success in the actual chromatography step; however, the results are useful for column packing reproducibility.

Usually a small, un-retained probe molecule is used for standard column tests such as calculation of height equivalent to a theoretical plate (HETP). Most chromatographers use a UV-absorbing molecule such as p-aminobenzoic acid (PABA) or acetone. Alternatively, concentrated sodium chloride spikes are monitored using a conductivity detector. Many more companies use sodium chloride because it is almost always used in the mobile phase of applications. Injection volume becomes more important as particle size decreases. A 0.1% column volume injection is a good starting point. The flow velocity for such a test should be 60–80 cm/ hr for best results. Data can be analyzed by computer if recorded digitally, or if not, data can be calculated by hand. In some cases, less than optimal column performance values may be tolerated because of the column's function. For instance, higher HETPs may be acceptable when the column is used for a simple capture step with a step elution. Tailings may also be acceptable if no closely eluting impurities are found and the extra volume is handled easily in subsequent unit operations.

The packing quality during operation of a column can also be tested by measuring the HETP (see Chapter 4 and Appendix A). Whatever sample is used or however one measures HETP it is essential to use the same method each time to compare packing performance and stability. Ideally, packing should be measured after every five runs to ensure that the column packing has not deteriorated (Sofer *et al.*, 1997). In addition to HETP, the peak asymmetry (As) is also a valuable parameter that measures the quality of a packed column (see Appendix A). The ranges of acceptable HETP and As values will be determined by comparing these values with column process performance. Specification of the frequency of checking HETP and As is also beneficial for maintaining control over the process. If a change in column performance (such as in product purity or flowrate) is observed, HETP measurements allow one to determine if the column packing has deteriorated or if there is another problem. Chapter 4 however, showed the danger of over reliance on HETP as a performance metric whereby deterioration in bed stability was not picked up by the widely used HETP testing procedure.

9.3 Process performance qualification

Process performance can be defined by a combination of criteria such as the purity and recovery of the product (in addition to the productivity and cost used in the previous analyses). Purity and recovery are a function of the sample load, flowrate, particle size and particle size distribution of the media, non-specific adsorption and the chromatographic selectivity. Yields for steps must be documented and it is also essential to ensure that the chromatography operation does not impair biological activity of the product.

During process development function tests should have been established. The load material must be assayed for antibody concentration prior to loading, usually by an analytical Protein A affinity assay. For adsorption techniques the dynamic capacity should be tested under actual running conditions. As demonstrated in Chapter 7, a batch of material is typically split into equal load volumes to ensure equivalent process performance over the cycles of operation. Further to this it has been shown that under-utilising the column capacity or loading with a safety factor is sometimes advantageous to processing needs. Given that loading proceeds to below

breakthrough and therefore before absorbance can be detected from the column outlet, measurement of load volume becomes extremely important and sensitive. In case the measurement of load volume is inaccurate, it is important to have an air sensor on the load line to end loading in case the load runs out early. During elution, the pool begins when the absorbance reaches a predetermined value. The pooling may also end when with absorbance or volume reaches a predetermined value.

9.3.1 Purity considerations

The fundamental use of chromatography techniques is impurity removal. Purity requirements for therapeutic products are extreme. There are six main purity considerations for the recovery of pharmaceutical antibodies.

1. Host cell proteins – typically present in high amounts (see Chapter 7 and 8) in the harvested cell culture fluid. Documented HCP levels can be achieved through quantitative measurements by Elisa (Chen, 1996) and qualitatively by SDS-PAGE (Farhner *et al.*, 2001).

2. DNA – is also present in large quantities (>1,000,000pg/mg) and must be removed to <10ng/dose levels. During validation studies DNA maybe spiked into the load of small scale studies to demonstrate clearance. The level of DNA may be measured though an assay kit (e.g. Molecular Devices Threshold DNA kit).

3. Aggregate - the main product related variant that must be reduced is aggregated forms of the antibody product (mostly dimer) because of the possible immunogenicity of the aggregate. Aggregate levels are typically measured through size exclusion chromatography.

4. Small molecules - the harvested cell culture fluid contains many small molecules, originating from the media components and created during cell culture by the CHO cells. Rather than determining the level of all small molecules a few representative

marker molecules are measured, the levels of which are determined through a competition ELISA.

5. Leached Protein A – during the Protein A step, some Protein A leaches from the column and ends up in the antibody pool. Protein A can be immunogenic and cause other physiological reactions (Gagnon, 1996). Leached Protein A must be cleared during the downstream steps (post initial capture). The level of Protein A may be determined by a sandwich ELISA (Lucas *et al.*, 1988).

6. Virus-Harvested cell culture fluid may have 10^4 or more retrovirus-like particles per mL and biological pharmaceuticals are allowed to have 1 theoretical virus particle per 10^6 doses, so the recovery process must provide significant virus clearance. The validation and test procedures are beyond the scope of this chapter. In general, the Protein A step provides the majority of virus clearance in the process through selective removal (during loading) and through the use of low pH inactivation (during elution).

Frequency of testing varies from batch lots to cycle lots depending on the frequency of cycling. Chapter 7 and 8 demonstrated how impurity levels increased due to capacity degradation on resins. The rate of degradation and therefore impurity remained constant, eventually increasing exponentially after extended cycling. Testing procedures would need to be more frequent when validating a process for extended cycles of operation. The cost of the frequent and varied validation testing adds greatly to the overall cost of production.

9.3.2 Resin re-use

A significant proportion of the analysis and design that has been presented in this thesis has been based on the re-use of chromatographic resins. The performance of a quantity of resin should be the same in the last run as in the first (Sofer, 1987). As has been discussed for an early step in the process the frequency of repacking or replacing the resin will be generally high. The proposed lifetime of the media should

be defined when applying for a license to manufacture a product by chromatography. Documentation of data such as the number of runs achieved at the pilot scale is essential to support the validation of chromatography processes. Indications of resin deterioration include changes in flow rate and/or pressure, elution profile, regeneration profile (e.g. pH, conductivity) and decreasing product recovery. Using a resin to its functional lifetime maximises the cost basis of that resin and may be beneficial if the resin is expensive (as in the case of Protein A) or the number of cycles in its functional lifetime is low. For a relatively inexpensive resin, economic considerations other than cost or cycles many influence the useful lifetime (O'Leary *et al.*, 2001). For example, using a resin for the duration of a campaign and then packing a fresh column for the next might be more convenient. That reduces the need to store used resin and it saves both storage space and resources that would be used to track resins. Generally, the resin lifetime will be determined by preventative maintenance methods, build-up of material on the column, efficacy of the cleaning methods employed and the stability of the resin to the cleaning methods. It is this final factor which has formed the basis of the resin lifetime calculations employed in this study whereby the resin capacity degradation caused by the harsh hydroxide cleaning was modelled.

The useful lifetime of a resin can be determined in several ways, including through validation studies performed concurrently at manufacturing scale or prospectively at small –scale. For both methods predefined acceptance criteria should be established in advance of the study; and in the case of failure, a predefined action plan is needed. From a validatory viewpoint, determining column lifetime is problematic prior to manufacturing a product, since it is unlikely that many full-scale runs will have been performed. For this reason, scaled down studies with production feed stream can be useful in providing data to regulatory agencies. This data can also be used in within the modeling framework presented in Chapter 5 to allow for more realistic resin lifetime estimates. The overall amount of resources used in small scale validation is likely to be less than those needed for manufacturing scale validation although resources in the latter case are spread over a longer period of time. Sample handling, completely traceable at small scale, is easier than sample handling from good manufacturing practice (GMP) production runs. Prospective determination of

column lifetime is particularly advantageous to a multi-product company, when analytical resources are stretched among many processes and products. Although prospective small-scale validation requires resources before regulatory submission, it can significantly reduce the amount of analysis required for each marketed run. In addition the manufactured lots are now placed on hold pending extensive analysis. This can ensure speedier release of marketable product. Rarely if ever does resin performance go from 100% to 0%. Rather a slow deterioration occurs (e.g. Equation 5.20). Monitoring systems for these parameters should be developed during process development and at pilot-scale. The parameters that most affect the separation should be determined and a decision made on when to replace the resin. A crucial way a company can maximise the lifetime of its chromatographic systems is through conscientious resin sanitization and cleaning (Sofer, 1987).

9.3.3 Column cleaning and sanitisation

Cleaning validation is a critical consideration in the pharmaceutical industry. Inadequate cleaning can result in contamination of drug products with bacteria, endotoxins, active pharmaceuticals from previous batch runs, and cleaning solution residues. Such contaminants must be reduced to safe levels, both for regulatory approval and to ensure patient safety.

A validated pharmaceutical cleaning process must use principles that are scientifically sound and reproducible. It is the pharmaceutical company's responsibility to set acceptance criteria and to explain the scientific basis for those limits to the regulatory authorities. Companies must have written SOPs in place that detail the cleaning processes used for individual pieces of equipment or systems. Protocols should contain sampling procedures, analytical methods and their sensitivities, and descriptions of methods and materials, including cleaning agents used in all processes. Instructions should be included for disassembly and reassembly of equipment when necessary, removal of previous batch identification, protection of equipment from contamination before use, and inspection of equipment immediately before use, as well as maximum time lapse permitted between the end of a production process and the start of cleaning procedure (Linsay, 1996).

In addition, pharmaceutical companies must provide the regulatory authorities with a validation report, approved by management, which demonstrates the effectiveness of the cleaning process. The report must include data indicating that residues specific to the drug product and the process in question, are reduced to acceptable levels by the cleaning process. Such regulatory scrutiny of cleaning processes means that pharmaceutical companies must carefully consider the cleanability of new equipment and to the systems already in place for cleaning existing equipment. Construction material should be a primary consideration in selecting equipment and establishing cleaning protocols. Equipment should not be reactive, additive, or adsorptive with the process materials that contact them. Materials such as seals, valves, gaskets, hoses, or tank surfaces that come in contact with drug products cannot cause contamination. Possible interactions of equipment materials with cleaning products must also be examined.

Other things to consider for equipment design include difficult to clean areas such as piping, connections, and valves. Surfaces should be smooth and the system should have no dead legs where sediment can settle. Piping and instrumentation diagrams can identify problem areas. Depending on the drug product being manufactured, different cleaning methods and analyses may be required. First one must identify the substances to be removed. The chemical and physical properties of the residues determine the best method to remove these from equipment surfaces. Some characteristics to consider include solubility, hydrophobicity, and reactivity. In addition, removal of the cleaning agent will have to be demonstrated, so its composition must be known.

9.4 Online process monitoring

The FDA recently published guidelines in which the importance of process understanding is emphasised when validating a process (Rathore *et al.*, 2002). These guidelines promote the use of process analytical tools such as multivariate data acquisition and analysis, modern process analysers and process monitoring. The FDA also states that the ability to predict process behaviour shows process understanding, and a greater process understanding gives more freedom in changing process conditions within the scope of the original approved validation

documentation. The cost of validation often hinders process development and implementation of new process equipment in existing production processes for pharmaceuticals. The ability to implement technology which can produce real-time data such as that described by the schematic in Figure 9.1 will significantly reduce these costs.

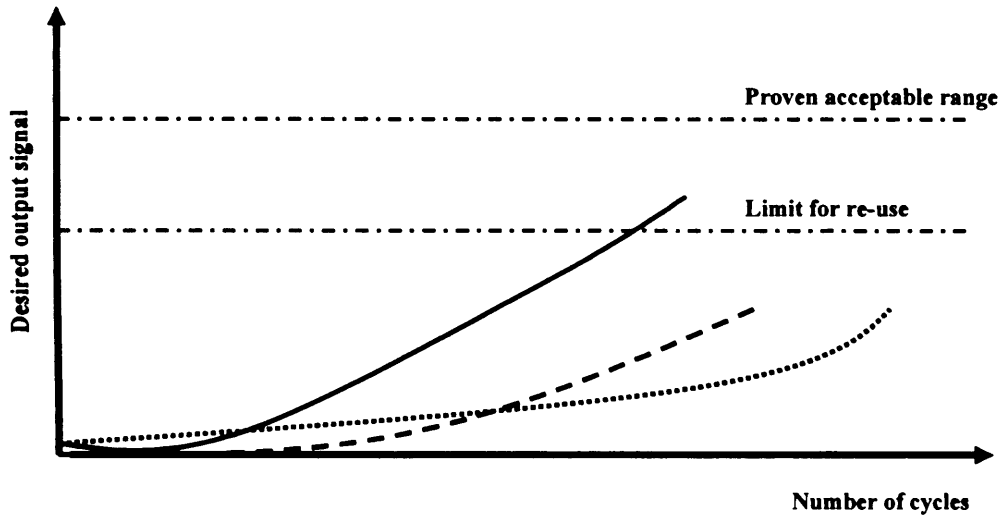

Figure 9.1 Determining resin re-use: (——) denotes back pressure trace; (— — —) denotes product purity and (·····) represents product loss.

9.5 Conclusions

Validation is documented evidence that a process does what it should. The fundamental basis of the validatory strategy is to present the understanding required to control and limit variability in a process so as to provide a means to manufacture a safe product. This chapter highlights the various procedures and considerations that should be undertaken to ensure the purification steps in the MAb process are (and remain) robust and reliable. The key point to note here is that constant testing and documentation procedures are required to provide successful validation of a purification process, which is important from a commercial and regulatory perspective. It is important to note that the limits of the validation range should encompass the operating range that is expected to be used for routine process control rather than the edge of failure limits.

10 CONCLUSIONS

It is likely that as the number of biopharmaceuticals moving toward large-scale production increases, so will the importance of addressing issues of process design and operation. To meet growing cost pressures companies will need to develop efficient and robust processes for manufacture of increasingly sophisticated biological entities.

A large percentage of potential biopharm products are monoclonal antibodies (MAbs). MAbs represent the most useful and diverse class of therapeutic, contributing to the treatment of infectious diseases, cancers and autoimmune diseases. As such, demands for such wide ranging products are high resulting in a high cost of manufacture as firms strive to produce the quantities of MAb required.

As outlined in **Chapter 1**, purification operations account for more than 40% of the overall cost of the production of such high value products. Due to its high selectivity and stability chromatography has become the pre-eminent separation technique for the large-scale purification of MAbs and accounts for the majority of the purification cost. Improving the economy and efficiency of chromatographic systems is therefore important in reducing total production costs. Cheaper and more productive manufacture allows firms the opportunity of fulfilling the wide-spread demand of therapeutic drugs at a lower cost to the consumer.

The particular focus of this thesis was the reduction in cost and increase in productivity of large scale chromatography systems through improved process design. Biotech companies currently have only limited tools available for the predictive design of chromatographic steps and the determination of the most suitable conditions of operation. In this work, a tool has been developed which tries to encompass the typical needs of both the technical and business perspectives of chromatographic manufacturing processes. A described in detail in **Chapter 2**, the design of large-scale chromatography is complex and multi-factorial. A variety of different tools and techniques have been described throughout this study, each

addressing a particular consideration in the design and operation of a chromatographic separation.

Chapter 3 explored the limits of large-scale chromatographic operation. An empirical methodology was described which allowed the prediction of the maximal flow rate possible through production scale columns from experimental data obtained from bench scale columns.

An equation of the form:

$$u_{crit}L_0 = \left(\left(4.76\times10^{-5}\right)\mu^{-0.83}u_{10\%} - \left(2.32\times10^{-8}\right)\mu^{-0.74}\right)\left(\frac{L_0}{D}\right) + \left(\left(4.22\times10^{-8}\right)\mu^{-0.91}e^{1304u_{10\%}}\right)$$

(Equation 3.11)

was found to predict successfully the variation in critical velocity (u_{crit}) of compressible agarose resins at scale. Here, (D) is the column diameter, (L_0) is the gravity settled bed height, (μ) is the mobile phase viscosity and ($u_{10\%}$) the resin rigidity.

Results showed the accuracy of the predictive capability, of the model developed, to be within ±17% of published data for production scale columns. Using such techniques could potentially save large quantities of expensive chromatographic resin and buffer and as well the developmental time that would be required if such tests were only conducted at manufacturing scale.

The empirical model developed in Chapter 3 was then extended in **Chapter 4** to investigate the impact of varying buffer type on the stability of chromatographic resins at large scale. Resin stability was shown to be strongly affected by buffer choice. Closer analysis showed that a variation in the size of the resin beads is dependent on the pH of the buffer employed for the test. Increasing the resin stability greatly reduced the tendency for bead swelling and contraction under different buffer conditions. However there was evidence that long term use of the resin under such

varying physicochemical conditions could cause losses in structural integrity which were not detectable by traditional testing procedures of peak analysis. Such findings emphasise the need for the validation of the mechanical stability of resins for the number of cycles of desired use.

Having investigated the limits of chromatographic operation, a verified mathematical model was described in **Chapter 5** to predict column performance in terms of its separation performance. To gain a realistic view of large scale column processing, scheduling considerations, resin degradation and lifetime, the fluctuations in binding capacity with flow rate and the cost consideration of the process were also implemented into this base model. Also incorporated was the empirical model developed in Chapter 3, which gives an indication of the compressive effects that occur at the large-scale, limiting flow rate.

Combining these techniques into a single consistent framework provides for a structured, fully integrated approach to designing large-scale high resolution systems. This can facilitate more informed decision making when evaluating manufacturing alternatives. The design, implementation and application of the framework was applied to a Protein A affinity capture step in the production of monoclonal antibodies based on cell culture in **Chapter 6**. Protein A chromatography was specifically selected for investigation given its sizeable impact on production as a whole, making its design and development key for successful processing. The combined effects of column size, resin type and membrane filtration area were investigated so as to identify the optimal configuration to adopt for a given process duty. Results are presented through the Windows of Operation technique with column performance quantified in terms of productivity and cost of goods per gram ($COG/g_{specific}$). Further design criteria and/or extra constraints can be easily added on. The method shows how the feasible area of operation is simulated and used to support key design decisions and to identify suitable trade-offs between operating strategies given the discrete nature of commercially available column sizes, yield losses associated with the addition of a concentrating step and the use of rigid high-throughput resins.

Results showed that productivity fluctuates with linear velocity for large diameter columns due to the under-utilisation of these large columns when they are not loaded to capacity. However, small diameter columns can suffer from over-utilisation which restricts their use due to scheduling constraints. It was shown that the minimum value of $COG/g_{specific}$ varies according to the velocity used for smaller columns. As resin volume start to dominate costs with the use of larger columns the effect of velocity on $COG/g_{specific}$ diminishes.

Bed length was shown to have a significant effect on the maximum flow allowable through the column. This in turn influences cycle times which effect column scheduling to fit DSP shift patterns. The results drawn through the use of the tool provide a valuable insight into the feasible process strategies which can be used.

Flexibility in the use of the modelling framework was demonstrated through modelling the effects of variation in the process flowsheet. This was exemplified with a case study involving the addition of a concentrating step prior to initial capture. The tool can be used to select design criteria for both the chromatography and concentrating effect and it was shown that reducing the batch volume to be processed provided for a design solution when the cost and productivity of the Protein A step alone were infeasible. Further to this, the model provided a suitable platform for investigating the use of the new generation of Protein A resins as another design alternative. It was shown that despite the greater expense of these resins, the gains in performance which could be attained through operation at higher flow velocities allowed intensive performance constraints to be met without the introduction of a pre-concentrating step into the process flowsheet.

It was shown that loading flow rate plays an important part, not only in the productivity of the process but also in its economy. Reducing loading flowrate reduces the required number of cycles to process a given batch, therefore decreasing buffer consumption and operation time. In some cases it is much more prudent to

operate at a lower flowrate to benefit from reduced manufacturing costs as productivity is not impacted too greatly.

Chapter 7 further extended the use of the integrated model outlined in Chapter 6 and showed how the model could be used to investigate the effects of a post-load washing section of the chromatographic cycle. Two different washing strategies were modelled, highlighting the flexibility of the framework in simulating different processing options. It was found that it would be necessary to under-utilise the column, through use of a safety factor, during the loading stage to ensure acceptable losses in expensive product.

Results indicated that a minimum specific COG/g can be attained when operating with a low safety factor and a low loading velocity. This is due to the reduction in the number of cycles required to process a batch of material as well as the high yields attained which are characteristic of operation with low safety factors.

Operation with high safety factors when loading at low velocity could increase COG/g despite the reduction in the overall number of cycles required for processing. This was due to the losses in yield associated with over utilisation of the stationary phase. Washing velocity was itself shown to have a significant effect on the process yield. A reduction in washing velocity was shown not to significantly reduce the productivity of the process but lead to a lower overall cost of production. The feature of such analysis was to show that loading and washing strategies must be considered simultaneously in order to optimise both productivity and cost; emphasising again the need for integrated chromatography design.

Chapter 8 demonstrated of the framework as a management tool where the model was used in resin selection. Two resins were evaluated: a compressible agarose based resin, MabSelect^{TM} and an incompressible controlled pore glass (CPG) based resin, Prosep vA Ultra®. These were chosen to reflect the most prominent groups of resins in industry. Results showed that whilst binding characteristics in

both resins were extremely similar, the operating strategies used for both resin varied significantly.

Despite the higher linear velocities with which Prosep could be operated, its attainable productivity was severely diminished given the long cleaning times required for the resin. Despite this, the productivities which could be attained were still higher than those with MabSelect™ under similar conditions. Cost proved to be the "Achilles heel" of the Prosep vA Ultra® as its per litre price was found to be almost twice that of MabSelect, making cost constraints difficult to satisfy. However, the operational envelope of the Prosep vA Ultra® given by its incompressible nature allows for greater operational flexibility with this resin than for MabSelect™.

The work within this thesis highlights the benefits of adopting an integrated approach when considering the process-business interface in large-scale chromatography for the manufacture of biopharmaceuticals. This has been realised through the design and application of a simulation tool. The tool can be used in the sizing and operation of a chromatographic step. It is envisaged that such a tool is useful for process management, resource utilisation, cost analysis and process efficiency assessments, all of which together bear on the examination of column size and operation for different process options. The developmental framework proposed aids in providing an understanding about how the chromatographic process has to be implemented at scale. The simulation results can then be used to build a consensus amongst decision-makers. Effective use of the simulation outcomes can lead to concentrated R&D efforts, more effective use of resources, faster time to market and improved overall economic performance which is of benefit to both the firm and the consumer.

11 CONSIDERATIONS FOR FURTHER WORK

11.1 Introduction

By its very nature research tends to raise as many questions as it answers. The following areas highlighted for further study represent those which are of direct relevance to chromatography design. There are three main areas where further work would be of benefit:

11.2 Addition of particulate fouling into the resin compression analysis.

Chapter 3 showed the impact on the critical velocity (u_{crit}) of a compressible resin with variation in the column geometry, resin rigidity and mobile phase viscosities. A further parameter that could be added to this study and incorporated into the model formulation is particulate fouling. Only a few investigations on the effect of fouling of packed bed chromatography columns have been reported in the literature (Levsion *et al.*, 1990; Staby *et al.*, 1998; Shephard *et al.*, 2000) which shows how binding capacity for the protein product can be reduced in the presence of contaminants in the feed material, and also how foulants can affect resin lifetime. However, there has been no quantification of the impact of fouling on the pressure-flow characteristics and critical velocity of a chromatographic system. Intuitively, one would expect a fouled stream to reduce u_{crit} whilst shifting the pressure-flow curve backwards. This can be attributed to particulates occupying inter-particle void volume restricting fluid flow and therefore increasing the pressure-drop inside the column. However, the extent of such an impact on critical velocity has yet to be quantified, nor has there been any measurements correlating the degree of fouling with u_{crit}.

Knowledge of such entities becomes important in manufacturing to ensure that the chromatographic step is able to continue processing with any variations in the feed stream. Such variation may be caused through the output of the clarification steps prior to initial capture. Additionally, knowledge of the trade-offs between additional processing effort to clean up a process stream and the benefits in terms of

performance of the subsequent chromatographic steps is key to achieving efficient bioprocess operation. Ideally one would aim to minimise the extent of feed pre-treatment prior to column-based separation without affecting chromatographic performance and column lifetime.

This type of fouling study provides an evaluation in terms of cleaning strategy. Pressure drop may be found not to vary significantly when processing a fouled feed during the initial cycle of operation on fresh resin. However, inefficient cleaning may cause a build up of fouled material during subsequent processing on the same resin.

11.3 Optimisation of washing velocity

Chapter 7 showed that reducing the post-load washing velocity relative to that of the load velocity allowed for improved yields when loading with a safety factor. This is because the second (lower) velocity enables re-binding of product which had become unbound in the wash onto stationary phase sites that were less accessible at the higher velocity. This causes a slight decrease in the outlet concentration of the protein as a greater proportion of the incoming protein now binds to the column. Traditional operation involves running the post-load wash stage at the maximum possible velocity that can be attained.

Optimisation may be performed to calculate the optimal post-loading wash velocity relative to the load velocity. To accomplish any optimisation in preparative chromatographic systems, one needs to consider four different factors: objective function, parameters, decision variables and constraints. For this case, an optimisation routine can be employed to maximise productivity (defined by Equation 5.24) with respect to three independent decision variables (i.e., the variables that are changed during optimisation), loading velocity, washing velocity and load volume/safety factor. At any point, the dynamic capacity will be a function of each of these variables and can be calculated through the modelling framework presented in Chapter 5. In addition, a weighted combination of cost and can be used as an objective function to address the conflicting demands of simultaneously high capacity through increases in column size (see Chapter 6) and productivity.

Constraints can define the region of the operating space in which the optimisation process can be carried out. The physical constraint that can be applied is the maximum value of operating velocity (assuming a compressible resin is used). In addition, load volume can be assumed to take place no later than at 1% breakthrough since further loading would be discontinued in most industrial processes.

11.4 Novel engineering of chromatography hardware

This thesis has been geared towards producing tools to enable rapid process development and improving approaches to chromatographic design and operation. Improved speed of design has been necessary given the exponential market demand of therapeutic products. Increased competition together with high throughput requirements in the manufacturing of these entities has made process economics and efficiency a key design constraint. Currently, chromatographic operations are limited by the maximum column size that can be feasibly employed. The largest practical column sizes have been limited to <2m in diameter due to scale up issues (wall support). As cell culture titre for antibodies increase (titres of ~10g/L are now being projected) and the production demands for even more products reach several hundred kilograms per year, downstream purification starts to become the rate-limiting step in the manufacturing process. Chromatography, for the time-being, remains the optimal purification technique open to the biopharmaceutical industry given that it is well understood, validatable and is easily installable into platform processes. To circumvent this problem therefore, new engineering design should be applied to this existing technology. Investigation can be directed at mitigating the column wall support phenomena, allowing for larger column with greater allowable velocities. Increasing the maximum allowable velocities through large diameter columns (>2m in diameter) permits their use in manufacturing. Feasible operation on large diameter columns also solves the capacity concerns which lead to process bottlenecks. Figure 11.1 shows a schematic of a potential new column design utilising structural 'spines' ('F' in Figure 11.1) inside the column, lending additional support to the column walls by effectively reducing its cross-sectional area. It is envisaged that such a structure will cause a reduction in the compressive force on the resin bed given the increase in support provided by the added wall support inside the column.

Implementation of this structure would necessitate a change in the design of the column adaptor also. This may take the form of a supplementary cap which may be fitted onto the end of the frit of an existing adaptor. This supplementary cap would be indented/segmented so as to allow the adaptor to rest on the top of the support spines if necessary. This will depend on how high the internal spines of the column will need to be as well as the packed bed height. Certainly, it is noted that an idea as to the packed bed height may be required before the height of the column spines can be estimated.

Flow distribution will also need to be investigated for this design to become viable. There will, for instance, be a disruption the traditional plug flow of the column whereby the initial plug will be split into smaller plugs as soon as flow reaches the support spines. Furthermore, increasing the number of column walls will increase the formation of eddies and therefore mixing that will occur close to the edges of the column walls will also increase. This is presumed to cause band broadening in the chromatographic resolution the extent to which is something to research. However, the application of such a large column which requires the use of such a design will typically be at the initial capture stage where yield is of primary concern and not that of column resolution. Certainly, the design poses many questions in terms of packing techniques, column aspect ratio, spine support height to bed height ratio, flow distribution and chromatographic resolution. However, if investigation shows that these issues are manageable then it may be advantageous to implement such a design given the gains in throughput and capacity that are possible.

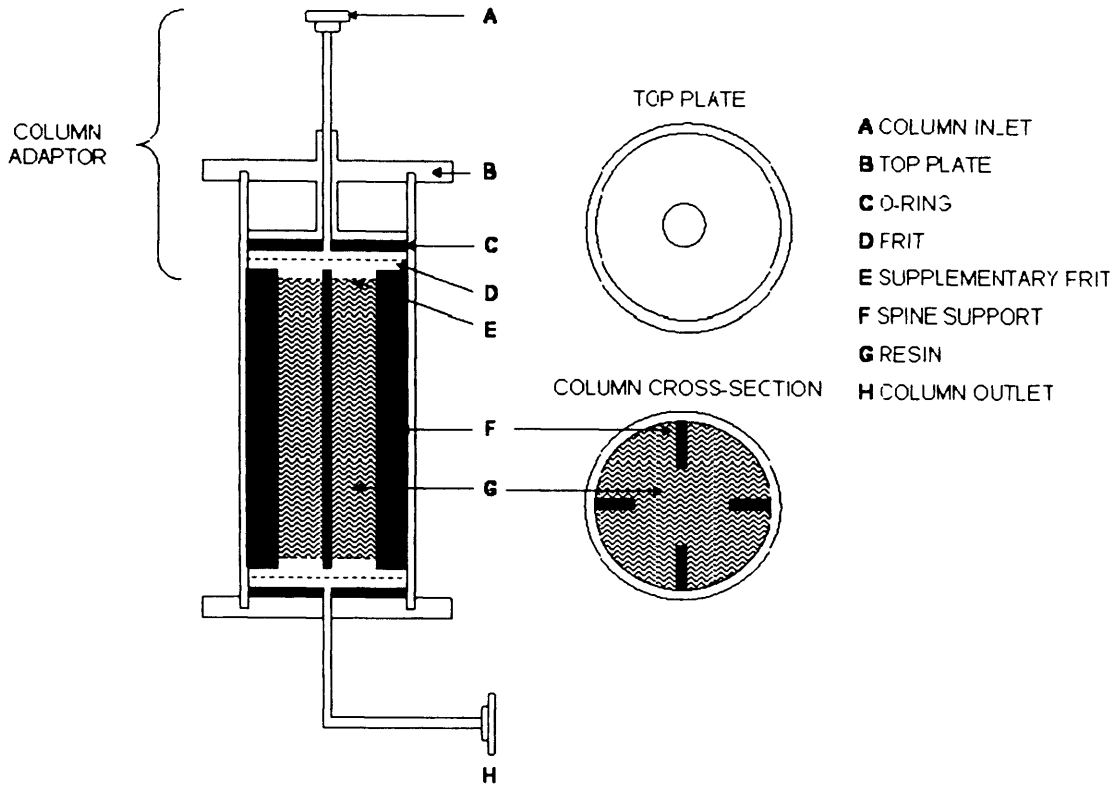

Figure 11.1 Schematic of an approach to the design of a chromatography column. Spine supports implemented inside the column provide added wall support allowing for greater column diameters to be realised.

12 APPENDICES

A. CALCULATION OF CHROMATOGRAPHIC EFFICIENCY

A.1 Quality testing packed beds.

The efficiency of a column depends on how well it is packed. A poorly packed column gives rise to uneven flow, resulting in zone broadening and reduced resolution. It is thus important to have a method by which the column can be tested before it is put into operation. It is also an advantage if the same method can be used to monitor column performance over its working life, so that it is easy to determine when the medium should be re-packed or replaced.

Pulsed-input height equivalent of a theoretical plate (HETP) testing is commonly used to measure column packing efficiency (Hoffman, 1998; Gondkar *et al.*, 2001; Moscariello *et al.*, 2001). These values were determined easily through the application of a 1M NaCl solution, to the column after packing. Before sample application, the column was equilibrated (>2 column volumes). Sample volume was approximately 1% of the total bed volume and was loaded at the operational loading flow velocity. Packing tests were run three times to ensure the values are stable.

A Gaussian HETP calculation using moment analysis was used to estimate plate height with the assumption that the solute response peak is a Gaussian distribution. The Gaussian HETP, $HETP_G$, was determined by:

$$HETP_G = \frac{L}{5.54 \cdot \left[\frac{V_{max}}{V_d - V_c}\right]^2} \qquad \textbf{(A. 1)}$$

where the response data on the chromatogram is volume-based (V) instead of time-based. On this basis, V_c and V_d are the values of V, at 50% of $(dC/dV)_{max}$, such that $V_d > V_c$. This calculation is commonly used to estimate HETP (Gondkar *et al.*, 2001; Hofmann, 1998). An increase in the HETP value corresponds to decreased efficiency of the chromatography column.

The asymmetry factor, *As*, was determined by:

$$As = \left(\frac{V_b - V_{max}}{V_{max} - V_a} \right) \qquad \textbf{(A. 2)}$$

where V_{max}, is the value of V corresponding to $(dC/dV)_{max}$ and V_b and V_a are the values of V at 10% of $(dC/dV)_{max}$, such that $V_b > V_a$. This calculation has been described previously (Hofmann, 1998). Decreasing asymmetry factor values are indicative of early transition breakthrough, which may be associated with an integrity breach. Increasing asymmetry factor values are indicative of tailing in the transition, which can be associated with mixing in the column's headspace. Increasing asymmetry values could also be associated with a major integrity failure in which the majority of flow passes through the channel; however, this has not been observed by the authors in practice. A perfectly symmetrical peak has an asymmetry value of 1.

Acceptable criteria were based on manufacturer's recommendations. The resins tested in Chapter 3 were procured from GE Healthcare Biosciences (Uppsala, Sweden). They recommended *As* values to be 0.8- 1.2 and $HETP_G$ values to be > 0.025 cm. Similar specifications were used when testing resins *X* and *Z* (Chapter 4). However, vendor specifications changed when the *ApA* ligand was attached. For resins, X_{ApA} and Z_{ApA} , As specifications remained in between 0.8-1.2 where $HETP_G$ values were recommended to be in the region of >0.04 cm. Resins used in packed beds studies in this thesis were packed to these individual specifications.

A.1.2 Quality testing during operation: Transition Analysis

Process monitoring and testing plays an essential role in the production of protein biologics. The complexity of protein chemistry can make it difficult to predict and evaluate the effects of process variations on product quality. Therefore, consistency in the protein manufacturing process becomes of critical importance. In the case of protein purification, monitoring the performance of liquid

chromatography columns is necessary to ensure the quality of final product (Larson *et al.*, 2003).

As protein production rates grow, it has become increasingly difficult to review chromatographic data in real time, as operations are occurring. More importantly, it can be difficult to visually detect subtle changes in chromatographic performance. These subtle changes can evolve into problems that affect the validated function of chromatographic operations. To address these difficulties, the use of transition analysis was investigated in Chapter 4 during the cycling studies. Transition analysis utilises process data to monitor the performance of packed bed columns. A chromatographic transition is the response at the outlet of a column to a step change at the column's inlet. For example, a column equilibrated with a low salt buffer and eluted with a high salt buffer will have a low-to-high transition, which can be measured by a conductivity meter at the column's outlet. Transition analysis utilises pH, conductivity, and optical density data from a column's outlet to assess the condition of the packed bed in the column. The data derived from transition analysis are quantitative and sensitive to subtle changes in performance.

In the cycling studies conducted in Chapter 4 the transition used was that of a step change in conductivity, where 1M NaCl was added to the pH 3 buffer as may be the case in a typical elution buffer. This analysis was used to evaluate if chromatographic efficiency decreased in column over times. Once again, HETP was used to estimate the efficiency of the column; however, in this case there was no pulse input. Given this, a non-Gaussian HETP was estimated. This being a more accurate measurement than $HETP_G$ as it does not make the assumption that the peak derivative of the step response curve is in Gaussian shape.

The non-Gaussian HETP, $HETP_N$, is given by:

$$HETP_N = \frac{L \cdot \sigma^2}{\left(\frac{M_1}{M_0}\right)^2} \qquad \textbf{(A. 3)}$$

where L is the column length, σ^2 is the variance, M_1 is the first moment, and M_0 is the zeroth moment (McCoy and Goto, 1994). All three of these quantities are derived from the frequency distribution of the solute signal. The variance can be expressed in terms of the distribution's moments:

$$\sigma^2 = \frac{M_2}{M_0} - \left(\frac{M_1}{M_0}\right)^2 \qquad \textbf{(A. 4)}$$

where M_2 is the second moment of the frequency distribution (McCoy and Goto, 1994). The equations for the moments of order k that result from a step, not pulse, change at the column inlet are defined as:

$$M_K = \int t^k \frac{dF(t)}{dt} dt \qquad \textbf{(A. 5)}$$

where t is time and $F(t)$ is the solute step response at the outlet of the column (Garcia *et al.*, Pires, 1993). As with the other calculations, the data is volume-based (V) instead of time-based. The symbol C refers to the normalised solute signal data array which occurs as a result of the step change. Practically speaking, C may represent, UV, conductivity, pH or any measurement that can record the change that occurs on a step input. Therefore, the moment equations become:

$$M_K = \int V^k \frac{dC}{dV} dV \qquad \textbf{(A. 6)}$$

The non-Gaussian HETP is determined by calculating the zeroth, first, and second moments using Equation (A1.6), calculating the variance using Equation (A1.4), and then calculating $HETP_N$ using Equation (A1.3). As with the cumulative error calculation, the integrals were estimated using a trapezoidal approximation. This method of calculating HETP takes into account the entire solute response curve, without making any assumptions about the distribution of the curve. It is referred to as the non-Gaussian method because it does not make the traditional assumption that the solute response is a Gaussian distribution. This more common method, denoted Gaussian HETP, is described later in this section. An increase in the HETP, or height equivalent of a theoretical plate, value corresponds to decreased efficiency of the chromatography column (Moscariello *et al.*, 2001).

B. THEORETICAL FITTINGS TO EXPERIMENTAL DATA

B.1 Variation in viscosity with product titre

Measurements to determine the change in viscosity with titre for varying degrees of pre-concentration as described in Chapter 5 and applied in Chapter 6 were extrapolated from experimental data reported by Pradipasena *et al.*, (1977) and is shown below.

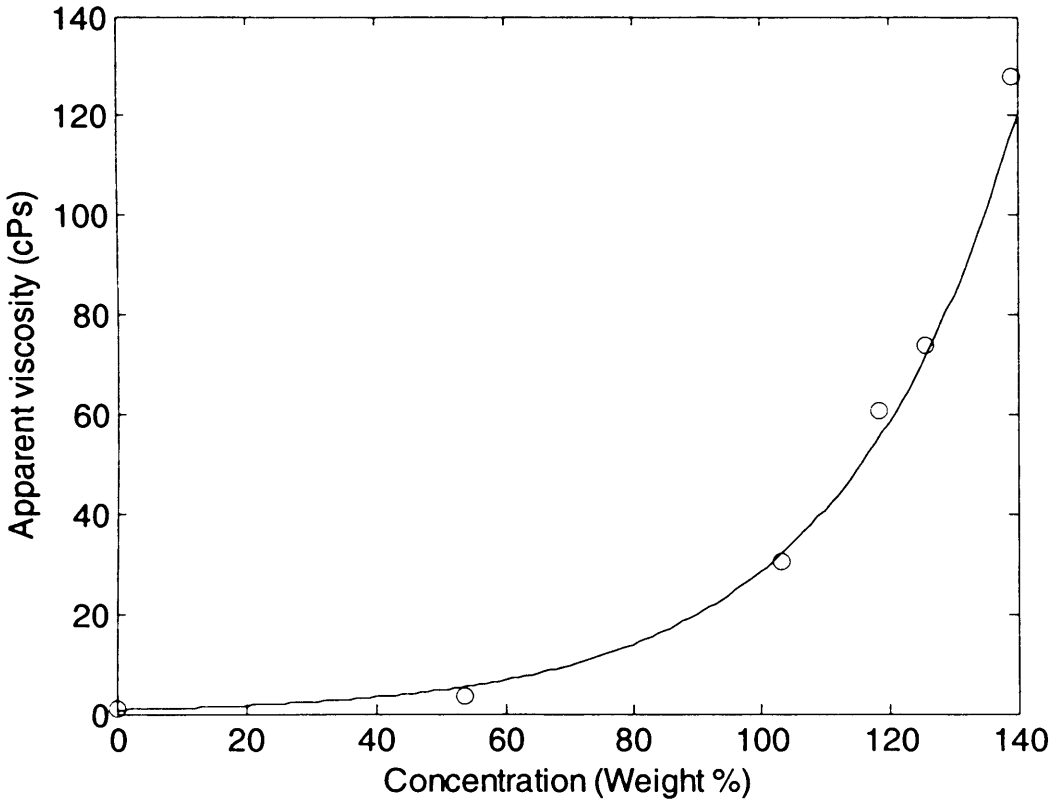

Figure B. 1 Effect of concentration on apparent viscosity of globular protein solutions (adapted from Pradipasena *et al.*, 1977). Data points refer to experimental data. Solid line refers to model fit. Linear regression coefficient found was 0.98.

The fitted model correlation was found to be:

$$Viscosity = 0.776^{0.036(Concentration)} \qquad \textbf{(B. 1)}$$

B.2 Calibration of the general rate model

Calibration of the general rate model to simulate binding onto various Protein A resins was performed through the use of a nonlinear unconstrained optimisation routine FMINSEARCH in the MATLAB programming environment (The Mathworks Inc., Natick, MA, USA, 2004). Experimental data for adsorption isotherms and some mass transfer parameters (Tables 5.2-5.4) were inputted into the model. The remaining model parameters necessary to use the correlations outlined in Table 5.1 were fitted through the optimisation routine described above. The model was fitted/calibrated to experimental binding capacity vs. loading velocity curves found from literature and vendor handbooks/websites. Figure B.2 shows the process flowchart used for estimating the unknown model parameters. All the trapeziums and boxes are labeled numerically, while the decision blocks (diamond-shaped figures) are labeled using Roman numerals. The procedure is as follows:

Trapezium 1: Compile the experimental chromatographic data of the process (in this work, from literature sources).

Trapezium 2: Program the model of the process in the chosen modelling software (in this work, MatLab is used).

Box 3: Set the bounds for the parameters to be estimated. The parameters are estimated within the range imposed by the bounds.

Box 4: Initialise the values of the estimated parameters. During all the test runs, the parameter estimation will use these values as initial guesses.

Box 5: Carry out the parameter estimation (in this work,Matlab function FMINSEARCH is used).

Decision i: Determine if the model prediction fits the shape of the experimental data (in this work, binding capacity vs. flowrate curves) given in Trapezium 1. If it does, proceed to the next step; otherwise return to Box 4 and change the values for initialisation.

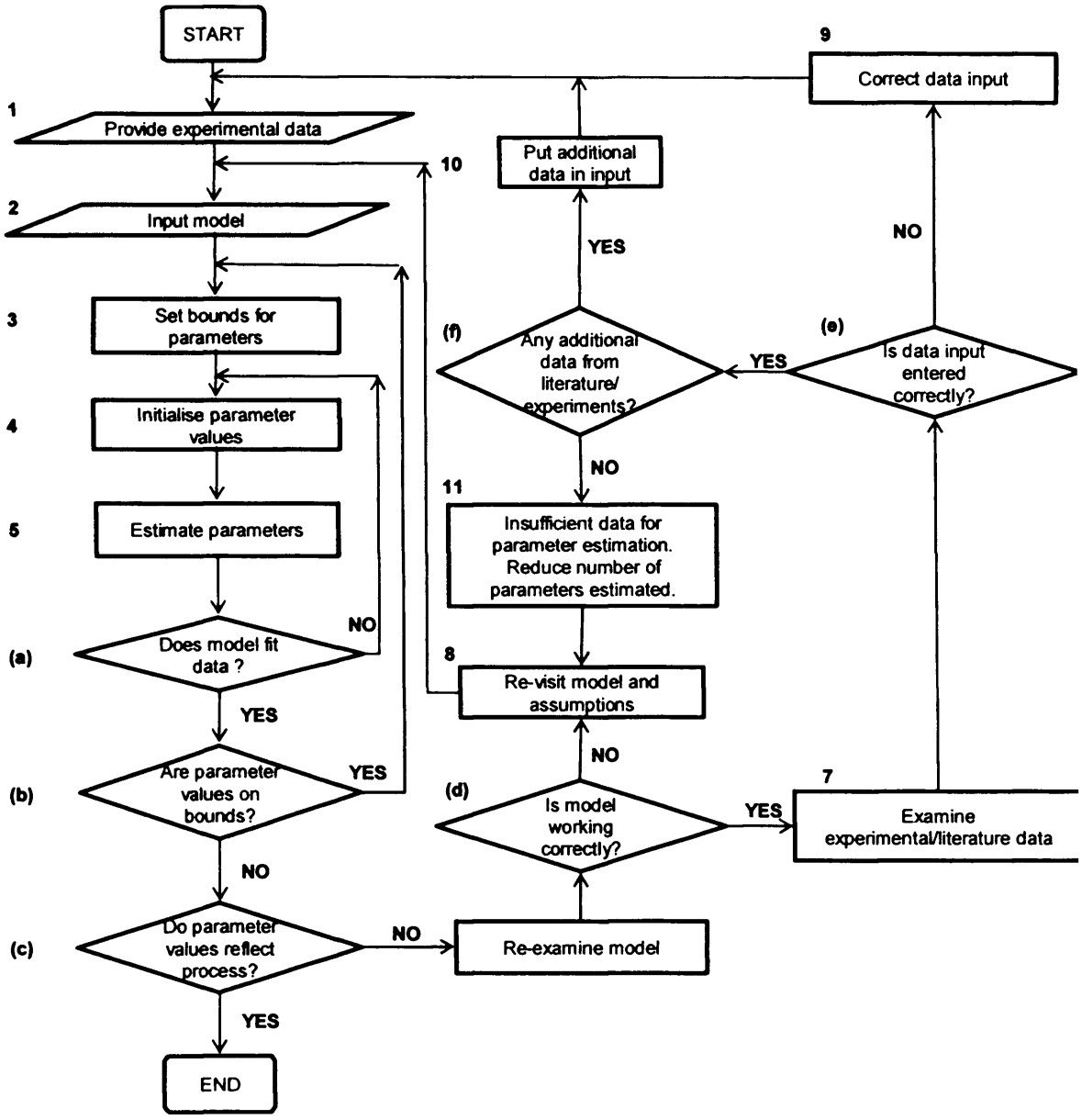

Figure B. 2 Process flowchart for model parameter estimation.

Decision ii: Check that the estimated parameter values do not lie on the bounds set in Box 3. If they do, return to Box 3 to increase the bounds; if not proceed to the next step. (If values lie on the bound, it may mean the parameter estimation has been constrained by the bounds on that parameter.)

Decision iii: Check that the estimated parameter values obtained reflect the process accurately based on previous knowledge of the process. With the limited data provided for parameter estimation, the estimated parameters may not reflect certain aspects of the behavior correctly, e.g. the elution order or band width. If it does reflect the actual process, then the parameter estimation comes to an end. However, if it does not, then proceed to Box 6.

Box 6: Examine the model equations to determine why there is a discrepancy between the model prediction and the experimental data.

Decision iv: If the model is working correctly but the discrepancy is still present, proceed to Box 7. If it is determined not to be working correctly, then proceed to Box 8.

Box 7: Examine that the experimental data used in the estimation is correctly entered and proceed to Decision v.

Box 8: Revisit the model and the modeling assumptions. Return to Trapezium 2.

Decision v: If the experimental data input has been entered wrongly for the parameter estimation, proceed to Box 9. If the experimental data given is correct, proceed to Decision vi.

Box 9: Correct the experimental data input and return to Trapezium 1.

Decision vi: Determine if there is any additional data available on the experiment. If there is additional data, proceed to Box 10. If there is no additional data on the experiment, proceed to Box 11.

Box 10: Add the additional experimental data to the input data and return to Trapezium 1.

Box 11: There is probably insufficient data for accurate parameter estimation. Since there is no additional data to be gathered, reduce the number of parameters to be estimated by making additional simplifying assumptions, e.g. by fixing some of the parameters. This entails returning to Box 8 and revisiting the model.

The procedure ends successfully when the parameters estimated reflect the process at Decision iii to a predetermined level of tolerance, or unsuccessfully if there is insufficient data for parameter estimation. The figures below present the experimental data found together with the calibrated model outputs.

Linear fits of the form of Equation (5.20) were used when modelling the rate of degradation found caused by harsh clean-in-place (CIP) protocols. In these cases, the Q_{max} of the adsorption isotherm for each resin was decreased by a certain quantity (given through Equation 5.20) after every cycle of operation. This reduction in static capacity was assumed to simulate the inactivation of Protein A ligands caused by the harsh conditions.

B.2.1 Parameter fits for rProtein A Sepharose FF™

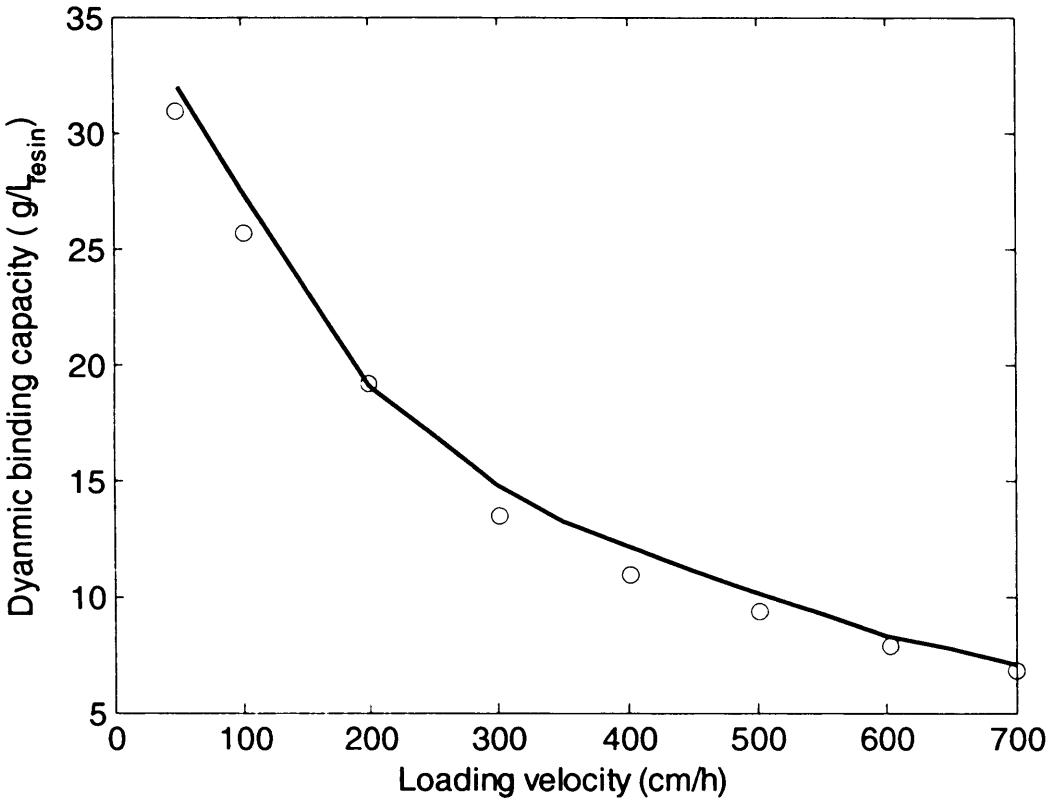

Figure B. 3 Dynamic binding capacity vs. loading velocity. Experimental data (data points) taken from Hahn *et al.*, 2003 and derived at 2.5 % breakthrough using a bed height of 10cm. Modelled fits (solid line) were found to have a regression coefficient of 0.971. Parameter values found in attaining these fits are displayed in Table 5.2.

B.2.2 Parameter fits for MabSelect™

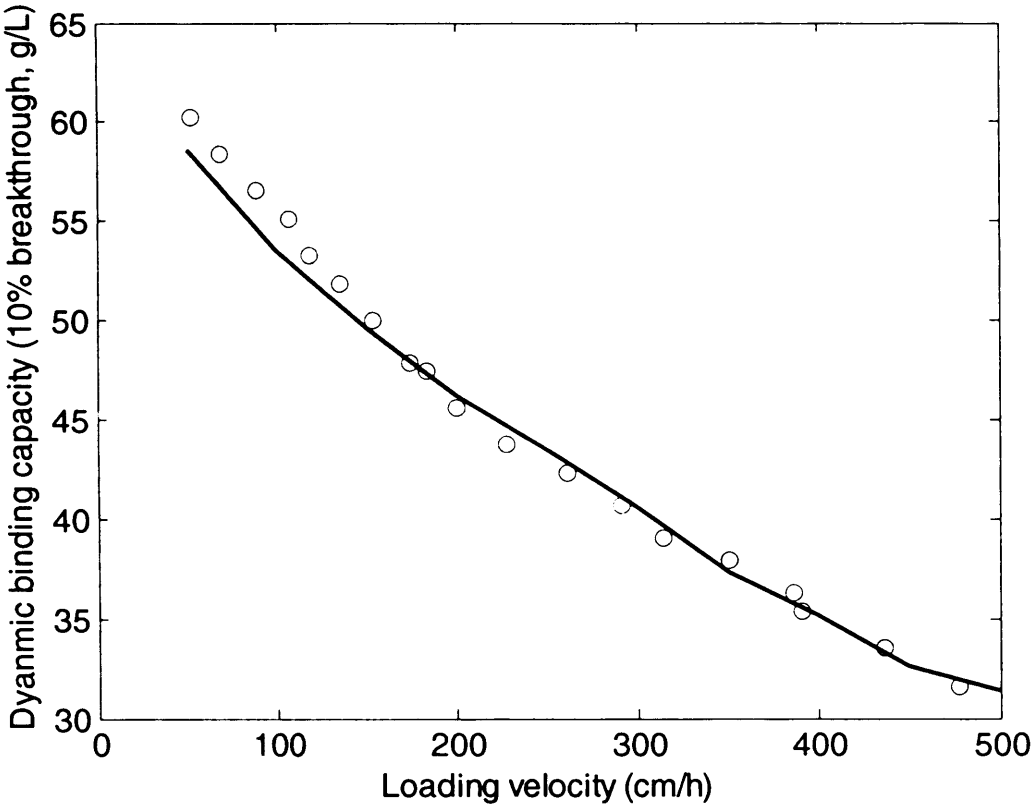

Figure B. 4 Dynamic binding capacity vs. flowrate. Experimental data (data points) taken from www.gelifesciences.com, MabSelect™ product data file and derived at 10% breakthrough using a bed height of 20cm. Modelled fits (solid line) were found to have a regression coefficient of 0.985. Parameter values found in attaining these fits are displayed in Table 5.3.

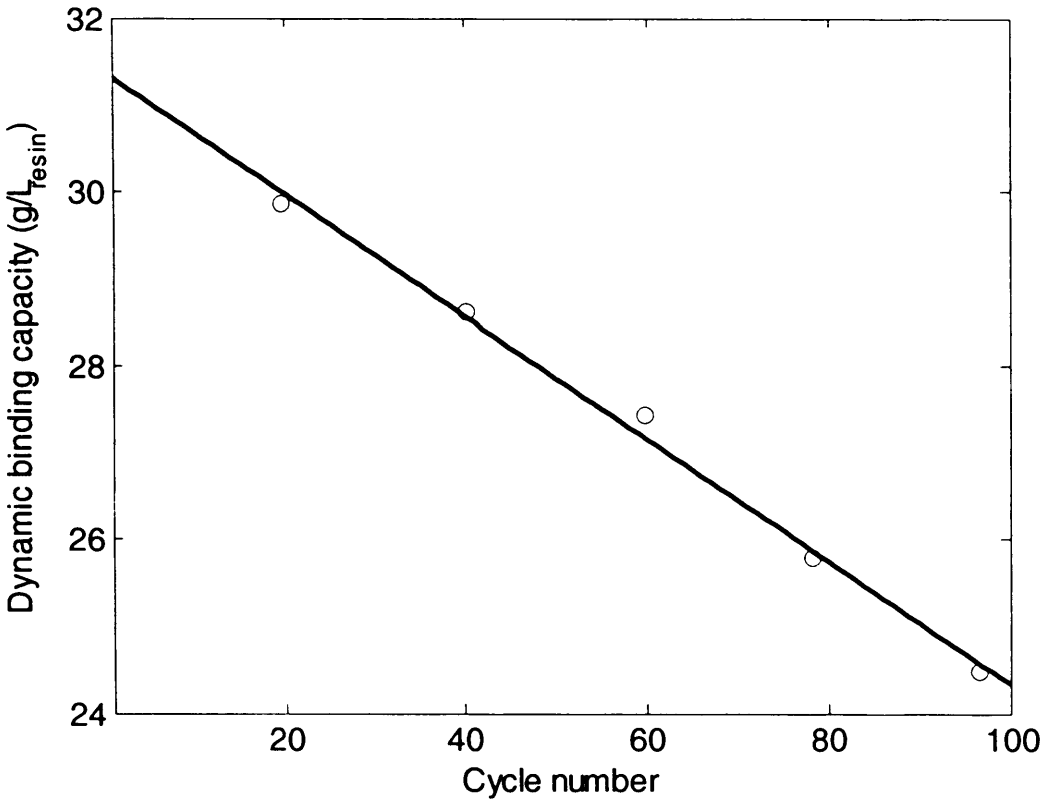

Figure B. 5 Decrease in dynamic binding capacity on resin re-use when using a cleaning-in-place (CIP) protocol consisting of 250mM NaOH + 1M NaCl. Contact time was 15 minutes. Binding capacity was measured at 10% breakthrough using a linear loading velocity of 336 cm/h. Packed bed height was 10 cm and product titre was 2.5 g/L. Experimental data (data points) was taken from Johansson *et al.* (2002). Model fit (given by Equation (5.20), solid line) had a regression coefficient of 0.99. After 100 cycles of operation dynamic binding capacity decreased by 18%.

B.2.3 Parameter fits for Prosep vA Ultra®

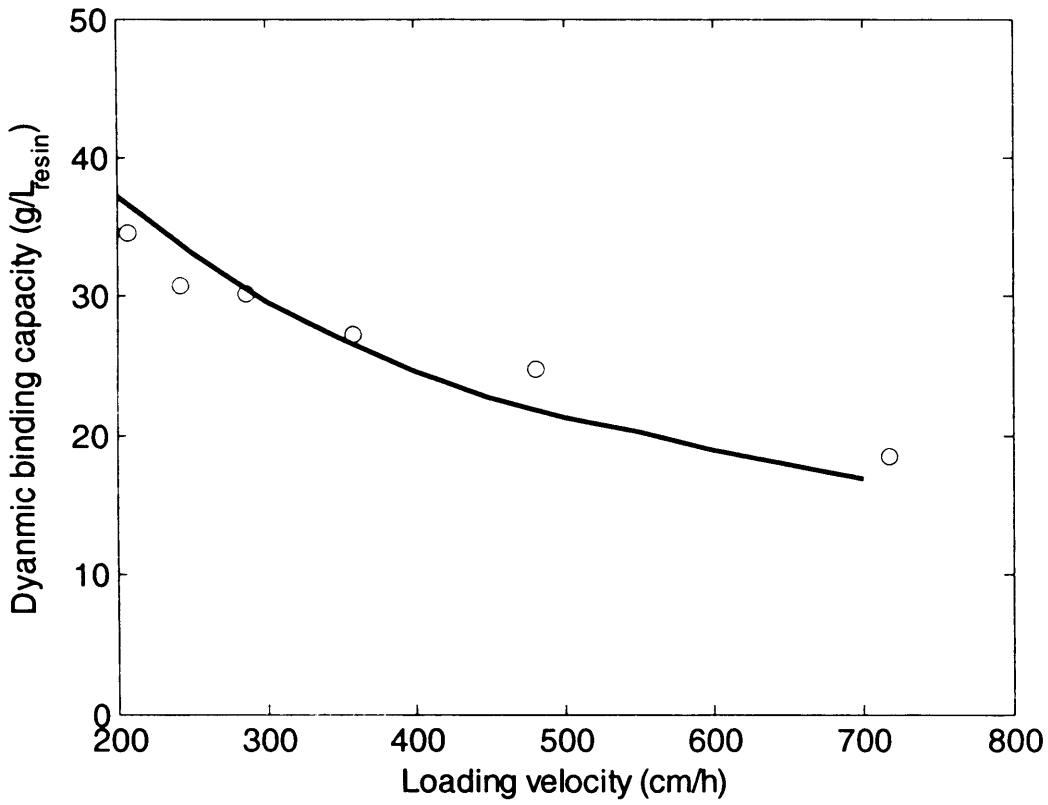

Figure B. 6 Dynamic binding capacity vs. flowrate. Experimental data (data points) taken from Hahn *et al.* (2005), Prosep vA Ultra® product data file and derived at 10% breakthrough using a bed height of 10cm. Modelled fits (solid line) were found to have a regression coefficient of 0.94. Parameter values found in attaining these fits are displayed in Table 5.4.

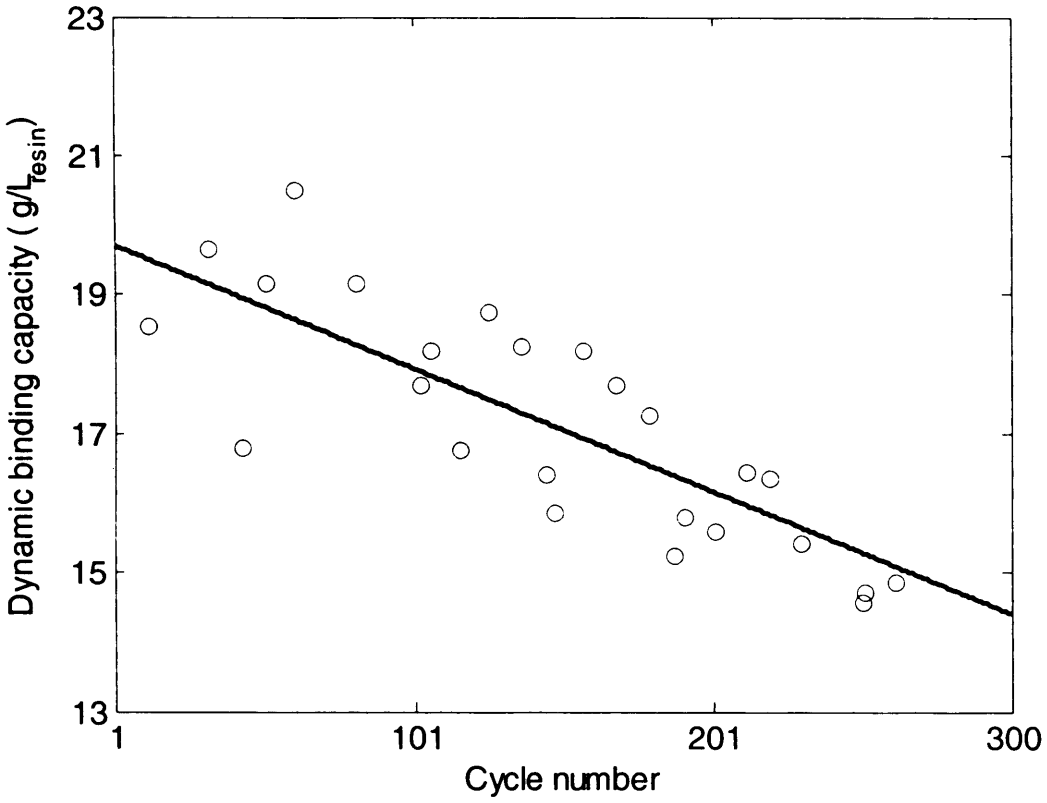

Figure B. 7 Decrease in dynamic binding capacity on resin re-use when using a cleaning-in-place (CIP) protocol consisting of 0.1M H_3 PO_4, contact time was 15 minutes and 6M guanidine, contact time 60 minutes. Binding capacity was measured at 10% breakthrough using a linear loading velocity of 350 cm/h. Packed bed height was 5 cm and product titre was assumed to be 1 g/L. Experimental data (data points) was taken from Lute *et al.* (2005). Model fit (given by Equation (5.20), solid line) had a regression coefficient of 0.8.

C. PUBLICATIONS ARISING FROM THIS RESEARCH

Joseph, J; Zhou, Y; Lacki, K; Titchener-Hooker, N.J. (2007) A Framework to Assess the Impact of Operating Strategy on Initial Capture Chromatography during Large-Scale Manufacture. AIChE J (submitted for review).

Tran, R; Joseph, J; Bracewell, DG; Zhou, Y; Titchener-Hooker, N.J. (2007) A Framework for the Prediction of Scale-Up When Using Compressible Chromatographic Packings. *Biotechnology Progress,* 23 (2), 413-422 .

Joseph, J. R., Sinclair, A., Zhou, Y. and Titchener-Hooker, N. J. (2006). A structured tool to assess the impact of initial capture steps in the production of monoclonal antibodies, presented (poster) at *Recovery of Biological Products* 12, Phoenix, Arizona, USA, 2-7 April.

Joseph, J., Sinclair, A., Titchener-Hooker, N.J., Zhou, Y. (2006). A framework for assessing the solutions in chromatographic process design and operation for large-scale manufacture, *Journal of Chemical Technological Biotechnology,* 81, 1009-1020.

Tran, R; Joseph, J; Bracewell, DG; Zhou, Y; Titchener-Hooker, NJ. A Generic Framework for the Prediction of Scale-Up when Using Compressible Chromatographic Packings. *12th European Congress on Biotechnology*, Copenhagen, Denmark, Presented (poster) on 22nd August 2005.

Joseph, J; Sinclair, A; Titchener-Hooker, NJ; Zhou, Y. A tool for combining the business and process aspects in the design of chromatographic steps.*10th World Congress of Chemical Engineering*, Glasgow, Scotland, presented (oral + poster) on 11th July 2005.

Joseph, J; Sinclair, A; Titchener-Hooker, NJ; Zhou, Y. A Decision-Support Tool for the Specification of a Chromatographic Step. *BIA Bioprocess UK Annual Forum*, Newcastle, UK, presented (poster) on 24th November 2004.

13 REFERENCES

Aguilera Soriano, G., Titchener-Hooker, N.J. and Ayazi Shamlou, P. (1997) The effects of processing scale on the pressure drop of compressible gel supports in liquid chromatographic columns. Bioprocess Engineering.17: 115-119.

Aldridge, S. (2006) Downstream processing needs a boost. Genetic Engineering and Biotechnology News. 26, 1. January.

Andrews, B.A., Nielsen, S. and Asenjo, J.A. (1996) Partitioning and purification of monoclonal antibodies in aqueous two-phase systems. Bioseparation 6: 303.

Arnold, F.H., Blanch, H.W. and Wilke, C.R. (1985) Analysis of affinity separations. I: Predicting the performance of affinity adsorbers. Chemical Engineering Journal. 30, 2: B9-B23.

Arshady, R. (1990) Development of new hydrophilic polymer supports based on dimethylacrylamide. Colloid and Polymer Science.268: 948.

Arshady. R. (1991) Beaded polymer supports and gels II: Physicochemical criteria and functionalization. Journal of Chromatography. 586: 199-219.

Arve, B.H. and Liapis, A.I. (1987) Modelling and analysis of biospecific adsorption in a finite bath. American Institute of Chemical Engineering Journal. 33,2: 179-193.

Baines, D., Burton, M., Pearson, J., Burton, S. and Curling, J. (2001) Synthetic ligand affinity adsorbents for highly selective purification of human plasma proteins. Presented at Recovery of Biological Products X, Mexico, USA, June 3-8.

Becker, T., Ogez, J. R. and Builder, S. E. (1983) Downstream processing of proteins. Biotechnology Advances. 1: 247-261.

Belfort, G., Davis, R.H. and Zydney, A.L. (1994) The behaviour of suspensions and macromolecular solutions in cross-flow microfiltration. Journal of Membrane Science. 96: 1-58.

Biblia, T.A. and Robinson, D.R. (1995) In Pursuit of the Optimal Fed-Batch Process for Monoclonal Antibody Production. Biotechnology Progress. 11:1-13.

Birch, J.R. (2005) The importance of developing a high yield of product. Presented at European Antibody Congress, Harrowgate, UK, June 5–9.

Birch, J.R., Bonnerjea, J., Flatman, S. and Vranch, S. (1995) Production of monoclonal antibodies. Monoclonal antibodies: Principles and application, Wiley-Liss, Inc.: New York, USA, pp231-265.

Bird, R.B., Stewart, W.E. and Lightfoot, E.N. (1960) Transport phenomena, Wiley (Pub) New York, USA, pp.193-194.

Blank, G. (2005) The future of process development for monoclonal antibody manufacturing. Presented at IBC Conference on antibody production and downstream processing, San Diego, California, USA, March.

Blank, G.S., Zapata, G., Fahrner, R.L., Milton, M., Yedinak, C., Knudsen, H. And Schmelzer, C. (2001) Expanded bed adsorption in the purification of monoclonal antibodies: A comparison of process alternatives. Bioseperation. 10: 65-71.

Blank, G.S. (1997) Protein purification by Protein A chromatography. U.S. Patent 6,127,526.

Blatt, W.F., Dravid, A., Michael, A.S. and Nelsen, L. (1970) Solute polarization and cake formation in membrane ultrafiltration causes consequences and control techniques. In: Flinn, F.E. (Ed.), Membrane Science and Technology. Plenum, New York, pp. 47-97.

Boschetti, E. (1994) Advanced sorbents for preparative affinity chromatography. Journal of Chromatography A. 658:207-236.

Boschetti, E., Judd, D., Schwartz, W. and Tunon, P. (2000) Hydrophobic charge induction chromatography. Genetic Engineering News. 20, 13: 1-4.

Boschetti, E. (2002) Antibody separation by HCIC. Trends in Biotechnology. 20, 8: 333-337.

Breece, T.N., Fahrner, R.L., Gorrell, J.R., Lazzarechi, K.P., Lester, P.M. and Peng, D. (2005) Protein Purification. U.S. Patent WO 6,870,034.

Brough, A.V.J., Epton, R., Marr, G., Shackleu, A.T. and Sniezko-Blocki, A.G. (1978) Chromatography of synthetic and biological macromolecules, Vol 1, Ellis Horwood, Chichester, pp 70-90.

Brown, M.E., Renner G., Field R.P. and Hassell T. (1992) Process development for the production of recombinant antibodies using the glutamine synthetase (GS) system. Cytotechnology. 9: 231–236.

Burgoyne, R.F., Priest, M.C., Roche, K.L. and Vella, G. (1993) Systematic development and validation of sanitization protocols for a chromatographic system designed for biotherapeutics purification. Journal of Pharmaceutical and Biomedical Analysis. 11:1317-1325.

Burton, D.R. (1985) Immunoglobulin G: Functional sites. Molecular Immunology. 22: 161-206.

Burton, S.C. and Harding, D.R.K. (1998) Hydrophobic charge induction chromatography: salt independent protein adsorption and facile elution with aqueous buffers. Journal of Chromatography A. 814: 71-81.

Cabatingan, M. (2005) Impact of virus stock quality on virus filter validation: A case study. Reprinted with permission from BioProcess International 3(10) 39-43, November.

Chadd, H.E. and Chamow S.M. (2001) Production of chimeric antibodies by transgenic chicken bioreactors. Current Opinion in Biotechnology. 12: 188-194.

Chase, H.A. (1994) Purification of proteins by adsorption chromatography in expanded beds. Trends in Biotechnology. 12, 8:296-303.

Chase, H.A. (1984) Prediction of the performance of preparative affinity chromatography. Journal of Chromatography. 297: 179-202.

Colby, C.B., O'Neill, B.K. and Middelberg, A.P.J. (1996) A modified version of the volume averaged continuum theory to predict pressure-drop across compressible packed beds of Sepharose big beads SP. Biotechnology Progress. 12: 92-99.

Cowan, G.H., Gosling, I.S. and Sweetenham, W.P. (1989) Modelling methods to aid the design and optimisation of batch stirred-tank and packed –bed column adsorption and chromatography units. Journal of Chromatography A. 484:187-210.

Curling, J. (2004) Affinity chromatography: from textile dyes to synthetic ligands by design. Part 2. Biopharm international. August, 60-65.

Curling, J. (2001) Biospecific affinity chromatography: intelligent combinatorial chemistry. Genetic Engineering News. 21, 20: 1-3.

Danckwerts, P.V. (1953) Continuous flow systems, Chemical Engineering Science. 2: 1-13.

Danilov, A.V., Vagenina, I.V., Mustaeva, L.G., Moshnikov, S.A., Gobunova, E.Y.,

Cherskii, V.V. and Baru, M.B. (1997) Liquid chromatography on soft packing material, under axial compression; Size exclusion chromatography of polypeptides. Journal of Chromatography A. 773: 103-114.

De Koning, H.W.M., Chamuleau, R.A.F.M. and Bantjes, A. (1984) Cross-linked agarose encapsulated sorbents resistant to steam sterilisation – preparation and mechanical properties. Journal of Biomedical Materials Research , 18, 1-13.

De Palma, A. (2002) Protein products push large-scale cell culture. Genetic Engineering News. 22, 7: 58, 61.

DeVault, D., (1943) The Theory of Chromatography, Journal of the American Chemical Society. 65: 532.

Diesenhoder, J. (1981) Crystallographic refinement and atomic models of a human Fc fragment and its complex with fragment B of Protein A from staphylococcus aureus at 2.9 and 2.8A resolution. Biochemistry. 20, 9: 2361-2370.

Duel, M.W. (2002) Improved process economics for MAb purification using Fractoprep® and MAbsorbent. Presented at IBC's 3rd International Conference on Recovery and Purification, San Diego, California, USA, November.

Dünnebier, G., Fricke, J. and Klatt, K. (2000) Optimal design and operation of simulated moving bed chromatographic reactors. Industrial and Engineering Chemical Research. 39 ,7: 2290 -2304.

Eklund, M., Axelsson, L., Uhlen, M. and Nygren, P.A. (2002) Anti-idiotypic protein domains selected from Protein A-based affibody libraries. Proteins: Structure Function and Genetics. 48: 454.

Fahrner, R.L., Knudsen, H. L., Basey, C.D., Galan, W., Feuerhelm, D., Vanderlaan, M. and Blank, G. Industrial purification of Pharmaceutical Antibodies: Development,

Operation, and Validation of Chromatography Processes (2001). Biotechnology and Genetic Engineering Reviews.18: 301 – 327.

Fahrner, R.L., Iyer, H.V., Blank, G.S. (1999a) The optimal flow rate and column length for the maximum production rate of Protein A affinity chromatography. Bioprocess Engineering. 21:287-292.

Fahrner, R.L., Whitney, D.H., Vanderlaan, M. and Blank, G.S. (1999b) Performance comparison of Protein A affinity chromatography sorbents for purifying recombinant monoclonal antibodies. Journal of Biotechnology and applied Biochemistry. 30: 121-128.

Fahrner, R.L., Blank, G. And Zapata, G. (1999c) Expanded bed Protein A affinity chromatography of a human monoclonal antibody: Process development, operation and comparison with a packed bed method. Journal of Biotechnology. 75: 273-280.

Fahrner, R.L. and Blank, G.S. (1999d) Real-time monitoring of recombinant antibody breakthrough during Protein A affinity chromatography. Journal of Biotechnology and Applied Biochemistry. 29:109-112.

Fahrner, R.L., Whitney, D.H., Vanderlaan and M; Blank, G.S. (1998) Performance comparison of Protein A affinity-chromatography sorbents for purifying recombinant monoclonal antibodies. Journal of Biotechnology and Applied Biochemistry. 30:121-128.

Farid, S.S. (2006) Process economics of industrial monoclonal antibody manufacture. Journal of Chromatography B., 848, 1, 8-18.

Farid, S.S. (2001) A decision-support tool for simulating the process and business perspectives of biopharmaceutical manufacture. PhD Thesis. University College London, UK.

Fassina, G., Ruvo, M., Palombo, G., Verdoliva, A. and Marino, M. (2001) Novel ligands for the affinity chromatography antibodies. Journal of Biochemical and Biophysical Methods. 49, 481-490.

Fassina, G., Verdoliva, A., Palombo, G., Ruvo, M. And Cassani, G. (1998) Immunoglobulin specificity of TG19318: a novel synthetic ligand for antibody affinity purification. Journal of molecular recognition. 11: 128-133.

Fassina, G., Verdoliva, A., Odierna, M.R., Ruvo, M. and Cassani, G. (1996) Protein A mimetic peptide ligand for affinity purification of antibodies. Journal of Molecular Recognition. 9: 564-569.

Felinger, A. and Guiochon, G. (1998) Comparing the optimum performance of the different modes of preparative liquid chromatography. Journal of Chromatography A 796, 1: 59-74.

Felinger, A. and Guiochon, G. (1996) Multicomponent interferences in overloaded gradient elution chromatography. Journal of Chromatography A 1996, 724, 1-2: 27-37.

Felinger, A. and Guiochon, G. (1994) Optimizing experimental conditions for the minimum production cost in preparative chromatography. American Institute of Chemical Engineering Journal. 40:594-605.

Ferreira, G.M., Dembecki, J. Patel, K., Arunakumari, A. (2007) Chromatography: A two-column process to purify antibodies without Protein A. BioPharm International, May 1.

Ferris, K.F., Risser, S.M., Wagner-Brown, K.B., Kiel, J.L. and Albanese, R.A.(1999) Effects of conformational diversity and structural dynamics on the optical properties of diazoluminmelanin. Presented at The Materials Research Society Meeting, Boston, Massachusetts, USA, Nov 29–Dec 3.

Follman, D. and Fahrner, R.L. (2004) Factorial screening of antibody processes using three consecutive steps without Protein A. Journal of Chromatography A. 1024: 79-85.

Gagnon, P. (1996) Protein A affinity chromatography Purification tools for monoclonal antibodies, Validated Biosystems Inc., Tuscon, Arizona, USA, pp. 155-158.

Geisow, M .J. (1992) Pore for thought in bioseparations and bioassay matrices. Trends in Biotechnology. 10: 373-375.

Ghose, S. (2005) Purification of monoclonal antibodies and Fc-fusion proteins – Protein A and beyond. PhD Thesis. Rensselaer Polytechnic Institute, USA.

Ghose, S., Nagrath, D., Hubbard, B., Brooks, C. and Cramer, S., (2004) Use and optimisation of a dual-flowrate loading strategy to maximise throughput in Protein-A affinity chromatography. Biotechnology Progress 20:830-840.

Ghose, S., Hubbard, B. and Cramer, S. (2006) Evaluation and comparison of alternatives to Protein A chromatography mimetic and hydrophobic Charge Induction chromatographic stationary phases, Journal of Chromatography A. 1122, 1:144-152.

Golshan-Shirazi, S. and Guiochon, G. (1992) Comparison of various kinetic models of non-linear chromatography. Journal of Chromatography. 603: 1-1 1.

Gottschlich, N. and Kasche, V. (1997) Purification of monoclonal antibodies by simulated moving bed chromatography. Journal of Chromatography A. 765: 201-206.

Gu, T., Hsu, K. and Syu, M. (2003) Scale up of affinity chromatography for purification of enzymes and other proteins. Enzyme and Microbial Technology. 33: 430-437.

Gu, T. (1995) Mathematical modelling and scale up of liquid chromatography. Springer Press, Berlin, Germany.

Guerrier, L., Girot, P., Schwartz, W. and Boschetti, E. (2000) New method for the selective capture of antibodies under physiological conditions. Bioseparation. 9: 211-221.

Guiochon, G. and Lin, B. (2003) Modelling of preparative chromatography, Elsevier, Amsterdam, Netherlands.

Gura, T. (2002) Therapeutic antibodies: Magic bullets hit the target. Nature Biotechnology. 417: 584-586.

Hahn, R., Schlegel, R. and Jungbauer, A. (2003) Comparison of Protein A affinity sorbents. Journal of Chromatography A, 790: 35-51.

Hahn, R., Bauerhansl, P., Shimahara, K., Wizniewski, C., Tscheliessnig, A. and Jungbauer, A. (2005) Comparison of Protein A Sorbents II. Journal of Chromatography A. 1093:98-110.

Hahn, R, Bauerhansl, P., Shimahara, K., Wizniewski, C., Tscheliessnig, A. and Jungbauer, A. (2006) Comparison of Protein A sorbents III: Lifetime study. Journal of Chromatography A. 1102 :224-31.

Hale, G., Drumm, A., Harrison, P. and Phillips, L. (1994) Repeated cleaning of a Protein A affinity column with sodium hydroide. Journal of Immunological Methods. 171: 15-21.

Hamers, M.N. (1993) Multiuse biopharmaceutical manufacturing. Biotechnology, May, 561-570.

Hand D.B. (1934) Correlation of the viscosity of protein solutions with their ability to crystallize. Journal of General Physiology. 17: 847-852.

Hinckley, P.H., Shukla, A.A. and Hubbard, B. (2002) Productivity comparisons on Protein A affinity chromatography. Presented at ACS National meeting, Boston, Massachusetts, USA, August.

Hjlem, H., Sjodahl, J. and Sjoquist, J. (1975) Immunologically active and structurally similar fragments of Protein A from staphylococcus aureus. European Journal of Biochemistry. 57: 395-403.

Hjlem, H., Hjlem, K. and Sjoquist, J. (1972) Protein A from staphylococcus aureus. XXIII. Its isolation by affinity chromatography and its use as an immunoadsorbent for isolation of immunoglobulins. FEBS Letters. 28, 1: 73-76.

Horstman, B.J. and Chase, H.A. (1989) Modelling the affinity adsorption of immunoglobulin-G to protein-A immobilized to agarose matrixes. Chemical Engineering Research and Design. 67: 243-254.

Hubbard, B.H. and Shukla, A.A. (2005) Platform approaches to monoclonal antibody purification. Presented at IBC Conference on antibody production and downstream processing, San Diego, California, USA, March.

Hubbard, B. (2003) Post-approval changes to the downstream Enbrel commercial process. Presented at IBC conference on Antibody Production and Downstream Development Processing, La Jolla, California, USA, March.

Hunt, B. Goddard, C. Middelberg, A.P.J. and O'Neill, B.K. (2001) Economic analysis of immunoadsorption systems. Biochemical Engineering Journal. 9:135-145.

Hunter, A.K. and Carta, G. (2001) Effects of bovine serum albumin heterogeneity on frontal analysis with anion-exchange media. Journal of Chromatography A. 937: 13-19.

Huse, K., Bohme, H.J. and Scolz, G.H. (2002) Purification of antibodies by affinity chromatography. Journal of Biochemical and Biophysical Methods. 51: 217-231.

Iyer, H., Henderson, F., Cunningham, E., Webb, J., Hanson, J., Bork, C. and Conley, L. (2002) Considerations during development of a Protein A antibody purification Process, BioPharm 5, 1: 14-20.

Jacobson, S.C.,Felinger, A. and Guiochon, G. (1992) Optimising the sample –size and the retention parameters to achieve maximum production-rates for enantiomers in chiral chromatography. Journal of Biotechnology and Bioengineering. 10: 1210-1217.

Jandera, P., Komers, D. and Guichon, G. (1997) Effects of the gradient profile on the production in reversed-phase gradient elution overload chromatography. Journal of chromatography A. 760: 25-39.

Johannsson, H., Mottaqui-Taber, A. and Karlsson, S. (2004) New affinity media for purification of monoclonal antibodies. Presented at ACS National Meeting, Anaheim, California, USA, March.

Johansson, H. and Lacki, K. (2003) Comparison and optimisation of different operating principles for capture step on Protein A resin. Presented at PREP 2003, Washington DC, USA, July 1.

Johansson, H.J., Bergenstrahle, A., Rodrigo, G., and Oberg, K. (2002) The use of NaOH for CIP of rProtein A media: a 300 cycle study. (http://www5.amershambiosciences.com/applic/upp00738.nsf/vLookupDoc/250173076-P516/$file/18117764AA.pdf). Accessed 10/04/2004.

Jones, S.C.B. and Smith, M.P. (2005) Evaluation of an alkali stable Protein A resin versus Protein A Sepharose Fast Flow and considerations on process scale-up to 20,000L. Downstream Gab04 abstracts. Extended reports from the 3rd International Symposium on Downstream Processing of Genetically Engineered Antibodies and Related Molecules. GE Healthcare publication code 11-0027-25.

Joustra, M.K., Emneus, A. and Tibbling, P. (1967) Large-scale gel filtration. Protides of the Biological Fluids. 12: 575-579.

Jungbauer, A. (1996) Insights into the chromatography of proteins provided by mathematical modelling. Current Opinions in Biotechnology. 7, 2: 210.

Kabir, S. (2002) Immunoglobulin purification by affinity chromatography using Protein A mimetic ligands prepared by combinatorial chemical reaction. Immunological Investigation. 31: 263.

Kamihira, M., Hatti-Kaul, R. and Mattiasson, B. (2000) found in Aqueous Two-Phase Systems: Methods and Protocols. Hatti-Kaul, R. (ed). Humana Press (online).

Kang, K.A. and Ryu, D.D.Y. (1991) Studies on scale-up parameters of an immunoglobulin separation system using Protein A affinity chromatography. Biotechnology progress. 7: 205-212.

Karlsson, D., Jakobsson, N., Axelsson, A. and Nilsson, B. (2004) Model-based optimisation of a preparative ion-exchange step for antibody purification. Journal of Chromatography A 1055:29-39.

Keener, R.N., Maneval, J.E. and Fernandez, E.J. (2004a) Toward a robust model for packing and scale-up for chromatographic beds.1: Mechanical compression. Biotechnology Progress. 20: 1146-1158.

Keener, R.N., Maneval, J.E. and Fernandez, E.J. (2004b) Toward a robust model for packing and scale-up for chromatographic beds.2: Flow packing. Biotechnology Progress. 20: 1159-1168.

Keener, R.N., Maneval, J.E., Ostergren, K.C.E. and Fernandez, E.J. (2002) Mechanical deformation of compressible chromatographic columns. Biotechnology Progress.18: 587-596.

Keller, K., Friedmann, T. and Boxman, A. (2001) The bioseparation needs for tomorrow. Trends in Biotechnology. 19, 11, 438-441.

Kelley, B.D., Tannatt, M., Magnusson, R., Hagelberg, S. and Booth, J (2004) Development and validation of an affinity chromatography step using a peptide ligand for cGMP production of factor VIII. Journal of Biotechnology and Bioengineering. 87: 400-412.

Kelly, B.D. (2001) Bioprocessing of therapeutic proteins. Current Opinion in Biotechnology. 12: 173–174.

Kemp, G., Hamilton, G., Quinones-Garcia, I., McCue, J., Mann, F. and Low, D (2002) PROSEP®-A media: Meeting the demands in process-scale antibody purification for high capacity and throughput. Presented at the BioPhex Conference, Santa Clara, California, USA. October 22-24.

Klyushnichenko, V. (2003) Protein crystallisation: From HTS to kilogram-scale. Current Opinion in Drug Discovery and Development 6: 848-854.

Koh, J., Broyles, B.S., Guan-Sajonz, H., Hu, M.Z.C. and Guiochon, G. (1998) Consolidation and column performance of several packing materials for liquid chromatography in a dynamic axial compression column. Journal of Chromatography A. 813: 223-238.

Köhler, G. and Milstein, C. (1975) Continuous cultures of fused cells secreting antibody of predefined specificity. Nature. 256: 495–497.

Kunin, R. (1976) Safety practices in ion exchange technology. Amber-HiLites. No 153. Rohm and Haas Company.

Langone, J.J. (1982) Protein A of staphylococcus aureus and related immunlogloulin receptors produced by streptococci and pneumonococci. Advanced Immunology. 32: 157-252.

Larson, T.M., Davis, J., Lam, H. and Cacia, J. (2003) Use of process data to assess chromatographic performance in production-scale protein purification columns. Biotechnology Progress. 19, 2: 485-492.

Lawrence , S. (2007) Billion dollar babies—biotech drugs as blockbusters. Nature Biotechnology. 25: 380 -382.

Lebreton, B., Lin Ai, P., Amy, L., Judy, H., Polly, M. and Sharma, M. (2006) High-yielding process within and beyond existing plant capacity. Presented at Recovery of Biological Products XII, Litchfield, Arizona, USA. April 2-7.

Lee, T.S., Vaghjiani, J.D., Lye, G.J. and Turner, M.K. (2000) A systematic approach to the large-scale production of protein crystals. Enzyme and Microbial Technology. 26: 582.

Levison, P.R., Badger, S.E. and Toome, D.W. (1992) Economic considerations important in the scale-up of an ovalbumin separation from hen egg-white on the anion exchange cellulose DE92. Journal of Chromatography. 590: 49-58.

Li, R., Dowd, V., Stewart, D., Burton, S.J. and Lowe, C.R. (1998) Design synthesis and application of a Protein A mimetic. Nature Biotechnology. 16: 190-195.

Lim, A.C. (2004) A decision-support tool for strategic decision-making in biopharmaceutical manufacture. PhD Thesis. University College London, UK.

Lindsay, J. (1996) Cleaning and cleaning validation: A biotechnology perspective. Interpharm Press Inc,USA.

Low, D., O'Leary, R. and Pujar, N.S. (2007) Future of antibody purification. Journal of Chromatography B. 15: 48-63.

Lowe, C., Burton, S., Burton, N., Alderton, W., Pitts, J. and Thomas, J. (1992) Designer dyes: Biomimetic ligands for the purification of pharmaceutical proteins by affinity chromatography. TIBTECH. 10: 442-448.

Lucas, C., Nelson, C., Peterson, M.L., Frie, S., Vetterlein, D., Gregory, T. And Chen, A.B. (1988) Enzyme-linked immunoadsorbant purification of recombinant assays (ELISAs) for the determination of contaminants resulting from the immunoaffinity purification of recombinant proteins. Journal of Immunological Methods, 133: 113-122.

Lute, S., Norling, L., Hanson, M., Emery, R., Stinson, D., Khuu, W., Xu, Y., Blank, G.; Chen, Q. and Brorson, K. (2005) Robustness of viral removal by Protein A chromatography is independent of media lifetime and mechanism of degradation. Presented at the 11th Annual FDA Science Forum. April 27-28.

Madani, H., Hershberg, R. and Hubbard, B. (2003) Enbrel product lifecycle from Phase I to market launch and beyond. Presented at Recovery of Biological Products XI, Banff, Canada, September.

Malmquist, G., Lacki, K.M., Ljunglof, A. and Johansson, H. (2003) Engineering a new generation of affinity media for antibody purification. Presented at PREP conference, Washington D.C., USA, May.

Mao, Q.M., Prince, I.G. and Hearn, T.W. (1996a) Optimisation of operating parameters for protein purification with chromatographic columns. Journal of Chromatography A. 52: 204-222.

Mao, Q.M. and Hearn, M.T.W. (1996b) Optimisation of affinity and ion-exchange chromatographic processes for the purification of proteins. Journal of Biotechnology and Bioengineering. 52:204-222.

Marra, R.A. and Cooney, D.O. (1973) An equilibrium theory for sorption accompanied by sorbent bed shrinking and swelling. American Institute of Chemical Engineering Journal. 19, 1: 181-183.

Martin, A. J. P. and Synge, R. L. M. (1941) A new form of chromatogram employing two liquid phases : A theory of chromatography. 2. Application to the micro-determination of the higher monoamino-acids in proteins, The Biochemical Journal. 35, 12: 1358.

McCue, J.T., Kemp, G., Low, D. and Quinones-Garcia, I. (2003) Evaluation of Protein A chromatography media. Journal of Chromatography A. 989: 139-153.

Merkle, H.P. and Jen, A. (2002) A crystal clear solution for insulin delivery. Nature Biotechnology. 20: 789.

Millipore Technical Brief, TB1026EN00, (2006) Increasing Purity on Prosep- vA Affinity Chromatography Media using an Intermediate Wash Step. (http://www.millipore.com/publications.nsf/docs/tb1026en00), accessed 01/06/2007.

Millipore Technical Brief TB1024EN00, Improving Purity on Protein A Affinity Chromatography Media through use of an Arginine Intermediate Wash Step, http://www.priorartdatabase.com/IPCOM/000127319/, accessed 01/06/2007.

Millipore technical publication: Data sheet - DS4241EN00. ProSep®–vA Ultra Chromatography Media: http://www.millipore.com/publications.nsf/docs/ds1013en00 , accessed 01/06/2007.

Mohammed, A.W., Stevenson, D.G. and Wankat, P.C. (1992) Pressure drop correlations and scale-up of size exclusion chromatography with compressible packing. Industrial Engineering and Chemical Research. 31:549-561.

Moks, T., Abrahmsen, L., Nilsson, B., Hellman, U., Sjoquist, J. and Uhlen, M. (1986) Staphylococcal Protein A consists of five IgG-binding domains. European Journal of Biochemistry. 156: 637-643.

Morrow, K. J. (2006) Development and production of antibodies: Looking at the needs and challenges and considering the range of possible alternatives. Genetic Engineering News 26, 15, 54-58.

Moscho, A., Hodits, R.A., Janus, F. and Leiter, J.M.E. (2000) Deals that make sense, Nature. Biotechnology.18, 7:719.

Muller, E., Chung, J.-T., Zhang, Z. and Sprauer, A. (2005) Characterisation of the Mechanical Properties of Chromatographic Particle by Micromanipulation. Journal of Chromatography A. 1097: 116-123.

Myers, J. (2000) Economic consideration in the development of the downstream steps for large-scale commercial biopharmaceutical processes. Presented at Production and economics of biopharmaceutical conference, San Diego, California, USA.

Naveh, D. and Siegel, R.C. (1991) Large-scale downstream processing of monoclonal antibodies. Bioseparation. 1: 351-366.

Nelson, K. (1998) Cell culture manufacturing: An economic perspective from an engineering consultant. Presented at US Biotechnology Symposium, Washington DC, USA, Nov 29 – Dec 1.

Newcombe, A.R., Cresswell, C., Davies, S., Watson, K., Harris, G., O'Donovan, K. and Francis, R. (2005) Optimised affinity purification of polyclonal antibodies from hyper immunised ovine serum using synthetic Protein A adsorbent, MAbsorbent A2P. Journal of Chromatography B. 814: 209-215.

Ngiam, S. H., Zhou Y.H., Turner M.K., and Titchener-Hooker N.J., (2001) Graphical frameworks for facilitating the study of chromatographic separations, Journal of Chromatography A, 937: 1–11.

O'Leary, R.M., Feuerhelm, D., Peers, D., Xu, Y. and Blank, G.S. (2001) Determining the useful lifetime of chromatography resins. BioPharm International.10-18.

Osborne, A. (1997) Evaluation of project economic viability. Presented at MBI Training Programme: Desogn II, University College London, UK, May.

Ostergren, K.C.E., Tragardh, A.C.,Enstad, G.G. and Mosby, J. (1998) Deformation of a chromatographic bed during steady state liquid flow. American Insitiute of Chemical Engineers Journal. 44: 2-12.

Ostlund, C. (1996) Large-scale purification of monoclonal antibodies. Trends in Biotechnology. 166: 288-293.

Peakman, T.C., Worden, J., Harris, R.H., Cooper, H., Tite, J., Page, M.J. Gewert, D.R., Bartholemew, M., Crowe, J.S. and Brett, S. (1994) Comparison of expression of a humanized monoclonal antibody in mouse NSO myeloma cells and Chinese hamster ovary cells. Human Antibody Hybridomas. 5: 65–74.

Pechenov, S., Shenoy, B., Yang, M.X., Basu, S.K. and Margolin, A.L. (2004) Injectable controlled release formulations incorporating protein crystals. Journal of Controlled Release 96, 1: 149-158.

Persson, J. and Lester, P. (2004) Purification of antibody and antibody-fragment from E. coli homogenate using 6, 9-diamino-2-ethoxyacridine lactate as precipitation agent. Journal of Biotechnology and Bioengineering. 87, 3: 424-434.

Peters, M.S., Timmerhaus, K.D. (1991) Plant design and economics for chemical engineers. McGrw-Hill: New York, USA, Chapter 6.

Petrides, D., Koulouris, A. and Siletti, C. (2002) Throughput analysis and debottlenecking of biomanufacturing facilities a job for process simulators. BioPharm. August.

Pisano, G.P. (1997) The development factory: Unlocking the potential of process innovation. Harvard Business School press, Massachusetts, USA.

Pradipasena, P. and Rha, C. (1977) Effect of concentration on apparent viscosity of a globular protein solution. Polymer Engineering and Science, 17, 12: 861-864.

Rathore, A.S., Noferi, J.F., Arling, E.R., Sofer, G., Walter, P. and O'Leary, R. (2002) Process validation: How much to do and when to do it. BioPharm International. 15,10: 18-28.

Remer, D.S., Idrovo, J.H. (1991) Cost-estimating factors for biopharmaceutical process equipment. Pharmaceutical Technology International, March: 36-42.

Rito-Palomares, M. (2004) Practical application of aqueous two-phase partition to process development for the recovery of biological products. Journal of Chromatography B 807, 1: 3-11.

Roque, A.C.A., Lowe, C.R., Taipa, M.A. (2004) Antibodies and genetically engineered related molecules: Production and purification. Biotechnology Progress. 20: 639-654.

Rouf, S.A., Douglas, P.L., Moo-Young, M. and Scharer, J.M. (2001) Economics of fed-batch operation: A computer aided approach. Bioprocess and Biosystems Engineering. 24: 65-71.

Russell, C., Baines, D. and Burton, S. (1999) Application of a synthetic adsorbent of the purification of immunglobulins. Presented at Recovery of Biological Products IX, Whistler, Canada.

Sada, E., Katoh, S., Sukai, K., Tohma, M. and Kondo, A. (1986) Adsorption equilibria in immuno-affinity chromatography with polyclonal and monoclonal antibodies. Journal of Biotechnology and Bioengineering, XXVIII: 1497-1502.

Sainio, T. and Paatero, E. (2007) Mass coordinates for dynamic simulation of column operations involving dimensional changes of packing material. Computers and Chemical Engineering. 31: 374-383.

Salisbury, R.S., Bracewell, D. G. and Titchener-Hooker, N. J. (2006) A methodology for the graphical determination of operating conditions of chromatographic sequences incorporating the trade-offs between purity and yield. Journal of Chemical Technology & Biotechnology, 81, 11: 1803-1813.

Schmidt, S., Havekost, D., Kaiser, K., Kauling J. and Henzler, H.-J. (2005) Crystallization for the downstream processing of proteins. Engineering in Life Sciences. 5: 273.

Schuler, G. and Reinacher, M. (1991) Development and optimisation of a single step procedure using Protein A affinity chromatography to isolate murine IgG1 monoclonal antibodies from hybridoma supernatant. Journal of Chromatography. 587: 61-70.

Schwartz, W., Judd, D., Wysocki, M., Guerrier, L., Brick-Wilson, E. and Boscheti, E. (2001) Comparison of HCIC with affinity chromatography on Protein A for harvest and purification of antibodies. Journal of Chromatography A. 908: 251-263.

Schwartz, C.E. and Smith, J.M. (1953) Flow distribution in packed beds. Industrial and Engineering Chemistry. 45, 6: 1209.

Scott, R.P.W. (1987) Techniques and practice of chromatography. CRC, New York/ London.

Sengupta, J., Sinha, P., Mukhopadhyay, C. and Ray, P.K. (1999) Molecular modelling and experimental approached toward designing a minimalisitic protein having the Fc-binding activity of staphylococcal Protein A. Biochemical and Biophysical Research Communications. 256: 6-12.

Shadday, M.A.(2006) A one-dimensional transient model of down-flow through a swelling packed porous bed. Chemical Engineering Science. 61: 2688-2700.

Shadle, P.J., Mills, G., Erickson, J.C., Scott, R.G., Collingwood, N.J. and Smith, T.M. (1995) US Patent 5,429,746, July 4.

Shire, S.J., Shahrokh, Z. and Liu, J. (2004) Challenges in the development of high protein concentration formulations. Journal of Pharmaceutical Sciences. 93: 1390-1402.

Shukla, A.V., Hubbard, B., Tressel, T., Guhan, S. And Low, D. (2007) Downstream processing of monoclonal antibodies – Application of platform approaches. Journal of Chromatography B. 848: 28-39.

Sinha, J., Dey, P.K. and Panda, T. (2000) Aqueous two-phase: the system of choice for extractive fermentation. Applied Microbiology and Biotechnology 54: 476.

Sinha, P., Sengupta, J. and Ray, P.K. (1999) Functional mimicry of Protein A of staphylococcus aureus by a proteolytically cleaved fragment. Biochemical and Biophysical Research Communications. 260: 111-116.

Sinott, R.K. (1997) Coulson and Richardson's Chemical Engineering Handbook, Pergamon Press, Oxford, UK.

Sinott, R.K. (1993) Coulson and Richardson's Chemical engineering handbook (Chemical Engineering Design), Pergamon Press, Oxford, UK, Vol 6, pp 209-244.

Snyder, L. R. and Glajch, J. L. (1990) Computer-Assisted Method Development for High Performance Liquid Chromatography, Elsevier, Amsterdam, Netherlands.

Sofer, G.K. and Nystrom, L.E. (1989) Process hygiene in process chromatography, a practical guide, New York, Academic Press, pp 93-105.

Sofer, G.K. (1987) Increasing media lifetime for cost-effective chromatography. Nature Biotechnology. 5.

Sofer,G. and Hagel, L. (1997) Handbook of process chromatography; A guide to optimisation, scale-up and validation; Academic Press: San Diego, USA, pp100-101, 361-365.

Solomons, G. (1996) Organic Chemistry, John Wiley John Wiley & Sons Inc Somerset, New Jersey, USA, pp 140-155.

Sommerfeld, S. and Strube, J. (2005) Challenges in biotechnology production—generic processes and process optimisation for monoclonal antibodies. Chemical Engineering Processing. 44, 10:1123-1137.

Stickel, J.J. and Fotopoulos A. (2001) Pressure-flow relationships for packed beds of compressible chromatography media at laboratory and production scale. Biotechnology Progress 17, 4:744-751.

Swinnen, K., Krul, A., Van Goidsenhoven, I., Van Tichelt, N., Roosen, A. and Van Houdt, K. (2007) Performance comparison of Protein A affinity resins for the purification of monoclonal antibodies. Journal of Chromatography B. 848: 97-107.

Tejeda-Mansir, A., Espinoza, R., Montesinos, R.M. and Guzman, R. (1997) Modelling regeneration effects on Protien A chromatogrpahy. Bioprocess Engineering. 17: 39-44.

Teng, S.F., Sproule, K., Hussain, A. and Lowe, C.R. (2000) Affinity chromatography on immobilized "biomimetic" ligands: Synthesis, immobilization and chromatographic assessment of an immunoglobulin G-binding ligand. Journal of Chromatography B. 740: 1-15.

Teng, S.F., Sproule, K., Hussain, A. and Lowe, C.R. (1999) A strategy for the generation of biomimetic ligands affinity chromatography – combinatorial synthesis and biological evaluation of an IgG binding ligand. Journal of Molecular Recognition. 12: 67-75.

Teoh H.K., Turner M., Titchener-Hooker N.J. and Sorensen E. (2001) Experimental verification and optimisation of a detailed dynamic high performance liquid chromatography column model. Computers and Chemical Engineering, 25, 4: 893-903.

Terman, D.S. and Bertram, J.H. (1985) Antitumor effects of immobilized Protein A and staphylococcal products: Linkage between toxicity and efficacy, and identification of potential reagents. European Journal of Cancer and Clinical Oncology. 21, 10: 1115-1122.

Thommes, J. and Etzel, M. (2007) Alternatives to Chromatographic Separations. Biotechnology Progress. 23,1:42-45.

Thommes, J., Conley, L., Pieracci, J. and Sonnenfled, A. (2003) Protein A affinity simulated moving bed chromatography for continuous monoclonal antibody purification. Presented at Recovery of Biological Products XI, Banff, Canada, September.

Torphy, T.J. (2002) Pharmaceutical biotechnology - Monoclonal antibodies: boundless potential, daunting challenges. Current Opinion in Biotechnology. 13: 589.
Trägardh, G. (1989) Membrane cleaning. Desalination.71:325–335.

Tscheliessnig, A., Hahn, R. and Jungbauer, A. (2005) In situ determination of adsorption kinetics of proteins in a finite bath. Journal of Chromatography A. 1069: 23-30.

Tu, Y.T., Primus, F.J. and Goldenberg, D.M. (1988) Temperature affects binding of murine monoclonal IgG antibodies of Protein A. Journal of Immunological Methods. 109: 43-47.

van Reis, R., Banerjess, D., Fontes, N., Harinarayan, C., Lebreton, B., Lin,A. and Mehta, A. (2006) Future Trends in Bioseperations. Presented at Recovery of Biological Products XII, Litchfield, Arizona, USA, April 2-7.

van Reis, R., Brake, M., Charkoudian, J., Burns, D. B. and Zydney, A. L. (1999) High-performance tangential flow filtration using charged membranes. Journal of Membrane Science. 159: 133-142.

Vandevyver, C. and Freitag, R. (2004) Purification of antibodies by chromatographic methods. Antibodies, Volume I: Production and Purification. Subramanian, G (ed.), Kluwer Academic/ Plenum Publishers, New York, USA, pp. 133-168.

Verdoliva, A., Pannone, F., Rossi, M., Catello, S. and Manfredi, V. (2002) Affinity purification of polyclonal antibodies using a new all-D synthetic peptide ligand: Comparison with Protein A and Protein G. Journal of Immunological Methods. 271: 77.

Walsh, G. (2000) Biopharmaceutical benchmarks. Nature Biotechnology. 18: 831–833.

Walsh, G. and Headon, D. (1994) Protein biotechnology, J Wiley and Sons Ltd. United Kingdom, p66.

Weaver, L.E. and Carta, G. (1996) Protein adsorption on cation exchangers: Comparison of macroporous and gel-composite media. Biotechnology Progress. 12: 342-355.

Whitely, R. D., Brown, J. M., Karajgikar, N. P. and Wang, N-H. L. (1989) Determination of ion-exchange equilibrium parameters of amino acid and protein systems by an impulse response technique. Journal of Chromatography. 483: 263-287.

Whitley, R. D., Berninger, J. A., Rouhana, N. and Wang, N.-H. L. (1991) Nonlinear gradient isotherm parameter estimation for proteins with consideration of salt competition and multiple forms. Biotechnology Progress. 7: 554-553.

Wilson, J.N. (1940) A theory of chromatography, Journal of the American Chemical Society, 6, 62: 1583.

Wilson, E.J. and Geankoplis, C.J. (1966) Industrial & engineering chemistry fundamentals. Industrial Engineering and Chemical Fundamentals. 5: 9.

Wurm, F.M. (2004) Production of recombinant protein therapeutics in cultivated mammalian cells. Nature Biotechnology. 22: 1393-8.

Xie, L. and Wang, D.I.C. (1996) High cell density and high monoclonal antibody production through medium design and rational control in a bioreactor. Journal of Biotechnology and Bioengineering. 51:725-729.

Yamamoto, S. and Sano, Y. (1992) Short-cut method for predicting the productivity for affinity chromatography. Journal of Chromatography A. 597:172-179.

Yang, M.X., Shenoy, B., Disttler, M., Patel, R., McGrath, M., Pechenov, S. and Margolin, A.L. (2003) Crystalline monoclonal antibodies for subcutaneous delivery Proceedings from the National Academy of Sciences. U.S.A. 100: 6934.

Yau, W.W., Kirkland, J.J, Bly, D.D. (1979) Modern Size-exclusion Liquid Chromatography: Practice of Gel Permeation and Gel Filtration Chromatography. Wiley-Interscience, New York.

Yuan, O.S., Rosenfeld, A., Root, T.W., Klingengerg, D.J. and Lightfoot, E.N. (1999) Flow distribution in chromatographic columns. Journal of Chromatography A. 831: 149-165.

Zenz, F.A. and Othmer, D.F. (1960) Fluidisation and fluid-particle systems. Reinhold publishing Corporation, New York, USA, pp 74-80.

Zhou, Y., H. and Titchener-Hooker, N.J. (1999) Visualizing integrated bioprocess designs through "windows of operation". Biotechnology and Bioengineering. 65, 5:550-557.

Zhou, J.X., Tressel, T. (2006) Basic concepts in Q membrane chromatography for large-scale antibody production. Biotechnology Progress. 22: 341-349.

14 NOMENCLATURE

$\&$	And
$\$_{MAb}$	Theoretical manufacturing MAb price ($)
b	Empirical constant (m^2/s) , Stickel correlation (3.5)
b'	Empirical constant (m^2/s) , Equation (3.10)
b''	Empirical constant (-)
C	Cost ($)
C_b	Solute concentration in bulk fluid phase ($g/L_{solution}$)
C_0 , Titre	Feed concentration of a solute (g/L)
C_p	Solute concentration in pore fluid (g/L_{resin})
$C_{\$\ buffer}$	Buffer costs ($/$L_{buffer}$)
$C_{\$\ col+rig}$	Cost of column hardware (capital cost and installation) (Equation 5.17) ($)
$C_{\$\ col+rig\ dep}$	Column and rig depreciation costs ($)
$C_{\$\ E}$	Capital cost of column hardware ($)
$C_{\$\ resin}$	Resin costs ($/$L_{resin}$)
$C_{\$\ time}$	Labour costs in terms of time ($/h)
CHO	Chinese hamster ovaries
CIP	Clean-in-Place
COG/g	Process cost of goods per gram of product produced ($/g)
$COG/g_{specific}$	Specific chromatographic cost of goods per gram of product produced ($/g)

CPG	Controlled pore glass (-)
CV	Column volume (L)
d	Molecular diameter of the solute (μm)
D	Column diameter (m) (Chapter 3)
D_b	Axial diffusion (cm^2/s)
D_c	Inner diameter of column (cm)
D_{eff}	Effective diffusitiy (cm^2/s)
D_m	Molecular diffusivity (cm^2/s)
d_p	Mean resin particle diameter (μm)
f_d	Frictional drag force (N)
f_L	Lang factor (-)
HCP	Host cell proteins (-)
K_d	Dissociation constant ($g/L_{solution}$)
k_f	External film mass transfer coefficient (cm/s)
L	Bed height (cm)
L_o	Gravity settled bed height (m)
M	Amount of solute lost during breakthrough (g)
m	Empirical constant (m^2/s) , Stickel correlation (3.5)
m'	Empirical constant (m) , Stickel correlation (3.8)
m''	Empirical constant (m^2/s) , Stickel correlation (3.9)
MAb	Monoclonal antibody
MW	Molecular weight of solute (g/mol)

N	Number of cycles (-)
N_{Life}	Resin lifetime (cycles)
P	Productivity (g/h)
Q	Equipment capacity (Equation 5.18)
Q_0	Initial binding capacity (g/L)
Q_{max}	Saturation capacity (g/L)
Q_N	Binding capacity after N number of cycles (g/L)
q_s	Solute concentration on a pore free basis (Equation 5.1) ($g/L_{skeletal\ resin}$)
R	Radial position in column (Equation 5.1)
Re	Reynolds Number
R_p	Distance from centre of particle to boundary (Equation 5.2) (-)
r_p	Particle radius (cm)
t	Time units
T	Total time of column operation (h)
t_b	Time taken for loading until desired breakthrough (h)
t_c	Total cycle time (h)
t_e	Time taken for elution stage (h)
t_{equ}	Time taken for equilibration (h)
t_F	Time taken for column clean-up after the final cycle (h)
t_p	Time taken for column preparation before the first cycle (h)
t_w	Time taken for wash stage (h)
u	Superficial fluid velocity (m/s)

$u_{10\%}$	Superficial fluid velocity causing 10% reduction in bed height (m/s)
u_{crit}	Critical superficial fluid velocity (m/s)
V_{load}	Load volume (L)
Z	Axial position coodinates inside the column

Greek letters

ε_b / ε	Interstitial bed porosity (-)
ε_0	Initial interstitial bed porosity before compression
ε_p	Particle porosity (-)
$\varepsilon_{peffective}$	Effective particle porosity (-)
λ	Bed compression (dimensionless) (-)
λ_{crit}	Bed compression at critical velocity (-)
μ	Viscosity of mobile phase (kg/ms)
ΔP	Hydrodynamic pressure drop across a packed bed (Pa)
ρ	Density (kg/m^3)
Φ	Constant in the degradation function (Equation (5.20)) (g/L)
τ	Tortuosity factor(-)